



**UNIVERSIDADE FEDERAL DO PARÁ  
CENTRO DE GEOCIÊNCIAS  
CURSO DE PÓS-GRADUAÇÃO EM GEOLOGIA E GEOQUÍMICA**

---

**TESE DE DOUTORADO**

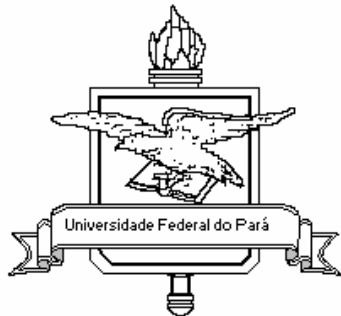
**MODELOS DE EVOLUÇÃO E COLOCAÇÃO DOS  
GRANITOS PALEOPROTEROZÓICOS DA SUÍTE JAMON,  
SE DO CRÁTON AMAZÔNICO**

**Tese apresentada por:**

**DAVIS CARVALHO DE OLIVEIRA**

---

**BELÉM  
2006**



**Universidade Federal do Pará  
Centro de Geociências  
Programa de Pós-Graduação em Geologia e Geoquímica**

**MODELOS DE EVOLUÇÃO E COLOCAÇÃO DOS GRANITOS  
PALEOPROTEROZÓICOS DA SUÍTE JAMON, SE DO CRÁTON  
AMAZÔNICO**

TESE APRESENTADA POR

**DAVIS CARVALHO DE OLIVEIRA**

Como requisito parcial à obtenção do Grau de Doutor em Ciências na Área de GEOQUÍMICA E PETROLOGIA.

Data de Aprovação: **27 / 10 / 2006**

**Comitê de Tese**

---

ROBERTO DALL'AGNOL (Orientador)

---

TAPANI RÄMÖ

---

SÉRGIO PACHECO NEVES

---

RICARDO IVAN FERREIRA DA TRINDADE

---

ROBERTO VIZEU LIMA PINHEIRO

Belém

A todas as pessoas que acreditaram na realização  
deste trabalho, em especial, à minha família.

## **AGRADECIMENTOS**

Este espaço é dedicado a algumas pessoas e instituições que, por diferentes razões, deram a sua contribuição para que esta tese fosse realizada. Deixo aqui meus agradecimentos sinceros:

À Universidade Federal do Pará pela infra-estrutura e suporte financeiro;

Aos órgãos financiadores: Coordenação de Aperfeiçoamento de Pessoal de Nível Superior (CAPES) à concessão da bolsa de pesquisa no período de novembro de 2001 a março de 2004; Conselho Nacional de Desenvolvimento Científico e Tecnológico (CNPq) pela disponibilidade de uma bolsa de estudo durante parte do período de realização da presente tese (abril de 2004 a novembro de 2005);

Ao Projeto PRONEX (FADESP/CNPq, proj. nº 103/98 - Proc. 66.2103/1998-0), através de seu coordenador Roberto Dall'Agnol, pelo suporte financeiro nas diversas etapas de elaboração deste trabalho e por ter possibilitado em diversas ocasiões a divulgação do mesmo;

Ao Professor Roberto Dall'Agnol, por compartilhar comigo seu tema de pesquisa, sendo um interlocutor disposto a oferecer estímulos e, principalmente, a percorrer novos caminhos, ouvir com interesse e ânimo todas as questões, dúvidas e problemas que surgiam durante o processo de reflexão. Por ser um interlocutor paciente e generoso e pela coragem de ousar trabalhar com novas idéias e conceitos, correndo os riscos inerentes a esta atitude. Por sua amizade, principalmente;

Aos Professores João Batista Corrêa da Silva pela importante e imprescindível participação no estudo gravimétrico dos granitos Bannach e Redenção e José Luiz Gouvêa, pelo auxílio no cálculo da Anomalia Bouguer do Granito Bannach;

Ao Professor Sérgio Pacheco Neves pelas importantes discussões sobre os resultados obtidos no estudo de ASM, bem como pelas importantes idéias colocadas sobre colocação de corpos graníticos;

Aos professores: Gorki Mariano pela valiosa colaboração nas etapas de campo e Paulo B. Correia pela utilização do Laboratório de Geofísica Prof. Helmo Rand da Universidade Federal de Pernambuco, durante a aquisição dos dados de Anisotropia de Suscetibilidade Magnética, bem como pelas discussões indispensáveis para o entendimento desta ferramenta;

*In Memoriam.* Ao Professor Nilson Teixeira, pelo incentivo e colaboração na etapa inicial deste trabalho;

À Mineração Jenipapo (Grupo Western Mining Company – WMC) pela disponibilidade dos dados gravimétrico obtidos sobre o Granito Redenção, somente possível através da colaboração com o Geólogo Grant Osborne;

À CPRM, através da Geóloga Lúcia Travassos, pela concessão das imagens aerogeofísicas da Província Mineral de Carajás;

Aos colegas/colaboradores José de Arimatéia Costa de Almeida e Marcelo Augusto Oliveira pela ajuda nas etapas de amostragem para o estudo de ASM, assim como pelas discussões e sugestões nos diversos temas que integram este trabalho. Ao primeiro por permitir nossa colaboração no estudo do granito Bannach;

Aos funcionários/colaboradores: Carlos Alberto pela ajuda nas etapas de campo do mapeamento geológico e na etapa inicial de amostragem para o estudo de ASM e Afonso Quaresma pela importante colaboração na aquisição de dados gravimétricos no Granito Bannach e da etapa complementar de amostragem do estudo de ASM do Granito Redenção;

Ao colegiado do curso de geologia do Campus Sul-Sudeste do Estado Pará – Marabá, pela compreensão e liberação das atividades acadêmicas durante a etapa final deste trabalho;

À colega Karen Volp pelo auxílio na preparação do volume final da tese, assim como pelo suporte na língua inglesa;

Ao Bibliotecário Hélio Braga Martins (Biblioteca Raimundo Montalvão – CG) pela revisão bibliográfica e de norma;

Aos demais colegas do Grupo de Pesquisa Petrologia de Granitóides (GPPG) pelas discussões e sugestões, bem como, pelo companheirismo e descontração nas diversas etapas de execução deste trabalho.

Todos são co-autores deste trabalho.

*Uma educação que possibilite ao homem a discussão corajosa de sua problemática. De sua inserção nesta problemática. Que o coloca em diálogo constante com o outro. Que o predispõe à constantes revisões. À análise crítica de seus ‘olhados’. A uma certa rebeldia no sentido mais humano da expressão. Que o identifique com métodos e processos científicos.*

PAULO FREIRE

## SUMÁRIO

<b>DEDICATÓRIA</b>	i
<b>AGRADECIMENTOS</b>	ii
<b>EPÍGRAFE</b>	iv
<b>RESUMO</b>	1
<b>ABSTRACT</b>	3
<b>1 – INTRODUÇÃO</b>	5
1.1 – APRESENTAÇÃO E LOCALIZAÇÃO DA ÁREA	6
1.2 – CONTEXTO GEOLÓGICO REGIONAL	9
1.3 – MAGMATISMO ANOROGÊNICO DA PROVÍNCIA MINERAL DE CARAJÁS	14
1.4 – APRESENTAÇÃO DO PROBLEMA	16
1.5 – OBJETIVOS	17
REFERÊNCIAS BIBLIOGRÁFICAS	19
<b>2 - GEOCHEMISTRY AND MAGMATIC EVOLUTION OF THE PALEOPROTEROZOIC, ANOROGENIC A-TYPE REDENÇÃO GRANITE OF THE JAMON SUITE, EASTERN AMAZONIAN CRATON, BRAZIL</b>	27
Davis Carvalho de Oliveira	
Roberto Dall’Agnol	
Carlos Eduardo M. Barros	
<i>Submetido: CANADIAN MINERALOGIST</i>	
Letter of Submission	
<b>Abstract</b>	28
<b>1. Introduction</b>	29
<b>2. Geologic Setting</b>	31
<b>3. Redenção granite</b>	33
3.1. Field relationships with country rocks	33
3.2. Petrography and facies relationships	35
3.3. Whole-rock geochemistry	43
3.3.1. Analytical procedure	43
3.3.2. Results	46
3.3.3. The behaviour of Rb, Sr, and Ba	51
3.3.4. Rare Earth Elements	53
<b>4. Discussion</b>	56
4.1. Granite typology	56
4.2. The oxidized character of the Redenção A-type granites	56
4.3. The magmatic evolution of the Redenção granites	59
<b>5. Summary and conclusions</b>	60
<b>Acknowledgments</b>	60
<b>References</b>	61

**3 – OXIDIZED, MAGNETITE-SERIES, RAPAKIVI-TYPE GRANITES OF CARAJÁS, BRAZIL: IMPLICATIONS FOR CLASSIFICATION AND PETROGENESIS OF A-TYPE GRANITES** ..... 68

Roberto Dall'Agnol  
Davis Carvalho de Oliveira  
*In Press: LITHOS*

<b>Abstract</b> .....	69
<b>1. Introduction</b> .....	70
<b>2. A-type granites of the Carajás province</b> .....	70
2.1. Geologic setting, geochronology and Nd isotope geochemistry .....	70
2.2. Petrography and mineral chemistry .....	72
2.3. Elemental geochemistry .....	73
2.4. Magnetic susceptibility and Fe-Ti oxides .....	73
<b>3. Comparison with the Proterozoic A-type granites of Fennoscandia and Laurentia</b> .....	73
<b>4. Granite classifications and their applicability to A-type rapakivi granites</b> .....	73
<b>5. Geochemical distinction of oxidized A-type granites</b> .....	77
<b>6. <math>\text{FeO}_t/(\text{FeO}_t+\text{MgO})</math> ratios versus magnetite-series and ilmenite-series</b> .....	80
<b>7. Experimental constraints on the origin of oxidized A-type granites</b> .....	81
<b>8. Conclusions</b> .....	84
<b>Acknowledgments</b> .....	85
<b>References</b> .....	85

**4 - GRAVIMETRIC, RADIOMETRIC, AND MAGNETIC SUSCEPTIBILITY STUDY OF THE PALEOPROTEROZOIC REDENÇÃO AND BANNACH PLUTONS: IMPLICATIONS FOR ARCHITECTURE AND ZONING OF A-TYPE GRANITES** ..... 88

Davis Carvalho de Oliveira  
Roberto Dall'Agnol  
João Batista C. da Silva  
José de Arimatéia C. de Almeida  
*Submetido: JOURNAL SOUTH AMERICA EARTH SCIENCE*

Letter of Submission	
<b>Abstract</b> .....	89
<b>1. Introduction</b> .....	90
<b>2. Geologic Setting</b> .....	92
<b>3. General aspects of the studied plutons</b> .....	94
<b>4. Zoning of the plutons</b> .....	95
4.1. Petrographic and geochemical data .....	95
4.2. Magnetic susceptibility data .....	100
4.3. Remote sensing and aerogamma spectrometry .....	101
<b>5. Gravity method</b> .....	104
5.1. Gravity survey and corrections .....	104

<i>5.1.1 Bannach Area</i>	104
<i>5.1.2 Redenção Área</i>	104
5.2. Density measurements	105
5.3. Inversion methodology	106
5.4. Results	107
<b>6. Discussion</b>	111
6.1. Tridimensional shape of the plutons	111
6.2. Tectonic setting and emplacement of the studied plutons	114
6.3. Internal zoning of the plutons	115
<b>7. Conclusions</b>	116
<b>Acknowledgments</b>	117
<b>References</b>	118

**5 - ANISOTROPY OF MAGNETIC SUSCEPTIBILITY OF THE REDENÇÃO GRANITE, EASTERN AMAZONIAN CRATON: IMPLICATIONS FOR THE EMPLACEMENT OF A PALEOPROTEROZOIC ANOROGENIC A-TYPE PLUTON** 126

Davis Carvalho de Oliveira

Sérgio Pacheco Neves

Roberto Dall'Agnol

Gorki Mariano

Paulo B. Correia

*Submetido: PRECAMBRIAN RESEARCH*

Letter of Submission	
<b>Abstract</b>	127
<b>1. Introduction</b>	128
<b>2. Geologic Setting</b>	130
<b>3. The Redenção pluton: general outline</b>	132
3.1. Field relationships and magmatic evolution	132
3.2. 3-D Geometry	134
<b>4. Anisotropy of magnetic susceptibility study</b>	135
4.1. Sampling and measurements	135
4.2. Results	136
4.2.1. Magnetic susceptibility	136
4.2.2. Shape and anisotropy of AMS ellipsoids	138
4.2.3. Magnetic fabric	142
<b>5. Discussion</b>	149
5.1. Regional context of pluton emplacement	149
5.2. Zoning and magnetic susceptibility	151
5.3. Magnetic fabric and emplacement model	152
5.4. Perspectives on the application of the AMS technique in the structural study of A-type granites	155
<b>6. Conclusions</b>	156
<b>Acknowledgments</b>	156

<b>References</b>	.....	157
<b>6 - DISCUSSÕES E CONCLUSÕES FINAIS</b>	.....	<b>167</b>

## LISTA DE ILUSTRAÇÕES

### FIGURAS

#### **1 – Introdução**

Figura 1 - Mapa de localização da região onde se situam os corpos estudados.	7
Figura 2 - Províncias geocronológicas do Cráton Amazônico.	10
Figura 3 - Mapa geológico do Terreno Granito- <i>Greenstone</i> de Rio Maria.	12

#### **2 - Geochemistry And Magmatic Evolution Of The Paleoproterozoic, Anorogenic A-Type Redenção Granite Of The Jamon Suite, Eastern Amazonian Craton, Brazil**

Figure 1 - Sketch map of the Amazonian craton and Geological map of the RMGGT.	32
Figure 2 - Detailed geological map of the Redenção region	34
Figure 3 - QAP and Q-(A+P)-M diagrams	37
Figure 4 - Redenção pluton showing the areal distribution of dominant facies	38
Figure 5 - Textural aspects of the Redenção pluton	40
Figure 6 - Sequence of crystallization	42
Figure 7 - Whole-rock geochemical plots for the Redenção plúton.	47
Figure 8 - Harker-variation diagrams of major element compositions (wt%).	48
Figure 9 - Trace element variation diagrams for Redenção Granite samples.	50
Figure 10 - (a) Rb vs. Sr, (b) Sr vs. Ba, (c) Rb/Sr vs. Sr/Ba plots.	52
Figure 11 - Chondrite normalized (Evensen et al., 1978) REE patterns.	54
Figure 12 - Geochemical plots for the Redenção granite samples.	57
Figure 13 - Whole-rock diagrams comparing the composition of the Redenção pluton with oxidized and reduced A-type and calc-alkaline granites.	58

#### **3 - Oxidized, Magnetite-Series, Rapakivi-Type Granites Of Carajás, Brazil: Implications For Classification And Petrogenesis Of A-Type Granites**

Figure 1 - Location of the studied area and geological map of the Carajás Province.	71
Figure 2 - Diagrams showing composition of A-type granites compared with calc-alkaline granites.	78
Figure 3 - Composition of oxidized and reduced A-type compared with calc-alkaline granites.	79
Figure 4 - Composition of oxidized and reduced A-type compared with calc-alkaline granites.	82
Figure 5 - Compositional fields of calc-alkaline and A-type granites and reduced and oxidized A-type granites and calc-alkaline granites.	83

#### **4 - Gravimetric, radiometric, and magnetic susceptibility study of the Paleoproterozoic Redenção and Bannach plutons: implications for architecture and zoning of A-type granites**

Figure 1 - Sketch map of the Amazonian craton and Geological map of the RMGGT.	93
Figure 2 - Geological map of the Redenção and Bannach plutons.	96
Figure 3 - Geological map of the Redenção pluton with areal distribution of granitic facies.	98
Figure 4 - Geological map of the Bannach pluton with areal distribution of granitic facies.	99
Figure 5 - Variation of bulk magnetic susceptibility values in the Redenção and Bannach plutons.	101
Figure 6 - SRTM /Gamma thorium integrated product.	103
Figure 7 - Outline of a 2D gravity source.	107
Figure 8 – Bouguer anomaly, gravity inversion profiles, and contour map of the Redenção pluton.	108
Figure 9 – Bouguer anomaly, gravity inversion profiles, and contour map of the Bannach pluton.	110
Figure 10 - Three-dimensional geometry of the Redenção and Bannach plutons.	112
Figure 11 - Diagram length/width ( $L/W$ ) as a function of the ratio width/thickness ( $W/T$ ).	113

#### **5 - Anisotropy of Magnetic Susceptibility of the Redenção Granite, Eastern Amazonian Craton: Implications for the Emplacement of a Paleoproterozoic Anorogenic A-type Pluton**

Figure 1 - Sketch map of the Amazonian craton and Geological map of the RMGGT.	131
Figure 2 - Geological map of the Redenção region and distribution of granitic facies.	133
Figure 3 - Perspective views of the three-dimensional geometry of the Redenção plúton.	135
Figure 4 - Frequency histogram showing the variation of bulk magnetic susceptibility values.	137
Figure 5 - Relationships between magnetic susceptibility and modal compositions.	138
Figure 6 - Sample sites in the Redenção Pluton, variation of bulk magnetic susceptibility, magnetic fabric intensity, and magnetic susceptibility shape factor.	143
Figure 7 – Variation between fabric intensity, magnetic susceptibility, and AMS ellipsoid shape.	144
Figure 8 - Principal AMS axes angular departure.	144
Figure 9 - AMS directional data types.	145
Figure 10 – AMS directional data: magnetic foliations.	146
Figure 11 - AMS directional data: magnetic lineations.	147
Figure 12 - . Magnetic fabric trajectories.	148
Figure 13 - Model for the generation of the Paleoproterozoic bimodal magmatism in the RMGGT.	150
Figure 14 - Proposed emplacement model for the Redenção granite.	154

#### **TABELAS**

##### **1 – Introdução**

Tabela 1 – Dados geocronológicos das rochas arqueanas do TGGRM.	13
---	----

Tabela 2 – Dados geocronológicos dos granitos proterozóicos da Província de Carajás.	15
<b>2 - Geochemistry And Magmatic Evolution Of The Paleoproterozoic, Anorogenic A-Type Redenção Granite Of The Jamon Suite, Eastern Amazonian Craton, Brazil</b>	
Table 1 – Modal Compositions of the Redenção Granite.	36
Table 2 – Geochemical composition.	44
<b>3 - Oxidized, Magnetite-Series, Rapakivi-Type Granites Of Carajás, Brazil: Implications For Classification And Petrogenesis Of A-Type Granites</b>	
Table 1 - Modal compositions of the A-type granites of the Jamon Suite.	72
Table 2 - Chemical compositions of the Jamon Suite.	74
<b>4 - Gravimetric, radiometric, and magnetic susceptibility study of the Paleoproterozoic Redenção and Bannach plutons: implications for architecture and zoning of A-type granites</b>	
Table 1 - Mean density values of the Redenção and Bannach granites and country rocks.	106
<b>5 - Anisotropy of Magnetic Susceptibility of the Redenção Granite, Eastern Amazonian Craton: Implications for the Emplacement of a Paleoproterozoic Anorogenic A-type Pluton</b>	
Table 1 – Parameters of AMS for individual sample sites.	139

## RESUMO

A Suite Jamon de 1.88 Ga e diques associados são intrusivos em granitóides arqueanos (2.97-2.86 Ga) do Terreno Granito-Greenstone de Rio Maria a sul da Serra dos Carajás, no SE do Craton Amazônico. Aspectos petrográficos e geoquímicos associados a estudos de susceptibilidade magnética e aerogeofísica mostraram que os plútuns da Suíte Jamon são normalmente zonados. Relações de magma *mingling* indicam injeções múltiplas de magma na construção dos plutons. Eles foram formados, em geral, por dois pulsos magmáticos: (1) um primeiro pulso magmático foi fracionado *in situ* após a colocação em níveis crustais rasos gerando uma série de monzogranitos equigranulares grossos com proporções variáveis de biotita e hornblenda; (2) um segundo pulso, ligeiramente mais jovem, localizado nas porções centrais dos plutons, é composto de um magma mais evoluído de onde leucogranitos equigranulares derivaram. Intrusões anelares são identificadas no plúton Redenção. O zoneamento magmático é marcado por um decréscimo do conteúdo modal de minerais máficos, das razões plagioclásio/K-feldspato e anfibólito/biotita e do conteúdo de anortita do plagioclásio. O conteúdo de TiO<sub>2</sub>, MgO, FeOt, CaO, P2O5, Ba, Sr e Zr diminuem e os de SiO<sub>2</sub>, K<sub>2</sub>O e Rb aumentam na mesma direção. A diferenciação magmática foi controlada pelo fracionamento das fases minerais cristalizadas precocemente, incluindo anfibólito ± clinopiroxênio, andesina-oligoclásio cálcico, ilmenita, magnetita, apatita e zircão. A Suíte Jamon é subalcalina, metaluminosa a peraluminosa e possui assinatura geoquímica de granitos intraplaca do tipo-A. A ocorrência de magnetita e titanita, bem como os altos valores de susceptibilidade magnética demonstra que os granitos da Suíte Jamon foram formados em condições oxidantes. Granitos tipo-A oxidados possuem altas razões de FeOt/(FeOt+MgO), TiO<sub>2</sub>/MgO e K<sub>2</sub>O/Na<sub>2</sub>O e baixos valores de CaO e Al<sub>2</sub>O<sub>3</sub> comparado aos granitos cálcio-alcalinos. Porém, o caráter oxidado da Suíte Jamon são similares aos granitos mesoproterozóicos do tipo-A da série magnetita do SW da América do Norte e difere dos granitos rapakivi reduzidos do Escudo da Fennoscandia e das suítes Serra dos Carajás e Velho Guilherme da Província Mineral de Carajás em vários aspectos, provavelmente pela diferença de fontes magmáticas. A Suíte Jamon cristalizou próximo ou levemente acima do tampão óxido níquel-níquel (NNO) e uma fonte biotite-honblende quartzo-diorítica sanukitoid arquena foi proposta para os magmas oxizados da Suíte Jamon.

O estudo gravimétrico indica que os plútuns Redenção e Bannach são intrusões tabulares com ~ 6.0 km e ~2.2 km de espessura máxima, respectivamente. Estes plútuns possuem

dimensões lacolíticas e são similares neste aspecto aos clássicos plútuns graníticos rapakivi. Os dados gravimétricos sugerem que o crescimento da parte norte do pluton Bannach resultou da amalgamação de plútuns tabulares menores intrusivos em seqüência de noroeste a sudeste. Os plútuns da Suíte Jamon foram colocados em um ambiente tectônico extensional com o esforço seguindo o trend NNE-SSW to ENE-WSW, como indicado pela ocorrência de enxames de diques de diabásio e granito pórfiro, de orientação WNW-ESE a NNW-SSE e coexistentes com a Suíte Jamon. Os plútuns graníticos paleoproterozóicos e stocks de Carajás estão dispostos ao longo de um cinturão que segue o *trend* geral definido pelos diques. A geometria tabular dos batólitos estudados e o alto contraste de viscosidade entre os granitos e suas rochas encaixantes arquenás pode ser explicado pelo transporte de magma via diques.

Os mecanismos responsáveis pela colocação dos plútuns graníticos, em particular de plútuns anorogênicos do tipo-A, são ainda discutidos. Desse modo, estudo da trama magnética através de medidas de anisotropia de susceptibilidade magnética (ASM) tem sido aplicado no plúton Redenção na tentativa de compreender a sua história de colocação. Os altos valores de suscetibilidade magnética ( $1 \times 10^{-3}$  SI to  $54 \times 10^{-3}$  SI) indicam que a trama magnética é controlada principalmente pelos minerais ferromagnéticos. Os baixos valores do grau de anisotropia ( $P'$ ) e os aspectos texturais (ausência de feições deformacionais) indicam que a trama magnética é de origem magmática. A trama magnética é bem definida e caracterizada por uma foliação concêntrica de alto ângulo associada com linhas com mergulho moderado a fraco. A falta de uma trama linear unidirecional bem definida na escala do plúton sugere uma influência reduzida ou nula dos esforços (stresses) regionais durante a colocação do corpo granítico. A forma tabular e a ocorrência de foliações magnéticas de alto ângulo são interpretadas principalmente como resultado de: (1) ascensão vertical de magmas através de diques alimentadores noroeste-sudeste e acomodação pela translação ao longo dos planos da foliação regional E-W; (2) mudança do fluxo vertical para um espalhamento lateral do magma, com subsidência do assoalho criando espaço para injeção de pulsos magmáticos sucessivos; (3) expansão *in situ* da câmara magmática em resposta às intrusões mais tardias na porção central, acompanhada pela injeção do magma residual através de fraturas anelares.

## ABSTRACT

The 1.88 Ga, anorogenic, A-type Jamon suite and associated dikes intruded 2.97 – 2.86 Ga-old Archean granitoids of the Rio Maria Granite-Greenstone Terrane which lies to the south of Serra dos Carajás, in the southeastern domain of the Amazon Craton, northern Brazil. Petrographic and geochemical aspects associated with magnetic susceptibility and gamma-ray spectrometry data showed that the Redenção and the northern part of Bannach plutons are normally zoned, with mingling relationships that indicate multiple magma injections in their construction. Both were formed by two magmatic pulses: (1) a first magma pulse which fractionated in situ after shallow crustal emplacement and generated a series of coarse, even-grained monzogranites with variable modal proportions of biotite and hornblende; (2) a second, slightly younger magma pulse, localised in the center of both plutons, and composed of a more evolved liquid from which even-grained leucogranites were derived. Seriated and porphyritic biotite monzogranite facies intruded the coarse (hornblende)-biotite monzogranites and formed anellar structures within the Redenção pluton. The magmatic zoning is marked by a systematic decrease in mafic mineral modal content, plagioclase/potassium feldspar and amphibole/biotite ratios, and anorthite content of plagioclase.  $TiO_2$ ,  $MgO$ ,  $FeO_t$ ,  $CaO$ ,  $P_2O_5$ ,  $Ba$ ,  $Sr$ , and  $Zr$  decreased, and  $SiO_2$ ,  $K_2O$ , and  $Rb$  increased in the same fashion. Magmatic differentiation was controlled by fractionation of early crystallized phases, including amphibole $\pm$ clinopyroxene, andesine to calcic oligoclase, ilmenite, magnetite, apatite, and zircon. The Jamon suite is subalkaline, metaluminous to mildly peraluminous, ferroan alkali-calcic, and displays geochemical affinities with within-plate A-type granites. The ubiquitous occurrence of magnetite and titanite as well as high magnetic susceptibility values demonstrate that granites of the Jamon suite are oxidized in character. Oxidized A-type granites have high  $FeOt/(FeOt+MgO)$ ,  $TiO_2/MgO$ , and  $K_2O/Na_2O$  ratios and low  $CaO$  and  $Al_2O_3$  compared to calc-alkaline granites. The oxidized character of the Jamon suite makes it more akin to the USA Mesoproterozoic magnetite-series A-type granites but differs from the reduced rapakivi granites of the Fennoscandian Shield, and Serra dos Carajás and Velho Guilherme suites of the Carajás province, probably because of different magmatic sources. The Jamon suite probably crystallized near or slightly above the nickel-nickel oxide (NNO) buffer and an Archean sanukitoid biotite-hornblende quartz diorite source was proposed for the oxidized Jamon magmas.

Gravity modelling indicates that the Redenção and Bannach plutons are sheeted-like composite laccolithic intrusions, ~6 km and ~2 km thick, respectively. These plutons follow the general power law for laccolith dimensions and are similar in this respect to classical rapakivi granite plutons. Gravity data suggest that the growth of the northern part of the Bannach pluton was the result of the amalgamation of smaller sheeted-like plutons which successively intruded in sequence from northwest to southeast. Jamon suite plutons were emplaced in an extensional tectonic setting with the principal stress oriented approximately along NNE-SSW to ENE-WSW, as indicated by the occurrence of diabase and granite porphyry dike swarms, orientated WNW-ESE to NNW-SSE and coeval with the Jamon suite. The 1.88 Ga A-type granite plutons and stocks of Carajás are disposed along a belt defined by the general trend of the dike swarms. The inferred tabular geometry of the studied plutons can be explained by magma transport via dikes and it is supported the high contrast of viscosity between the granites and their Archean country rocks.

Mechanisms responsible for emplacement of granitic plutons, and in particular of anorogenic A-type plutons, are still debated. A magnetic fabric study derived from anisotropy of magnetic susceptibility (AMS) measurements was applied to the Redenção pluton in order to understand its emplacement history. High magnetic susceptibilities ( $K$  from  $1 \times 10^{-3}$  SI to  $54 \times 10^{-3}$  SI) indicated that magnetic fabrics are primarily carried by ferromagnetic minerals (magnetite). Low  $P'$  values and absence of intracrystalline deformation features indicated that the magnetic fabric is of magmatic origin. The magnetic fabric is well organized and characterized by concentric steep foliations associated with moderately to gently plunging lineations. The lack of a well-defined unidirectional linear fabric at pluton scale suggests the reduced or null influence of regional stresses during granite emplacement. Three stages are proposed for construction of the Redenção pluton, which reconcile the tabular shape of the intrusion with the occurrence of steep magnetic foliations: (1) ascent of magmas in vertical, northwest-striking feeder dikes and accommodation by translation along east-west-striking regional foliation planes; (2) switch from upward flow to lateral spread of magma with space for injection of successive magma pulses created by floor subsidence; and (3) in situ inflation of the magma chamber in response to the central intrusion of late facies, accompanied by evacuation of resident magmas through ring fractures.

# CAPÍTULO - 1

## *INTRODUÇÃO*

## INTRODUÇÃO

### 1.1 – APRESENTAÇÃO E LOCALIZAÇÃO DA ÁREA

A Província Mineral de Carajás (PMC), de idade arqueana, é caracterizada pela sua grande variedade de recursos minerais, destacando-se os depósitos de ferro, ouro, manganês, níquel e cobre (DOCEGEO 1988). O conhecimento sobre a geologia da PMC deve-se em grande parte a trabalhos de mapeamento geológico e prospecção executados pelas equipes da DOCEGEO e CPRM. O Grupo de Pesquisa Petrologia de Granitóides (GPPG) e o Laboratório de Geologia Isotópica do Centro de Geociências - UFPA destacaram-se nos últimos anos pelos trabalhos de detalhe na região, em particular sobre as rochas granitóides.

O GPPG tem concentrado suas atividades na porção sul da Amazônia Oriental, visando o estudo da evolução das rochas granitóides, bem como sua caracterização petrológica e geoquímica. Paralelamente, o grupo tem desenvolvido o estudo sistemático de suscetibilidade magnética e dos minerais óxidos de Fe e Ti, através da linha de pesquisa Petrologia Magnética e suas aplicações práticas e teóricas, registradas em vários trabalhos (Dall'Agnol et al. 1988, Magalhães 1991, Magalhães & Dall'Agnol 1992, Magalhães et al. 1994, Oliveira 1998, Figueiredo 1999, Oliveira 2001, Oliveira et al. 2002, Figueiredo et al. 2003, Nascimento 2006). Os granitos anorogênicos presentes na província de Carajás têm sido sistematicamente estudados pelo GPPG. Um conhecimento expressivo foi acumulado sobre maciços que constituem as suítes Jamon (granitos Jamon, Musa e Redenção), Serra dos Carajás (granitos Central, Cigano e Pojuca), Velho Guilherme (granitos Antônio Vicente e Velho Guilherme), entre outros. Outros maciços foram até então estudados de maneira menos detalhada. Entre eles inclui-se o batólito granítico Bannach, situado junto à cidade homônima no sul da província, que foi estudado de maneira mais detalhada durante a realização deste trabalho, por meio do desenvolvimento da dissertação de mestrado de José de Arimatéia Costa de Almeida (Almeida 2005) e o plutônio Marajoara, um pequeno *stock* situado entre Rio Maria e Redenção, cujo estudo foi desenvolvido vinculado ao Trabalho de Conclusão de Curso de Gerson Luiz Dias da Rocha Jr (Rocha Jr. 2004). Vários desses granitos foram datados e forneceram idades próximas de 1,88 Ga (Macambira & Lafon 1995).

Com o objetivo de contribuir para o avanço do conhecimento da Suíte Jamon, a partir de um estudo integrado dos principais maciços graníticos, foi realizada esta pesquisa no nível de doutorado, iniciada em Dezembro de 2001 e vinculada ao programa de Pós-Graduação em

Geologia e Geoquímica da Universidade Federal do Pará. A área selecionada para pesquisa está situada no Terreno Granito-*Greenstone* de Rio Maria, estendendo-se entre as cidades de Rio Maria e Redenção, e prolongando-se para oeste até os domínios do município de Bannach (Figura 1).

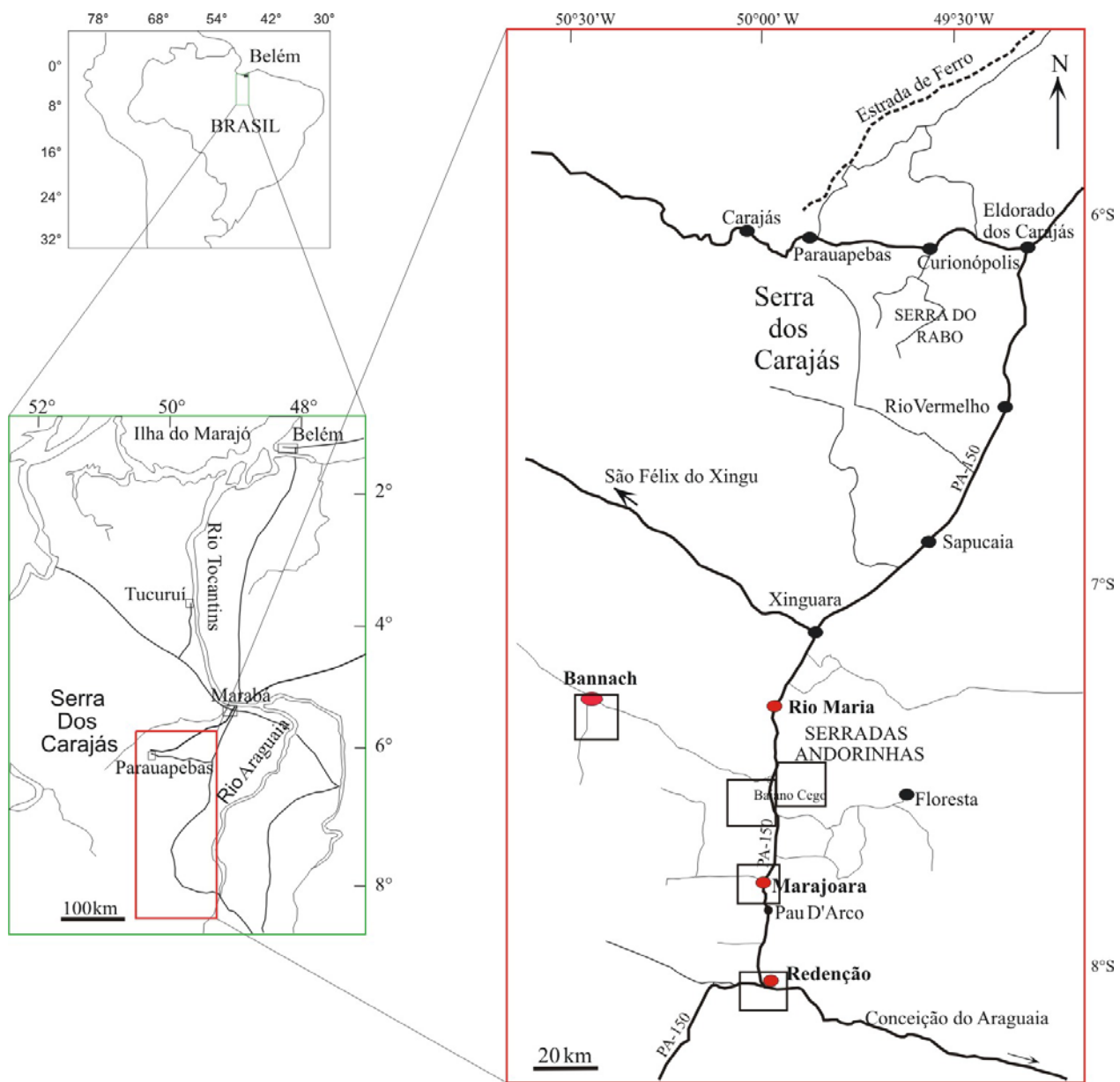


**Figura 1** - Mapa de localização da região de ocorrência dos principais corpos graníticos da Suíte Jamon. os retângulos assinalam as áreas onde se situam os corpos estudados.

A presente tese de doutorado, intitulada “**Modelos de Evolução e Colocação dos Granitos Paleoproterozóicos da Suíte Jamon, SE do Cráton Amazônico**”, foi estruturada na forma de integração de artigos científicos de acordo com as normas gerais definidas pela Comissão da Pós-Graduação em Geologia e Geoquímica da Universidade Federal do Pará. Este trabalho inclui um capítulo introdutório, onde é abordado o contexto geológico regional, destacando-se os principais aspectos geológicos e geocronológicos da Província Mineral de Carajás e a caracterização do magmatismo anorogênico paleoproterozóico. Em seguida são definidos os principais problemas geológicos que motivaram esta proposta de trabalho, a partir dos quais foram definidos os objetivos da pesquisa. As atividades e procedimentos metodológicos que viabilizaram alcançar os objetivos propostos serão descritos e discutidos nos capítulos subseqüentes. Os resultados alcançados neste trabalho são apresentados e discutidos na forma de quatro artigos científicos (Capítulos 2, 3, 4 e 5), e abordados de forma integrada no capítulo final (Capítulo 6).

**Capítulo 2 - Artigo 1 - GEOCHEMISTRY AND MAGMATIC EVOLUTION OF THE PALEOPROTEROZOIC, ANOROGENIC A-TYPE REDENÇÃO GRANITE OF THE JAMON SUITE, EASTERN AMAZONIAN CRATON, BRAZIL.** Submetido à revista *CANADIAN MINERALOGIST*. Apresenta os dados de campo, petrográficos e geoquímicos, bem como discute as relações entre as variedades faciológicas e os processos envolvidos na evolução magmática do Granito Redenção. Os dados geoquímicos também foram utilizados para discutir a tipologia e estabelecer o caráter oxidado do Granito Redenção e compará-lo com outros granitos tipo-A de caráter redutor.

**Capítulo 3 - Artigo 2 - OXIDIZED, MAGNETITE-SERIES, RAPAKIVI-TYPE GRANITES OF CARAJÁS, BRAZIL: IMPLICATIONS FOR CLASSIFICATION AND PETROGENESIS OF A-TYPE GRANITES.** Aceito para publicação na revista *LITHOS*. Apresenta as características geoquímicas e petrogenéticas que podem ser usadas para distinguir granitos tipo-A oxidados da série magnetita de outros grupos de granitos tipo-A e daqueles da série de granitóides cálcico-alcalinos. Para isto, os granitos tipo-A da Província Carajás são comparados com granitos tipo-A do Escudo Fennoscandiano (granitos rapakivi), do Cráton Norte-Americano, do Lachlan Fold Belt e com granitos cálcico-alcalinos tipo-I.

**Capítulo 4 - Artigo 3 - GRAVIMETRIC, RADIOMETRIC, AND MAGNETIC SUSCEPTIBILITY STUDY OF THE PALEOPROTEROZOIC REDENÇÃO AND BANNACH PLUTONS: IMPLICATIONS FOR ARCHITECTURE AND ZONING OF A-TYPE GRANITES.** Submetido para publicação ao *JOURNAL SOUTH OF AMERICAN EARTH SCIENCES*. Discute com base em dados geofísicos e no zoneamento interno dos granitos paleoproterozóicos Redenção e Bannach, a forma tridimensional e processos envolutivos das intrusões, assim como o ambiente tectônico responsável pela colocação dos corpos da Suíte Jamon.

**Capítulo 5 - Artigo 4 - ANISOTROPY OF MAGNETIC SUSCEPTIBILITY OF THE REDENÇÃO GRANITE, EASTERN AMAZONIAN CRATON: IMPLICATIONS FOR THE EMPLACEMENT OF A PALEOPROTEROZOIC ANOROGENIC A-TYPE PLUTON.** Submetido para publicação à revista *PRECAMBRIAN RESEARCH*. Discute os mecanismos de colocação envolvidos na construção do Granito Redenção com base em estudo de anisotropia de suscetibilidade magnética, aliado aos dados petrográficos, geoquímicos e gravimétricos.

## 1.2 – CONTEXTO GEOLÓGICO REGIONAL

A Suíte Jamon está localizada na Província Carajás, borda sudeste do Cráton Amazônico (Dall’Agnol et al. 2005). A Província Carajás faz parte da Província Amazônia Central (Tassinari & Macambira 2004; Figura 2) e é dominada por terrenos arqueanos intrudidos por granitos anorogênicos do Paleoproterozóico. Esta província é limitada a norte pela Província Maroni-Itacaiúnas (Figura 2) formada durante o Evento Trans-Amazônico (2.2-2.1 Ga); a leste, é bordejada pelo Cinturão Araguaia do Neoproterozóico, relacionado ao Ciclo Brasiliano (Pan-Africano), o qual não afetou significativamente o Cráton Amazônico; a oeste, é limitado por um terreno dominado por granitóides paleoproterozoicos e assembléias vulcânico-piroclásticas do Supergrupo Uatumã, com idades próximas de 1.88 Ga (Teixeira et al. 2002; Figura 2).

A Província Carajás é subdividida atualmente em dois domínios tectônicos arqueanos: o Terreno Granito-*Greenstone* de Rio Maria com idade de 3.0 – 2.86 Ga (Macambira & Lafon 1995, Dall’Agnol et al. 2006) e a Bacia tipo *rift* de Carajás composta predominantemente de rochas matavulcânicas, formações ferríferas bandadas e granitóides com idades de 2.76 – 2.55 Ga (Machado et al. 1991, Macambira & Lafon 1995, Barros et al. 2001). A Suíte Jamon é

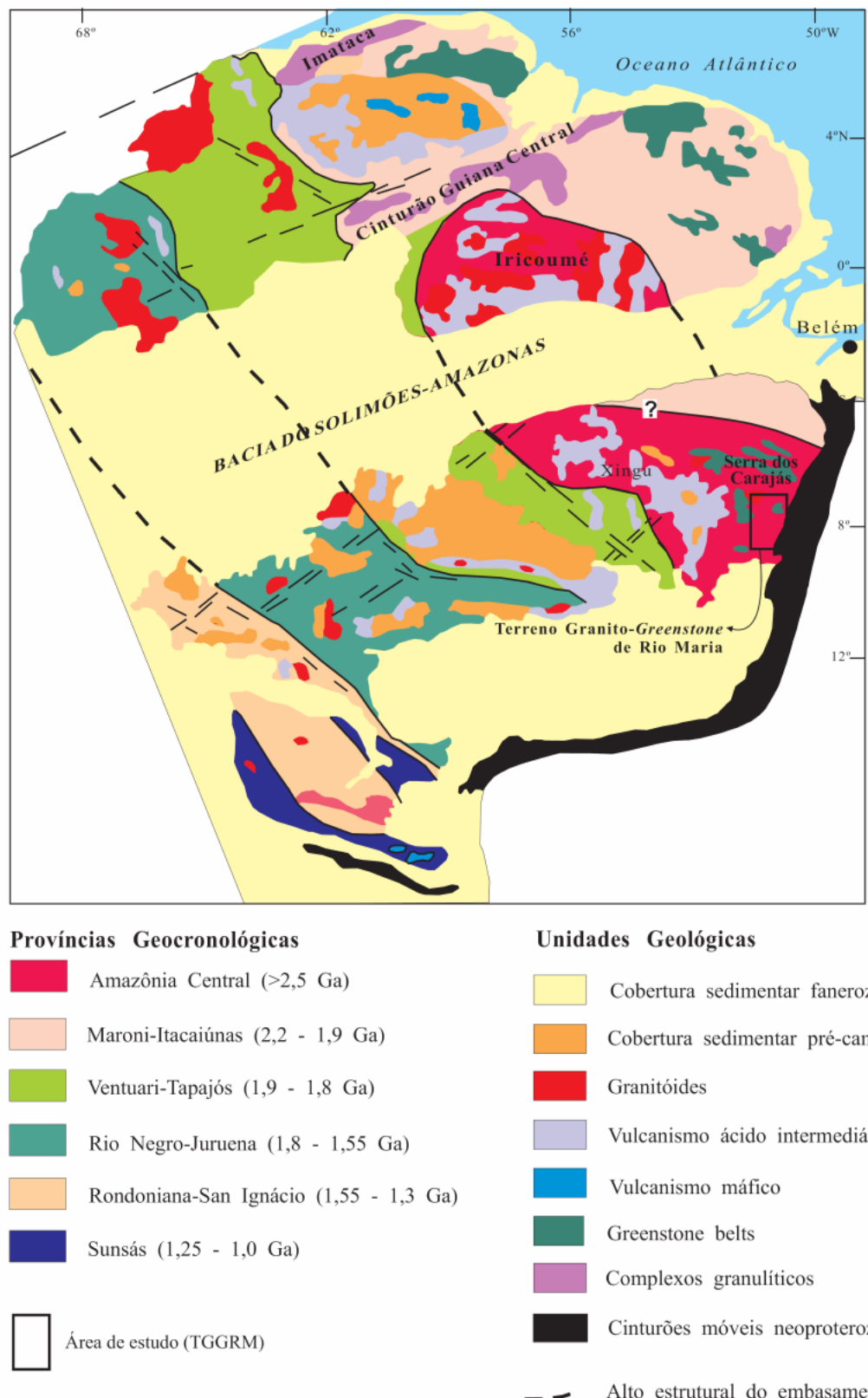


**Figura 2** - Províncias geocronológicas do Cráton Amazônico (Tassinari & Macambira 2004).

intrusiva em granitóides arqueanos e *greenstone belts* do Terreno Granito-Greenstone de Rio Maria, que corresponde à parte sul da Província Metalogenética de Carajás (Figura 3). Esta região corresponde a um terreno arqueano cortado por granitos anorogênicos paleoproterozóicos (Figura 3; Ramo et al. 2002, Dall'Agnol et al. 2005, 2006), onde predominam granitóides e supracrustais do tipo *greenstone belts* com idades U/Pb - Pb/Pb em cristais de zircão de 2.97 – 2.86 (Macambira & Lafon 1995, Macambira & Lancelot 1996, Leite et al. 2004, Dall'Agnol et al. 2006) cobertas por rochas sedimentares, mais jovens, porém ainda arqueanas, da Seqüência Rio Fresco. Os *greenstone belts* do Supergrupo Andorinhas são as rochas mais antigas da região e são compostos por komatiitos e basaltos toleíticos (Souza & Dall'Agnol 1995). Baseado em critérios petrográficos, geoquímicos e geocronológicos (Tabela 1), Macambira & Lafon (1995), Althoff et al. (2000), Leite et al. (2004), Dall'Agnol et al. (2006) e Oliveira et al. (Submetido a), dividiram os granitóides arqueanos da região de Rio Maria em quatro grupos principais: (1) Granitóides da série tonalítica -trondhjemítica-granodiorítica (tipo TTG) mais antiga (2.97 – 2.93 Ga; Tabela 1), sendo representada pelo Tonalito Arco Verde e Complexo Tonalítico Caracol; (2) Granitóides com alto-Mg, do tipo sanukítioide (2.87 Ga), representados pelo Granodiorito Rio Maria e rochas maficas e intermediárias associadas, os quais são intrusivos na seqüência *greenstone* e no Tonalito Arco Verde; (3) Série TTG mais jovem (~2.87 Ga), representada pelos trondhjemitos Mogno e Água Fria que exibem fortes similaridades petrográficas e geoquímicas com a Série TTG mais antiga, porém com idades não coincidentes (Tabela 1). As relações de campo mostram que o Trondhjemito Mogno secciona o Granodiorito Rio Maria; (4) Leucogranitos potássicos de afinidade cárlico-alcalina, representados pelos granitos Xingura, Mata Surrão, Guarantã e correlatos. O Granito Guarantã possui idade de cristalização em torno de 2,93 Ga (Althoff et al. 2000) diferenciando-se neste aspecto dos granitos Xinguara e Mata Surrão (Tabela 1), que apresentam idade de 2.86 Ga e são intrusivos no Tonalito Arco verde e Granodiorito Rio Maria. Na tabela 2 estão sintetizados os principais dados geocronológicos sobre as rochas arqueanas do Terreno Granito-Greenstone de Rio Maria. Corpos graníticos anorogênicos de idade paleoproterozóica (1,88 Ga; Machado et al. 1991; Barbosa et al. 1995; Dall'Agnol et al. 1999a), exemplificados principalmente pelos maciços Jamon, Musa, Redenção, Marajoara e Bannach, cortam as unidades arqueanas deste domínio e são enquadrados na Suíte Jamon (Gastal 1987, Dall'Agnol et al. 2005, Oliveira et al. 2005, Dall'Agnol et al. 2006, Almeida et al. submetido).

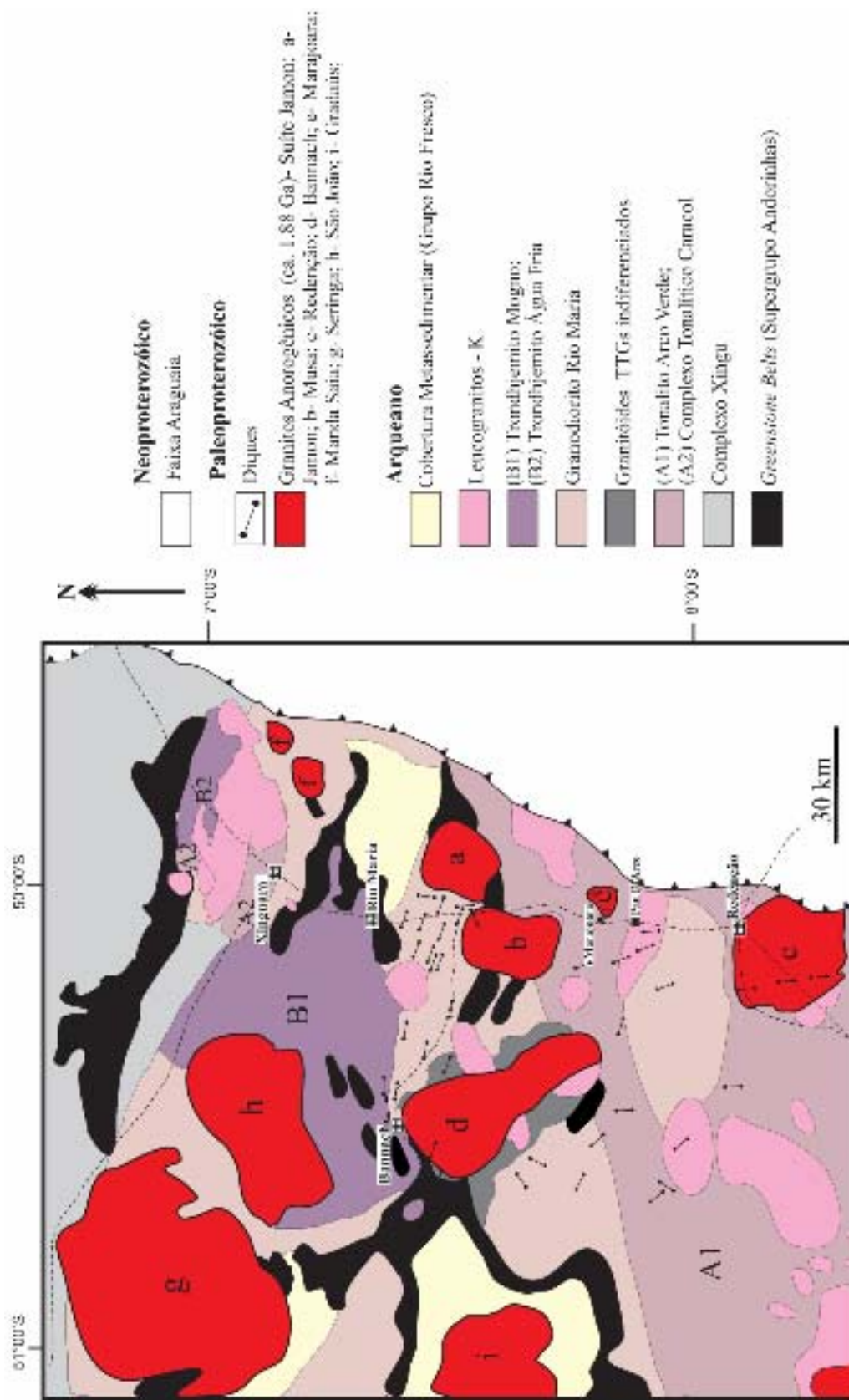


**Figura 3** - Mapa geológico do Terreno Granito-Greenstone de Rio Maria (Modificado de Almeida 2005).

**Tabela 1** – Dados geocronológicos das rochas arqueanas do Terreno Granito-Greenstone de Rio Maria.

Unidades Estatigráficas	Tipo de Rocha	Método	Material Analisado	Idade/Referência
<b>Leucogranitos</b>				
<b>Cálcico-Alcalinos</b>				
Granito Xinguara	Leucogranito	Pb-Pb	Zircão	$2865 \pm 1$ Ma (1)
	Leucogranito	Pb-Pb	Zircão	$2875 \pm 11$ Ma (2)
Granito Mata Surrão	Leucogranito (área tipo)	Pb-Pb	Rocha total	$2872 \pm 10$ Ma (3)
	Leucogranito (Marajoara)	Pb-Pb	Zircão	$2868 \pm 5$ Ma (4)
Granito Guarantã	Leucogranito	Pb-Pb	Zircão	2930 Ma (5)
<b>Granitoids Sanukítoides</b>				
Granodiorito Rio Maria e rochas associadas	Granodiorito	U-Pb	Zircão	$2874 + 9/-10$ Ma (6)
	Granodiorito	U-Pb	Zircão, Titanita	$2872 \pm 5$ Ma (7)
	Quartzo-diorito	Pb-Pb	Zircão	$2878 \pm 4$ Ma (8)
	Granodiorito	Pb-Pb	Zircão	$2879 \pm 4$ Ma (2)
				$2877 \pm 6$ Ma (9)
<b>Série TTG Jovem</b>				
Trondhjemito Mogno	Trondhjemito	U-Pb	Titanita	$2871 \pm ?$ Ma (7)
Trondhjemito Água Fria	Trondhjemito	Pb-Pb	Zircão	$2864 \pm 21$ Ma (1)
<b>Série TTG Antiga</b>				
Complexo Tonalítico Caracol	Tonalito	Pb-Pb	Zircão	$2948 \pm 5$ Ma (1)
	Tonalito	Pb-Pb	Zircão	$2936 \pm 3$ Ma (1)
	Tonalito	Pb-Pb	Zircão	$2942 \pm 2$ Ma (1)
Tonalito Arco Verde	Tonalito	U-Pb	Zircão	$2957 + 25/-21$ Ma (6)
	Tonalito	Pb-Pb	Zircão	$2948 \pm 7$ Ma (2)
	Tonalito	Pb-Pb	Zircão	$2981 \pm 8$ Ma (9)
				$2936 \pm 4$ Ma (4)
<b>Greenstone Belts</b>				
Supergrupo Andorinhas	Metagrauvaca	U-Pb	Zircão	$2971 \pm 18$ Ma (6)
	Metavulcânica Félsica	U-Pb	Zircão	$2904+29/-22$ Ma (6)
	Metavulcânica Félsica	U-Pb	Zircão	$2972 \pm 5$ Ma (7)

Fonte dos Dados: (1) Leite et al. (2004), (2) Rolando & Macambira (2002), (3) Lafon et al. (1994), (4) Dall'Agnol et al. (2005), (5) Althoff et al. (2000), (6) Macambira (1992), (7) Pimentel & Machado (1994), (8) Dall'Agnol et al. (1999a), (9) Rolando & Macambira (2003).

### 1.3 - MAGMATISMO ANOROGÉNICO DA PROVÍNCIA MINERAL DE CARAJÁS

Durante o Paleoproterozóico, tanto o Terreno Granito-*Greenstone* de Rio Maria como o Bloco Carajás foram palco de um magmatismo granítico anorogênico (Dall'Agnol et al. 2005, 2006) representado, entre outros, pelos granitos Jamon (Dall'Agnol 1999b, c), Musa (Gastal 1987, 1988), Marajoara (Rocha Jr. 2004), Bannach (Huhn et al. 1988, Duarte 1992, Almeida 2005, Almeida et al. submetido), Redenção (Montalvão et al. 1982, Vale & Neves 1994, Barbosa et al. 1995, Oliveira et al. 2002, 2005, Oliveira et al. Submetido b,c), Serra dos Carajás (Javier Rios et al. 1994a, b, Barros et al. 1995), Cigano (Gonçalez et al. 1988), Antônio Vicente e Velho Guilherme (Teixeira et al. 2002). Estes granitos anorogênicos, quando datados pelo método U/Pb e Pb/Pb em zircões e Pb/Pb em rocha total, forneceram idades de cristalização e colocação próximas de 1,88 Ga (Barbosa et al. 1995, Dall'Agnol et al. 1999a). Na tabela 2 estão sintetizados os principais dados geocronológicos sobre os granitos proterozóicos da Província Metalogenética de Carajás. São granitos não foliados, de alto nível crustal, os quais são colocados em uma crosta rígida e cortam discordantemente suas rochas encaixantes. Nas zonas de contato, xenólitos das rochas encaixantes são comumente encontrados nestes granitos e efeitos termais nas rochas adjacentes alcançam metamorfismo de contato na fácie hornblenda hornfels (Soares 1996, Dall'Agnol et al. 2006). Diques félscos a máficos, de modo geral contemporâneos dos granitos, ocorrem sob forma de corpos subverticais, tabulares, com espessuras de até 10 a 20 metros, cortando as unidades arqueanas, bem como localmente os granitos proterozóicos (Gastal 1987, Huhn et al. 1988, Rivalenti et al. 1998, Souza et al. 1990, Silva Jr. et al. 1999).

Os granitos anorogênicos da Província Mineral de Carajás possuem característica metaluminosa a peraluminosa e assinatura tipo-A. Entretanto, mostram diferenças significativas em termos de geoquímica, suscetibilidade magnética (SM) e mineralizações associadas. Com base nestes critérios, três suítes ou grupos de granitos puderam ser distinguidos (Dall'Agnol et al. 2005): 1 – Suíte Jamon formada por granitos da série magnetita que possuem alta razão Fe/(Fe+Mg), alto valor de SM e localmente, mineralizações de wolframita associada; é representada pelos plútôns Jamon, Musa, Redenção, Marajoara, Banach e Manda Saia (Figura 3); 2 – Suíte Serra dos Carajás, formada por granitos com moderada SM, com razão Fe/(Fe+Mg) muito alta e, às vezes, com molibdenita e sulfeto de cobre disseminados (maciços Serra dos Carajás, Cigano e Pojuca); 3 – Suíte Velho Guilherme, formada por maciços mineralizados a estanho, dominados por leucogranitos extremamente evoluídos, também com alta razão

Fe/(Fe+Mg) e, geralmente, mostrando baixos valores de SM; exemplificados pelos maciços Xingu, Mocambo, Ubim, Antônio Vicente e Velho Guilherme. Os magmas graníticos anorogênicos são provavelmente derivados de fusão parcial de rochas da crosta inferior (Dall'Agnol et al. 1994, Dall'Agnol & Magalhães 1995, Dall'Agnol et al. 1999b,c, 2005, Dall'Agnol & Oliveira 2006). Contrastos na natureza das fontes, bem como na temperatura de fusão, conteúdo de água e fugacidade de oxigênio dos magmas (Scaillet et al. 1995, Dall'Agnol & Oliveira 2006), podem explicar as diferenças observadas entre os grupos de granito distinguidos. Os granitos anorogênicos e rochas afins do Cráton Amazônico são atualmente correlacionados com os granitos rapakivi dos escudos da Fennoscandia e da América do Norte (Bettencourt et al 1995, Rämö & Happala 1995, Dall'Agnol et al. 1999a, Dall'Agnol & Oliveira 2006).

**Tabela 2** – Dados geocronológicos dos granitos proterozóicos da Província Metalogenética de Carajás.

Unidade Estratigráfica	Método	Material Analisado	Idade/Referência
<b>Bloco Carajás</b>			
<b>Suíte Serra dos Carajás</b>			
Granito Cigano	U-Pb	Zircão	1883 ± 2 Ma (1)
Granito Serra dos Carajás	U-Pb	Zircão	1880 ± 2 Ma (1)
Granito Pojuca	U-Pb	Zircão	1874 ± 2 Ma (1)
<b>Terreno Granito-Greenstone de Rio Maria</b>			
<b>Suíte Jamon</b>			
Granito Musa	U-Pb	Zircão	1883 +5/-2 Ma (1)
Granito Jamon	Pb-Pb	Zircão	1885 ± 32 Ma (2)
Granito Redenção	Pb-Pb	Rocha Total	1870 ± 68 Ma (3)
Granito Seringa	Pb-Pb	Zircão	1892 ± 30 Ma (4)
Granito Marajoara	Rb-Sr	Rocha Total	1724 ± 50 Ma (6)
<b>Região Xingu</b>			
<b>Suíte Velho Guilherme</b>			
Granito Velho Guilherme	Pb-Pb	Rocha Total	1873 ± 13 Ma (5)
Granito Antônio Vicente	Pb-Pb	Zircão	1867 ± 4 Ma (7)
Granito Mocambo	Pb-Pb	Zircão	1865±2 (7)
Rio Xingu	Pb-Pb	Zircão	1866±3 (7)

*Fonte dos Dados:* (1) – Machado et al. (1991); (2) – Dall’Agnol et al. (1999b); (3) - Barbosa et al. (1995); (4) - Avelar (1996); (5) - Rodrigues et al. (1992); (6) - Macambira (1992); (7) - Teixeira (1999).

#### 1.4 - APRESENTAÇÃO DO PROBLEMA E JUSTIFICATIVA

O magmatismo anorogênico proterozóico do Cráton Amazônico é um dos mais expressivos do mundo. Ele encerra um grande volume de rochas granítóides e vulcânicas maficas, intermediárias e félsicas, com subordinadas variedades plutônicas maficas (Issler & Lima 1987, Bettencourt et al. 1999, Dall'Agnol et al. 1999b, Dall'Agnol et al. 2005, 2006). Esse magmatismo se assemelha, em idades, características geoquímicas e evolução magmática, àqueles que ocorrem na Província Proterozóica Norte Americana e no Escudo Fennoscandiano (Anderson & Bender 1989, Haapala & Rämö 1990, Emslie 1991, Rämö & Haapala 1995).

O estágio atual de conhecimento sobre corpos graníticos anorogênicos paleoproterozóicos do Cráton Amazônico deve-se, em grande parte, a estudos realizados em maciços que constituem a Suíte Jamon, em especial aos maciços Jamon, Musa e Redenção, principalmente no que diz respeito ao mapeamento geológico, estudos petrográficos, geoquímicos, geocronológicos, petrologia magnética e isótopos de Nd, Sr e Pb. Entretanto, o grande número de informações obtidas sobre os batólitos Redenção (Oliveira 2001, Oliveira et al. 2002, Oliveira et al., 2005), principalmente quanto ao zoneamento e diferenciação do corpo, demonstrou a necessidade de reavaliar as interpretações anteriores sobre a evolução magmática da Suíte Jamonos, baseado sobretudo nos dados existentes sobre os maciços Jamon e Musa. Além disso, paralelamente a este trabalho foram realizados estudos em detalhe em corpos ainda pobemente estudados (granitos Bannach e Marajoara). A caracterização faciológica, geoquímica e de petrologia magnética do Granito Bannach foram realizados durante o desenvolvimento da dissertação de mestrado de José de Arimatéia Costa de Almeida (Almeida 2005, Almeida et al. submetido) e o mapeamento das fácies e estudo petrográfico do Granito Marajoara foram efetuados durante o Trabalho de Conclusão de Curso de Gerson Luiz Dias da Rocha Jr. (Rocha Jr. 2004). Contudo, tais maciços carecem ainda de estudos detalhados para a resolução de uma série de problemas e questões, ligados, sobretudo, a processos de geração, evolução, interação e colocação dos líquidos. Para isso é necessário levar em consideração: a) relação de diques maficos e intermediários com o magma granítico; b) presença ou não de magmatismo bimodal; c) processos de *mixing* ou *mingling*; d) interação entre magmas félsicos; e) processos magmáticos envolvidos na diferenciação e colocação das fácies dos corpos da suíte.

Além do aspecto acima, uma das principais questões ainda não esclarecidas em termos da evolução dos granitos anorogênicos da Província Carajás diz respeito aos mecanismos de sua colocação e arquitetura dos corpos. Procurou-se responder a estas questões no presente trabalho, em termos da Suíte Jamon, a partir de levantamentos geofísicos efetuados nos batólitos Redenção e Bannach, aliados a estudos de anisotropia de suscetibilidade magnética (ASM) realizados no primeiro. A introdução de métodos geofísicos no estudo da arquitetura e colocação dos granitos anorogênicos representa um aspecto inovador, capaz de permitir um salto qualitativo no conhecimento pois tais métodos ainda não haviam sido empregados no estudo de granitos paleoproterozóicos. Da mesma forma, os métodos de ASM revelaram-se uma ferramenta de grande valia, pois permitiram a determinação de feições estruturais (foliação e lineação magnéticas), no plúton Redenção, um granito anorogênico, isotrópico, em que as feições deformacionais clássicas como foliações e lineações são pouco desenvolvidas ou ausentes.

A pesquisa desenvolvida visou aprofundar a caracterização da Suíte Jamon, aprimorando o conhecimento de determinados aspectos da sua evolução não aprofundados em trabalhos anteriores. Estima-se que o preenchimento dessas lacunas represente uma contribuição importante para a compreensão deste tipo de magmatismo, não só na Província Mineral de Carajás e no Cráton Amazônico, mas também a nível internacional.

## 1.5 – OBJETIVOS

O objetivo principal deste trabalho é ampliar e integrar os dados sobre os granitos paleoproterozóicos da Suíte Jamon, avaliar a forma tridimensional e condições de colocação e reavaliar os processos magmáticos responsáveis pela distribuição das fácies e zoneamento dos corpos. Deste modo, os estudos realizados durante o desenvolvimento da tese visaram aos seguintes objetivos:

1- Mapeamento geológico do corpo Bannach na escala 1:100.000, definindo suas relações de contato, e levando à identificação de suas fácies e da distribuição espacial de cada uma delas (tema da dissertação de J. A. C Almeida, desenvolvida em colaboração com a presente tese).

2– Reavaliar os dados geológicos, petrográficos e geoquímicos disponíveis sobre o plúton Redenção, efetuar a sua caracterização geoquímica e propor um modelo para explicar a sua evolução magmática;

3- Propor modelos sobre a forma tridimensional dos corpos Redenção e Bannach e definir a natureza de seus contatos, bem como estimar as condições de colocação dos magmas graníticos com base em relações de campo, dados de anisotropia de suscetibilidade magnética (corpo Redenção), distribuição espacial e características petrográficas e geoquímicas das diferentes fácies;

4- Estabelecer comparações entre os diversos corpos graníticos da Suíte Jamon e destes com associações análogas de outros continentes;

5- Estabelecer um modelo de colocação para os corpos graníticos que constituem a Suíte Jamon e procurar esclarecer os mecanismos e processos magnáticos responsáveis pela distribuição espacial das fácies, bem como pelo zoneamento dos corpos.

## REFERÊNCIAS BIBLIOGRÁFICAS

- ALMEIDA, J.A.C. 2005. *Geologia, petrografia e geoquímica do granito anorogênico Bannach, Terreno Granito-Greenstone de Rio Maria, PA.* Belém, Universidade Federal do Pará. Centro de Geociências. 171 p. (Dissertação de Mestrado).
- ALMEIDA, J.A.C.; DALL'AGNOL, R.; OLIVEIRA, D.C. Submetido. Geologia, petrografia e geoquímica do granito anorogênico Bannach, Terreno Granito-Greenstone de Rio Maria, Pará. *Revista Brasileira de Geociências*.
- ALTHOFF, F.J.; BARBEY, P.; BOULLIER, A.-M. 2000. 2.8–3.0 Ga plutonism and deformation in the SE Amazonian craton: the Archean granitoids of Marajoara (Carajás mineral province). *Precambrian Research*, 104 : 187– 206.
- ANDERSON, J. L.& BENDER, E. E. 1989. Nature and origin of Proterozoic A-Type granitic magmatism in the southwestern United States of America. In: GORBATSCHEV, R. (Ed.), *Proterozoic Geochemistry. Lithos*, 23:19-52.
- AVELAR, V.G. 1996. *Geocronologia Pb-Pb por evaporação em monocrystal de zircão, do magmatismo da região de Tucumã, SE do Estado do Pará, Amazônia oriental.* Belém, Universidade Federal do Pará. (Dissertação de Mestrado).
- BARBOSA, A.A.; LAFON, J.M.; NEVES, A.P.; VALE, A.G. 1995. Geocronologia Rb-Sr e Pb-Pb do Granito Redenção, SE do Pará: Implicações para a evolução do magmatismo Proterozóico da região de Redenção. *Boletim do Museu Paraense Emílio Goeldi, série Ciências da Terra*, 7:147-164.
- BARROS, C.E.M.; BARBEY, P.; BOULLIER, A.M. 2001. Role of magma pressure, tectonic stress and crystallization progress in the emplacement of the syntectonic A-type Estrela Granite Complex (Carajás Mineral Province, Brazil). *Tectonophysics*, 343: 93-109.
- BARROS, C.E.M.; DALL'AGNOL, R.; VIEIRA, E.A.P.; MAGALHÃES, M.S. 1995. Granito Central da Serra dos Carajás: avaliação do potencial metalogenético para estanho com base em estudos da borda oeste do corpo. *Boletim Museu Paraense Emílio Goeldi, Série Ciências da Terra*, 7:93-123.

- BETTENCOURT, J.S.; TOSDAL, R.; LEITE, W.B. JR.; PAYOLLA, B.L. 1995. Overview of the rapakivi granites of the Rondônia Tin Province (RTP). In: SYMPOSIUM ON RAPAKIVI GRANITES AND RELATED ROCKS. Belém, 1995. *Excursion Guide and Programs...* Belém, p. 5-14.
- BETTENCOURT, J.S.; TOSDAL, R.; LEITE, W.B. JR.; PAYOLLA, B.L. 1999. Mesoproterozoic rapakivi granites of Rondônia Tin Province, southwestern border of the Amazonian craton, Brazil. Reconnaissance U-Pb geochronology and regional implications. *Precambrian Research*. **95**: 41-67.
- DALL'AGNOL, R. & MAGALHÃES, M.S. 1995. Geochemistry and petrogenesis of the anorogenic Jamon and Musa granites, eastern Amazonian craton, Brazil: implications for the genesis of A-type proterozoic granites. In: DALL'AGNOL, R.; MACAMBIRA, M.J.B.; COSTI, H.T. (Ed.). In: SYMPOSIUM ON RAPAKIVI GRANITES AND RELATED ROCKS. Belém. Universidade Federal do Pará. Center for Geosciences. 22-23.
- DALL'AGNOL, R. & OLIVEIRA, D.C. 2006. Oxidized, magnetite-series, rapakivi-type granites of Carajás, Brazil: implications for classification and petrogenesis of A-type granites. *Lithos* (In press).
- DALL'AGNOL, R.; COSTI, H.T.; LEITE, A.A.S.; MAGALHÃES, M.S.; TEIXEIRA, N.P. 1999b. Rapakivi granites from Brazil and adjacent areas. *Precambrian Research* **95**, 9-39.
- DALL'AGNOL, R.; LAFON, J.M.; MACAMBIRA, M.J.B. 1994. Proterozoic anorogenic magmatism in the Central Amazonian province, Amazonian Craton. Geochronological, Petrological and Geochemical aspects. *Mineralogy and Petrology*, **50**:113-138.
- DALL'AGNOL, R.; OLIVEIRA, M.A.; ALMEIDA, J.A.C.; ALTHOFF, F.J.; LEITE, A.A.S.; OLIVEIRA, D.C.; BARROS, C.E.M. 2006. Archean and Paleoproterozoic granitoids of the Carajás metallogenic province, eastern Amazonian craton. In: DALL'AGNOL, R.; ROSA-COSTA, L.T.; KLEIN, E.L. (eds.). Symposium on Magmatism, Crustal Evolution, and Metallogenesis of the Amazonian Craton. *Abstracts Volume and Field Trips Guide*. Belém, PRONEX-UFPB/SBG-NO, 150p.
- DALL'AGNOL, R.; RAMÖ, O.T.; MAGALHÃES, M.S.; MACAMBIRA, M.J.B. 1999a. Petrology of the anorogenic, oxidised Jamon and Musa granites, Amazonian Craton: implications for the genesis of Proterozoic, A-type Granites. *Lithos*. **46**: 431-462.

- DALL'AGNOL, R.; SAUCK, W.A.; GONÇALEZ, M.G.B. 1988. Suscetibilidade magnética em granitóides da Amazônia: Um estudo preliminar. In: CONG. BRAS. GEOL., 35, Belém, 1988. *Anais...Belém, SBG.* v. 3, p. 1664-1173.
- DALL'AGNOL, R.; SCAILLET, B.; PICHAVANT, M. 1999c. *Evolution of A-type granite magmas: an experimental study of the Lower Proterozoic Jamon Granite, eastern Amazonian craton, Brazil.* *Journal of Petrology.* 40 (11): 1673-1698.
- DALL'AGNOL, R.; TEIXEIRA, N.P.; RÄMÖ, O.T.; MOURA, C.A.V.; MACAMBIRA, M.J.B.; OLIVEIRA, D.C. 2005. Petrogenesis of the Paleoproterozoic, rapakivi, A-type granties of the Archean Carajás Metallogenic Province, Brazil. *Lithos,* 80 : 101-129.
- DOCEGEO (Rio Doce Geologia e Mineração - Distrito Amazônia) 1988. Revisão litoestratigráfica da Província Mineral de Carajás, Pará. In: CONGRESSO BRASILEIRO DE GEOLOGIA, 35, Belém. Anexos. Belém, SBG. Vol. Província Mineral de Carajás-Litoestratigrafia e Principais Depósitos Minerais. p. 11-54.
- DUARTE, K.D. 1992. *Geologia e geoquímica do Granito Mata Surrão (SW de Rio Maria-PA): um exemplo de granito “stricto sensu” Arqueano.* Belém, Universidade Federal do Pará. Centro de Geociências. 217 p. (Dissertação de Mestrado).
- EMSLIE, R., 1991. Granitoids of rapakivi granite-anorthosite and related associations. In: I. HAAPALA AND K.C. CONDIE (Ed.), Precambrian Granitoids-Petrogenesis, Geochemistry and Metallogeny. *Precambrian Res.,* 51, pp. 173-192.
- FIGUEIREDO, M.A.B.M. 1999. *Minerais óxidos de Fe e Ti e suscetibilidade magnética em vulcânicas e granitóides proterozóicos da Vila Riozinho, Província Aurífera do Tapajós.* Belém, Universidade Federal do Pará, Centro de Geociências. (Dissertação de Mestrado).
- FIGUEIREDO, M.A.B.M.; DALL'AGNOL, R.; LAMARÃO, C.N.; OLIVEIRA, D.C. 2003. Petrologia Magnética do Granito São Jorge Antigo, Província Aurífera do Tapajós. *Revista Brasileira de Geociências,* 33 (2):149-158.
- GASTAL, M.C.P. 1987. *Petrologia do Maciço Granítico Musa, Sudeste do Pará.* Belém, Universidade federal do Pará. Centro de Geociências. 316 p. (Dissertação de Mestrado).
- GASTAL, M.C.P. 1988. Magmatismo ácido-intermediário do Proterozóico Médio da região de Rio Maria, SE do Pará: discussão quanto à tipologia. In: CONGRESSO BRASILEIRO DE GEOLOGIA, 35, Belém, 1988. *Anais.* Belém, SBG. v. 3, p. 1147-1163.

- GONÇALEZ, M.G.B.; DALL'AGNOL, R.; VIEIRA, E.A.P.; MACAMBIRA, M.J.B.; DELLA SENTA, N. 1988. Geologia do maciço anorogênico Cigano, Vale do Rio Parauapebas-PA, In: CONGR. BRAS. GEOL., 35, Belém, 1988, Belém, SBG. p. 1132-1146.
- HAAPALA, I. & RÄMÖ, O.T. 1990. Petrogenesis of the Proterozoic rapakivi granites of Finland. In: H.J. STEIN & J.L. HANNAH (Editors), *Ore-bearing granite systems; Petrogenesis and mineralizing processes*. Geol. Soc. Am. pp. 275-286. (*Spec. Pap.*, 246).
- HUHN, S.R.B.; SANTOS, A.B.S.; AMARAL, A.F.; LEDSHAM, E.J.; GOUVEIA, J.L.; MARTINS, L.B.P.; MONTALVÃO, R.M.G.; COSTA, V.G. 1988. O terreno granito-greenstone da região de Rio Maria - Sul do Pará. In: CONGRESSO BRASILEIRO DE GEOLOGIA, 35, Belém, 1988. *Anais*. Belém, SBG. v. 3, p. 1438-1453.
- ISSLER, R.S. & LIMA, M.I.C. 1987. Amazonic Craton (Brazil): granitogenesis and its relation to geotectonic units. *Revista Brasileira de Geociências*, 17: 426-441.
- JAVIER RIOS, F.; VILLAS, R.N.N.; FUZIKAWA, K. 1994a. Estudo preliminar de Inclusões Fluidas (IF) em veios hidrotermais do Granito Cigano, Serra dos Carajás, PA. In: CONGR. BRAS. GEOL., 38, Camboriú, *Boletim de resumos expandidos*, 1994, Camboriú, SBG. p. 639-640.
- JAVIER RIOS, F.; VILLAS, R.N.N.; PIMENTA, M.A. 1994b. Fluidos relacionados com o hidrotermalismo do Granito Musa (PA): indicações das Inclusões Fluidas (IF) em quartzo de veios mineralizados da Jazida de W de Pedra Preta. In: CONGR. BRAS. GEOL., 38, Camboriú, *Boletim de resumos expandidos*, 1994, Camboriú, SBG. p. 644-645.
- LAFON, J.M.; RODRIGUES, E.; DUARTE, K.D. 1994. Le granite Mata Surrão: un magmatisme monzogranitique contemporain des associations tonalitiques-trondhjemítiques-granodiorítiques archéennes de la région de Rio Maria (Amazonie Orientale, Brésil). *Comptes Rendus de la Academie de Sciences de Paris*, t. 318, serie II, p. 642-649.
- LEITE, A.A.S.; DALL'AGNOL, R.; MACAMBIRA, M.J.B.; ALTHOFF, F.J. 2004. Geologia e geocronologia dos granitóides arqueanos da região de Xinguara (PA) e suas implicações na evolução do Terreno Granito-Greenstone de Rio Maria. *Revista Brasileira de Geociências*, 34 : 447-458.
- MACAMBIRA, M.J.B. 1992. *Chronologie U/Pb, Rb/Sr, K/Ar et croissance de la croûte continentale dans l'Amazonie du sud-est; exemple de la région de Rio Maria, Province de Carajas, Brésil*. Montpellier, Université Montpellier II-France. 212 p. (Tese de Doutorado).

- MACAMBIRA, M.J.B. & LAFON, J.M. 1995. Geocronologia da Província Mineral de Carajás; Síntese dos dados e novos desafios. *Boletim do Museu Paraense Emílio Goeldi, Série Ciências da Terra*, Belém, (7): 263-287.
- MACAMBIRA, M.J.B. & LANCELOT, J.R. 1996. Time constraints for the formation of the Archean Rio Maria crust, southeastern Amazonian craton, Brazil. *Intern. Geol. Rev.*, **38** : 1134-1142.
- MACHADO, N.; LINDENMAYER, Z.; KROGH, T.E.; LINDENMAYER, D. 1991. U/Pb geochronology of Archean magmatism and basement reactivation in the Carajás Área, Amazon Shield, Brazil. *Precambrian Research*, **49**: 329-354.
- MAGALHÃES, M.S. 1991. *Minerais opacos e suscetibilidade magnética de granitóides da Amazônia Oriental: Implicações Petrológicas*. Belém, UFPA. CG. 274 p. (Dissertação de Mestrado).
- MAGALHÃES, M.S & DALL'AGNOL, R. 1992. Estudos de minerais opacos e suscetibilidade magnética nos Granitos Musa e Jamon (Região de Rio Maria - SE do Pará) e suas implicações petrológicas. *Rev. Bras. Geoc.*, Belém. 22, 2.
- MAGALHÃES, M.S.; FIGUEIREDO, M.A.B.M.; ALTHOFF, F.J. 1994. Comportamento magnético do Tonalito Arco Verde e do Granito Guarantã, Rio Maria, Pará: suscetibilidade magnética e minerais opacos. In: SIMP. GEOL. AMAZ., **4**, Belém,
- MONTALVÃO, R.M.G.; BEZERRA, P.E. L.; PRADO, P.; FERNANDES, C.A.C.; SILVA, G.H.; BRIM, R.J.P. 1982. Características petrográficas e geoquímicas do Granito Redenção e suas possibilidades metalogenéticas. In: CONG. BRAS. GEOL., **32**, Salvador, 1982. Anais... Salvador, SBG. v. 2, p. 520 - 548.
- NASCIMENTO, F.G.C. 2006. *Petrologia magnética das associações magmáticas arqueanas da Região de Canaã dos Carajás – PA*. Belém. Universidade Federal do Pará. Centro de Geociências. 177 p. (Dissertação de Mestrado).
- OLIVEIRA, D.C. 1998. *Petrografia, suscetibilidade magnética e minerais óxidos de Fe e Ti do Granito Redenção, sudeste do estado do Pará*. Belém. Universidade Federal do Pará. Centro de Geociências. 68p. (Trabalho de Conclusão de Curso).

- OLIVEIRA, D.C. 2001. *Geologia, geoquímica e petrologia magnética do Granito Paleoproterozóico Redenção, SE do Cráton Amazônico*. Belém. Universidade Federal do Pará. Centro de Geociências. 207 p. (Dissertação de Mestrado).
- OLIVEIRA, D.C.; DALL'AGNOL, R.; BARROS, C.E.M.; FIGUEIREDO, M.A.B.M. 2002. Petrologia magnética do Granito Paleoproterozóico Redenção, SE do Cráton Amazônico. In: KLEIN, E.L., VASQUEZ, M.L., ROSA-COSTA, L.T. (Ed.) *Contribuições à Geologia da Amazônia*, v. 3, p. 115-132.
- OLIVEIRA, D.C.; DALL'AGNOL, R.; BARROS, C.E.M.; VALE, A.G. 2005. Geologia e Petrografia do Granito Paleoproterozóico Redenção, SE do Cráton Amazônico. *Boletim do Museu Paraense Emílio Goeldi*, Série Ciências Naturais, Belém, 2 (1), p: 155-172.
- OLIVEIRA, D.C.; DALL'AGNOL, R.; SILVA, J.B.C.; ALMEIDA, J.A.C. Submetido b. Gravimetric, radiometric, and magnetic susceptibility study of the Paleoproterozoic Redenção and Bannach plutons: implications for architecture and zoning of A-type granites. *Journal of South American Earth Sciences*.
- OLIVEIRA, D.C.; NEVES, S.P.; DALL'AGNOL, R.; MARIANO, G.; CORREIA, P.B. Submetido c. Anisotropy of magnetic susceptibility of the Redenção granite, Eastern Amazonian Craton: Implications for the emplacement of a Paleoproterozoic anorogenic A-type pluton. *Journal of Structural Geology*.
- OLIVEIRA, M.A.; DALL'AGNOL, R.; ALTHOFF, F. J. Submetido a. Petrografia e geoquímica do Granodiorito Sanukítóide Arqueano Rio Maria da região de Bannach e comparações com as demais ocorrências no Terreno Granito-Greenstone de Rio Maria. *Revista Brasileira de Geociências*.
- PIMENTEL, M.M. & MACHADO, N. 1994. Geocronologia U-Pb dos Terrenos granito-greenstone de Rio Maria, Pará. In: CONGRESSO BRASILEIRO DE GEOLOGIA, 38, Camboriú, 1988. *Boletim de Resumos Expandidos*. Camboriú, SBG. p. 390-391.
- RÄMÖ, O.T. & HAAPALA, I. 1995. One hundred years of rapakivi granite. *Mineralogy Petrology*, 52: 129-185.
- RÄMÖ, O.T.; DALL'AGNOL, R.; MACAMBIRA, M.J.B.; LEITE, A.A.S.; OLIVEIRA, D.C. 2002. 1.88 Ga oxidized A-type granites of the Rio Maria region, eastern Amazonian craton, Brazil: Positively anorogenic! *Journal of Geology*, 110 : 603-610.

- RIVALENTI, G.; MAZZUCHELLI, M.; GIRARDI, V.A.V.; CAVAZZINI, G.; FINATTI, C.; BARBIERI, M.A.; TEIXEIRA, W. 1998. Petrogenesis of the Paleoproterozoic basaltic-andesite-rhyolite dyke association in the Carajás region, Amazonian craton. *Lithos* **43**, 235-265.
- ROCHA Jr., G.L.D. 2004. *Caracterização petrográfica do Granito Paleoproterozóico Marajoara, Terreno Granito-Greenstone de Rio Maria, SE do estado do Pará. Belém.* Universidade Federal do Pará. Centro de Geociências. 45p. (TCC).
- RODRIGUES, E.M.S.; LAFON, J.M.; SCHELLER, T. 1992. Geocronologia Pb-Pb em rochas totais da Província Mineral de Carajás: primeiros resultados. In: CONGRESSO BRASILEIRO DE GEOLOGIA, 37., São Paulo, 1992. *Boletim de Resumos Expandidos.* São Paulo, SBG. v. 2, p. 183-184.
- ROLANDO, A.P. & MACAMBIRA, M.J.B. 2002. Geocronologia dos granitóides arqueanos da região da Serra do Inajá, novas evidências sobre a formação da crosta continental no sudeste do Cráton Amazônico, SSE Pará. In: CONGRESSO BRA SILEIRO GEOLOGIA, 41. *Anais.... João Pessoa.* SBG. p. 525.
- ROLANDO, A.P. & MACAMBIRA, M.J.B. 2003. Archean crust formation in Inajá range area, SSE of Amazonian Craton, Brazil, basead on zircon ages and Nd isotopes. In: SOUTH AMERICAN SYMPOSIUM ON ISOTOPE GEOLOGY, 4, Salvador, 2003. *Expanded Abstracts.* Salvador: CD-ROM.
- SCAILLET, B.; PICHAVANT, M.; DALL'AGNOL, R. 1995. Experimental determination of phase equilibria of the Jamon Granite, eastern Amazonian Province. In: SYMPOSIUM RAPAKIVI GRANITES AND RELATED ROCKS, IGCP-315. University of Pará, Belém, 1995, pp. 69.
- SILVA Jr., R.O.; DALL'AGNOL, R.; OLIVEIRA, E.P. 1999. Geologia, petrografia e geoquímica dos diques proterozóicos da região de Rio Maria, sudeste do Pará. *Geochimica Brasiliensis*, 13.
- SOARES, C.M. 1996. *Estudo das relações de contato do granodiorito Rio Maria com os granitos Jamon e Musa e com diques do proterozóico.* Belém, Universidade Federal do Pará. 165p. (Dissertação de Mestrado).

- SOUZA, Z.S. & DALL'AGNOL, R. 1995. Geochemistry of metavolcanic rocks in the Archean Greenstone Belt of Identidade, SE, Pará, Brazil. *Anais da Academia Brasileira de Ciências*, **67**: 217-233.
- SOUZA, Z.S.; MEDEIROS, H.; ALTHOFF, F.J.; DALL'AGNOL, R. 1990. Geologia do terreno granito-greenstone Arqueano da região de Rio Maria, Sudeste do Pará. In: CONGRESSO BRASILEIRO DE GEOLOGIA, **36**., Natal, 1990. *Anais*. Natal, SBG. v. 6, p. 2913-2928.
- TASSINARI, C.C.G. & MACAMBIRA, M. 2004. A evolução tectônica do Craton Amazonico. In: MANTESSO – NETO, V.; BARTORELLI, A.; CARNEIRO, C.D.R.; BRITO NEVES, B.B. (Eds.), *Geologia do Continente Sul Americano: Evolução da obra de Fernando Flávio Marques Almeida*. São Paulo, p. 471-486.
- TEIXEIRA, N.P. 1999. *Contribuição ao estudo dos granitóides e mineralizações associadas da Suíte Intrusiva Velho Guilherme, Província Estanífera do sul do Pará*. São Paulo, Universidade de São Paulo. V.1 e 2, 508p. (Tese de Doutorado).
- TEIXEIRA, N.P.; BETTENCOURT, J.S.; MOURA, C.A.V.; DALL'AGNOL, R.; MACAMBIRA, E.M.B. 2002. Archean crustal sources for Paleoproterozoic tin-mineralized granites in the Carajás Province, SSE Pará, Brazil: Pb-Pb geochronology and Nd isotope geochemistry. *Precambrian Research*, 119 : 257-275.
- VALE, A.G. & NEVES, P.N. 1994. O Granito Redenção: Estado do Pará. In: CONGRESSO BRASILEIRO DE GEOLOGIA, **38**, Balneário Camboriú-SC, 1994. *Anais....* Camboriú, SBG. V. 1, p. 149 - 150.

## CAPÍTULO - 2

### ***GEOCHEMISTRY AND MAGMATIC EVOLUTION OF THE PALEOPROTEROZOIC, ANOROGENIC A-TYPE REDENÇÃO GRANITE OF THE JAMON SUITE, EASTERN AMAZONIAN CRATON, BRAZIL***

**Davis Carvalho de Oliveira**

**Roberto Dall'Agnol**

**Carlos Eduardo M. Barros**

*Submetido: CANADIAN MINERALOGIST special issue of IGCP-510 (A-type Granites and Related Rocks through Time).*



September 25, 2006

Page 1 of 1

UNIVERSITY OF HELSINKI  
Department of Geology  
Division of Geology and Mineralogy

To whom it may concern:

This is to certify that the manuscript "*Geochemistry and magmatic evolution of the Paleoproterozoic, anorogenic A-type Redenção granite of the Jamon Suite, eastern Amazon Craton, Brazil*" by Davis Carvalho de Oliveira, Roberto Dall'Agnol, and Carlos Eduardo de Mesquita Barros has been submitted to will be considered for publication in the upcoming Canadian Mineralogist special issue of IGCP-510 (*A-type Granites and Related Rocks through Time*).

Sincerely,

A handwritten signature in blue ink, appearing to read "Tapani Rämö".

O. Tapani Rämö, Ph.D.  
Professor of Geology and Mineralogy  
Guest Editor of IGCP-510 Canadian Mineralogist special issue  
Co-leader of IGCP Project 510

**GEOCHEMISTRY AND MAGMATIC EVOLUTION OF THE PALEOPROTEROZOIC,  
ANOROGENIC A-TYPE REDENÇÃO GRANITE OF THE JAMON SUITE, EASTERN  
AMAZONIAN CRATON, BRAZIL**

Davis Carvalho de Oliveira, Roberto Dall'Agnol, Carlos Eduardo de Mesquita Barros

Group of Research on Granite Petrology, Centro de Geociências, Universidade Federal do Pará,  
Caixa Postal 8608, 66075-100 Belém, PA, Brazil

\*Corresponding author. Tel.: +55 91 3183 1477; fax +55 91 3183 1609. E-mail address:  
[robdal@ufpa.br](mailto:robdal@ufpa.br)

**Abstract**

The Paleoproterozoic anorogenic Redenção batholith is located in the Amazon Craton to the south of Serra dos Carajás where it had intruded Archean rocks of the Rio Maria Granite-Greenstone Terrane. The granitic pluton is comprised of essentially of monzogranites disposed in near-concentric zones. The less evolved facies is a coarse biotite-hornblende monzogranite, locally enriched in cumulitic amphibole ± clinopyroxene, which occurs in the southern part of the pluton. The main facies of the pluton is a coarse (hornblende)-biotite monzogranite and the central portion comprises evolved leucogranites. Seriated and porphyritic biotite monzogranite facies intruded the coarse (hornblende)-biotite monzogranite forming an annular structure located in the central and southern areas of the pluton. Locally, in coarse or porphyritic rocks, rapakivi and anti-rapakivi textures are present. The magmatic zoning is marked by a systematic decrease in mafic mineral modal content, the ratios of plagioclase/potassium feldspar and

amphibole/biotite, and anorthite content of plagioclase.  $\text{TiO}_2$ ,  $\text{MgO}$ ,  $\text{FeO}_t$ ,  $\text{CaO}$ ,  $\text{P}_2\text{O}_5$ ,  $\text{Ba}$ ,  $\text{Sr}$ , and  $\text{Zr}$  decrease, and  $\text{SiO}_2$ ,  $\text{K}_2\text{O}$ , and  $\text{Rb}$  increase in the same fashion. The magmatic evolution of the pluton involved several distinct processes. The clinopyroxene-amphibole rich facies was derived from a hornblende-biotite monzogranite liquid locally enriched in cumulitic amphibole and clinopyroxene. The biotite-hornblende monzogranites and biotite monzogranites were probably linked by fractional crystallization processes predominantly controlled by the early crystallization of andesine-calcic oligoclase, amphibole, magnetite, ilmenite, zircon, and apatite. The leucogranites were probably derived from an independent magma. The porphyritic facies is considered a hybrid product the result of mingling processes involving coarse biotite monzogranites and leucogranites. The Redenção pluton is subalkaline, metaluminous to peraluminous and shows high  $\text{FeOt}/(\text{FeOt}+\text{MgO})$  (0,83 a 0,95) and  $\text{K}_2\text{O}/\text{Na}_2\text{O}$  (1 to 2) and moderate  $\text{K/Rb}$  (100-300) ratios. These granites are typical ferroan alkali-calcic A-type granites and display geochemical affinity with within-plate granites. The oxidized character of the Redenção pluton is revealed by the ubiquitous occurrence of magnetite and titanite, and geochemical features, such as relatively lower  $\text{FeO}_t/(\text{FeO}_t+\text{MgO})$  ratios, which distinguish it from reduced A-type granites, and allow it to be considered more akin to the Paleoproterozoic Jamon suite granites of the Amazon Craton. Broadly speaking the petrographic and geochemical characteristics and magmatic evolution of the Redenção pluton is similar to that of other plutons within the Jamon suite.

**Keywords:** A-type granite; oxidized; geochemistry; Paleoproterozoic; Amazonian craton

## 1. Introduction

The end of the Paleoproterozoic Era and the entire Mesoproterozoic Era were characterized by intense magmatic activity in different cratonic areas of the world. The rapakivi granite suites and associated rocks of the Fennoscandian Shield (Haapala and Rämö, 1992; Rämö and Hapala, 1995; Åhäll et al., 2000; Amelin et al., 1997; Eklund and Shebanov, 1999) and North American continent (Emslie, 1991; Frost et al., 1999; Anderson and Morrison, 2005) are typical examples of the rocks formed during these Proterozoic magmatic events. Similar magmatic events have also been identified in the Amazonian craton (Dall'Agnol et al., 1999a, 2005; Bettencourt et al., 1995).

Since the introduction of the term A-type granite (Loiselle and Wones, 1979), numerous papers have discussed their petrographic and geochemical features, source characteristics, petrogenesis, and tectonic setting (Collins *et al.*, 1982; Clemens *et al.*, 1986; Whalen *et al.*, 1987, 1996; Rogers and Greenberg, 1990; Eby 1990, 1992; Creaser *et al.*, 1991; King *et al.*, 1997; Dall'Agnol *et al.*, 2005; Dall'Agnol and Oliveira, 2006). A-type granites were defined as relatively anhydrous, reduced, anorogenic granites (Loiselle and Wones, 1979) and rapakivi granites were redefined by Haapala and Rämö (1992) as A-type granites characterized by the presence of rapakivi texture. Their origin is most commonly associated with anorogenic settings, such as rifted continental crust. Origins associated with crustal anatexis promoted by magmatic underplating have also been suggested (Huppert and Sparks, 1988; Rämö and Haapala, 1995; Dall'Agnol *et al.*, 1999a, b, c). These rocks are, however, also found in postcollisional settings (Whalen *et al.*, 1987; King *et al.*, 1997), and there is increasing evidence of oxidized A-type granites (Anderson and Bender, 1989; Anderson and Smith, 1995; Dall'Agnol *et al.*, 1997, 1999b, c; Anderson and Morrison, 2005; Dall'Agnol and Oliveira, 2006). Proposed sources vary from granodiorite, tonalite (Anderson and Cullers, 1978; Anderson, 1983; Creaser *et al.*, 1991), and quartz diorite (Dall'Agnol *et al.*, 1999 b, c) to tholeiites and their differentiates (Frost and Frost, 1997; Frost *et al.*, 1999). Fractional crystallization from alkaline basalts (Eby, 1992) or other mantle-derived magmas (Bonin, 1996) and melting of residual granulitic sources (Collins *et al.*, 1982; Clemens *et al.*, 1986) have also been proposed for the origin of A-type granites.

The Redenção granite belongs to the Paleoproterozoic, oxidized A-type Jamon suite of the Archean Rio Maria Granite-Greenstone Terrane in the eastern Amazonian craton (Dall'Agnol *et al.*, 1999b, c; 2005). The granites of that suite have been dated at 1.88 Ga (Machado *et al.*, 1991; Dall'Agnol *et al.*, 1999b, 2005 and references therein) and were intruded into a ~3.0 to 2.86-Ga-old crust composed of greenstone belts and granitoids rocks which comprise the Rio Maria Granite-Greenstone Terrane. The A-type granites of the Jamon suite show many similarities with the Mid-Proterozoic granites of the western United States. They are metaluminous to mildly peraluminous, magnetite-bearing, oxidized granites, displaying high K<sub>2</sub>O and HFSE (Dall'Agnol and Oliveira, 2006).

The aim of this paper is to present field, petrographic, and geochemical data and to discuss the magmatic evolution on the Redenção pluton, which is representative of the Paleoproterozoic anorogenic, oxidized A-type granites of the Jamon Suite. The good exposure

and extensive sampling allowed for a better understanding of the relationships between different granite varieties of the pluton and their magmatic evolution. Geochemical data was employed to discuss the typology of the Redenção Granite and the criteria applied in order to establish its oxidized character in contrast with reduced A-type granites.

## 2. Geological setting

The Redenção granite is situated in the eastern border of the Central Amazonian province of the Amazon Craton (Tassinari and Macambira, 2004; Fig 1a) within the Archean Rio Maria Granite-Greenstone Terrane, comprising the southern part of the Carajás metallogenetic province (DOCEGEO, 1988). This province is limited in the north by the Maroni-Itacaiúnas province (Fig. 1a) which formed in the 2.2-2.1 –Ga Trans-Amazonian event. To the east, it is bordered by the Neoproterozoic Araguaia Belt which is related to the Brasiliano (Pan-African) cycle that did not significantly affect the Amazon Craton.

The Rio Maria Granite-Greenstone Terrane is an Archean terrane intruded by Paleoproterozoic anorogenic granites (Fig. 1b; Dall'Agnol et al., 1999b, 2005; Rämö et al., 2002). The area is dominated by granitoids and supracrustal greenstone belts with zircon ages of 2.97 to 2.86 Ga (Macambira and Lafon, 1995; Macambira and Lancelot, 1996; Leite et al., 2004) and younger, yet Archean, sedimentary rocks of the Rio Fresco sequence. The greenstone belts (Andorinhas Supergroup) are composed dominantly of komatiites and tholeiitic basalts (Souza and Dall'Agnol, 1995) and three principal groups of Archean granitoids have been distinguished (Althoff et al., 2000; Leite, 2001; Oliveira et al., submitted a, Dall'Agnol et al., 2006): (1) Granitoids of the tonalitic-trondhjemite series (TTG) represented by the Arco Verde and Caracol tonalites (2.96 to 2.93 Ga) and Mogno trondhjemite (2.87 Ga); (2) 2.87 Ga sanukitoid Rio Maria granodiorite and associated intermediate rocks, which had intruded the greenstone sequence; and (3) Potassic leucogranites of calc-alkaline affinity, represented by the Xinguara, Mata Surrão, and Guarantã granites.

The eastern part of the Amazon Craton was stabilized in the Archean and remained stable until 1.88 Ga when an episode of distension and underplating led to the generation and emplacement of oxidized A-type granites of the Jamon suite and associated coeval mafic and felsic dikes (Dall'Agnol et al., 1994, 1999b, 2005). The Redenção pluton intruded the Arco Verde tonalite and potassic leucogranites (Vale and Neves, 1994; Oliveira, 2001; Oliveira et al.,

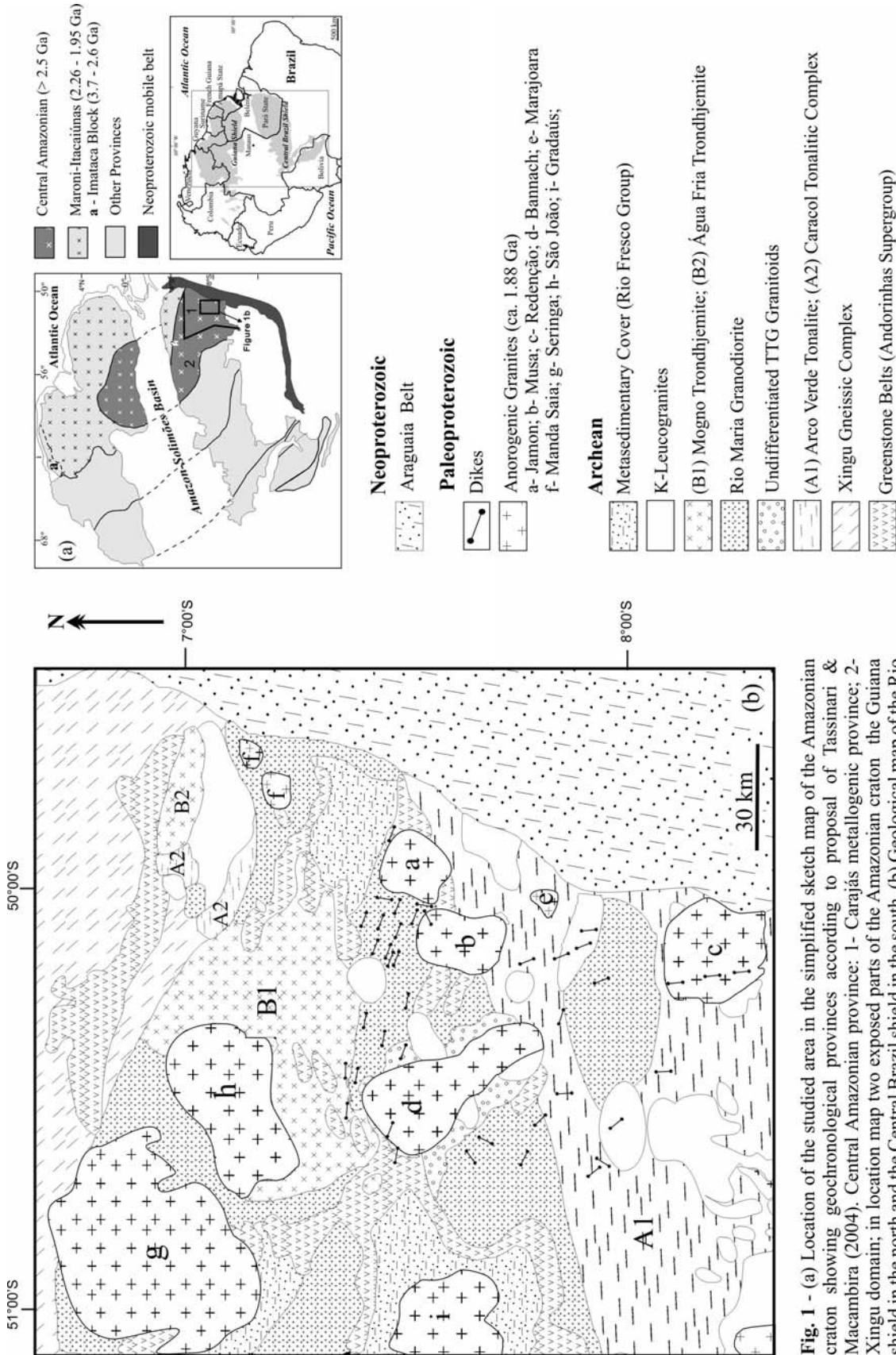


**Fig. 1 -** (a) Location of the studied area in the simplified sketch map of the Amazonian craton showing geochronological provinces according to proposal of Tassinari & Macambira (2004). Central Amazonian province: 1- Carajás metallogenetic province; 2- Xingu domain; in location map two exposed parts of the Amazonian craton the Guiana shield in the north and the Central Brazil shield in the south. (b) Geological map of the Rio Maria Granite-Greenstone Terrane showing the distribution of the Paleoproterozoic A-type granites of the Jamon suite (modified from Almeida, 2005, and references therein).

2005). In addition to the Redenção pluton, the Jamon Suite comprises the Jamon, Musa, Bannach, Marajoara, Manda Saia, Seringa, São João, and Gradaús plutons (Fig. 1b; Dall'Agnol et al., 2005; Almeida et al., submitted).

Nd isotope data for the Jamon Suite show that their  $E_{Nd}$  (at 1880 Ma) values are strongly negative ranging generally from -10.5 to -8.1 (mean value -9.4) and showing relatively little variation. On the other hand,  $T_{DM}$  ages are all Archean but show considerable variation (~2.60 to 3.02 Ga; Dall'Agnol et al., 1999b, 2005; Rämö et al., 2002). The Nd evolution lines of Archean granitoids suggest that the Paleoproterozoic A-type granites of the Jamon Suite were derived from deeper parts of the Archean crust.

Unlike other anorogenic granites of the Carajás metallogenic province, the Redenção granite is not mineralized. Wolframite mineralization is associated, however, with quartz veins emplaced in metasedimentary and metavolcanic rocks of the Pedra Preta greenstone belt has been described in the western border of the Musa Pluton (Javier Rios, 1995).

### 3. Redenção granite

#### 3.1. Field relationships with country rocks

The Redenção and other plutons of the Jamon Suite are generally unfoliated and, excepting local magmatic foliation developed on the border, deformational structures are restricted to fracturing and faulting. The Redenção pluton cross-cuts the E-W to NW-SE structural trends of the Archean granitoids (Fig. 2). Contacts are remarkably discordant and sharp. Angular xenoliths of the Arco Verde tonalite are commonly observed near the border of the pluton, indicating a high viscosity contrast between the granite magma and Archean bedrock. In the case of the Redenção pluton, contact effects were not studied in detail, but for other plutons of the Jamon suite, Archean country rocks are strongly affected by contact metamorphism. Hornblende hornfels contact metamorphism aureoles have been identified around the Jamon and Musa plutons and are well developed in both granitoid and greenstone rocks (Dall'Agnol et al., 1994, 1999b, c). Moreover, on the basis of Al content in hornblende from the granite and of mineral assemblages developed in the contact aureole, Dall'Agnol et al. (1999c, 2006) suggested that these plutons were emplaced at shallow crustal levels (~1 to 3 kbar).

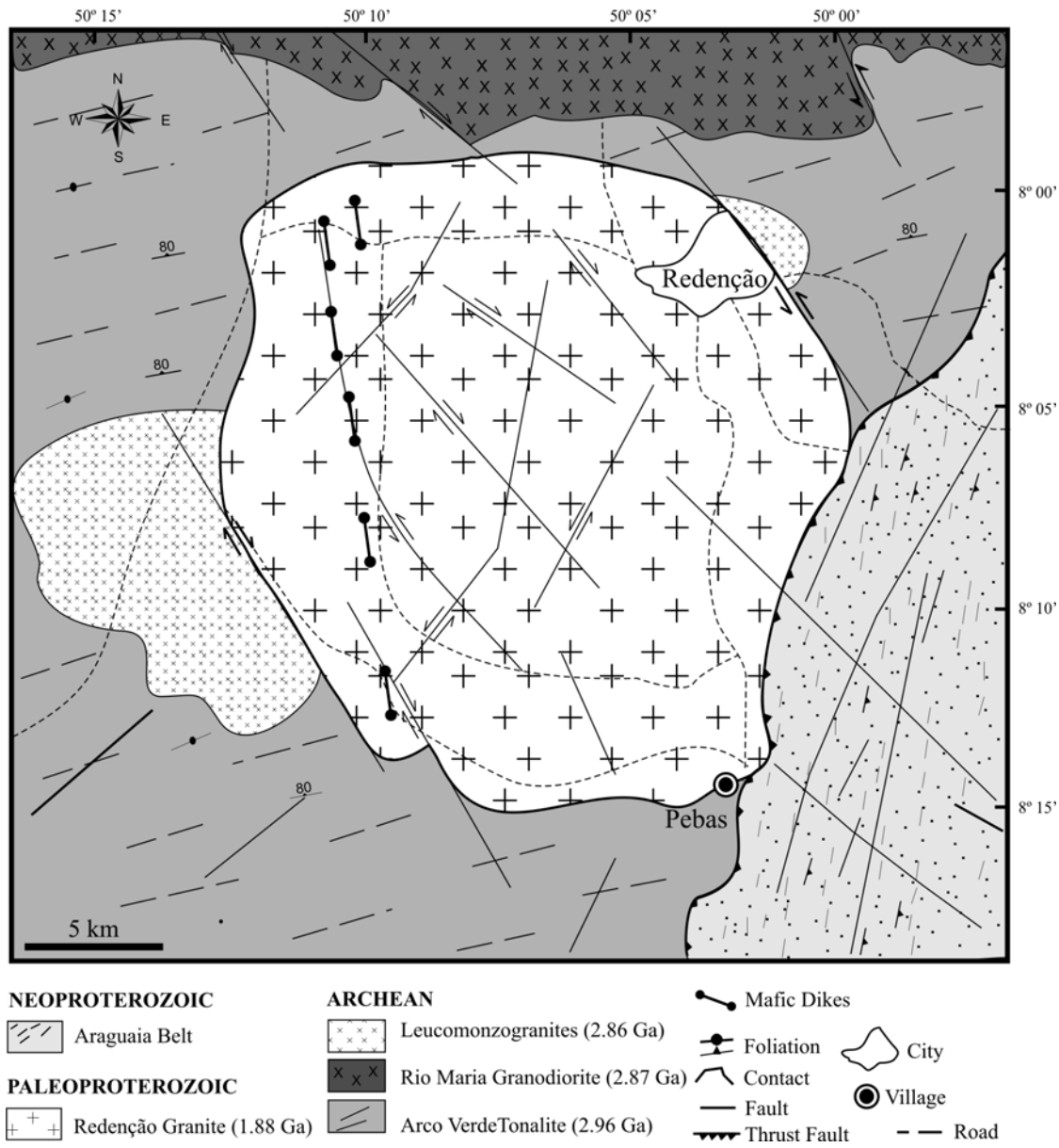


**Fig. 2** - Detailed geological map of the Redenção region (Oliveira et al. 2005).

Swarms of mafic and felsic dikes are associated with the Jamon Suite. Composite dikes of granite porphyry associated with diabase which cross-cut the sanukitoid Rio Maria granodiorite have been locally described (Dall'Agnol et al., 2005). The felsic rock in the composite dike yielded a Pb-Pb zircon age of  $1885 \pm 4$  and shows evidence of mingling with the associated mafic dike, demonstrating that the mafic and felsic magmas were contemporaneous. Another felsic dike gave an age of  $1885 \pm 2$  Ma (Oliveira D.C., unpublished data). The occurrence of dike swarms that

are coeval with the granites of the Jamon suite indicates that the granite plutons were emplaced in an extensional tectonic regime. This is consistent with the laccolithic shape of the Redenção pluton, suggested by gravity data (Oliveira et al., submitted b), which is dominant in rapakivi batholiths (Vigneresse, 2005).

### 3.2. Petrography and facies relationships

The petrography and magmatic evolution of the Redenção Granite was discussed in detail by Oliveira (2001). All granite varieties are isotropic and their color varies from grayish to reddish passing to brick red in the more strongly oxidized leucogranites. Granite facies display coarse-grained, equigranular or coarse- to medium-grained seriated textures with subordinate porphyritic and medium, even-grained types. They are leucocratic, with mafic mineral content normally between 15% and 6%, reaching > 25% in the less evolved facies, and decreasing to < 3% in the differentiated leucogranites (Table 1). All the granite varieties have relatively uniform modal composition, being essentially composed of monzogranites with rare syenogranite limited to dikes (Table 1; Figs. 3 and 4). The different facies have similar proportions of K-feldspar, quartz, and plagioclase, associated with biotite, and, in the less evolved facies, amphibole ± clinopyroxene.

In this subcircular granitic pluton, the distribution of the different facies is relatively well ordered with the more evolved varieties occupying the center (Fig. 4). The less evolved rocks are even-grained coarse monzogranites (MzG) which are concentrated in the southern border of the pluton (Fig. 4). They contain variable proportions of hornblende and biotite (BHMzG, HBMzG), and are locally enriched in amphibole ± clinopyroxene (CBHMzG). The clinopyroxene-bearing facies (Fig. 5a, b) is found only in contact with coarse amphibole-biotite monzogranite (Fig. 4). Coarse biotite monzogranites (cBMzG) are dominant in the northern, eastern, and western borders of the pluton. Coarse- to medium-grained seriated (sBMzG) and porphyritic (pBMzG) biotite monzogranites form annular structures in the central-southern and central parts of the pluton and had intruded coarse-grained hornblende-biotite and biotite monzogranites. The more evolved leucogranites are found in the central part of the pluton. The syenogranitic dikes have limited distribution and coincident orientation with the main fracturing systems.

**Table 1** – Modal Compositions of the Redenção Granite.

<i>Facies</i>	CBHMzG	BHMzG	HBMzG	cBMzG	sBMzG	pBMzG	sLMzG	eLMzG	LMcSg
<i>Mineral</i>	(4)	(6)	(10)	(10)	(7)	(8)	(10)	(3)	(7)
Plagioclase	33.0	33.0	29.3	29.0	31.4	27.8	24.7	27.8	21.8
Alkali-Feldspar	20.3	25.9	30.5	33.7	29.8	34.0	39.0	40.0	42.7
Quartz	21.5	25.8	29.2	30.4	32.7	31.8	33.6	30.5	32.5
Clinopyroxene	1.4	Tr	-	-	-	-	-	-	-
Amphibole	11.2	6.2	2.5	0.3	<0.1	0.3	-	-	-
Biotite	7.9	5.9	5.6	4.4	4.1	3.0	1.0	0.6	1.3
Chlorite	-	0.1	0.2	0.4	0.7	1.3	0.4	0.6	0.7
Opaques	3.5	2.1	1.8	1.1	0.8	0.8	0.6	0.4	0.6
Titanite	1.1	0.8	0.8	0.8	0.6	0.4	<0.1	Tr	0.2
Allanite	0.1	-	<0.1	0.1	<0.1	0.3	-	-	-
Fluorite	-	-	-	-	-	Tr	<0.1	0.7	<0.1
Others <sup>(Ap+Zr)</sup>	0.2	0.1	0.1	<0.1	<0.1	0.1	0.1	0.1	<0.1
Felsic	74.8	84.7	89.1	93.0	93.8	93.6	97.3	98.3	97.0
Mafic	25.5	15.1	11.1	6.9	6.3	6.2	2.6	1.7	2.8

**Note:** Data sources: Oliveira (2001); ( ) number of averaged samples; Tr= trace; Ap= apatite; Zr= zircon;

Abbreviations: C - clinopyroxene; B - biotite; H - hornblende ; MzG - monzogranite; L - leuco; Mc - micro; Sg - syenogranite; c - coarse, even-grained; s - medium- to coarse- grained seriated; p - porphyritic; e - medium-, even-grained.

Typical wiborgitic and pyterlitic textures (cf. Rämö and Haapala, 1995) have not been reported in the Jamon Suite, however, alkali feldspar megacrystals (2 to 5 cm) with mantles of plagioclase are common in the Redenção (Fig. 5c) and Bannach plutons (Oliveira et al., 2005; Almeida et al., submitted). Such rapakivi textures are more common in the coarse porphyritic facies and display evidence of interaction between different felsic magmas. In the Redenção pluton, evidence of magma mingling between mafic and felsic magmas is lacking and in the case of the entire Jamon suite is limited to local composite dikes (Dall'Agnol et al., 2005).

The pluton is dominated by hypidiomorphic granular textures and is composed of coarse perthitic alkali feldspar (20-43%), plagioclase (22-33%) and quartz (22-34%). In the porphyritic and seriated varieties two generations of quartz have been recognized (Fig. 5h): (1) coarse- or medium-grained, embayed bipyramidal crystals; and (2) medium- to fine-grained anhedral interstitial grains or fine-grained inclusions, concentrated in the K-feldspar or plagioclase outer zones and signalizing a late stage of feldspar crystallization. In all facies, plagioclase crystals are normally zoned, sometimes with an oscillatory character.

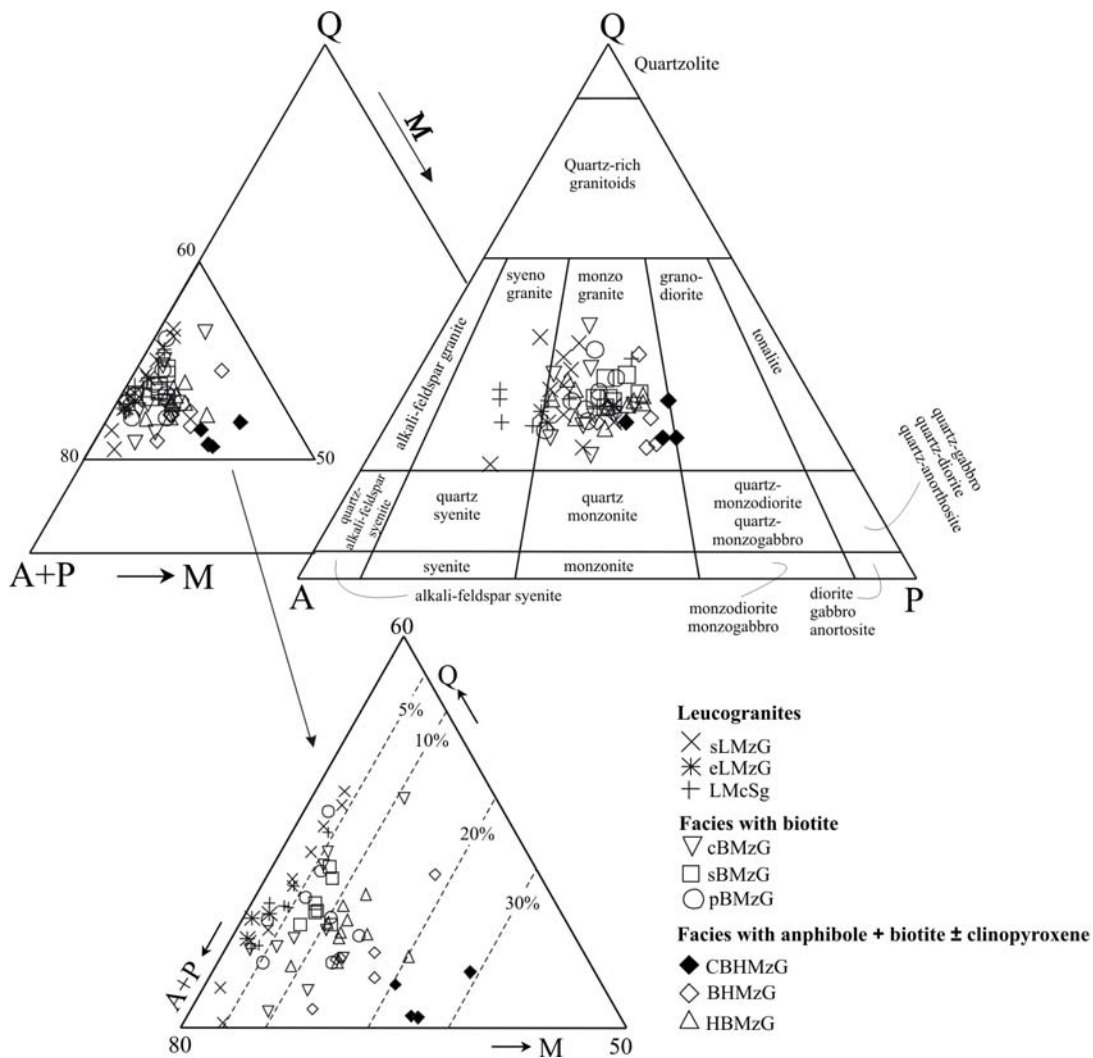


**Fig. 3.** QAP and Q-(A+P)-M diagrams (Streckeisen, 1976), showing the modal compositions of the Redenção Granite and the decrease in mafic mineral content with increase in alkali-feldspar/plagioclase ratio. CBHMzG = clinopyroxene-biotite-hornblende monzogranite; BHMzG = biotite-hornblende monzogranite; HBMzG = hornblende-biotite monzogranite; cBMzG = coarse, even-grained biotite monzogranite; sBMzG = medium- to coarse-grained seriated biotite monzogranite; pBMzG = porphyritic biotite monzogranite; sLMzG = medium- to coarse-grained seriated leuco-monzogranite; eLMzG = medium-, even-grained leuco-monzogranite; LMcSg = Leucomicro-sienogranite. Abbreviations as in Table 1.

The earlier crystallized plagioclase form euhedral to subhedral strongly zoned crystals with andesine to calcic oligoclase cores grading to sodic oligoclase in the border zones, and showing local albitic rims, preferentially in contact with K-feldspar. The latter crystallized plagioclase form subhedral to anhedral crystals of sodic oligoclase to albite, generally found as local interstitial grains or in the matrix of porphyritic varieties. In the hornblende-biotite monzogranite, plagioclase cores have compositions between An<sub>32</sub> and An<sub>29</sub>, intermediate zones

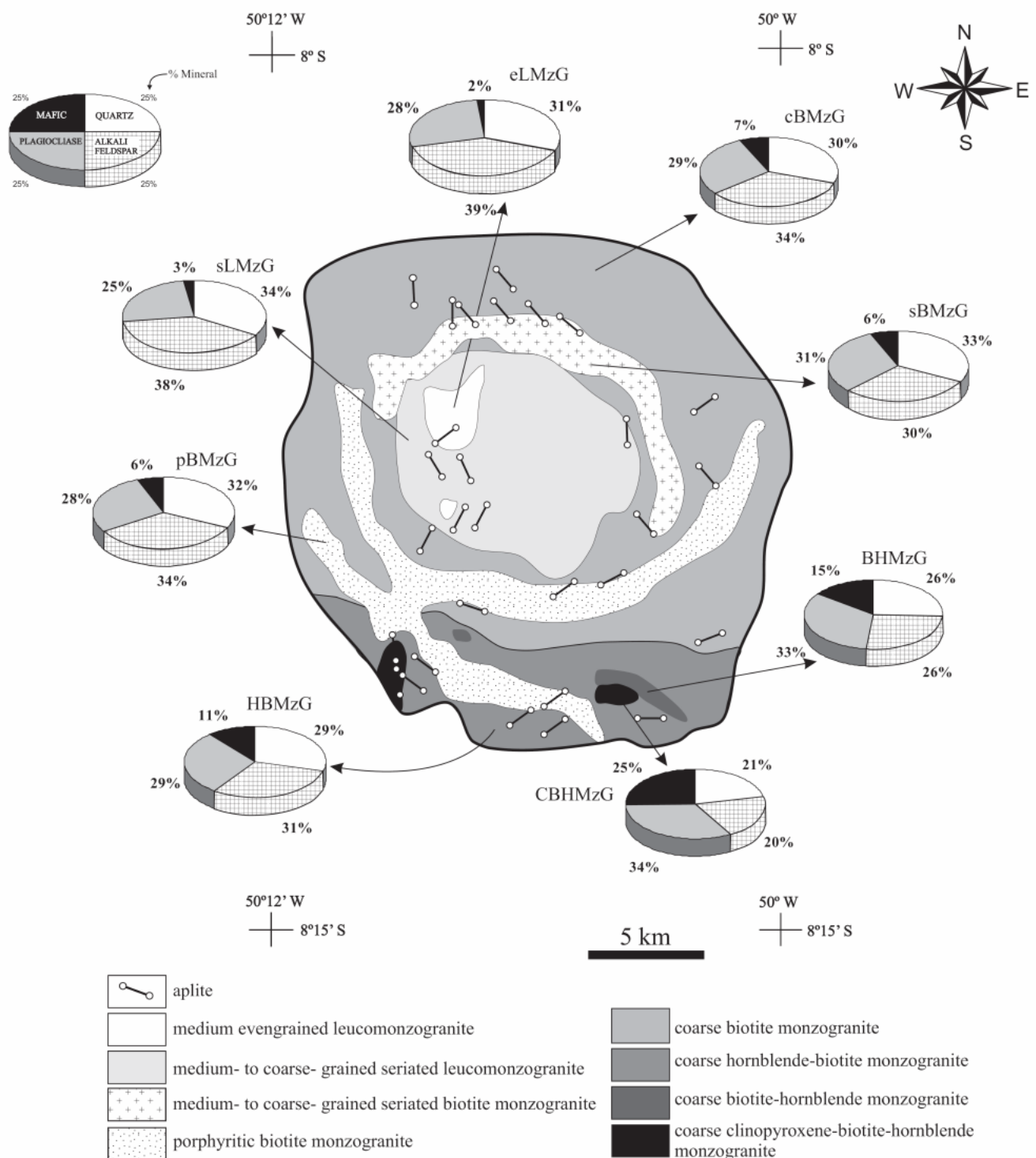


**Fig. 4.** Redenção pluton showing the areal distribution of dominant facies with the average modal mineral abundance for each facies in pie diagrams. Abbreviations as in Table 1. The mafic mineral component includes clinopyroxene, amphibole, biotite, and opaque minerals.

have a composition of An<sub>25-22</sub>, and border zones of An<sub>16-10</sub> to albite (An<sub>6-0</sub>). In the coarse- even-grained and porphyritic biotite monzogranite, most plagioclase crystals display subidiomorphic or idiomorphic cores up to An<sub>25</sub> and xenomorphic intermediate to outer zones with An<sub>16-10</sub> (Fig. 5d). In the medium- to coarse-grained seriated biotite monzogranite and leucogranites facies the plagioclase is sodic oligoclase-albite (Fig. 5i, j) without andesine-calcic oligoclase cores. Plagioclase crystals are weakly to intensely altered to sericite±epidote, especially in the cores (decalcification).

Late-magmatic granophyric quartz-K-feldspar intergrowths, subsolidus quartz-plagioclase myrmekitic textures, and K-feldspar albitization (*chess board albite*; Smith, 1974) are common in the more evolved facies. In the porphyritic facies, phenocrysts of plagioclase, quartz, and alkali-feldspar constitute about 40% of the rock (Fig. 5g) and granophyric textures are present locally in the matrix. The syenogranite facies has a porphyritic texture, with phenocrysts of quartz, oligoclase (An<22), and K-feldspar set in a fine-grained matrix.

In the Redenção pluton, biotite is the dominant ferromagnesian mineral, whereas amphibole, sometimes with relics of clinopyroxene (corona texture; Fig. 5b), is abundant only in the less evolved facies. Hornblende average modal contents (Table 1) are 6.2% in the biotite-hornblende monzogranite and 2.5% in the hornblende-biotite monzogranite; in the biotite monzogranites (Fig. 5e) amphibole is absent or just a relic phase (<0.5%). The clinopyroxene-bearing biotite-amphibole monzogranite is enriched in amphibole and clinopyroxene (average modal content of 11.2% and 1.4%, respectively). Amphiboles often contain inclusions of zircon, magnetite, ilmenite, and apatite. In the amphibole-biotite monzogranites, clusters of amphibole with aggregates of earlier crystallized plagioclase are common (except in biotite monzogranites) and associated with relics of clinopyroxene, biotite, Fe-Ti oxides, and other accessory minerals. Mafic mineral clusters are commonly found associated. Inclusions of apatite, zircon, allanite, and opaque minerals are common in the biotite. Biotite is locally altered to chlorite and fine grains of titanite. The assemblage of accessory minerals includes zircon, apatite, magnetite, ilmenite, sulphide phases (pyrite and chalcopyrite), allanite, and titanite (Fig. 5f). Magnetite with subordinate ilmenite are the main opaque minerals (Fig. 5b). Sericite, epidote, chlorite, and, in the more evolved facies, fluorite, are alteration products.

The modal compositions of the granite varieties indicate that the magmatic evolution of the Redenção pluton is marked by the systematic decrease of modal mafic mineral content,

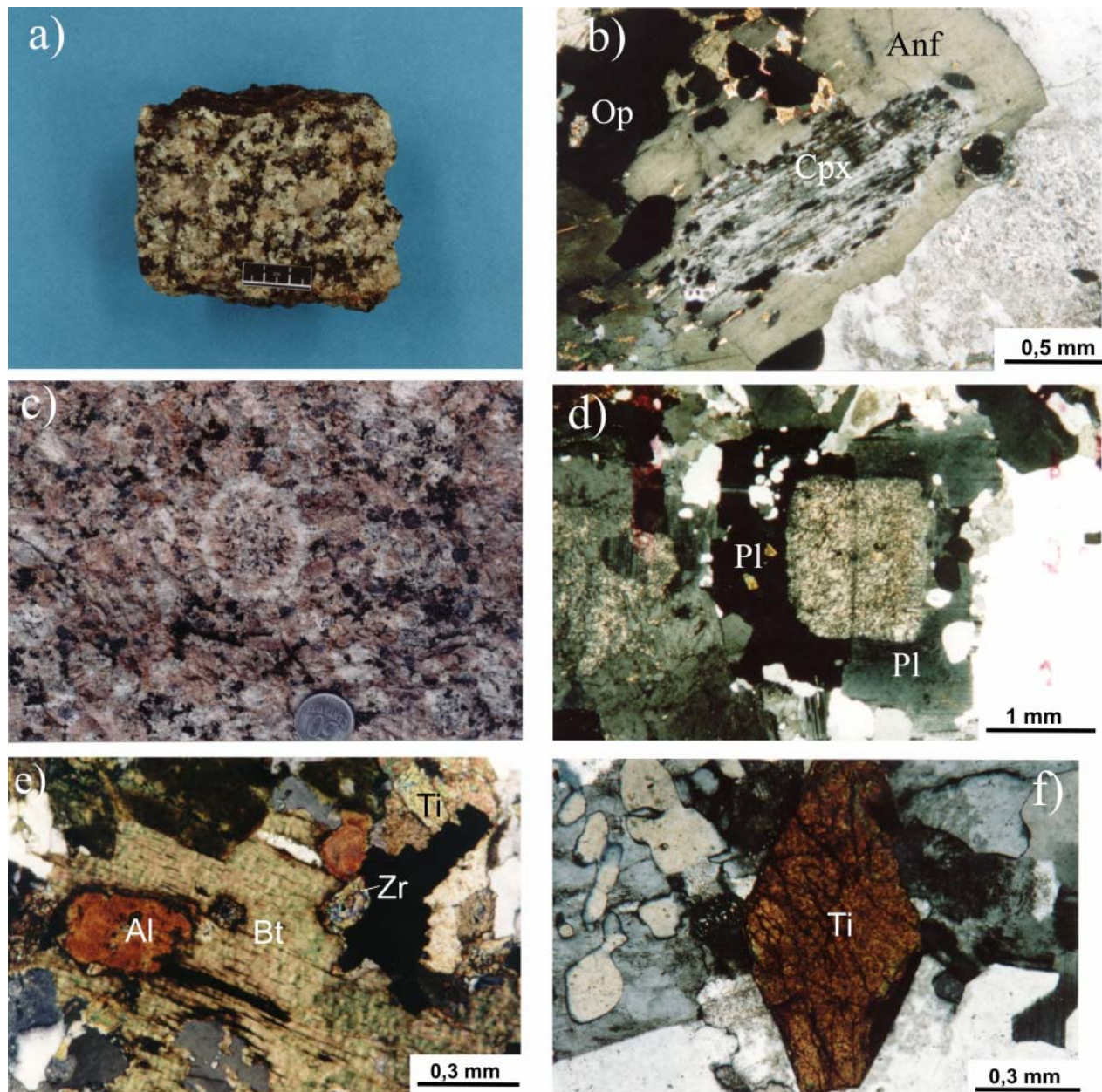


**Fig. 5.** Textural aspects of the Redenção pluton: a) clinopyroxene-bearing hornblende-enriched monzogranite; b) Amphibole with relic clinopyroxene core (corona texture) which is abundant only in the less evolved facies; c) Ovoid alkali feldspar megacrystal with mantle of plagioclase illustrating rapakivi texture, which is common in the Redenção pluton; d) Plagioclase crystals with idiomorphic andesine-calcic oligoclase cores showing evidence of synneusis structure (Vance, 1969) or epitaxial growth (Dowty, 1980); e) Mafic mineral cluster from coarse biotite monzogranite comprising a single biotite crystal with inclusions of zircon and allanite, associated with titanite, opaque minerals, and apatite; f) accessory magmatic idiomorphic titanite crystal from biotite monzogranite. (continued in the next page)

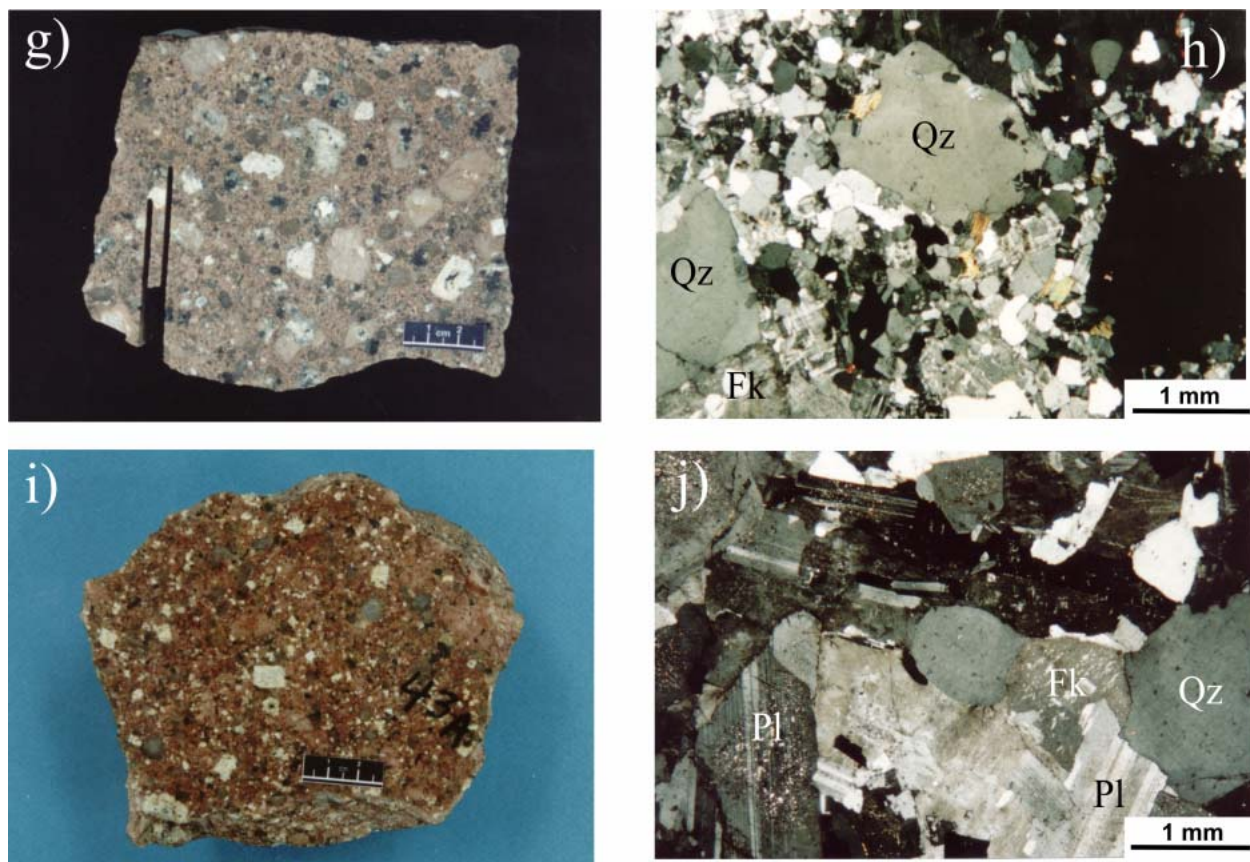


**Fig. 5** (continued). g) Porphyritic biotite monzogranite comprising phenocrysts of plagioclase, quartz, and alkali-feldspar set in a fine-grained matrix; h) Photomicrograph of porphyritic variety of the biotite monzogranite showing embayed quartz phenocrysts set in a fine-grained matrix constituted by quartz, plagioclase, and alkali-feldspar; i) Hand specimen sample of reddish seriated leucomonzogranite from the central portion of the pluton; j) Microscopic aspect of the leucomonzogranite showing a plagioclase of sodic oligoclase composition, less decalcified than those of coarse monzogranites. OP – opaque minerals; Cpx – clinopyroxene; Anf – amphibole; Pl – plagioclase; Al – allanite; Bt – biotite; Zr – zircon; Ti – titanite; Qz – quartz; Fk – potassic feldspar.

plagioclase/K-feldspar and amphibole/biotite ratios, and anorthite content of plagioclase (Table 1). The modal proportions of plagioclase and amphibole, as well as modal mafic content (Fig. 3), are greater in the clinopyroxene-bearing biotite+amphibole monzogranite and decrease toward the biotite monzogranites, attaining the lowest values in the leuogranoites, which form the center of the pluton (Fig. 4). On the other hand, the abundance of alkali feldspar and quartz increases towards the inner zone.

The crystallization sequence of the Redenção Granite magma was deduced from microscopic textural criteria in the clinopyroxene-bearing biotite+hornblende monzogranites, thought to most closely approximate the composition of the less evolved liquid. The crystallization sequence has been discussed by Oliveira (2001) and Oliveira et al. (2005) and is

presented in Fig. 6. Apatite, zircon, ilmenite, magnetite, and clinopyroxene (found locally as relics in amphibole; Fig. 5b) are the earliest phases in the crystallization sequence. They are followed by hornblende and andesine-calcic oligoclase ( $An < 41$ ), that commonly form clusters and is associated with biotite and early crystallized accessory minerals. In these clusters, plagioclase crystals with double idiomorphic cores (Fig. 5d; synneusis structure of Vance, 1969; cf. also Dowty, 1980) are common, showing that the magma had a low crystal/liquid ratio at this crystallization stage. Quartz began to crystallize relatively early and was followed by alkali feldspar. Biotite is later in the sequence and textural relationships suggest that it replaces hornblende. Titanite (Fig. 5f) and allanite begin to crystallize a little earlier but grow in major part synchronously with biotite. At this stage, the crystallizing plagioclase was a sodic oligoclase. At the subsolidus stage, calcic plagioclase cores, hornblende, and biotite were partially replaced by secondary phases (Fig. 6).

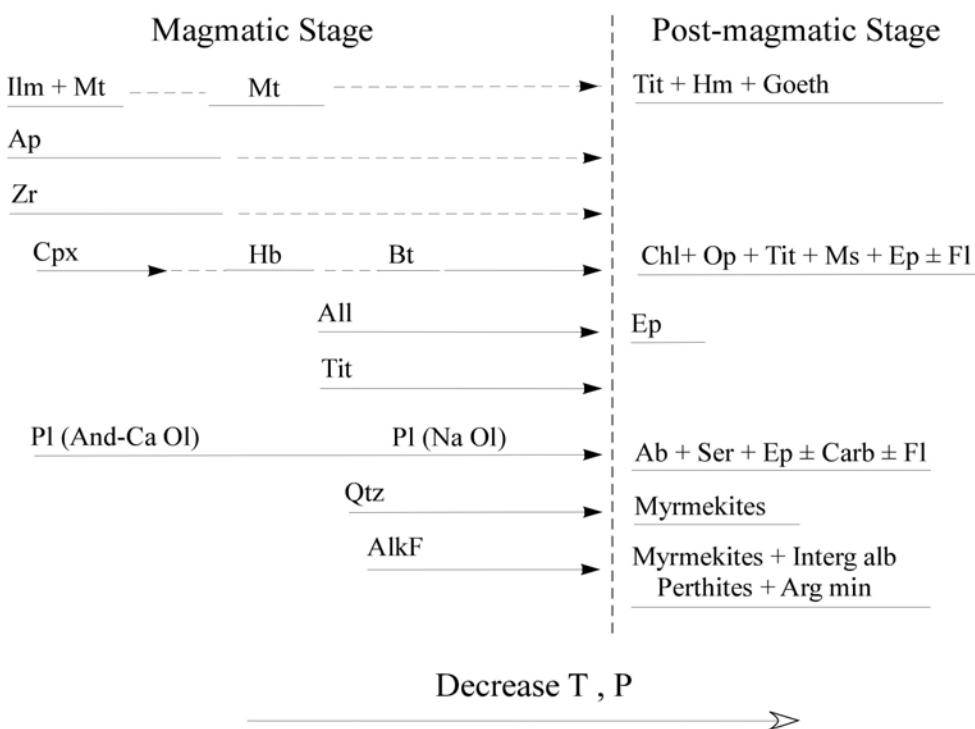


**Fig. 6.** Sequence of crystallization as deduced from petrographical observations in the hornblende + biotite  $\pm$  clinopyroxene monzogranites facies of the Redenção Granite (Oliveira, 2001 modified). Continuous lines mark the principal crystallization stage of the different minerals. IIm = ilmenite; Mt = magnetite; Ap = apatite; Zr = zircon; Cpx = clinopyroxene; Hb = hornblende; Bt = biotite; Tit = titanite; All = allanite; PI = plagioclase; And = andesine; Ca Ol = calcic oligoclase ( $An_{20-30}$ ); Na Ol = sodic oligoclase ( $An_{10-20}$ ); Qtz = quartz; AlkF = alkali-feldspar; Hem = hematite; Goeth = goethite; Chl = chlorite; Ab = albite; Interg. alb = intergranular albite; Ser = sericite; Ms = muscovite; Carb = carbonate; Fl = fluorite; Ep = epidote; Arg. Min = argillic minerals. T = temperature and P = pressure.

Therefore, in the Redenção magma, as observed in the Jamon pluton (Dall'Agnol et al., 1999b), the crystallization of hydrous silicates, and particularly that of amphibole, initiated at a relatively earlier stage. On the contrary, in other A-type granites, biotite is often reported as an interstitial or subsolidus phase, and, amphibole, although generally earlier than biotite in the crystallization sequence, is also commonly interpreted as a late phase (e.g. Clemens et al., 1986; Anderson and Bender, 1989; Emslie and Stirling, 1993; King et al., 1997; Rajesh 2000). This indicates Redenção magma amphibole and biotite crystallized at relatively higher temperatures when compared to other A-type granites. This contrast can be explained by the oxidizing character and the relatively higher water content of the Redenção magma, when compared to reduced, water-poor A-type magmas (Dall'Agnol et al., 1999c, 2005, Dall'Agnol and Oliveira, 2006).

In the biotite monzogranites, the magmatic crystallization sequence is similar to that described in the biotite-hornblende monzogranites, but andesine-calcic oligoclase and amphibole are less abundant and hornblende was almost entirely replaced by biotite. As a consequence, the plagioclase-amphibole clusters are less common in the biotite monzogranite, where smaller and more sodic plagioclase is dominant and hornblende is rare. In the porphyritic facies, the crystallization sequence was similar to that described in the even-grained biotite monzogranites, however, when the proportion of phenocrystals in the liquid was significant (40 to 60%), a sudden change in the magmatic conditions, possibly due to open-system degassing (Dall'Agnol et al., 1999b), which accelerated the crystallization of the liquid and generated the fine-grained matrix of these rocks (Fig. 5g, h). Finally, the leucogranites (Fig. 5i, j) are interpreted as having been precipitated from evolved liquids, which, if proposed to have been derived from the less evolved amphibole-biotite monzogranites, should be verified using geochemical data.

### 3.3. Whole-rock geochemistry

#### 3.3.1. Analytical procedure

Thirty four representative samples of the different granite facies of the Redenção pluton were analyzed for major and trace elements (Table 2). The chemical analyses were performed at the Lakefield-Geosol laboratories at Belo Horizonte, Brazil.  $\text{SiO}_2$ ,  $\text{TiO}_2$ ,  $\text{Al}_2\text{O}_3$ ,  $\text{Fe}_2\text{O}_{3\text{b}}$ ,  $\text{MnO}$ ,  $\text{MgO}$ ,  $\text{CaO}$ ,  $\text{K}_2\text{O}$ ,  $\text{Na}_2\text{O}$ ,  $\text{P}_2\text{O}_5$ ,  $\text{Rb}$ ,  $\text{Sr}$ ,  $\text{Ba}$ ,  $\text{Zr}$ ,  $\text{Y}$ ,  $\text{Nb}$ ,  $\text{Ga}$ , and  $\text{V}$  were analyzed by X-ray

**Table 2**  
a - Chemical composition of the Redenção Granite (analyse LAKEFIELD-GEOOL; to be continued)

	CBHMzG						BHBMzG						HBHMzG						cBMzG						sBMzG					
	DCR			DC			DCR			DCR			DCR			DCR			DC			DC			DC			DC		
	34A	63B	$\bar{X}$	63A	95A	62	$\bar{X}$	99	66A	38A	24	$\bar{X}$	50	60	14B	103	111	01D	08	$\bar{X}$	93B	105	69	29	$\bar{X}$	93B	105	69	29	$\bar{X}$
SiO <sub>2</sub> (wt.)	66.10	66.50	66.30	71.10	71.00	71.20	71.10	70.70	71.20	71.40	72.00	71.33	72.80	73.10	73.80	74.10	74.20	75.20	73.91	72.30	73.00	73.30	74.50	73.28						
TiO <sub>2</sub>	1.20	1.30	1.25	0.60	0.57	0.50	0.56	0.44	0.49	0.53	0.49	0.49	0.49	0.47	0.28	0.29	0.26	0.30	0.24	0.33	0.37	0.31	0.29	0.26	0.31					
Al <sub>2</sub> O <sub>3</sub>	13.10	12.00	12.55	13.50	13.70	13.60	13.60	14.20	14.20	13.40	13.40	13.80	13.20	13.60	13.40	13.10	13.30	12.70	13.24	13.60	13.90	13.70	12.80	13.50						
Fe <sub>2</sub> O <sub>3</sub>	3.47	4.21	3.84	2.19	1.69	1.74	1.87	1.24	1.53	1.39	1.35	1.38	1.74	1.85	1.29	1.29	1.05	1.31	1.02	1.36	1.85	1.15	1.24	1.22	1.37					
FeO	3.36	3.86	3.61	1.54	1.71	1.31	1.52	2.03	1.41	1.44	1.57	1.61	1.22	0.94	0.54	0.54	0.62	0.70	0.77	0.94	0.94	0.86	0.70	0.86						
MnO	0.13	0.17	0.15	0.07	0.08	0.06	0.07	0.06	0.05	0.06	0.06	0.06	0.06	0.04	0.04	0.04	0.04	0.05	0.07	0.07	0.04	0.04	0.05							
MgO	1.10	1.20	1.15	0.60	0.53	0.45	0.46	0.53	0.52	0.38	0.47	0.44	0.44	0.24	0.18	0.22	0.26	0.29	0.46	0.44	0.40	0.31	0.40							
CaO	2.80	2.60	2.70	2.10	1.80	1.90	1.93	1.60	1.80	1.70	1.60	1.68	1.60	1.50	1.10	1.20	1.10	1.10	1.24	1.70	1.40	1.40	1.20	1.43						
Na <sub>2</sub> O	3.70	3.50	3.50	3.70	3.40	3.60	3.57	3.50	3.70	3.60	3.40	3.55	3.40	3.40	3.20	3.40	3.30	3.30	3.34	3.50	3.40	3.30	3.10	3.33						
K <sub>2</sub> O	3.70	3.80	4.20	4.40	4.50	4.37	4.80	4.50	5.10	4.70	4.78	4.40	4.70	5.10	4.90	5.00	5.10	5.10	4.90	4.80	4.80	5.10	4.88							
P <sub>2</sub> O <sub>5</sub>	0.42	0.47	0.45	0.22	0.19	0.15	0.14	0.15	0.15	0.14	0.15	0.13	0.13	0.14	0.06	0.06	0.07	0.05	0.08	0.11	0.07	0.06	0.05	0.07						
Pf	0.32	0.65	0.49	0.38	0.43	0.29	0.37	0.35	0.31	0.25	0.21	0.28	0.51	0.53	0.39	0.39	0.33	0.28	0.31	0.36	0.39	0.40	0.38	0.33	0.30	0.38	0.38			
Total	99.60	99.78	100.2	99.50	99.30	99.67	99.52	99.89	99.53	99.30	99.56	99.99	100.6	99.44	99.80	99.43	100.1	100.1	99.92	100.1	99.83	99.72	99.68	99.83						
Ba (ppm)	919	1134	1027	1498	1309	1426	1411	1310	1499	1436	1301	1387	1197	1358	1172	930	799	795	1010	1044	812	928	756	885						
Rb	1.51	1.16	1.34	1.39	1.70	1.51	1.53	1.93	1.82	1.46	1.49	1.68	1.74	1.70	204	192	255	204	247	322	263	240	263	272						
Sr	241	228	235	332	268	285	295	271	273	286	252	271	243	302	228	216	163	196	169	217	266	209	219	205	225					
Zr	686	752	719	377	419	338	378	353	342	388	328	353	344	343	246	268	263	258	274	285	265	244	237	262	252					
Nb	29	31	30	16	20	19	20	20	12	21	18	23	17	14	20	21	21	19	22	10	20	19	18							
Y	80	95	50	49	47	49	43	40	36	43	41	57	43	40	58	45	71	51	52	72	36	50	49							
Ga	26	22	24	26	25	26	26	25	25	24	22	24	26	23	23	25	23	24	24	26	26	27	24	26						
Sc	14	11	13	<10	<10	<10	<10	<10	10	17	<10	<10	<10	<10	<10	<10	<10	<10	<10	<10	<10	<10	<10	<10	<10	<10	<10			
Th	<5	<5	<5	<5	<5	<5	<5	<5	<5	<5	<5	<5	<5	<5	<5	<5	<5	<5	<5	<5	<5	<5	<5	<5	<5	<5	<5			
U	<10	<10	<10	<10	<10	<10	<10	<10	<10	<10	<10	<10	<10	<10	<10	<10	<10	<10	<10	<10	<10	<10	<10	<10	<10	<10				
V	53	79	66	22	29	20	24	14	19	21	20	19	24	12	10	14	10	10	10	13	<10	12	18	<10	<15					
La (ppm)	102.9	80.2	91.5	60.5	49.0	54.7	82.0	82.0	71.8	40.2	73.9	71.8	44.6	60.5	43.3	44.2	43.7													
Ce	196.5	172.8	184.7	120.9	98.9	109.9	146.7	146.7	135.9	80.3	129.5	139.7	85.8	114.2	80.6	86.2	83.4													
Nd	84.5	87.2	85.8	48.4	42.8	45.6	46.6	46.6	45.6	48.7	29.2	40.6	51.7	30.3	40.1	29.6	29.4													
Sm	14.9	17.5	16.2	8.1	7.8	8.0	8.4	8.4	8.4	7.7	5.8	6.3	9.3	7.2	4.7	5.2														
Eu	1.6	2.0	1.8	1.5	1.5	1.4	1.4	1.4	1.4	1.2	1.1	0.7	1.4	1.0	0.6	0.6	0.6													
Gd	11.8	14.6	13.2	6.3	6.4	6.0	6.0	5.3	4.7	4.4	5.3	5.3	5.6	5.3	3.6	3.6	3.7													
Dy	7.9	11.9	9.4	4.3	4.4	3.8	3.8	3.8	3.8	2.9	3.3	2.3	5.0	4.1	3.5	2.3	2.3													
Ho	1.6	2.5	2.0	0.8	0.9	0.7	0.7	0.7	0.7	0.5	0.6	0.4	1.4	0.8	0.7	0.4	0.4													
Er	3.7	6.4	5.1	2.3	2.1	2.2	1.7	1.7	1.7	1.2	1.5	1.0	3.6	2.1	1.9	1.2	1.1													
Yb	2.9	4.8	3.8	1.8	1.5	1.7	1.2	1.2	1.2	0.8	1.2	0.7	2.8	1.5	1.4	1.0	0.8													
Lu	0.4	0.6	0.5	0.3	0.2	0.2	0.2	0.2	0.2	0.1	0.2	0.1	0.2	0.1	0.2	0.1	0.2													
Fe <sub>2</sub> O <sub>3</sub>	7.20	8.50	7.85	3.90	3.60	3.20	3.57	3.50	3.00	3.10	3.18	3.10	2.90	1.90	2.00	1.80	2.23													
FeMg	0.87	0.88	0.87	0.87	0.88	0.87	0.88	0.85	0.85	0.89	0.87	0.88	0.87	0.89	0.82	0.80	0.87													
ACNK	0.85	0.85	0.93	1.01	0.95	0.96	1.02	1.00	0.92	0.99	0.98	1.00	1.03	1.02	1.00	0.98	1.01													
K <sub>2</sub> O/Na <sub>2</sub> O	1.95	1.12	1.09	1.14	1.29	1.25	1.22	1.37	1.22	1.42	1.38	1.35	1.29	1.42	1.59	1.44	1.55													
K <sub>2</sub> O+Na <sub>2</sub> O	7.60	7.00	7.30	7.90	8.10	7.93	8.30	8.20	8.70	8.10	8.33	7.80	8.00	8.30	8.60	8.40	8.24													
La/Yb <sub>in</sub>	23.89	11.37	16.12	22.94	21.56	22.30	45.35	45.35	45.35	57	57	57	57	57	57	57	57													
Eu/Eu <sub>in</sub>	0.35	0.36	0.36	0.61	0.65	0.63	0.57	0.57	0.62	0.40	0.49	0.47	0.51	0.41	0.43	0.41	0.43													

**Table 2 (continued)**  
**b - Chemical composition of the Redenção Granite (analyse LAKEFIELD-GEOSOL)**

	pBMGp				sLMZG				eLMZG				LMcSg					
	DC		JCR 07	JCR 02	JCR 20A	JCR 07	JCR 02	JCR 83B	DCR		DCR 120	DCR 56A	DCR		DCR 42	DCR 07	$\bar{X}$	
SiO <sub>2</sub> (wt %)	74.20	74.40	74.60	75.00	74.55	73.20	74.50	75.10	75.20	76.20	74.84	76.30	76.00	76.15	75.30	75.80	75.90	75.67
TiO <sub>2</sub>	0.31	0.22	0.29	0.26	0.27	0.30	0.20	0.13	0.12	0.11	0.17	0.13	0.12	0.13	0.16	0.22	0.49	0.29
Al <sub>2</sub> O <sub>3</sub>	13.20	13.10	11.60	12.70	12.65	13.40	13.00	13.10	13.10	12.90	13.10	12.50	13.10	12.80	13.00	12.40	12.20	12.53
Fe <sub>2</sub> O <sub>3</sub>	1.67	1.01	0.89	1.41	1.25	1.68	1.05	1.03	0.62	0.93	1.06	0.95	0.65	0.80	1.12	0.78	1.06	0.99
FeO	0.38	0.53	0.54	0.62	0.52	0.46	0.31	0.15	0.31	0.28	0.15	0.31	0.31	0.21	0.43	0.55	0.39	0.46
MnO	0.04	0.04	0.04	0.03	0.04	0.09	0.09	0.06	0.06	0.05	0.07	0.04	0.03	0.04	0.06	0.05	0.04	0.05
MgO	0.23	0.18	0.22	0.21	0.18	0.22	0.18	0.22	<0.10	0.13	<0.10	0.13	<0.10	<0.10	<0.10	0.14	0.15	0.14
CaO	0.98	0.67	0.66	0.89	0.80	1.30	0.88	0.72	0.80	0.71	0.88	0.69	0.55	0.62	0.42	0.71	0.62	0.58
Na <sub>2</sub> O	3.40	2.80	3.30	3.23	3.10	3.30	3.60	3.60	3.30	3.38	3.40	3.40	3.10	3.25	3.40	3.00	2.70	3.03
K <sub>2</sub> O	5.30	5.30	4.80	5.18	5.50	5.30	5.10	5.20	5.00	5.22	4.90	5.40	5.15	5.30	5.40	5.80	5.50	5.50
P <sub>2</sub> O <sub>5</sub>	0.06	0.04	0.04	0.05	0.05	0.08	0.04	0.03	0.02	<0.01	0.03	0.02	0.01	0.02	0.02	0.02	0.02	0.02
PF	0.24	0.73	0.39	0.45	0.49	0.61	0.51	0.55	0.53	0.54	0.48	0.47	0.33	0.59	0.42	0.33	0.45	0.45
Total	100.0	99.62	97.37	99.18	99.78	99.50	99.53	99.71	99.90	99.68	99.72	99.44	99.58	99.94	99.50	99.69	99.71	
Ba (ppm)	880	489	626	686	670	1442	962	463	591	417	775	198	32	115	390	311	512	404
Rb	215	281	193	238	232	267	389	440	422	345	373	430	396	413	393	254	300	316
Sr	179	122	151	155	152	228	171	94	119	92	141	72	27	50	87	78	126	97
Zr	297	240	352	299	297	391	266	218	194	196	253	171	126	149	216	261	86	188
Nb	16	24	21	19	20	38	48	63	36	30	43	34	21	28	23	25	50	33
Y	52	62	34	89	59	101	86	74	62	66	78	64	30	47	61	65	175	100
Ga	24	27	22	26	25	30	28	32	30	29	30	30	27	29	24	24	19	22
Sc	<10	<10	<10	<10	<10	<10	<10	<10	<10	<10	<10	<10	<10	<10	<10	<10	<10	<10
Th	<5	<5	<5	<5	<5	<5	<5	<5	<5	<5	<5	<5	<10	<10	15	<5	26	15
U	<10	<10	17	11	<10	20	19	16	<10	20	19	16	<10	<10	20	<10	17	15
V	<10	<10	<10	<10	<10	<10	<10	<10	<10	<10	<10	<10	<10	<10	<10	<10	<10	<10
La (ppm)	56.8	79.0	67.9	58.4	58.4	42.8	44.6	48.6	48.6	42.8	44.6	48.6	11.9	11.9	61.8	56.2	59.0	
Ce	114.4	145.2	129.8	111.6	83.9	86.7	94.1	31.9	31.9	31.9	29.7	29.7	9.2	9.2	114.1	102.2	108.2	
Nd	36.3	47.1	41.7	33.3	33.3	28.4	27.3	28.4	27.3	28.4	27.3	28.4	27.3	29.7	24.6	30.9	27.8	
Sm	6.6	9.1	7.9	6.1	5.6	5.5	5.7	5.6	5.5	5.6	5.7	5.6	5.7	5.8	5.6	5.6	4.7	
Eu	0.7	1.0	0.8	1.0	0.9	1.0	1.0	1.0	1.0	1.0	1.0	1.0	0.2	0.2	0.4	0.4	0.4	
Gd	5.0	7.2	6.1	4.3	4.5	4.4	4.4	4.5	4.4	4.5	4.4	4.4	1.3	1.3	2.9	4.1	3.5	
Dy	3.9	4.6	4.2	2.1	2.1	3.7	3.1	3.0	3.0	3.0	3.0	3.0	0.8	0.8	1.5	2.4	2.0	
Ho	0.8	0.9	0.9	0.4	0.8	0.6	0.6	0.6	0.6	0.6	0.6	0.6	0.2	0.2	0.3	0.5	0.4	
Er	2.1	2.2	2.2	2.2	2.3	2.3	2.3	2.3	2.3	2.3	2.3	2.3	0.4	0.4	0.4	0.9	1.1	
Yb	1.9	1.5	1.7	0.6	0.6	2.8	1.8	1.7	1.7	1.7	1.7	1.7	0.4	0.4	0.8	0.8	0.8	
Lu	0.3	0.2	0.3	0.1	0.5	0.3	0.3	0.3	0.3	0.3	0.3	0.3	0.1	0.1	0.2	0.1	0.2	
Fe <sub>2</sub> O <sub>3</sub> T	2.10	1.60	1.50	2.10	1.83	2.20	1.20	1.20	0.97	1.10	1.37	1.30	1.00	1.15	1.60	1.40	1.50	
Fe/Mg	0.90	0.87	0.91	0.90	0.92	0.86	0.93	0.88	0.92	0.90	0.94	0.92	0.93	0.90	0.90	0.91	0.91	
ACNK	1.01	1.04	1.00	1.04	1.02	1.00	1.02	1.03	1.01	1.06	1.02	1.03	1.10	1.06	1.07	1.03	1.03	1.04
K <sub>2</sub> O/Na <sub>2</sub> O	1.56	1.56	1.89	1.45	1.60	1.77	1.61	1.42	1.44	1.52	1.44	1.74	1.59	1.56	1.80	2.15	1.81	
K <sub>2</sub> O+Na <sub>2</sub> O (La/Yb)N	8.70	8.70	8.10	8.40	8.60	8.70	8.80	8.30	8.60	8.30	8.70	8.40	8.30	8.70	8.40	8.50	8.53	
Eu/Eu*	0.37	0.35	0.35	0.36	0.57	0.51	0.62	0.56	0.56	0.56	0.56	0.56	0.29	0.29	0.37	0.26	0.31	

Data source: Oliveira (2001); C - clinopyroxene; H - hornblende; B - biotite; MgG - monzogranite; L - leucosome; Sg - syenogranite; c - coarse-grained; s - medium-grained seriated; e - medium, even-grained; x - Average; Fe/Mg = FeO/(FeO+MgO); óxidos (wt %); ACNK = Al<sub>2</sub>O<sub>3</sub>/(Na<sub>2</sub>O+CaO+K<sub>2</sub>O) mol.

fluorescence combined with atomic absorption spectrometry. Rare earth elements (REE) were analyzed using inductively coupled plasma (ICP) atomic emission spectrometry. FeO was analyzed by wet chemistry at the Geosciences Center of the Federal University of Pará.

### 3.3.2. Results

In the R1-R2 diagram (De La Roche et al., 1980), the samples of the Redenção Granite display a subalkaline trend (Fig. 7a) and, except for the clinopyroxene-bearing facies which has a chemical granodioritic composition, plot in the fields of syenogranite and monzogranite. The studied granites vary from metaluminous to slightly peraluminous with decreasing Fe + Mg + Ti content, corresponding with increasing silica (Fig. 7b; A-B diagram, Debon and Le Fort, 1983). Average A/CNK values vary from 0.85 to 1.06 (Table 2; the average for rapakivi granites is 0.99 and they also plot close to the metaluminosity-peraluminosity boundary; Rämö and Haapala, 1995). The varieties containing amphibole ± clinopyroxene are mostly metaluminous, the biotite monzogranites are essentially peraluminous, and the leucogranites display the more accentuated peraluminous character compared to the other facies. The total alkali contents display a positive correlation with SiO<sub>2</sub> and vary from 7.0 to 8.80 wt. % (Table 2). The K<sub>2</sub>O/Na<sub>2</sub>O ratios are between 1 and 2 (Fig. 7c) and increase from the biotite-amphibole monzogranites to the leucogranites. The FeO<sub>t</sub>/(FeO<sub>t</sub>+MgO)-SiO<sub>2</sub> diagram (Fig. 7d) shows that FeO<sub>t</sub>/(FeO<sub>t</sub>+MgO) is higher than 0.8 and also increases with SiO<sub>2</sub> (Table 2). These values are lower than those dominant in typical rapakivi granites (Rämö and Haapala, 1995). They are, however, consistent with those reported in oxidized A-type granites (Dall'Agnol and Oliveira, 2006).

In the Redenção granite, SiO<sub>2</sub> contents vary from 66.1 to 76.3 wt. % and Al<sub>2</sub>O<sub>3</sub> from 12.0 to 14.2 wt. % (Table 2). Except for the clinopyroxene-bearing granite, the major element compositions of the different facies overlap, but there is a general trend of increasing silica content from the biotite-amphibole monzogranites to the leucogranites, passing through the biotite monzogranites (Fig. 8). TiO<sub>2</sub>, Al<sub>2</sub>O<sub>3</sub>, Fe<sub>2</sub>O<sub>3t</sub>, MgO, CaO, and P<sub>2</sub>O<sub>5</sub> decreases, and K<sub>2</sub>O increase from the biotite-hornblende monzogranites to the leucogranites (Fig. 8). The decrease of TiO<sub>2</sub>, Fe<sub>2</sub>O<sub>3t</sub>, MgO, CaO, and P<sub>2</sub>O<sub>5</sub> may be correlated with the early crystallization of clinopyroxene, hornblende, magnetite, ilmenite, and apatite. Al<sub>2</sub>O<sub>3</sub> and, in part, CaO decrease can be explained by the early crystallization of andesine-calcic oligoclase. Na<sub>2</sub>O concentrations are relatively uniform.

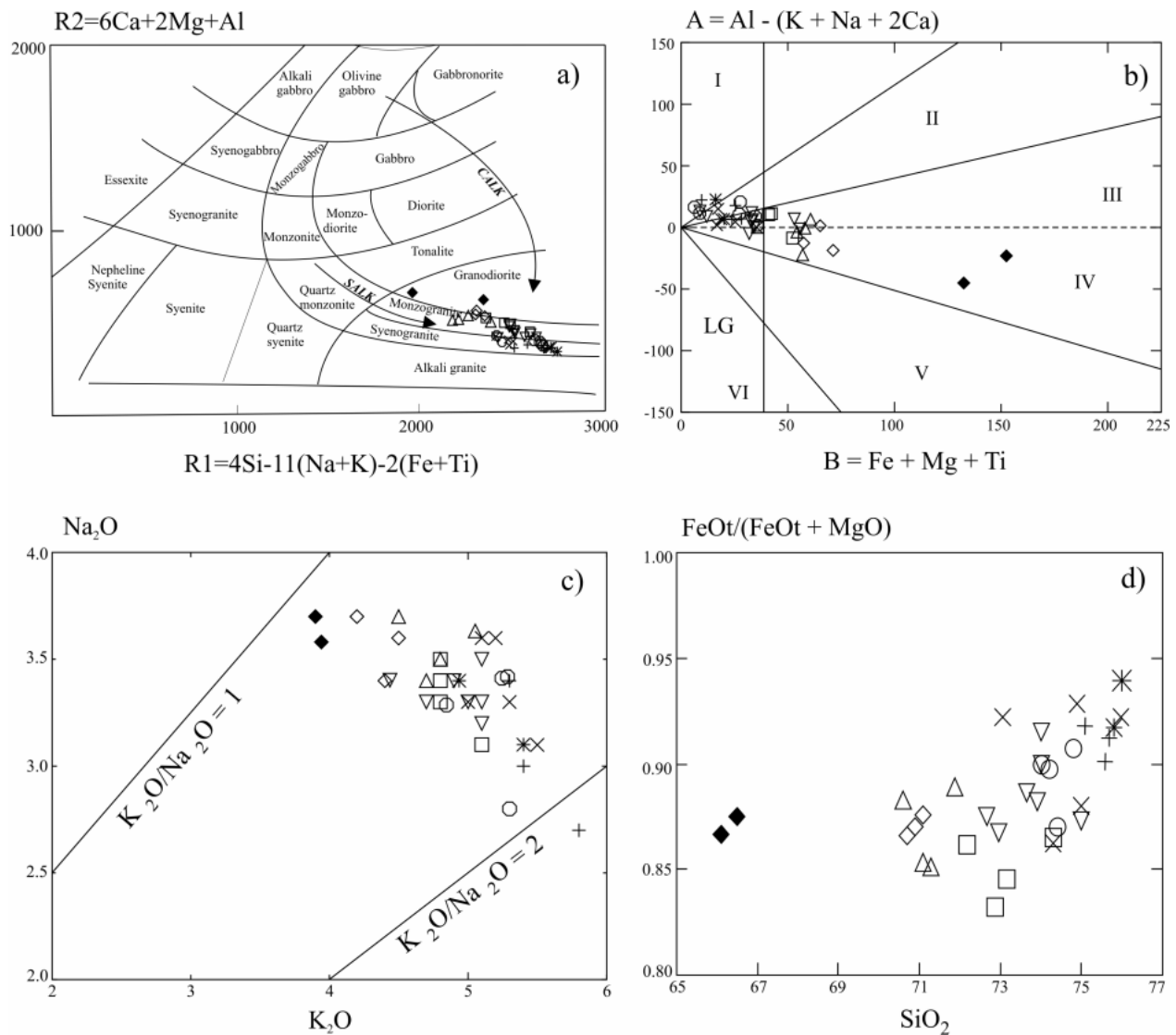


**Fig. 7.** Whole-rock geochemical plots for the Redençao pluton: (a) Classification using the parameters R1 and R2 (De la Roche et al. 1980), calculated from millication proportions; (b) A-B diagram after Debbon and Le Fort (1983) of Redençao granite samples – dashed line indicates boundary between peraluminous (above the dashed line) and metaluminous (below the dashed line) fields -; (c)  $\text{Na}_2\text{O}$  vs  $\text{K}_2\text{O}$  plot, showing the samples falling between 1 and 2; (d)  $\text{FeO}_t/(\text{FeO}_t + \text{MgO})$  vs  $\text{SiO}_2$  plot. Symbols as in Fig. 3.

Several major element chemical data features of the studied granites, including high  $\text{Fe}/\text{Mg}$ , medium to high  $\text{TiO}_2/\text{MgO}$ , and low  $\text{Al}_2\text{O}_3$ ,  $\text{CaO}$ , and  $\text{MgO}$ , are typical of A-type granites (Collins et al. 1982; Whalen, 1987; Anderson and Bender, 1989; Eby, 1992; Patiño Douce, 1997; Frost et al., 2001; Dall'Agnol and Oliveira, 2006).

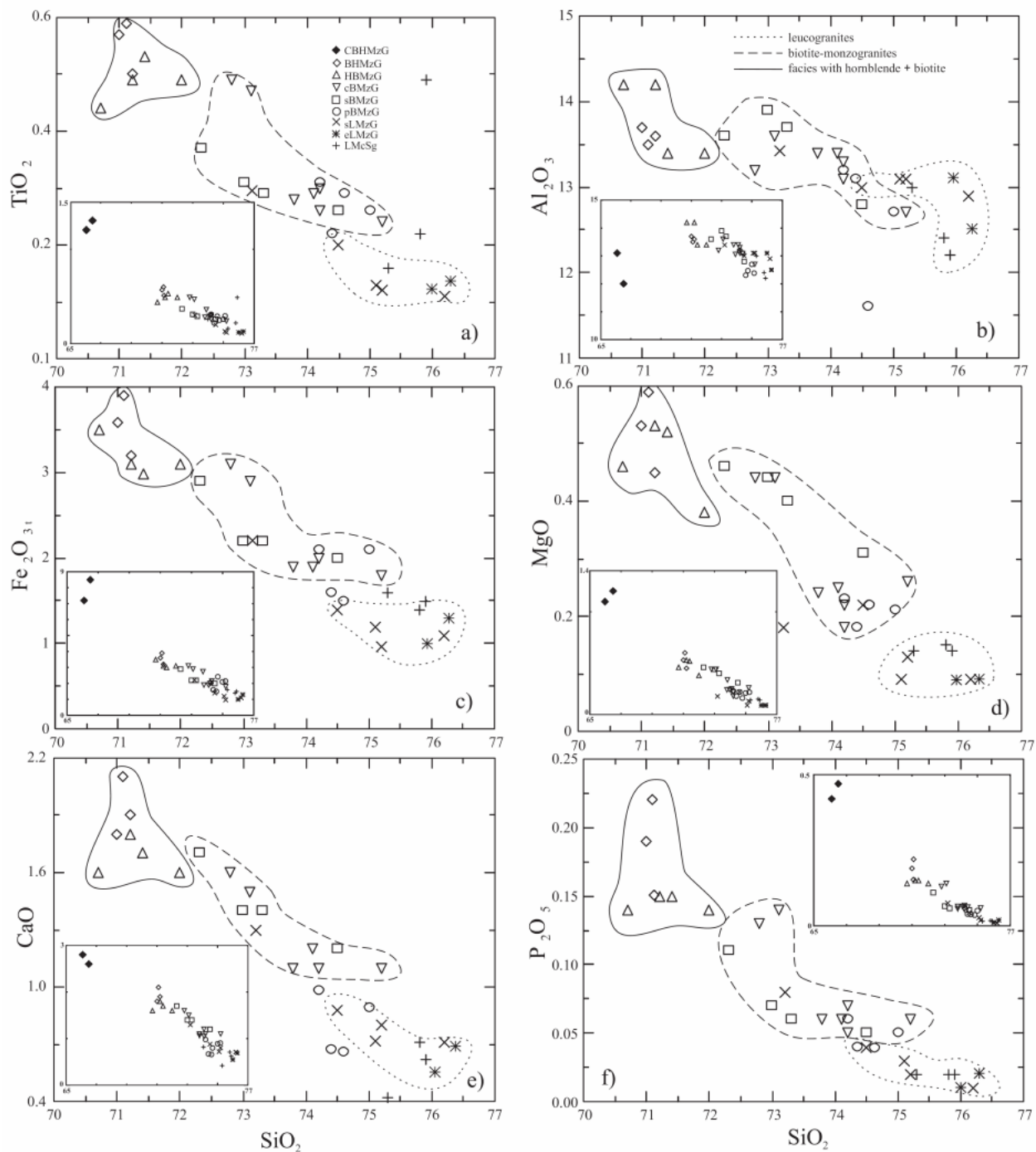


**Fig. 8.** Harker-variation diagrams of major element compositions (wt%) for Redenção granite samples. Insets illustrate the compositional gap between the clinopyroxene-bearing monzogranite and remaining facies. Abbreviations as in Table 1.

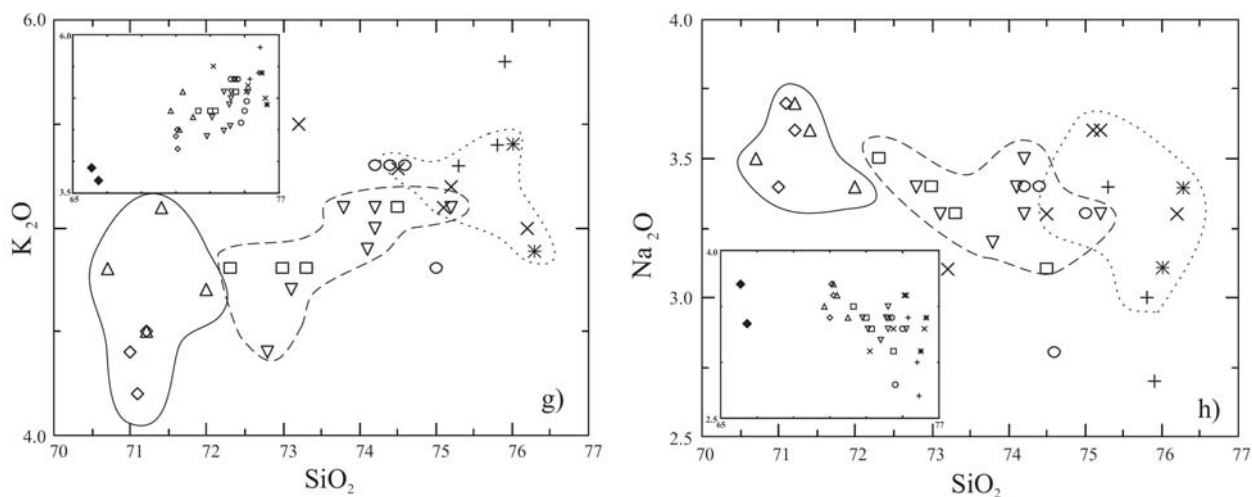


**Fig. 8** (continued). Harker-variation diagrams of major element compositions (wt%) for Redenção granite samples. Insets illustrate the compositional gap between the clinopyroxene-bearing hornblende-enriched monzogranite and remaining facies. Abbreviations as in Table 1.

Compared to the other varieties, the two analyzed samples of the clinopyroxene-biotite-amphibole monzogranites display the lowest content of SiO<sub>2</sub> and K<sub>2</sub>O, and the highest contents of TiO<sub>2</sub>, Fe<sub>2</sub>O<sub>3t</sub>, MgO, CaO, and P<sub>2</sub>O<sub>5</sub>. There is a large compositional gap between these rocks and those representative of others varieties (Fig. 8), which is a reflection of their higher mafic mineral content of and lower modal proportions of quartz and K-feldspar of the former (Table 1; Fig. 3). This feature, associated with field and textural evidence, is indicative of a cumulitic nature for the mafic clusters enriched in clinopyroxene observed in this facies.

Except for the clinopyroxene-bearing monzogranites, the biotite-amphibole monzogranites are geochemically the less evolved rocks. In spite of their textural contrasts, the seriated and the coarse even-grained biotite monzogranites have similar compositions. The general trends of the biotite monzogranites and leucogranites are not aligned in the TiO<sub>2</sub>, Fe<sub>2</sub>O<sub>3t</sub>, MgO, and P<sub>2</sub>O<sub>5</sub> Harker plots (Fig. 8), suggesting that the leucogranite magma is probably not a residual liquid derived from the biotite monzogranites by fractional crystallization. The less evolved facies are exposed in the south part and the more evolved in the central part of the pluton (Fig. 4).

The trace element Harker diagrams show a good negative correlation of Ba, Zr, and Sr with SiO<sub>2</sub>, and a positive correlation of Rb with SiO<sub>2</sub>. Rb displays a remarkable increase from the biotite-amphibole monzogranites to the leucogranites (Fig. 9a), having a clear incompatible behavior during the magmatic evolution of the Redenção pluton. On the other hand, Ba, Sr, and

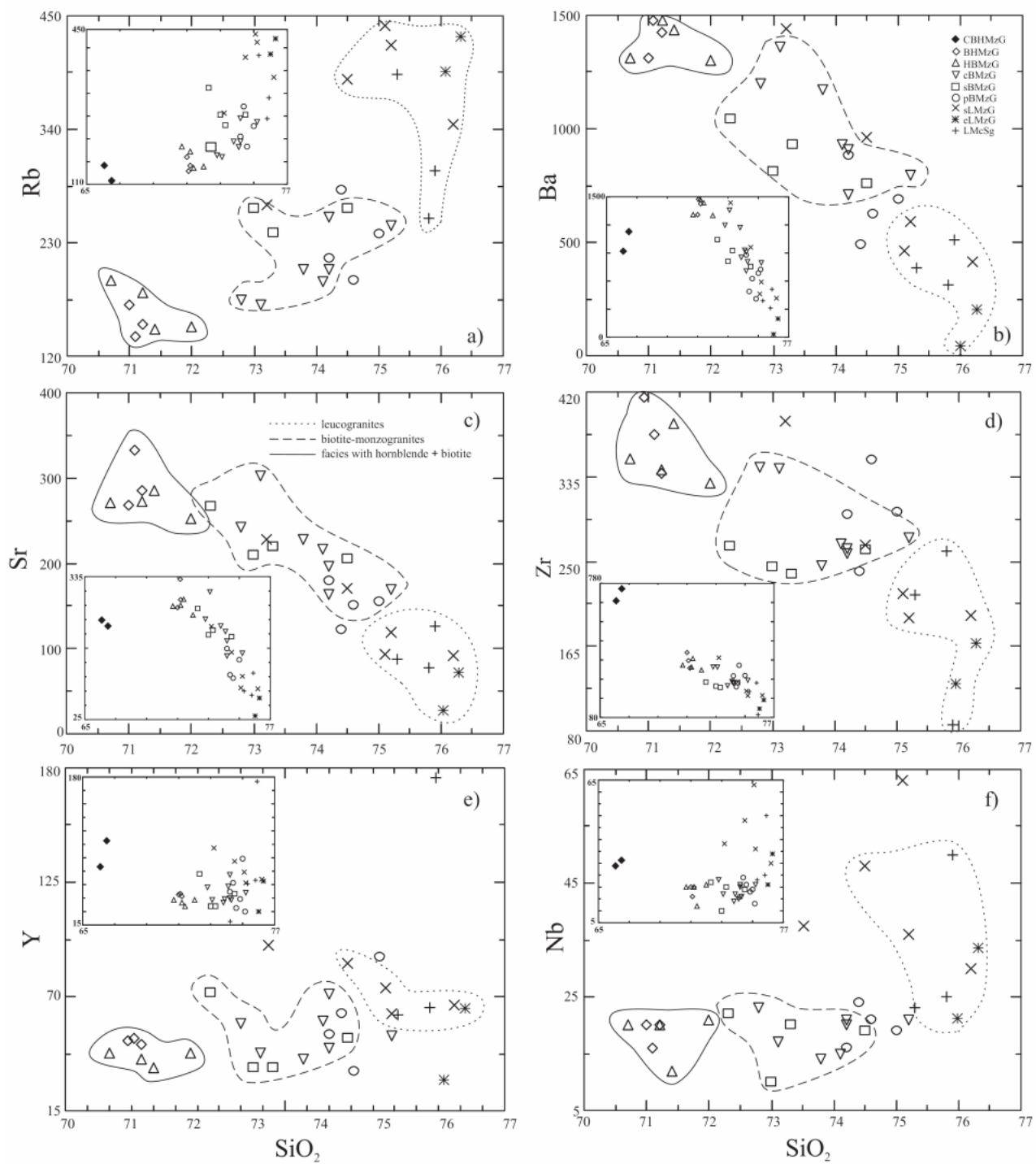


**Fig. 9.** Representative trace element variation diagrams for Redenção Granite samples. Insets illustrate the compositional gap between the clinopyroxene-bearing hornblende-enriched monzogranite and remaining facies. Symbols as in Fig. 3.

Zr, behave as compatible elements during the magmatic evolution (Figs. 9b, c, and d). Zr behavior (Fig. 9d) indicates that it was strongly compatible since early crystallization stages, which is consistent with petrographic evidence of zircon crystallization as a near liquidus phase (Fig. 6). Y and Nb do not define clear trends in Harker diagrams, but the leucogranites are enriched in these elements compared to the other facies (Fig. 9e, f).

### 3.3.3. The Behavior of Rb, Sr, and Ba

The contrasting behavior of Rb, Sr, and Ba, in different mineral phases is useful in estimating the extent of fractionation of distinct minerals and whether magmatic evolution was controlled dominantly by fractional crystallization, partial melting or more complex processes (Hanson, 1978, 1989; Rollinson, 1993; Dall'Agnol et al., 1999b). In addition to quartz, the most abundant minerals in the Redenção Granite are plagioclase, alkali feldspar, biotite, and amphibole. Considering the range of silica and other geochemical parameters, as well as textural evidence, it could be expected that plagioclase had an important role in the magmatic evolution of the granite. Hornblende was certainly also a significant phase during the early magmatic stage. On the other hand, the influence of alkali feldspar and biotite in the evolution of liquid composition should increase in the more felsic rocks, because in the more mafic varieties both are relatively late phases.

Ba and Sr are strongly compatible in granitic systems. They display a positive correlation (Fig. 10a) and show large variation, decreasing in the studied granite from the more mafic to the more felsic varieties (1498 to 32 ppm and 332 to 27 ppm, respectively; Table 2; Fig. 10a). Rb, on the other hand, behaves as an incompatible element and increases toward the leucogranites. As a consequence, Rb and Sr correlate negatively (Fig. 10b). In the Rb/Sr – Sr/Ba plot (Fig. 10c), a rapid increase in the Rb/Sr ratio from the low-silica to the more silica-rich samples is observed, while the Sr/Ba ratio remains almost constant. In these plots, the biotite monzogranites and the leucogranites tend to display distinct trends, suggesting that they could be derived from different liquids.

In the above-mentioned geochemical plots (Fig. 10), the analyzed rocks follow non linear trends. This aspect, associated with the large variations of Rb, Sr, Ba, and Rb/Sr are indicative of fractional crystallization with changes in the fractionating assemblage in contrast to partial melting or equilibrium crystallization dominated processes (Hanson, 1989; Caskie, 1984; Rämö,

1991; Dall'Agnol et al., 1999b). An alternative hypothesis is to admit the influence of more complex processes in the magma evolution. With the exception of local evidence for magma mingling processes, generally involving porphyritic varieties, there is little evidence in the pluton of processes such as magma mixing that could explain these geochemical characteristics.

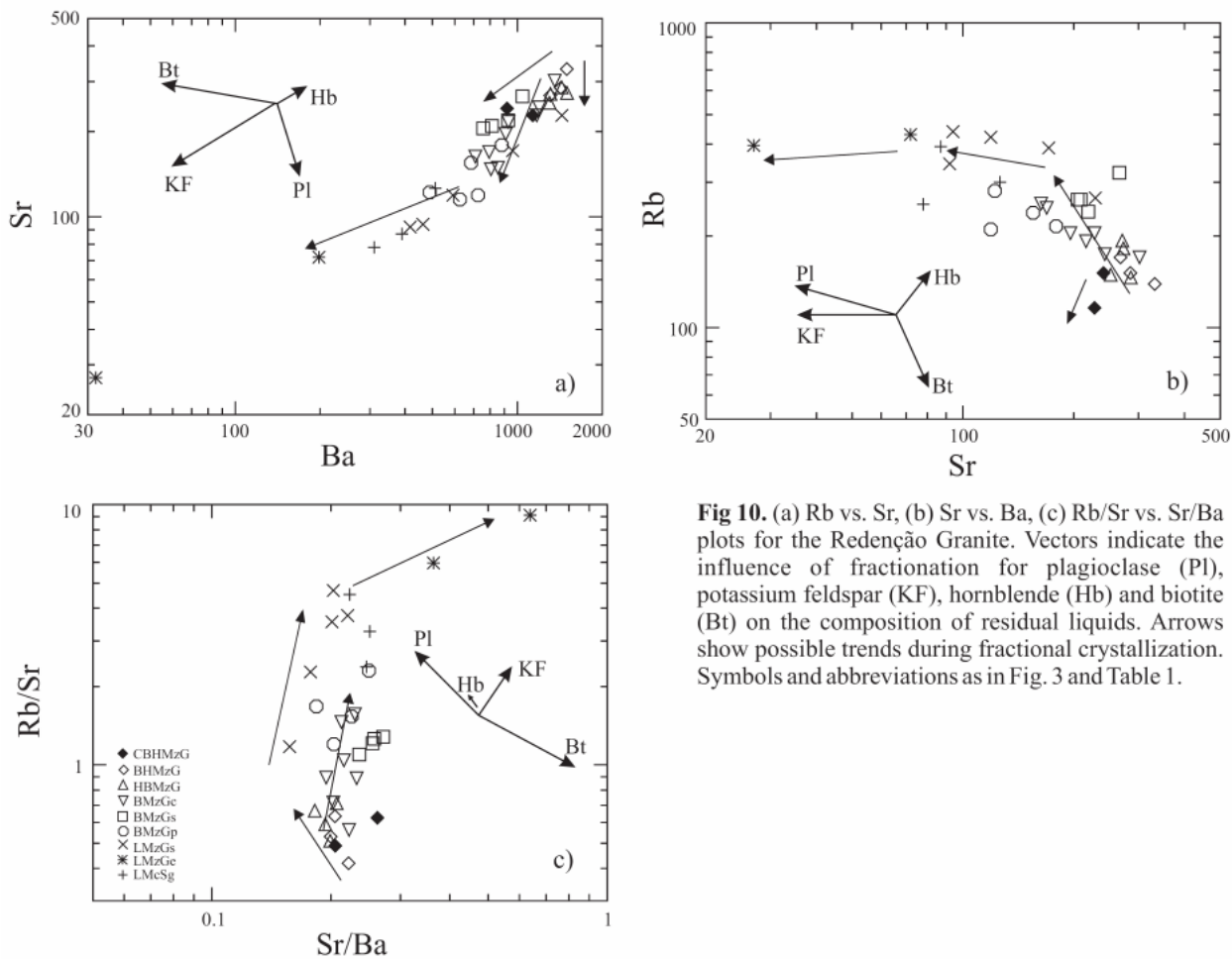


**Fig 10.** (a) Rb vs. Sr, (b) Sr vs. Ba, (c) Rb/Sr vs. Sr/Ba plots for the Redenção Granite. Vectors indicate the influence of fractionation for plagioclase (Pl), potassium feldspar (KF), hornblende (Hb) and biotite (Bt) on the composition of residual liquids. Arrows show possible trends during fractional crystallization. Symbols and abbreviations as in Fig. 3 and Table 1.

In the Sr-Ba and Rb-Sr plots (Fig. 10a, b), the clinopyroxene-bearing hornblende-enriched monzogranites are impoverished in Rb, Sr, and Ba compared to the hornblende-biotite monzogranites. This feature could be explained by derivation of the less evolved, mafic-enriched varieties by cumulitic concentration of hornblende and clinopyroxene in the hornblende-biotite monzogranite magma. The magmatic evolution from the hornblende-biotite monzogranites to the biotite monzogranites was accompanied by decrease of Sr and Ba, and increase of Rb, resulting fast increase of Rb/Sr ratios with little variation of Sr/Ba (Fig. 10 a, b, c). This suggests fractional

crystallization controlled by plagioclase with the subordinate influence of hornblende and K-feldspar. Compared to the hornblende-biotite monzogranites, the leuogranites display a similar but apparently independent trend in the Rb/Sr vs Sr/Ba plot, while in the Sr-Ba and Rb-Sr plots they show clearly distinct trends that indicate a dominant influence of K-feldspar in the liquid evolution (Fig. 10a, b, c). Biotite apparently exerted a limited influence during the fractional crystallization of the studied granites, but the effects of mica fractionation could have been masked by the larger volume fractionation of alkali feldspar and plagioclase. Nevertheless, some of the silica-richer samples show relatively low Rb contents which indicate a greater extent of biotite fractionation in the more evolved liquids.

Geochemical data are not conclusive but several diagrams (Fig. 8a, c, d, e, f; 9b, c, f; 10a, c) reinforce the hypothesis of origin of at least some of the porphyritic biotite monzogranites by mingling between the biotite monzogranites and the leuogranites, as supported by field and petrographic data.

### 3.3.4. Rare Earth Elements

Rare earth element (REE) analytical data (Table 2) and the corresponding chondrite-normalized plots (Fig. 11) of representative samples of the different varieties of the Redenção pluton show that the studied granites display LREE-enrichment and a significant fractionation of HREE. Average  $(\text{La/Yb})_{\text{N}}$  ratios are relatively high and show strong variation, from a minimum of 16.12 in the clinopyroxene-amphibole monzogranite to a maximum of 50.23 in the syenogranite dike facies (Table 2), with the biotite monzogranites displaying average values of ~30. The internal fractionation of HREE is also significant with  $(\text{Gd/Yb})_{\text{N}}$  ratio ranging from 5.59 to 2.15. All varieties display negative Eu anomaly with average  $\text{Eu/Eu}^*$  ranging from 0.65 to 0.29 (Table 2), and generally decreasing from the biotite-hornblende monzogranites to the leuogranites. The exceptions are the clinopyroxene-hornblende monzogranites which show an accentuated negative Eu anomaly (average  $\text{Eu/Eu}^*$  of 0.36) and the seriated leucomonzogranites with a moderate anomaly, similar to that observed in the hornblende-biotite monzogranites. In general, the negative Eu anomalies increase from the rocks with lower silica to those with higher silica content which is consistent with important feldspar fractionation.

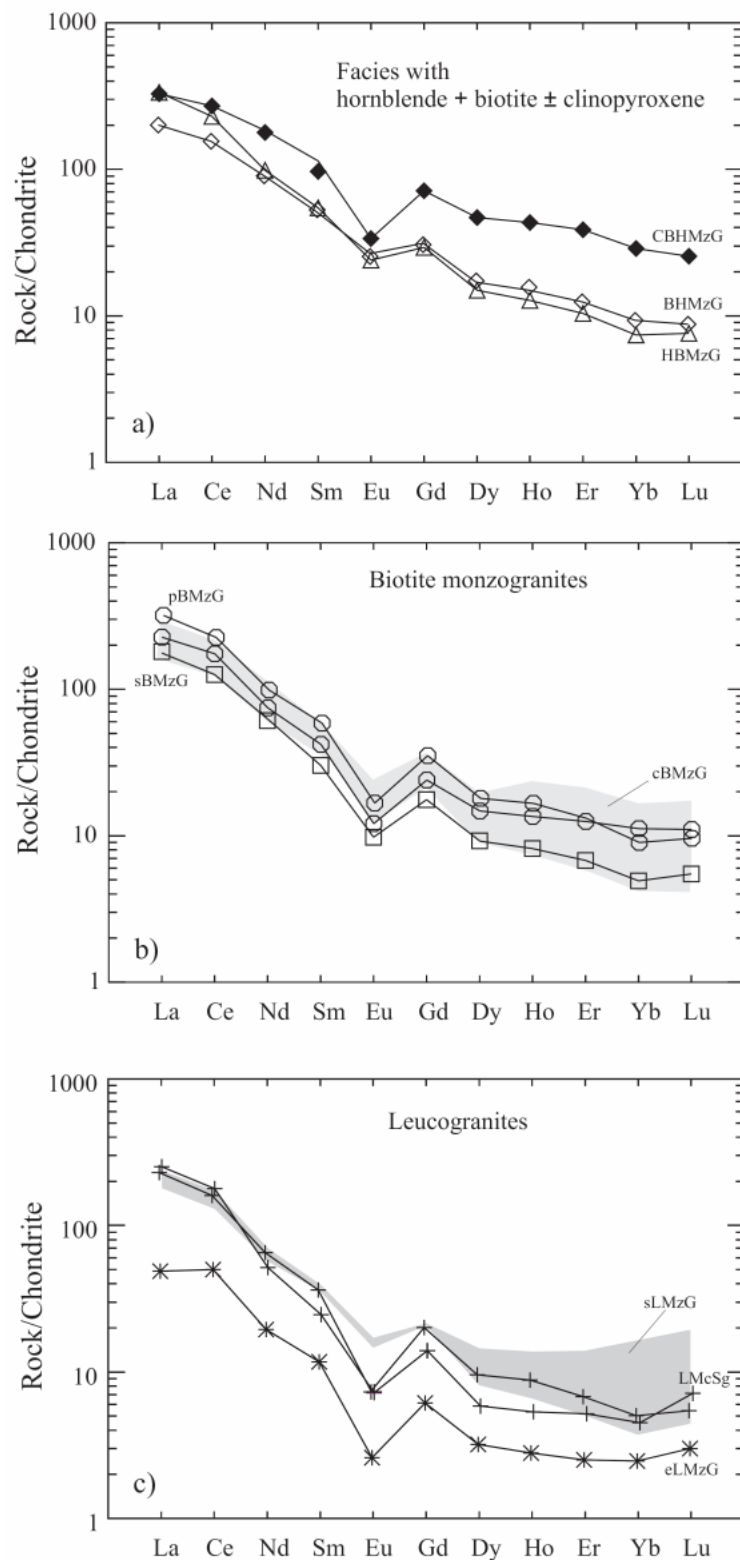


**Fig. 11.** Chondrite normalized (Evensen et al., 1978) REE patterns for representative samples of the Redenção Granite. Abbreviations and symbols as in Table 1.

The clinopyroxene-hornblende monzogranites are enriched in HREE and show a more accentuated negative Eu anomaly compared to the biotite-hornblende monzogranites (Fig. 11a). These aspects are not consistent with an origin of the latter by fractional crystallization processes from the clinopyroxene-hornblende facies but could be explained by admitting that the mafic-enriched rocks are derived from a biotite-hornblende monzogranite liquid modified mostly by cumulitic concentration of clinopyroxene and amphibole. The three varieties of biotite monzogranite display quite similar patterns (Fig. 11b) which differ from those of the hornblende-enriched facies only by the more accentuated negative Eu anomalies of the former. These patterns are consistent with the hypothesis of derivation of the biotite monzogranites from the biotite-hornblende monzogranites by fractional crystallization. The leucogranites patterns are distinct from those of other varieties of the Redenção pluton. They display a concave shape of the HREE branch (Fig. 11c) that is not observed in the other facies (Fig. 11a, b) and is indicative of important hornblende fractionation during their magmatic evolution. Another relevant aspect is the moderate negative Eu anomaly of the seriated leucomonzogranite (Fig. 11c; average Eu/Eu\* of 0.56, comparable to those of hornblende-biotite monzogranites; Table 2). This feature is not consistent with derivation of these rocks from the biotite monzogranites by fractional crystallization. On the other hand, the increase of negative Eu anomalies from the seriated to the equigranular leucomonzogranites and leucomicrosyenogranites, associated with other geochemical characteristics shown by these rocks, could suggest a derivation of the latter from the seriated leucomonzogranites.

In summary, REE data support the hypothesis of a comagmatic origin for the hornblende-biotite monzogranites and biotite monzogranites that could be related by fractional crystallization processes. The clinopyroxene-hornblende monzogranite is more probably derived from a liquid similar to the biotite-hornblende monzogranite but enriched in cumulitic mafic phases. The leucomonzogranites apparently have an origin independent to that of the other facies, being derived from a different liquid. This is not in contradiction with the hypothesis that all studied rocks are derived from similar magmatic sources, being cogenetic, but in the specific case of the leucogranites, not comagmatic.

## 4. Discussion

### 4.1. Granite Typology

In the Nb-Y and Rb-(Y+Nb) diagrams (Pearce et al., 1984), Redenção granite samples plot into the field of within-plate granites of attenuated continental crust (Fig. 12a). Ga/Al ratios vary from 3.0 to 4.8 and the highest values are encountered in the leuco granite varieties. In the diagrams proposed by Whalen et al. (1987) to distinguish geochemically A-type from S-, M-, and I-type granites, all analyzed samples plot into the A-type granite field (Fig. 12b). Moreover, Eby (1992) suggested that the Y/Nb ratio can be employed to distinguish A-type granites of mantle ( $Y/Nb < 1.2$ ; A1-subtype) or crustal ( $Y/Nb > 1.2$ ; A2-subtype) origin. All samples of the Redenção pluton have  $Y/Nb > 1.2$  and plot in the A2 field in the Rb/Nb-Y/Nb and Nb-Y-Zr/4 geochemical diagrams (Fig. 12c, d), suggesting that they are of dominantly crustal origin.

The geochemical characteristics of Redenção are similar to other studied plutons of the Jamon Suite, ie., Jamon, Musa, and Bannach. All these granites are classified as A-type granites (Dall'Agnol et al., 1999a, b, 2005; Dall'Agnol and Oliveira, 2006). The Jamon suite granites do not have calc-alkaline affinities as demonstrated by their high  $FeO_t/(FeO_t+MgO)$  ratios (Figs. 7d, 13a, b) and low  $Al_2O_3$  contents (Table 2; cf. detailed discussion in Dall'Agnol and Oliveira, 2006). They are anorogenic granites emplaced in an extensional setting (Oliveira et al., submitted b). Their origin is associated with anatexis of lower crustal rocks due to mafic underplating (Dall'Agnol et al., 1999a, 2005). It is concluded that the Redenção granite is an A-type granite but its oxidized character deserves further discussion.

### 4.2. The oxidized character of the Redenção A-type granites

All varieties of the Redenção pluton, as well as those found in other plutons of the Jamon suite, are oxidized granites. This is demonstrated by the characteristic occurrence in these rocks of magnetite as the dominant iron-titanium oxide mineral, their relatively high magnetic susceptibility values (Oliveira et al., 2002, submitted c), and the presence of the magmatic assemblage titanite – magnetite - quartz (Wones, 1989). It was estimated that the Jamon suite granites crystallized at  $fO_2$  conditions near NNO or HITMQ buffers (Dall'Agnol et al., 1997, 1999c, 2005) and, following the criteria of Ishihara (1981), they have been classified as magnetite series granites (cf. Dall'Agnol et al., 2005, and references therein).

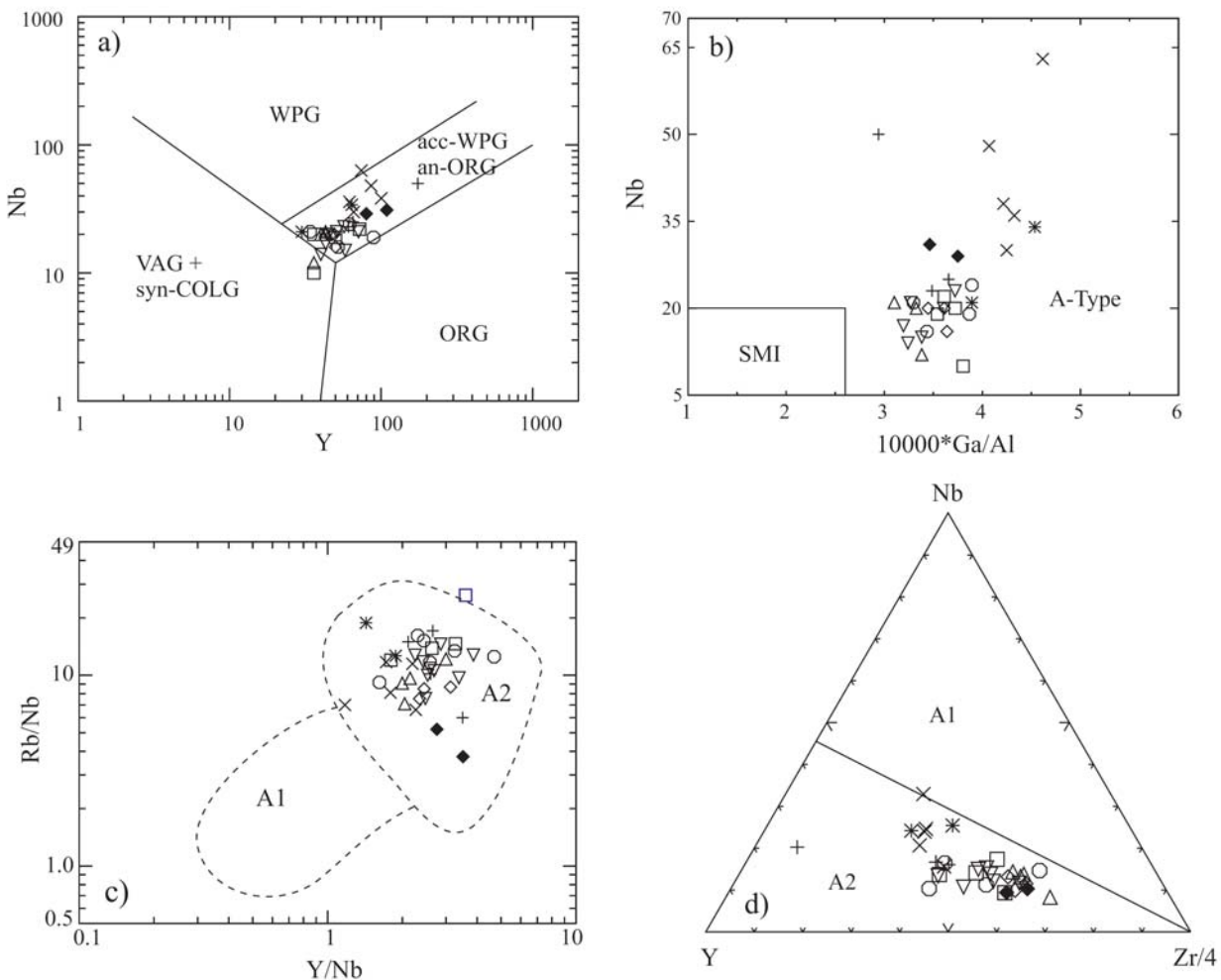


**Fig. 12.** Geochemical plots for the Redençao granite samples in: (a) Nb vs. Y tectonic discriminant diagram illustrating that Redençao Granite falls in the within-plate granite field after Pearce et al. (1984) - Syn-COLG: syn-collision granite; VAG: volcanic arc granite; WPG: within-plate granite; ORG: ocean ridge granite; (b) Nb vs.  $10000 * \text{Ga/Al}$  diagram of Whalen et al. (1987) showing A-type granite affinity; (c) the Rb/Nb vs. Y/Nb diagram of Eby (1992) with data from the Redençao pluton plotting between the fields of OIB and IAB (island-arc basalt); (d) Nb-Y-Zr/4 ternary diagram for the subdivision of A1- and A2-type granites (Eby, 1992) showing that the Redençao pluton was derived from a crustal source. Symbols as in Fig 3.

Dall'Agnol and Oliveira (2006) discussed the geochemical and petrological distinction between reduced and oxidized A-type granites and proposed some geochemical diagrams to distinguish these two sub-types. It is beyond the scope of the present paper to reproduce this discussion but some diagrams are presented here to illustrate the geochemical variation of the Redençao pluton and its oxidized A-type character (Figs. 13a, b, c). The  $\text{FeO}_t / (\text{FeO}_t + \text{MgO})$  vs.  $\text{SiO}_2$  plot (Fig. 13a) demonstrates clearly that the Redençao pluton granites are ferroan granites (Frost et al., 2001), differing from the magnesian or Cordilleran granites by their

$\text{FeO}_t/(\text{FeO}_t+\text{MgO})$  ratios higher than 0.8 and increasing from the less evolved to the more evolved varieties. The contrast between the Redenção granites and calc-alkaline granites is also evident in the  $\text{CaO}/(\text{FeO}_t+\text{MgO}+\text{TiO}_2)$  vs.  $\text{CaO}+\text{Al}_2\text{O}_3$  plot (Fig. 13b). The lower  $\text{CaO}$  and  $\text{Al}_2\text{O}_3$  contents of the oxidized A-type granites, compared to calc-alkaline granites allows for a clear separation of both granites. Finally, the  $\text{FeO}_t/(\text{FeO}_t+\text{MgO})$  vs.  $\text{Al}_2\text{O}_3/(\text{K}_2\text{O}+\text{Na}_2\text{O})$  plot (Fig. 13c) distinguishes between the oxidized and reduced A-type granites. The Redenção samples display  $\text{Al}_2\text{O}_3/(\text{K}_2\text{O}+\text{Na}_2\text{O})$  ratios that are lower than those found in calc-alkaline granites and similar to those of reduced A-type granites. Their  $\text{FeO}_t/(\text{FeO}_t+\text{MgO})$  ratios, however, vary between 0.83 and 0.94 and are generally lower than those displayed by typical reduced A-type granites, as for most classical rapakivi granites (Rämö and Haapala, 1995), allowing a clear distinction of both A-subtypes.

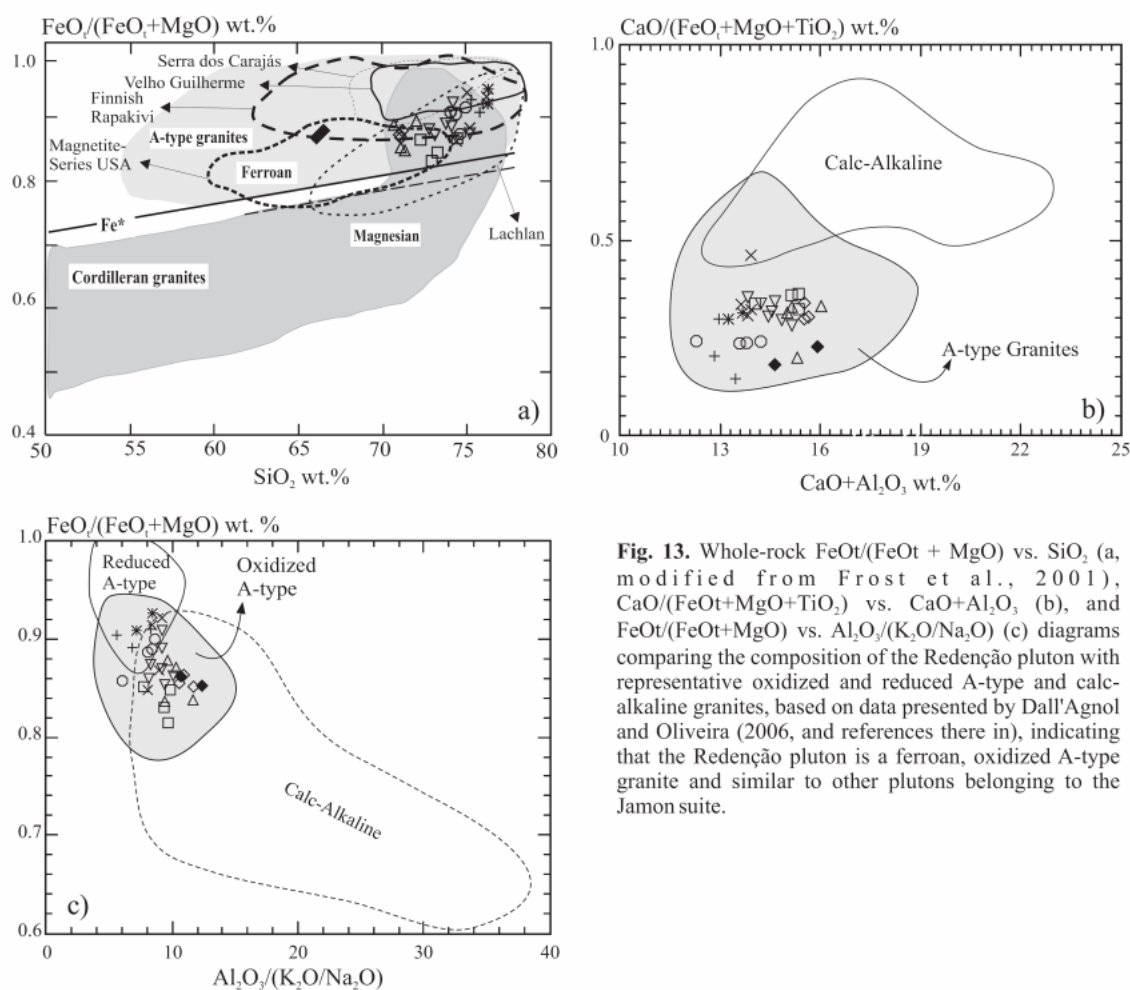


**Fig. 13.** Whole-rock  $\text{FeO}_t/(\text{FeO}_t + \text{MgO})$  vs.  $\text{SiO}_2$  (a), modified from Frost et al., 2001),  $\text{CaO}/(\text{FeO}_t+\text{MgO}+\text{TiO}_2)$  vs.  $\text{CaO}+\text{Al}_2\text{O}_3$  (b), and  $\text{FeO}_t/(\text{FeO}_t+\text{MgO})$  vs.  $\text{Al}_2\text{O}_3/(\text{K}_2\text{O}/\text{Na}_2\text{O})$  (c) diagrams comparing the composition of the Redenção pluton with representative oxidized and reduced A-type and calc-alkaline granites, based on data presented by Dall'Agnol and Oliveira (2006, and references therein), indicating that the Redenção pluton is a ferroan, oxidized A-type granite and similar to other plutons belonging to the Jamon suite.

#### 4.3. The magmatic evolution of the Redenção granites

At a first approach it could be supposed that the different varieties of the Redenção pluton derived from a unique magma by processes of fractional crystallization. A more detailed examination of geochemical data, however, revealed a more complex magmatic evolution. The restricted volume of the pluton, field relationships and the geochemical characteristics of the clinopyroxene-amphibole monzogranite are not consistent with the hypothesis that the less evolved primitive magma gave origin to the other varieties. The less evolved variety is interpreted as derived from a hornblende-biotite monzogranite liquid locally enriched in cumulitic amphibole and clinopyroxene. The biotite-hornblende monzogranites and biotite monzogranites were probably linked by fractional crystallization processes, their differentiation being controlled mostly by the early crystallization of andesine-calcic oligoclase, amphibole, magnetite, ilmenite, zircon, and apatite. The leucogranites, on the other hand, do not follow the general geochemical trends defined for the other varieties and are most probably derived from an independent magma. The geochemical characteristics of the porphyritic facies suggest that they could represent the hybrid product of mingling processes involving coarse biotite monzogranites and leucogranites.

Nd isotope data also show significant variations in the different facies of the Redenção pluton. Available data are limited to four samples, but  $\epsilon_{\text{Nd}}$  values vary from -8.8 in a coarse-grained biotite monzogranite to -10.5 in a porphyritic biotite monzogranite, with an intermediate value of -9.6 in the biotite-hornblende monzogranite (Rämö et al., 2002). The observed contrast in  $\epsilon_{\text{Nd}}$  values indicates that all the analyzed varieties are probably not comagmatic and suggests that different Archean sources could be indicated for the Redenção granites.

The proposed scheme of magmatic evolution is consistent with the sequence of emplacement proposed for the Redenção pluton by Oliveira et al. (submitted c). They admitted that the less evolved biotite-amphibole monzogranites and associated rocks were the first to be emplaced. The magma ascent was controlled by fractures and its transport was achieved via a series of dike feeder channels. The less evolved rocks are concentrated in the southern domain of the pluton, and they have been followed by the coarse biotite monzogranites that are dominant in the eastern, western and northern domains. The leucogranites are concentrated in the center of the pluton and should correspond to an independent intrusion of evolved magma. Finally, the seriated

and porphyritic biotite monzogranites were emplaced later along ring fractures probably generated by roof fracturing induce by the intrusion of the leucogranites.

## 5. Summary and conclusions

The 1.88 Ga Redenção pluton is anorogenic and displays a roughly circular zoned internal structure. Less evolved facies are located in the southern domain with more evolved leucogranites in the center of the pluton. The magmatic evolution is relatively complex involving several distinct processes whereby mafic phases accumulated in the clinopyroxene-amphibole rich facies; biotite monzogranites were derived from the biotite-hornblende monzogranites by fractional crystallization; leucogranites correspond to an independent felsic magma; and porphyritic varieties may have resulted from mingling between the coarse biotite monzogranite and leucogranite. The proposed models of magmatic evolution are considered consistent with the emplacement sequence presented for the pluton.

The geochemical characteristics of different varieties allow their classification as A-type granite and distinguish them from calc-alkaline series. The oxidized character of the Redenção granite is revealed, however, by some geochemical features, such as marginally lower  $\text{FeO}_t/(\text{FeO}_t+\text{MgO})$  ratios, that allow its distinction from reduced A-type granites. Preliminary Nd isotope data suggest that the Redenção granites are cogenetic but apparently not comagmatic. This point should be further investigated in the future.

In their broad aspects, the petrographic and geochemical characteristics and magmatic evolution of the Redenção pluton are similar to those of the other plutons belonging to the Jamon suite, e.g. the Jamon, Musa (Dall'Agnol et al., 1999b), and Bannach (Almeida et al., submitted) granites.

## Acknowledgments

To J.A.C. Almeida for participation in the field work and in the final draft of illustrations, and to our colleagues of the Group of Research on Granite Petrology for stimulating discussions about rapakivi and A-type granites geochemistry and petrogenesis. This research received financial support from CNPq (RD – 550739/2001-7, 476075/2003-3, 307469/2003-4; DCO – scholarship April04 to Nov05), CAPES (DCO – scholarship Nov01 to March04), and Federal University of Pará (UFPA). This paper is a contribution to PRONEX/CNPq (Proj. 103/98 – Proc. 66.2103/1998-0) and IGCP-510 project (IUGS-UNESCO).

## References

- Åhäll, K.I., Connelly, J.N., Brewer, T.S., 2000. Episodic rapakivi magmatism due to distal orogenesis: correlation of 1.69–1.50 Ga orogenic and inboard, “anorogenic” events in the Baltic Shield. *Geology* 28, 823– 826.
- Almeida, J.A.C., 2005. Geologia, petrografia e geoquímica do granito anorogênico Bannach, Terreno Granito-Greenstone de Rio Maria, PA. M.Sc. Thesis, Federal University of Pará, Belém, Brazil (in Portuguese), 171p.
- Almeida, J.A.C., Dall'Agnol, R., Oliveira, D.C., Submitted. Geologia, petrografia e geoquímica do granito anorogênico Bannach, Terreno Granito-Greenstone de Rio Maria, Pará. *Revista Brasileira de Geociências*.
- Althoff, F.J., Barbey, P., Boullier, A.-M., 2000., 2.8–3.0 Ga plutonism and deformation in the SE Amazonian craton: the Archean granitoids of Marajoara (Carajás mineral province). *Precambrian Research* 104, 187– 206.
- Amelin, Y.V., Larin, A.M., Tucker, R.D., 1997. Chronology of multiphase emplacement of the Salmi rapakivi granite–anorthosite complex, Baltic shield: implications for magmatic evolution. *Contributions to Mineralogy and Petrology* 127, 353–368.
- Anderson, J.L. 1983. Proterozoic anorogenic granite plutonism of North America. In: Medaris, L.G., Mickelson, D.M., Byers, C.W., Shanks, W.C. (Eds.), *Proterozoic Geology*. Geol.Soc. Am. Mem. 161, 133-154.
- Anderson, J.L., Bender, E.E., 1989. Nature and origin of Proterozoic A-type granitic magmatism in the southwestern United States of America. *Lithos* 23, 19-52.
- Anderson, J.L., Cullers, R.L. 1978. Geochemistry and evolution of the Wolf River Batholith, a Late Precambrian rapakivi massif in North Wisconsin, USA. *Precambrian Research*, 7:287-324.
- Anderson, J.L., Smith, D.R., 1995. The effects of temperature and  $fO_2$  on the Al-in-hornblende barometer. *American Mineralogist* 80, 549-559.
- Anderson, J.L., Morrison, J., 2005. Ilmenite, magnetite, and peraluminous Mesoproterozoic anorogenic granites of Laurentia and Baltica. *Lithos* 80, 45–60.
- Bettencourt, J.S., Tosdal, R., Leite, W.B., JR., Payolla, B.L., 1995. Overview of the rapakivi granites of the Rondônia Tin Province (RTP). In: *Symposium on Rapakivi Granites and*

- Related Rocks. Excursion Guide and Programs... Belém, pp. 5-14.
- Bonin, B., 1996, A-type granite ring complexes: mantle origin through crustal filters and the anorthosite-rapakivi magmatism connection. In: Demaiffe, D., (Ed.), Petrology and Geochemistry of Magmatic Suites of Rocks in the Continental and Oceanic Crusts. A volume dedicated to Professor Jean Michot, Université Libre de Bruxelles-Royal Museum for Central Africa (Tervuren), 201-218.
- Caskie D.R.M., 1984. Identification of petrogenetic processes using covariance plots of trace-element data. *Chemical Geology*, 42:325-341
- Clemens, J.D., Holloway, J.R., White, A.J.R., 1986. Origin of the A-type granite: experimental constraints. *American Mineralogist* 71, 317-324.
- Collins, W.J., Beams, S.D., White, A.J., Chappell, B.W., 1982. Nature and origin of A-type Granites with particular reference to Southeastern Australia. *Contributions to Mineralogy and Petrology* 80, 189-200.
- Creaser, R.A., Price, R.C., Wormald, R.J., 1991. A-type granites revisited: assessment of a residual-source model. *Geology* 19, 163-166.
- Dall'Agnol, R., Lafon, J.M., Macambira, M.J.B., 1994. Proterozoic anorogenic magmatism in the Central Amazonian province: geochronological, petrological and geochemical aspects. *Mineralogy and Petrology* 50, 113-138.
- Dall'Agnol, R., Pichavant, M., Champenois, M., 1997. Iron-titanium oxide mineral of the Jamon granite, Eastern Amazonian region, Brazil: implications for the oxygen fugacity in Proterozoic A-type granites. *Anais da Academia Brasileira de Ciências* 69, 325-347.
- Dall'Agnol, R., Costi, H.T., Leite, A.A., Magalhães, M.S., Teixeira, N.P., 1999a. Rapakivi granites from Brazil and adjacent areas. *Precambrian Research* 95, 9-39.
- Dall'Agnol, R., Rämö, O.T., Magalhães, M.S., Macambira, M.J.B., 1999b. Petrology of the anorogenic, oxidised Jamon and Musa granites, Amazonian craton: implications for the genesis of Proterozoic A-type granites. *Lithos* 46, 431-462.
- Dall'Agnol, R., Scaillet, B., Pichavant, M., 1999c. An Experimental Study of a Lower Proterozoic A-Type Granite from the Eastern Amazonian Craton, Brazil. *Journal of Petrology* 40, 1673-1698.
- Dall'Agnol, R., Teixeira, N.P., Rämö, O.T., Moura, C.A.V., Macambira, M.J.B., Oliveira, D.C., 2005. Petrogenesis of the Paleoproterozoic, rapakivi, A-type granites of the Archean Carajás

- Metallogenic Province, Brazil. *Lithos* 80, 101-129.
- Dall'Agnol, R., Oliveira, D.C., 2006. Oxidized, magnetite-series, rapakivi-type granites of Carajás, Brazil: implications for classification and petrogenesis of A-type granites. *Lithos* (In press).
- Dall'Agnol, R., Oliveira, M.A., Almeida, J.A.C., Althoff, F.J., Leite, A.A.S., Oliveira, D.C., Barros, C.E.M., 2006. Archean and Paleoproterozoic granitoids of the Carajás metallogenic province, eastern Amazonian craton. In: Dall'Agnol, R., Rosa-Costa, L.T., Klein, E.L. (eds.). *Symposium on Magmatism, Crustal Evolution, and Metallogenesis of the Amazonian Craton. Abstracts Volume and Field Trips Guide*. Belém, PRONEX-UFPB/SBG-NO, 150p.
- Debon, F., Le Fort, P., 1983. A chemical-mineralogical classification of common plutonic rocks and associations. *Trans. R. Soc. Edinburg: Earth Sciece* 73, 135-149.
- De La Roche, H., Leterrier, J., Grandclaude, P., Marchal, M., 1980. A classification of volcanic and plutonic rocks using  $Rj/Rj$ - diagram and major-element analyses - its relationships with current nomenclature. *Chemical Geology* 29, 183-210.
- DOCEGEO (Rio Doce Geologia e Mineração - Distrito Amazônia) 1988. Revisão litoestratigráfica da província Mineral de Carajás, Pará. In: Congresso Brasileiro de Geologia, 35, Belém. Anexos. Belém, SBG. Vol. Província Mineral de Carajás-Litoestratigrafia e Principais Depósitos Minerais. p. 11-54.
- Dowty, E., 1980. Synneusis reconsidered. *Contributions to Mineralogy and Petrology* 24, 7-29.
- Eby, G.N. 1990. The A-type granitoids: A review of their occurrence and chemical characteristics and speculations on their petrogenesis. In: A.R. Woolley and M. Ross (Editors), *Alkaline igneous rocks and carbonatites*. *Lithos*, 26, pp. 115-134.
- Eby, G.N., 1992. Chemical subdivision of the A-type granitoids: petrogenesis and tectonic implications. *Geology* 20, 641-644.
- Eklund, O., Shebanov, A.D., 1999. The origin of rapakivi texture by sub-isothermal decompression. *Precambrian Research*. 95, 129–146.
- Emslie, R.F., 1991. Granitoids of rapakivi granite-anorthosite and related associations. *Precambrian Research* 51, 173-192.
- Emslie, R.F., Stirling, J.A.R., 1993. Rapakivi and related granitoids of the Nain plutonic suite: geochemistry, mineral assemblages and fluid equilibria. *Canadian Mineralogist* 31, 821-847.

- Evensen, N.M., Hamilton, P.J., O'Nions, R.K., 1978. Rare earth abundance in chondritic meteorites. *Geochimica Cosmochimica Acta* 42, 1199-1212.
- Frost, C.D., Frost, B.R., 1997. Reduced rapakivi type granites: the tholeiitic connection. *Geology* 25, 647-650.
- Frost, C.D., Frost, B.R., Chamberlain, K.R., Edwards, B., 1999. Petrogenesis of the 1.43 Ga Sherman batholith, SE Wyoming USA: a reduced, rapakivi-type anorogenic granite. *Journal of Petrology* 40, 1771-1802.
- Frost, B.R., Barnes, C.G., Collins, W.J., Arculus, R.J., Ellis, D.J., Frost, C.D., 2001. A geochemical classification for granitic rocks. *Journal of Petrology* 42, 2033-2048.
- Haapala, I., Rämö, O.T., 1992. Tectonic setting and origin of the Proterozoic rapakivi granites of the southeastern Fennoscandia. *Transactions of the Royal Society of Edinburgh: Earth Sciences* 83, 165-171.
- Hanson, G.N. 1978. The application of trace elements to the petrogenesis of igneous rocks of granitic composition. *Earth and Planetary Science Letters*, 38: 26-43.
- Hanson, G.N., 1989. An approach to trace element modeling using a simple igneous system as an example, in *The Geology and Geochemistry of Rare Earth Elements* edited by Lipin and McKay, *Reviews in Mineralogy* 21, 79-97.
- Huppert H.E. & Sparks R.S.J. 1988. The generation of granitic magmas by intrusion of basalt into continental crust. *Journal of Petrology*, 29:599-624
- Ishihara, S., 1981. The granitoid series and mineralization. *Economic Geology*, 75 th Anniversary volume, pp. 458-484.
- Javier Rios, F., 1995. A jazida de wolframita de Pedra Preta, Granito Musa, Amazônia Oriental (PA): Estudo dos fluidos mineralizantes e isótopos estáveis de oxigênio em veios hidrotermais. PhD thesis, Federal University of Paraíba, Belém, Brazil (in Portuguese).
- King, P.L., White, A.J.R., Chappell, B.W., Allen, C.M., 1997. Characterization and origin of aluminous A-type granites from the Lachlan Fold Belt, southeastern Australia. *Journal of Petrology* 38, 371-291.
- Leite, A.A.S., 2001. Geoquímica, petrogênese e evolução estrutural dos granitóides arqueanos da região de Xinguara, SE do Cráton Amazônico. Belém, Centro de Geociências, Universidade Federal do Pará, 330p. Doctor Thesis. Curso de Pós-Graduação em Geologia e Geoquímica, Centro de Geociências, UFPa.

- Leite, A. A. S., Dall'Agnol, R., Macambira, M. J. B., Althoff, F. J., 2004. Geologia e geocronologia dos granitóides arqueanos da região de Xinguara (PA) e suas implicações na evolução do Terreno Granito-Greenstone de Rio Maria. Revista Brasileira de Geociências. 34, 447-458.
- Loiselle, M.C., Wones, D.R., 1979. Characteristics and origin of anorogenic granites. Geological Society of America Abstracts with Programs 11, 468.
- Macambira, M.J.B., Lafon, J.-M., 1995. Geocronologia da Província mineral de Carajás: síntese dos dados e novos desafios. Boletim do Museu Paraense Emílio Goeldi, Ciências da Terra 7, 263-288 (in Portuguese).
- Macambira, M.J.B., Lancelot, J.R., 1996. Time constraints for the formation of the Archean Rio Maria crust, southeastern Amazonian craton, Brazil. Intern. Geol. Rev. 38, 1134-1142.
- Machado, N., Lindenmayer, Z., Krogh, T.E., Lindenmayer, D., 1991. U-Pb geochronology of Archean magmatism and basement reactivation in the Carajás área, Amazon Shield, Brazil. Precambrian Research 49, 329-354.
- Oliveira, D.C., 2001. Geologia, geoquímica e petrologia magnética do granito paleoproterozóico Redenção, SE do Cráton Amazônico. M.Sc. Thesis, Federal University of Pará, Belém, Brazil (in Portuguese).
- Oliveira, D.C., Dall'Agnol, R., Barros, C.E.M., Figueiredo, M.A.B.M., 2002. Petrologia magnética do Granito Paleoproterozóico Redenção, SE do Cráton Amazônico. In: Klein, E.L., Vasquez, M.L., Rosa-Costa, L.T. (Eds.) Contribuições à Geologia da Amazônia. Sociedade Brasileira de Geologia Núcleo Norte, Belém, vol. 3, p. 115-132.
- Oliveira, D.C., Dall'Agnol, R., Barros, C.E.M., Vale, A.G., 2005. Geologia e Petrografia do Granito Paleoproterozóico Redenção, SE do Cráton Amazônico. Boletim do Museu Paraense Emílio Goeldi, Série Ciências Naturais, Belém, v. 2, n. 1, p. 155-172.
- Oliveira, M.A., Dall, Agnol, R., Althoff, F.J., Submitted a. Petrografia e geoquímica do Granodiorito Sanukítóide Arqueano Rio Maria da região de Bannach e comparações com as demais ocorrências no Terreno Granito-Greenstone de Rio Maria. Revista Brasileira de Geociências.
- Oliveira, D.C., Dall'Agnol, R., Silva, J.B.C., Almeida, J.A.C., Submitted b. Gravimetric, radiometric, and magnetic susceptibility study of the Paleoproterozoic Redenção and Bannach plutons: implications for architecture and zoning of A-type granites. Journal of

South American Earth Sciences.

- Oliveira, D.C., Neves, S.P., Dall'Agnol, R., Mariano, G., Correia, P.B., Submitted c. Anisotropy of magnetic susceptibility of the Redenção granite, Eastern Amazonian Craton: Implications for the emplacement of a Paleoproterozoic anorogenic A-type pluton. *Journal of Structural Geology*.
- Patiño Douce, A.E., 1997. Generation of metaluminous A-type granites by low-pressure melting of calc-alkaline granitoids. *Geology* 25, 743-746.
- Pearce, J.A., Harris, N.B.W, Tindle, A.C., 1984. Trace element discrimination diagrams for the tectonic interpretation of granitic rocks. *Journal of Petrology* 25, 956-983.
- Rajesh, H.M., 2000. Characterization and origin of a compositionally zoned aluminous A-type granite from South India. *Geological Magazine* 137, 291-318.
- Rämö, O.T., 1991. Petrogenesis of the Proterozoic rapakivi granites and related basic rocks of the southeastern Fennoscandian: Nd and Pb isotopic and general geochemical constraints. *Geological Survey of Finland Bulletin* 355.
- Rämö, O.T., Haapala, I., 1995. One hundred years of rapakivi granite. *Mineralogy and Petrology* 52, 129–185.
- Rämö, O.T., Dall'Agnol, R., Macambira, M.J.B., Leite, A.A.S., de Oliveira, D.C., 2002. 1.88 Ga oxidized A-type granites of the Rio Maria region, eastern Amazonian craton, Brazil: Positively anorogenic! *Journal of Geology* 110, 603-610.
- Rogers J., Greenberg J. 1990: Late-orogenic, post-orogenic, and anorogenic granites: distinction by major elements and trace element chemistry and possible origins. *Journal of Geology*. 98: 291-309.
- Rollinson, H. R., 1993. Using geochemical data: evaluation, presentation, interpretation. London, Longman, 352 p.
- Smith, J. V., 1974. Feldspar Minerals: Chemical and textural properties. New York, Springer Verlag v. 2.
- Souza, Z.S., Dall'Agnol, R., 1995. Geochemistry of metavolcanic rocks in the Archean Greenstone Belt of Identidade, SE, Pará, Brazil. *Anais Academia Brasileira de Ciências* 67, 217-233.
- Streckeisen, A., 1976. To each plutonic rock its proper name. *Earth Science Review* 12, 1-13.

- Tassinari, C. C. G., Macambira, M., 2004. A evolução tectonica do Craton Amazonico. In: Mantesso – Neto, V., Bartorelli, A., Carneiro, C.D.R., Brito Neves, B.B. (Eds.), Geologia do Continente Sul Americano: Evolução da obra de Fernando Flávio Marques Almeida, 471-486.
- Vale, A.G., Neves, P.N., 1994. O Granito Redenção: Estado do Pará. In: Congresso Brasileiro de Geologia, 38, Balneário Camboriú-SC. SBG, vol. 1, p. 149 - 150.
- Vance, J.A., 1969. On Synneusis. Contribution to Mineralogy and Petrology 24, 7-29.
- Vigneresse, J.L., 2005. The specific case of the Mid-Proterozoic rapakivi granites and associated suite within the context of Columbia supercontinent. Precambrian Research, 137, 1-34.
- Whalen, J.B., Currie, K.L., Chappell, B.W., 1987. A-Type granite: geochemical characteristics, discrimination and petrogenesis. Contributions to Mineralogy and Petrology 95, 407-419.
- Whalen, J.B., Jenner, G.A., Longstaffe, F.J., Robert, F., Gariepy, C. 1996. Geochemical and isotopic (O, Nd, Pb and Sr) constraints on A-type granite petrogenesis based on the Topsails Igneous Suite, Newfoundland Appalachians. Journal of Petrology 37, 1463-1489.
- Wones, D.R., 1989. Significance of the assemblage titanite+magnetite+quartz in granitic rocks. American Mineralogist 74, 744–749.

## CAPÍTULO - 3

### ***OXIDIZED, MAGNETITE-SERIES, RAPAKIVI-TYPE GRANITES OF CARAJÁS, BRAZIL: IMPLICATIONS FOR CLASSIFICATION AND PETROGENESIS OF A-TYPE GRANITES***

**Roberto Dall'Agnol**  
**Davis Carvalho de Oliveira**  
*In Press: LITHOS*



Available online at www.sciencedirect.com



LITHOS

Lithos xx (2006) xxx–xxx

www.elsevier.com/locate/lithos

# Oxidized, magnetite-series, rapakivi-type granites of Carajás, Brazil: Implications for classification and petrogenesis of A-type granites

Roberto Dall'Agnol \*, Davis Carvalho de Oliveira

*Group of Research on Granite Petrology, Centro de Geociências, Universidade Federal do Pará, Caixa Postal 8608, 66075-100 Belém, PA, Brazil*

Received 14 October 2004; accepted 30 March 2006

## Abstract

The varying geochemical and petrogenetic nature of A-type granites is a controversial issue. The oxidized, magnetite-series A-type granites, defined by Anderson and Bender [Anderson, J.L., Bender, E.E., 1989. Nature and origin of Proterozoic A-type granitic magmatism in the southwestern United States of America. *Lithos* 23, 19–52.], are the most problematic as they do not strictly follow the original definition of A-type granites, and approach calc-alkaline and I-type granites in some aspects. The oxidized Jamon suite A-type granites of the Carajás province of the Amazonian craton are compared with the magnetite-series granites of Laurentia, and other representative A-type granites, including Finnish rapakivi and Lachlan Fold Belt A-type granites, as well as with calc-alkaline, I-type orogenic granites. The geochemistry and petrogenesis of different groups of A-types granites are discussed with an emphasis on oxidized A-type granites in order to define their geochemical signatures and to clarify the processes involved in their petrogenesis. Oxidized A-type granites are clearly distinguished from calc-alkaline Cordilleran granites not only regarding trace element composition, as previously demonstrated, but also in their major element geochemistry. Oxidized A-type granites have high whole-rock  $\text{FeO}_t/(\text{FeO}_t + \text{MgO})$ ,  $\text{TiO}_2/\text{MgO}$ , and  $\text{K}_2\text{O}/\text{Na}_2\text{O}$  and low  $\text{Al}_2\text{O}_3$  and  $\text{CaO}$  compared to calc-alkaline granites. The contrast of  $\text{Al}_2\text{O}_3$  contents in these two granite groups is remarkable. The  $\text{CaO}/(\text{FeO}_t + \text{MgO} + \text{TiO}_2)$  vs.  $\text{CaO} + \text{Al}_2\text{O}_3$  and  $\text{CaO}/(\text{FeO}_t + \text{MgO} + \text{TiO}_2)$  vs.  $\text{Al}_2\text{O}_3$  diagrams are proposed to distinguish A-type and calc-alkaline granites. Whole-rock  $\text{FeO}_t/(\text{FeO}_t + \text{MgO})$  and the  $\text{FeO}_t/(\text{FeO}_t + \text{MgO})$  vs.  $\text{Al}_2\text{O}_3$  and  $\text{FeO}_t/(\text{FeO}_t + \text{MgO})$  vs.  $\text{Al}_2\text{O}_3/(\text{K}_2\text{O}/\text{Na}_2\text{O})$  diagrams are suggested for discrimination of oxidized and reduced A-type granites. Experimental data indicate that, besides pressure, the nature of A-type granites is dependent of  $f\text{O}_2$  conditions and the water content of magma sources. Oxidized A-type magmas are considered to be derived from melts with appreciable water contents ( $\geq 4$  wt.%), originating from lower crustal quartz-feldspathic igneous sources under oxidizing conditions, and which had clinopyroxene as an important residual phase. Reduced A-type granites may be derived from quartz-feldspathic igneous sources with a metasedimentary component or, alternatively, from differentiated tholeiitic sources. The imprint of the different magma sources is largely responsible for the geochemical and petrological contrasts between distinct A-type granite groups. Assuming conditions near the NNO buffer as a minimum for oxidized granites, magnetite-bearing granites formed near FMQ buffer conditions are not *stricto sensu* oxidized granites and a correspondence between oxidized and reduced A-type granites and, respectively, magnetite-series and ilmenite-series granites is not always observed.

© 2006 Elsevier B.V. All rights reserved.

**Keywords:** Carajás; Amazonian craton; Oxidized granites; Reduced granites; Magnetite-series; Ilmenite-series; Rapakivi; A-type granite

\* Corresponding author. Tel.: +55 91 3201 7123/3201 7477; fax: +55 91 3201 7537.

E-mail address: [robdal@ufpa.br](mailto:robdal@ufpa.br) (R. Dall'Agnol).

## 1. Introduction

A-type granites were defined as relatively anhydrous, reduced, anorogenic granites enriched in incompatible elements (Loiselle and Wones, 1979). Later, more detailed petrographic and geochemical criteria as well as petrogenetic models have been presented for A-type granites (Collins et al., 1982; Whalen et al., 1987; Eby, 1990, 1992; Whalen et al., 1996; Frost and Frost, 1997; Frost et al., 1999) and their exclusively anorogenic geotectonic setting has been questioned (e.g., Whalen et al., 1987; Sylvester, 1989; Whalen et al., 1996). Rapakivi granites were redefined by Haapala and Rämö (1992) as A-type granites characterized by the presence of rapakivi texture. The Mesoproterozoic A-type granites of the Laurentia–Baltica have been divided into three groups: ilmenite granites, magnetite granites and two-mica (peraluminous) granites (Anderson and Bender, 1989; Anderson and Morrison, 1992; Anderson and Smith, 1995; Anderson and Morrison, 2005). Most of the granite members of the anorthosite–mangerite–charnockite–rapakivi granite series (AMCG series; Emslie, 1991) belong to the ilmenite-series granites. Until recently, little attention has been given to the magnetite-series A-type granites. These are commonly seen with suspicion, because they do not follow strictly the original definition of A-type granites, and approach calc-alkaline and I-type granites in some aspects, e.g., in their oxidizing character.

Many authors have stressed the varying petrogenetic nature of A-type granites (Sylvester, 1989; Creaser et al., 1991; Eby, 1992; Hogan et al., 1992; Poitrasson et al., 1994; King et al., 1997; Patiño Douce, 1999; Rajesh, 2000; Dall'Agnol et al., 2005). Geochemical contrasts between typical peralkaline and metaluminous to mildly peraluminous A-type granites have also been emphasized (King et al., 1997; Patiño Douce, 1999; Costi, 2000). There is increasing evidence that the variations shown by A-type granites dominantly reflect contrasts in magma sources and petrological processes and are, thus, extremely relevant for the understanding of their petrogenesis. On the other hand, the relevance of oxidized A-type granites and their differences compared to ilmenite-series rapakivi granites were demonstrated in central and southwestern United States (Anderson and Bender, 1989; Anderson and Smith, 1995; Barnes et al., 2002; Anderson and Morrison, 2005) and eastern Amazonian craton (Dall'Agnol et al., 1997a, 1999a,b,c; Rämö et al., 2002; Dall'Agnol et al., 2005). Occurrences of oxidized, magnetite-series A-type granites have also been described in other continents (Rajesh, 2000; Bogaerts et al., 2003). Several chemical and petrogenetic classifications for granites have been proposed (see summaries by Barbarin,

1999; Frost et al., 2001). However, it should be evaluated how suitable they are for the discrimination of different A-type granite groups.

Experimental studies direct or indirectly concerning A-type magmas have been carried out (Clemens et al., 1986; Skjerlie and Johnston, 1993; Patiño Douce and Beard, 1995; Patiño Douce, 1997; Dall'Agnol et al., 1999c; Scaillet and Macdonald, 2001, 2003; Klimm et al., 2003). These studies established constraints for the origin and evolution of different A-type granite groups.

The aim of this paper is to present the geochemical and petrogenetic characteristics that can be used to distinguish between the oxidized, magnetite-series A-type granites from both other A-type granite groups, and calc-alkaline granitoid series. To do this, the A-type granites of the Carajás province of the Amazonian craton, Brazil, will be compared with representative A-type granites, including those of Laurentia–Baltica and Lachlan Fold Belt provinces, as well as with calc-alkaline, I-type orogenic granite series. In addition, major element geochemical diagrams for A-type granite classification and discrimination will be evaluated. The petrogenesis of oxidized A-type granites will be discussed taking into account constraints established by experimental petrology. This will be done in order to define the geochemical signature of oxidized A-type granites and to clarify the processes involved in their petrogenesis.

## 2. A-type granites of the Carajás province

A synthesis of the geological, tectonic, mineralogical, geochemical, isotopic, and petrogenetic aspects of the Paleoproterozoic A-type granites of the Carajás province of the eastern Amazonian craton and a brief comparison between them and the Mesoproterozoic A-type granites of Fennoscandia and Laurentia was presented by Dall'Agnol et al. (2005). More detailed information on the A-type granites of Carajás can be found in that paper and references therein. The aspects more relevant to the present paper will be reviewed in the following.

### 2.1. Geologic setting, geochronology and Nd isotope geochemistry

The Archean Carajás province of the Amazonian craton (Machado et al., 1991; Macambira and Lafon, 1995; Dall'Agnol et al., 1997b; Rämö et al., 2002) is divided into the Rio Maria Granite–Greenstone Terrane (3.0 to 2.86 Ga), and the rift-related Carajás Basin (2.76 to 2.55 Ga), located, respectively, in the southern and northern parts of the province. The Jamon, Serra dos Carajás, and Velho Guilherme Paleoproterozoic A-type,

rapakivi granite suites were recognized in the province (Fig. 1). These three suites differ in the degree of oxidation of their magmas and region of occurrence (see Dall'Agnol et al., 2005, and references therein). The oxidized granite plutons of the Jamon suite are found in the Rio Maria Granite–Greenstone Terrane (Dall'Agnol et al., 1997a; Althoff et al., 2000; Souza et al., 2001; Rämö et al., 2002; Dall'Agnol et al., 2005). The moderately reduced Serra dos Carajás suite plutons are exposed in the Carajás Basin (Dall'Agnol et al., 1994, 2005). The tin-mineralized, reduced Velho Guilherme suite plutons are located in the Xingu region, to the west of the province (Dall'Agnol et al.,

1993; Teixeira et al., 2002). The A-type granite plutons of the Carajás province were formed at ~1.88 Ga (Machado et al., 1991; Macambira and Lafon, 1995; Dall'Agnol et al., 1999a,b; Teixeira et al., 2002; Dall'Agnol et al., 2005), and were emplaced in an extensional tectonic regime, as indicated by dike swarms that are coeval with the granites (Dall'Agnol et al., 2005). Lamarão et al. (2002, 2005) and Dall'Agnol et al. (2005) postulated that the A-type granite magmatism of the Carajás province was related to a continental event that marks the beginning of the breakup of the Paleoproterozoic continent formed at the end of the Trans-Amazonian orogenic cycle.

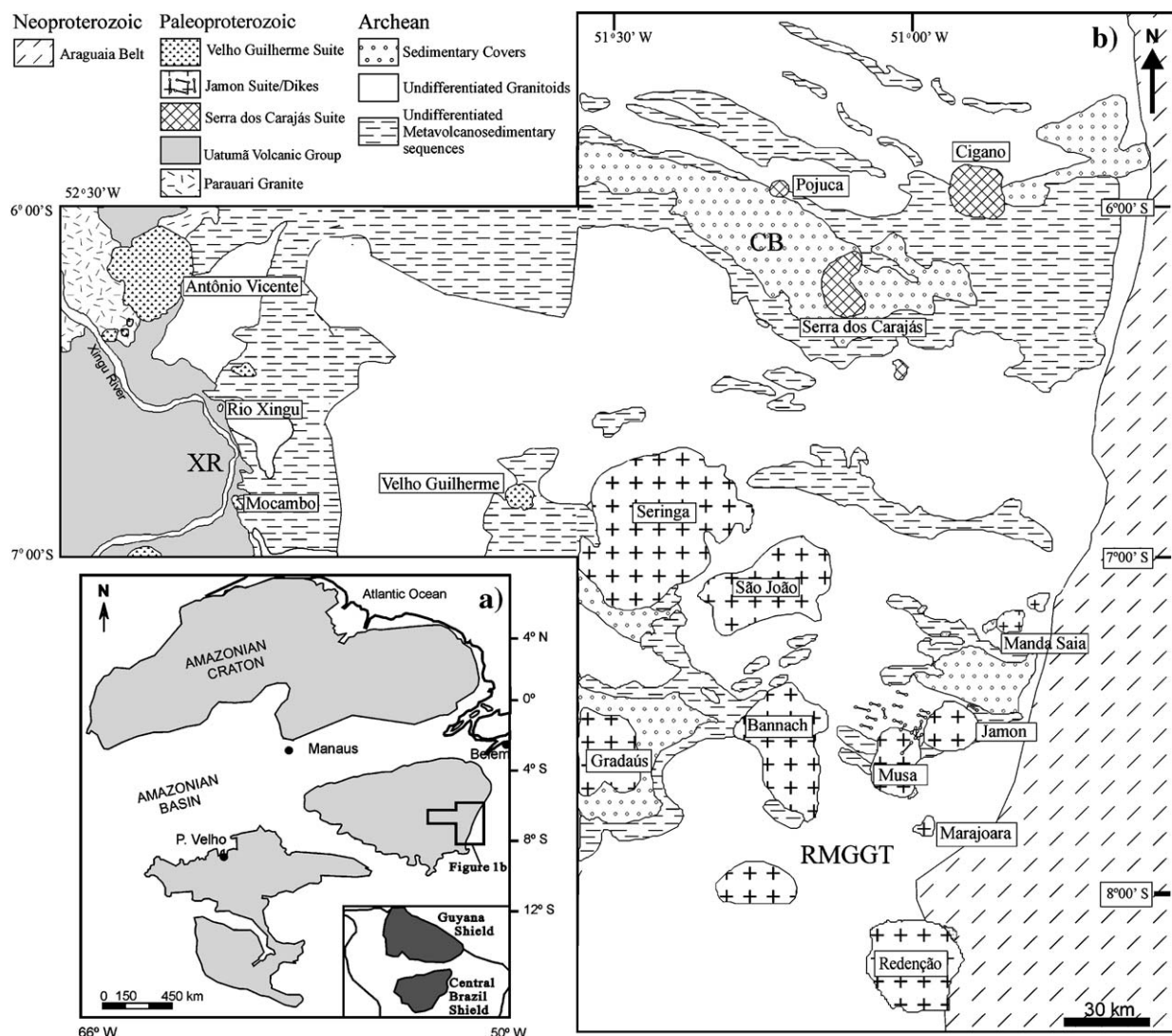


Fig. 1. (a) Location of the studied area in the Amazonian craton. (b) Simplified geological map of the Carajás Mining Province showing the distribution of Paleoproterozoic A-type granites (modified from Dall'Agnol et al., 2005, and references therein). RMGGT—Rio Maria Granite–Greenstone Terrane; CB—Carajás Basin; XR—Xingu Region. Inset in (a) shows the two exposed parts of the Amazonian craton—the Guiana shield in the north and the Central Brazil shield in the south.

Table 1  
Modal compositions of the Paleoproterozoic A-type granites of the Jamon Suite

Jamon (1)				Redenção (2)				Musa (3)				Bannach (4)				
HBMzG [9]	BmzG [4]	BMcG [1]	LMzG [6]	CBAMzG [4]	BHMzG [10]	BmzG [8]	BMzP [10]	BHMzG [3]	BHMzG [11]	BMzG [15]	BHMzG [1]	LzG [5]	BHMzG [9]	BHMzG [4]	BHMzG [14]	
Plagioclase	30.2	28.6	35.9	30.1	33.0	29.3	29.0	27.8	24.7	30.9	31.1	28.0	26.0	18.2	34.5	
Alkali-feldspar	29.4	33.4	35.1	32.5	20.3	25.9	30.5	33.7	34.0	39.0	27.6	31.5	33.4	46.6	17.8	
Quartz	31.9	31.0	32.0	30.1	21.5	25.8	29.2	30.4	31.8	33.6	31.0	29.5	31.3	33.8	26.0	
Clinopyroxene	<0.1	—	—	—	1.4	—	—	—	—	—	—	—	0.9	0.4	—	—
Amphibole	1.7	0.1	—	<0.1	11.2	6.2	2.5	0.3	—	4.0	1.7	0.3	—	16.4	5.3	1.4
Biotite	4.6	4.5	0.9	0.2	7.9	5.9	5.6	4.4	3.0	1.0	3.2	3.8	5.2	0.4	0.3	7.5
Chlorite	0.3	0.5	1.5	0.1	—	0.1	0.2	0.4	1.3	0.4	0.1	0.3	0.4	1.2	1.0	0.1
Opaques	0.8	0.8	0.6	0.7	3.5	2.1	1.8	1.1	0.6	1.7	0.8	0.6	0.5	0.4	3.8	1.9
Titanite	0.5	0.3	0.1	0.4	1.1	0.8	0.8	0.8	<0.1	0.6	0.8	0.5	0.3	1.0	0.4	0.1
Allanite	n.d.	n.d.	n.d.	0.1	—	<0.1	0.1	0.3	—	0.1	0.1	0.1	<0.1	0.2	0.2	0.3
Fluorite	n.d.	n.d.	n.d.	—	—	—	—	<0.1	<0.1	<0.1	0.1	0.1	—	0.2	—	0.1
Others(Ap+Zn)	0.4	0.5	0.5	0.2	0.2	0.1	0.1	<0.1	0.1	0.2	0.1	0.3	0.2	0.1	0.1	<0.1
Felsic	91.5	93.0	96.4	98.5	74.8	84.7	89.1	93.0	93.6	97.3	89.6	92.1	92.7	97.2	98.0	70.2
Mafic	8.4	6.9	3.6	1.5	25.5	15.1	11.1	6.9	6.2	2.6	10.4	7.7	7.3	2.8	2.0	29.8

(1) Dall'Agnol et al. (1990); (2) Oliveira (2000); (3) Gestal (1987) and Oliveira D.C. (unpubl. data); (4) Almeida et al., submitted for publication; [ ] number of averaged samples; n.d. = not determined; Ap = apatite; Zn = zircon; C = clinopyroxene; H = hornblende; B = biotite; MzG = monzogranite; McG = microgranite; SG = syenogranite; P = porphyritic; L = leuco.

Whole-rock Nd isotope data for the Jamon (Dall'Agnol et al., 1999b; Rämö et al., 2002), Velho Guilherme (Teixeira et al., 2002), and Serra dos Carajás (Dall'Agnol et al., 2005) suites imply remarkably similar  $\varepsilon_{\text{Nd}}$  (at 1880 Ma) values, ranging generally from −10.5 to −7.9. Data for the Jamon suite (Rämö et al., 2002) also indicate that the plutons were not disturbed and have retained their initial magmatic Nd isotope composition. The Nd isotope composition of the Archean country-rock granitoids complies with the idea that the Paleoproterozoic A-type Carajás granites were derived from deeper parts of the Archean crust (Dall'Agnol et al., 1999b; Rämö et al., 2002; Teixeira et al., 2002; Dall'Agnol et al., 2005).

## 2.2. Petrography and mineral chemistry

All three suites are composed essentially of granites *sensu stricto* (monzogranite to syenogranite with rare alkali feldspar granite; Dall'Agnol et al., 2005; modal compositions of the oxidized Jamon Suite granites are given on Table 1), with biotite or, in the less evolved facies, biotite and hornblende as the major mafic phases. Locally relict clinopyroxene crystals are associated with amphibole. Muscovite is present only in evolved, hydrothermally altered leucogranites. Isotropic, equigranular, coarse- or medium-grained and seriated rocks are dominant in most of the plutons. However, plagioclase mantled K-feldspar megacrysts are observed in every pluton and are quite common in some of them (e.g., Redençao, Bannach, and Serra dos Carajás). Nevertheless, the texture of the porphyritic facies of these plutons differs from typical wiborgitic rapakivi textures (cf. Rämö and Haapala, 1995) by the fact that tabular megacrysts are as common as ovoid megacrysts and that mantled K-feldspar megacrysts are subordinate relative to those unmantled by plagioclase.

The Fe/(Fe+Mg) in amphibole (0.47 to 0.73) and biotite (0.6 to 0.70), Fe–Ti oxide mineral data, and experimental studies (Dall'Agnol et al., 1997a, 1999c, 2005) demonstrate that the Jamon and associated felsic dike magmas evolved in relatively oxidizing conditions, above the NNO buffer. This is consistent with the presence of significant modal magnetite and titanite in all the facies of this suite.

In the Antonio Vicente complex of the Velho Guilherme suite (Teixeira, 1999; Dall'Agnol et al., 2005), the amphibole and biotite of the less evolved monzogranites have Fe/(Fe+Mg) between 0.74 and 0.85. In the alkali-feldspar granite, Fe/(Fe+Mg) in the amphibole and associated biotite are higher (0.95–0.98) than in the monzogranites. The biotite of the syenogranite has Fe/(Fe+Mg) of 0.85–0.89 and in the more evolved leucogranites of this suite, the mica is a siderophyllite with a Fe/(Fe+Mg) higher than 0.9. Except in the amphibole-bearing

monzogranite, where magnetite is found associated with ilmenite and titanite, magnetite and titanite are absent or very scarce. These data indicate that the dominant facies of the Velho Guilherme suite evolved under reducing conditions (Dall'Agnol et al., 2005). The amphibole-bearing monzogranite evolved in moderately reducing conditions, probably similar to those prevalent in the Serra dos Carajás suite (see below).

In the Cigano pluton, representative of the Serra dos Carajás suite, amphibole and biotite have, respectively,  $\text{Fe}/(\text{Fe} + \text{Mg})$  in the range 0.85–0.94 and 0.78–0.88. The dominant Fe–Ti oxide mineral is magnetite, demonstrating that these granites crystallized at  $f\text{O}_2$  above the FMQ buffer. However, their high whole-rock, amphibole, and biotite  $\text{Fe}/(\text{Fe} + \text{Mg})$  ratios are compatible with those of reduced granites. This was interpreted to imply oxygen fugacity just a little above the FMQ buffer (Dall'Agnol et al., 2005).

### 2.3. Elemental geochemistry

Representative chemical compositions of the major facies of some Jamon Suite plutons are given in Table 2. Previous works (Dall'Agnol et al., 1993, 1994; Barros et al., 1995; Dall'Agnol et al., 1999b; Dall'Agnol et al., 2005) have shown that granites from the three Carajás suites plot in the A-type field in the geochemical classification of Whalen et al. (1987) and in the within-plate field of Pearce et al. (1984). They also show geochemical affinity with Finnish rapakivi granites (Figs. 2, 3; see Dall'Agnol et al., 1999a). Compared to the oxidized Jamon suite granites, the reduced and moderately reduced granites of the Velho Guilherme and Serra dos Carajás suites show a geochemical signature more similar to that of the A-type rapakivi granites. These have higher  $\text{FeO}_t/(\text{FeO}_t + \text{MgO})$ ,  $\text{K}_2\text{O}/\text{Na}_2\text{O}$  (Fig. 2d,e), and HFSE contents than the Jamon Suite granites. The granites have silica content >65 wt.%, generally >70 wt.%, and are metaluminous to mildly peraluminous, ferroan granites according to the terminology of Frost et al. (2001; see Fig. 2c,d).

### 2.4. Magnetic susceptibility and Fe–Ti oxides

Magnetic susceptibility (MS) decreases from the oxidized Jamon suite ( $1.05 \times 10^{-3}$  to  $54.73 \times 10^{-3}$ , most values  $>5.0 \times 10^{-3}$ ; MS in International System volume units) to the moderately reduced Serra dos Carajás suite ( $1.0 \times 10^{-3}$  to  $5.0 \times 10^{-3}$ ); the lowest values are found in the syenogranites of the Velho Guilherme suite ( $<1.0 \times 10^{-3}$ ). The Jamon suite granites are typical magnetite-series according to the terminology of Ishi-

hara (1981) with modal contents of Fe–Ti oxide minerals generally between 0.5 and 2% and magnetite dominant over ilmenite. Compared to Jamon, the Serra dos Carajás suite granites and the amphibole-bearing monzogranite of the Antonio Vicente complex (Velho Guilherme suite) have lower contents (<1%) of magnetite and ilmenite. It is important to realize that the moderately reduced Serra dos Carajás granites and the amphibole-bearing monzogranite of the Velho Guilherme suite have more than 0.1% modal magnetite and thus belong to the magnetite-series (Ishihara, 1981). The Velho Guilherme suite syenogranites, with opaque mineral contents generally <0.1%, and magnetite absent in most of the studied samples, classify as ilmenite-series.

### 3. Comparison with the Proterozoic A-type granites of Fennoscandia and Laurentia

The country rocks and probably also the sources of the Paleoproterozoic, A-type granites of Carajás region are all Archean and the three studied granite suites are practically coeval (~1.88 Ga; Dall'Agnol et al., 2005). In contrast, in Fennoscandia and Laurentia the granite magma sources, with the exception of the Salmi batholith (Rämö and Haapala, 1995; Amelin et al., 1997), are essentially Paleoproterozoic to Mesoproterozoic and the ages of the granites show significant variation (~1.7 to 1.1 Ga). The three Carajás suites evolved in varying  $f\text{O}_2$  conditions, but do not exactly correspond to the three main granite groups identified in Laurentia by Anderson and Bender (1989). The oxidized Jamon suite granites crystallized at  $f\text{O}_2$  conditions near the NNO and HITMQ (Wones, 1989) buffers and are similar to the magnetite-series granites of Laurentia (Anderson and Morrison, 2005). The dominant syenogranites of the Velho Guilherme Suite are ilmenite-series. The amphibole-bearing monzogranite of the Antonio Vicente complex (Velho Guilherme suite) and the Serra dos Carajás granites are magnetite-bearing granites but are also relatively reduced. The Serra dos Carajás and Velho Guilherme granites evolved in  $f\text{O}_2$  conditions similar to those of the rapakivi granites of Laurentia and Fennoscandia and thus have affinities with the classic rapakivi series (Rämö and Haapala, 1995). Peraluminous two-mica granites, similar to those in Laurentia (Anderson and Morrison, 2005), have not been found in Carajás.

### 4. Granite classifications and their applicability to A-type rapakivi granites

The alphabetic classification, developed initially for I- and S-type granites of the Lachlan Fold Belt of

Table 2

Chemical compositions of representative samples of the Paleoproterozoic A-type granites of the Jamon Suite

	Jamon (1)				Redenção (2)						Musa (3)
	HBMzG	BMzG	BMcG	LMzG	CBAMzG	BHMzG	HBMzG	BMzG	BMzP	LMzG	BHMzG
	AU 391	AU 375	AU 397	AU 376	DCR 34	DCR 63A	JCR 09	JCR 01D	JCR 07	DCR 07	KM 144B
SiO <sub>2</sub> (wt.%)	71.12	73.71	75.47	75.97	66.10	71.10	70.70	74.20	74.40	76.00	69.18
TiO <sub>2</sub>	0.72	0.35	0.17	0.10	1.20	0.60	0.44	0.30	0.22	0.12	0.64
Al <sub>2</sub> O <sub>3</sub>	12.42	12.36	12.50	13.70	13.10	13.50	14.20	13.30	13.10	13.10	13.21
Fe <sub>2</sub> O <sub>3</sub>	4.52*	2.79*	1.61*	0.28	3.47	2.19	1.24	1.31	1.01	0.65	4.69*
FeO	n.d.	n.d.	n.d.	0.38	3.36	1.54	2.03	0.62	0.53	0.31	n.d.
MnO	0.07	0.04	0.01	0.01	0.13	0.07	0.06	0.05	0.04	0.03	0.06
MgO	0.68	0.32	0.20	0.04	1.10	0.60	0.46	0.22	0.18	<0.10	0.88
CaO	2.40	1.21	0.64	1.00	2.80	2.10	1.60	1.10	0.67	0.55	2.37
Na <sub>2</sub> O	3.37	3.27	3.47	3.87	3.70	3.70	3.50	3.50	3.40	3.10	3.59
K <sub>2</sub> O	3.70	4.75	4.97	4.06	3.90	4.20	4.80	5.10	5.30	5.40	4.01
P <sub>2</sub> O <sub>5</sub>	0.32	0.20	0.13	0.01	0.42	0.22	0.14	0.05	0.04	0.01	0.32
LOI	0.30	0.70	0.62	0.57	0.32	0.38	0.35	0.31	0.73	0.17	0.53
Total	99.62	99.7	99.79	99.99	99.60	100.2	99.52	100.1	99.62	99.44	99.48
Ba (ppm)	1320	718	443	99	919	1498	1310	909	489	32	1056
Rb	100	230	281	159	151	139	193	204	281	396	172
Sr	246	118	61	41	241	332	271	196	122	27	232
Zr	397	283	164	57	686	377	353	258	240	126	299
Nb	19	21	21	17	29	16	20	21	24	21	16
Y	65	79	137	14	80	50	43	71	62	30	47
Ga	26	31	28	n.d.	26	26	25	23	27	27	19
Sc	13	7	2.5	n.d.	14	<10	15	10	<10	<10	9.3
Th	9	25	29	n.d.	<5	<5	<5	<5	<5	<5	23
U	3.7	n.d.	5.56	n.d.	<10	<10	<10	<10	<10	<10	n.d.
V	23	9	5	n.d.	53	22	14	<10	<10	<10	44
Cr	8	5	5	n.d.	n.d.	n.d.	n.d.	n.d.	n.d.	n.d.	15
Co	5	n.d.	5	n.d.	n.d.	n.d.	n.d.	n.d.	n.d.	n.d.	14
Ni	5	5	5	n.d.	n.d.	n.d.	n.d.	n.d.	n.d.	n.d.	13
Cu	11	5	5	n.d.	n.d.	n.d.	n.d.	n.d.	n.d.	n.d.	11
Zn	69	48	36	n.d.	n.d.	n.d.	n.d.	n.d.	n.d.	n.d.	58
La	89.75	101.0	155.4	n.d.	102.9	60.5	82.0	71.8	56.8	11.9	88.13
Ce	154.6	178.0	172.5	n.d.	196.5	120.9	146.7	139.7	114.4	31.9	152.3
Nd	71.77	67.4	99.5	n.d.	84.5	48.4	46.6	51.7	36.3	9.2	65.87
Sm	14.53	12.8	21.94	n.d.	14.9	8.1	8.4	9.3	6.6	1.8	12.99
Eu	2.65	1.6	1.88	n.d.	1.6	1.5	1.4	1.4	0.7	0.2	2.12
Gd	11.88	10.5	19.76	n.d.	11.8	6.3	6.0	7.6	5.0	1.3	10.43
Dy	10.71	10.2	18.84	n.d.	7.9	4.4	3.8	5.0	3.9	0.8	8.77
Er	6.14	6.5	10.09	n.d.	3.7	2.3	1.7	3.6	2.1	0.4	4.89
Yb	5.98	7.5	10.31	n.d.	2.9	1.8	1.2	2.8	1.9	0.4	4.71
Lu	0.87	1.0	1.53	n.d.	0.4	0.3	0.2	0.4	0.3	0.1	0.76
FeO/(FeO <sub>t</sub> +MgO)	0.86	0.89	0.88	0.94	0.87	0.87	0.88	0.90	0.90	0.92	0.83
K <sub>2</sub> O/Na <sub>2</sub> O	1.10	1.45	1.43	1.05	1.05	1.14	1.37	1.46	1.56	1.74	1.12
Eu/Eu*	0.62	0.42	0.28	n.d.	0.35	0.61	0.57	0.49	0.37	0.29	0.56
(La/Lu) <sub>N</sub>	10.71	10.48	10.54	n.d.	26.70	20.94	42.59	18.63	19.66	12.37	12.04

(1) Dall'Agnol et al. (1994); (2) Oliveira (2001); (3) Dall'Agnol et al. (1999b); (4) Almeida et al. (submitted for publication); n.d. = not determined; \* = Fe<sub>2</sub>O<sub>3</sub> as total; C = clinopyroxene; H = hornblende; B = biotite; MzG = monzogranite; McG = micro-granite; SG = syenogranite; P = porphyritic; L = leuco.

Australia (Chappell and White, 1974, 2001), was expanded (Collins et al., 1982; King et al., 1997, 2001) to include A-type granites (originally defined by Loiselle and Wones, 1979). This classification has been largely adopted around the world; it has, however, been more commonly used as a geochemical rather than

genetic classification. There has also been dispute regarding the source of the granite magmas and tectonic settings inherent in this classification (e.g., Whalen et al., 1987; Pitcher, 1993; Frost et al., 2001).

In the Lachlan Fold Belt, A-type granites are subordinate relative to I- and S-type granites (Collins et al.,

				Bannach (4)				
HBMzG	BMzG	LMzG	LSG	CBHMzG	BHMzG	HBMzG	BMzP	LMzG
KM 32	CRE 37A	CRE 37B	CRE 140E	ADR 136I	ADR 67	ADR 241	ADR 45B	ADR 28B
71.80	72.62	74.97	76.20	58.12	70.39	72.36	75.70	76.86
0.45	0.38	0.20	0.08	2.41	0.56	0.42	0.33	0.15
13.08	12.66	12.35	12.28	9.17	13.09	12.75	11.11	11.45
3.41*	2.86*	1.95*	1.18*	6.87	2.71	2.09	1.90	1.23
n.d.	n.d.	n.d.	n.d.	8.86	1.00	0.95	0.64	0.10
0.04	0.07	0.02	n.d.	0.29	0.06	0.05	0.03	0.03
0.56	0.36	0.20	0.04	2.48	0.46	0.35	0.25	0.09
1.85	1.53	0.85	0.60	3.31	2.01	1.66	0.85	0.64
3.52	3.41	3.47	3.44	1.92	3.38	3.20	2.60	2.88
4.57	4.62	5.05	5.30	3.10	4.14	4.56	4.61	5.14
0.29	0.22	0.13	0.13	0.79	0.16	0.11	0.06	0.03
0.54	0.68	0.60	0.59	1.00	0.90	0.60	0.80	0.40
100.01	99.41	99.79	99.84	99.31	98.97	99.21	98.95	99.01
1053	698	216	282	427	1373.40	988.20	641.20	237.70
170	210	179	259	202	150.30	168.40	183.50	180.80
181	142	66	50	107	211.20	166.60	117.20	46.10
278	212	126	90	1683	394.70	317.60	276.40	125.40
14	20	19	12	65	21.90	21.30	10.10	17.20
34	46	22	7	234	55.00	57.50	27.50	22.20
23	23	23	14	26	20.30	19.40	18.60	18.70
7.9	5.4	3.7	1.7	33	9.00	8.00	3.00	2.00
25	35	75	39	15	18.90	22.50	41.20	13.00
n.d.	n.d.	n.d.	n.d.	7	2.80	3.30	4.20	2.40
26	16	5	5	129	21.00	11.00	6.00	<5
18	7	17	12	n.d.	n.d.	n.d.	n.d.	n.d.
16	13	19	20	n.d.	n.d.	n.d.	n.d.	n.d.
14	7	11	8	n.d.	n.d.	n.d.	n.d.	n.d.
8	5	5	11	n.d.	n.d.	n.d.	n.d.	n.d.
54	56	38	12	n.d.	n.d.	n.d.	n.d.	n.d.
61.15	87.91	173.6	33.61	157.90	88.90	99.70	197.00	35.60
108.1	140.1	198.5	54.72	378.90	185.30	210.20	409.80	66.40
44.28	47.20	46.15	14.30	206.80	70.40	75.50	103.90	23.40
9.0	8.76	6.75	2.85	43.80	12.20	13.20	11.80	4.00
1.55	1.28	0.81	0.52	2.43	2.32	1.80	1.29	0.60
8.45	6.79	5.21	3.22	39.32	10.26	10.17	6.70	3.51
5.84	5.98	3.48	1.44	36.72	9.08	9.45	4.51	3.57
3.34	3.76	2.48	1.15	21.53	5.42	5.57	2.62	2.22
3.37	4.31	3.33	1.49	17.90	4.84	4.54	2.53	2.35
0.65	0.86	0.71	0.34	2.58	0.74	0.69	0.44	0.38
0.85	0.88	0.90	0.96	0.86	0.88	0.89	0.90	0.93
1.38	1.35	1.46	1.54	1.61	1.22	1.43	1.77	1.78
0.54	0.51	0.42	0.52	0.18	0.63	0.47	0.44	0.49
9.77	10.61	25.38	10.26	6.33	13.18	15.75	55.85	10.87

1982; Whalen et al., 1987; King et al., 1997, 2001). King et al. (1997) emphasized the geochemical contrasts between true peralkaline and other A-type granites of the Lachlan Fold Belt and designated the latter as ‘aluminous A-type granites’ based on their metaluminous to weakly peraluminous character. However, King et al.

(2001) suggested the abandon of this terminology. They also stated that the Lachlan A-type granites are distinguished from felsic I-type granites by a greater abundance of high-field-strength elements and that they were produced by high-temperature, partial melting of quartz-feldspathic crustal sources, with limited H<sub>2</sub>O content,

relatively low  $fO_2$  and relatively high ( $TiO_2 + FeO_b$ )/MgO. Magnetite found in some of the Australian A-type granites was interpreted as secondary, and most of the Wangrah Suite granites evolved under reduced conditions, below the FMQ buffer (King et al., 2001). The A-type granites of Lachlan show relatively limited variation and, except for the Watergums granite that contains 0.2% modal magnetite (Clemens et al., 1986), magnetite-series granites were not generally described from the area. Accordingly, the White and Chappell classification can be useful to distinguish between I-, S-, and A-type granites of Lachlan, but it does not discriminate different A-type granite groups described from elsewhere.

Ishihara (1977, 1981) proposed a non-genetic classification for granites on the basis of magnetite content and magnetic susceptibility. The magnetite-series granites have more than 0.1 vol.% of magnetite and the ilmenite-series granites are magnetite-free. This classification was developed for the granites of Japan and has been extended to the circum-Pacific orogenic belt and also to anorogenic environments (Takahashi et al., 1980; Ishihara, 1981; Anderson and Bender, 1989; Dall'Agnol et al., 1997a). The contrasts between these series are considered to be related to differences in oxygen fugacity during magma evolution, the magnetite-series granites being oxidized and the ilmenite-series reduced. This classification has been applied to the Mesoproterozoic A-type granites of Laurentia and Fennoscandia (Anderson and Cullers, 1999; Anderson and Morrison, 2005). It presents, however, some contradictory aspects that need discussion. As observed in the Carajás region, some A-type granites that clearly classify as oxidized magnetite-series according to the terminology of Ishihara can also have high FeO/(FeO+MgO) ratios in whole-rock, amphibole, and biotite; this indicates that they evolved at relatively reducing conditions, probably not far from the FMQ buffer. On the other hand, granites which formed at moderately reduced conditions, on or a little above FMQ, can have significant modal contents of magnetite. These granites were formed in  $fO_2$  conditions between those of the ilmenite-series granites and the typical oxidized magnetite-series granites. Even granites and rhyolites with the classic fayalite+magnetite+quartz assemblage, that were unequivocally formed under low oxygen fugacity (FMQ; e.g., Frost, 1991), can have significant modal contents of magnetite (Galindo et al., 1995; Dall'Agnol et al., 1999d; McReath et al., 2002). These granites display magnetic susceptibility values that are higher than those of the ilmenite-series granites, which are devoid of magnetite. Hence not all magnetite-series granites of Ishihara (1981) have been evolved in oxidizing conditions and thus other aspects than Fe-Ti oxide minerals should

be used to distinguish them from the calc-alkaline or oxidized A-type magnetite-series granites.

Eby (1990, 1992) scrutinized the trace element composition of A-type granites and identified significant differences in their signatures. He proposed to divide the A-type granites into two subgroups (A1 and A2) with contrasting petrogenesis. The oxidized A-type granites (see Anderson and Bender, 1989, for Laurentia; Dall'Agnol et al., 1999b, for Amazonia), the rapakivi granites of Fennoscandian shield, and the A-type granites of Lachlan, all display the geochemical characteristics of the A2 subgroup. In contrast, the White Mountain Series and the Shira Nigerian Younger A-type granites are both classified as A1 (see Dall'Agnol et al., 1999b).

Barbarin (1999) proposed tectonic, geological, and geochemical criteria to distinguish between different granite series. He identified strongly peraluminous (S-types and their variants), calc-alkaline orogenic, and arc or mid-ocean tholeiitic granitoids. However, on that classification, A-type granites are represented only by peralkaline granites of inferred mantle origin. The metaluminous to mildly peraluminous A-type granites, represented by the rapakivi and similar A-type granites of crustal origin (Rämö and Haapala, 1995; Dall'Agnol et al., 1999a; Bettencourt et al., 1999) are not clearly represented in Barbarin's classification.

Patiño Douce (1999) distinguished six groups of felsic 'granitic' rocks on the basis of major element composition, petrogenesis, and tectonic setting: peraluminous leucogranites, S-type granites, peraluminous Cordilleran granites, calc-alkaline granites, metaluminous alkali-rich granites (MAGS), and rhyolites associated with continental flood-basalt provinces (FBRS). The MAGS are predominantly metaluminous A-type granites and rhyolites, including rapakivi granites. Strongly peralkaline granites and their volcanic equivalents as well as strongly peraluminous topaz rhyolites are excluded from MAGS by Patiño Douce (1999). The FBRS are distinctly metaluminous Fe-rich rocks that share some characteristics with MAGS. The clear differences between MAGS and peralkaline granites (Patiño Douce, 1999) require a refined classification of these two A-type granite groups. Patiño Douce's criteria to distinguish strongly peraluminous topaz rhyolites from MAGS are less evident, not least in view of the fact that topaz-bearing granites, similar in mineralogy and geochemistry to topaz rhyolites (Christiansen et al., 1986; Christiansen, 2003), are commonly associated with the more evolved facies of rapakivi granites (Haapala, 1977, 1995; Dall'Agnol et al., 1999a; Bettencourt et al., 1999; Lenharo et al., 2002). According to Patiño Douce (1999), peraluminous leucogranites are the only group that represents pure anatetic

crustal melts—the other groups correspond to crystal-rich magmas with residual phases or hybrid melts resulting from interaction of crustal rocks with mafic mantle-derived magmas.

Frost et al. (2001) proposed a non-genetic classification for granitic rocks considering their major element compositions. Their classification scheme uses three major element chemical parameters, the Fe-number (Fe or Fe\*), the modified alkali-lime index (MALI) and the aluminum saturation index (ASI) to distinguish 16 different kind of granites independent of their magma sources or tectonic environment. The Fe\* parameter [ $\text{FeO}_t/(\text{FeO}_t + \text{MgO})$ ] is a good discriminant between A-type and Cordilleran granites and also quite useful for a preliminary identification of A-type granites. In the  $\text{FeO}_t/(\text{FeO}_t + \text{MgO})$  vs.  $\text{SiO}_2$  diagram proposed by Frost et al. (2001) (Fig. 2d), A-type granites plot systematically in the ferroan field (high Fe\*). However, in the  $\text{Na}_2\text{O} + \text{K}_2\text{O} - \text{CaO}$  (MALI) vs.  $\text{SiO}_2$  diagram (Fig. 2b), A-type granites spread across several fields. This is probably due to the fact that whole-rock  $\text{Al}_2\text{O}_3$  content, commonly employed as a discriminating parameter (Irvine and Baragar, 1971; Ringwood, 1975; Wilson, 1989) is not considered in MALI.

Most of the classifications reviewed above do not discriminate the different A-type granite groups and some of them are unable to distinguish oxidized, magnetite-series A-type granites from the orogenic calc-alkaline and I-type granites.

## 5. Geochemical distinction of oxidized A-type granites

As emphasized by Patiño Douce (1999) and Frost et al. (2001), it is profitable to use major element chemical composition for granite classification, whereas genetic connotations should be left out. We will take the classification scheme of Frost et al. (2001) and the group of metaluminous, alkali granites (MAGS) of Patiño Douce (1999) as a starting point for our refined geochemical characterization of A-type granites. The scheme of Patiño Douce (1997) will also be used, mainly to differentiate between A-type and calc-alkaline granitoids.

In search of distinctive geochemical characteristics of oxidized, rapakivi A-type granites, we have employed a data set (available on request from the authors) with representative geochemical data from (1) the Carajás region granites (Jamon, Serra dos Carajás, and Velho Guilherme suites, Dall'Agnol et al., 2005); (2) the Finnish rapakivi granites (Wiborg area, Rämö, 1991, Rämö and Haapala, 1995; Bodom and Obbnäs plutons, Kosunen, 1999)—the Bodom and Obbnäs plutons were chosen because they dominant facies show significant

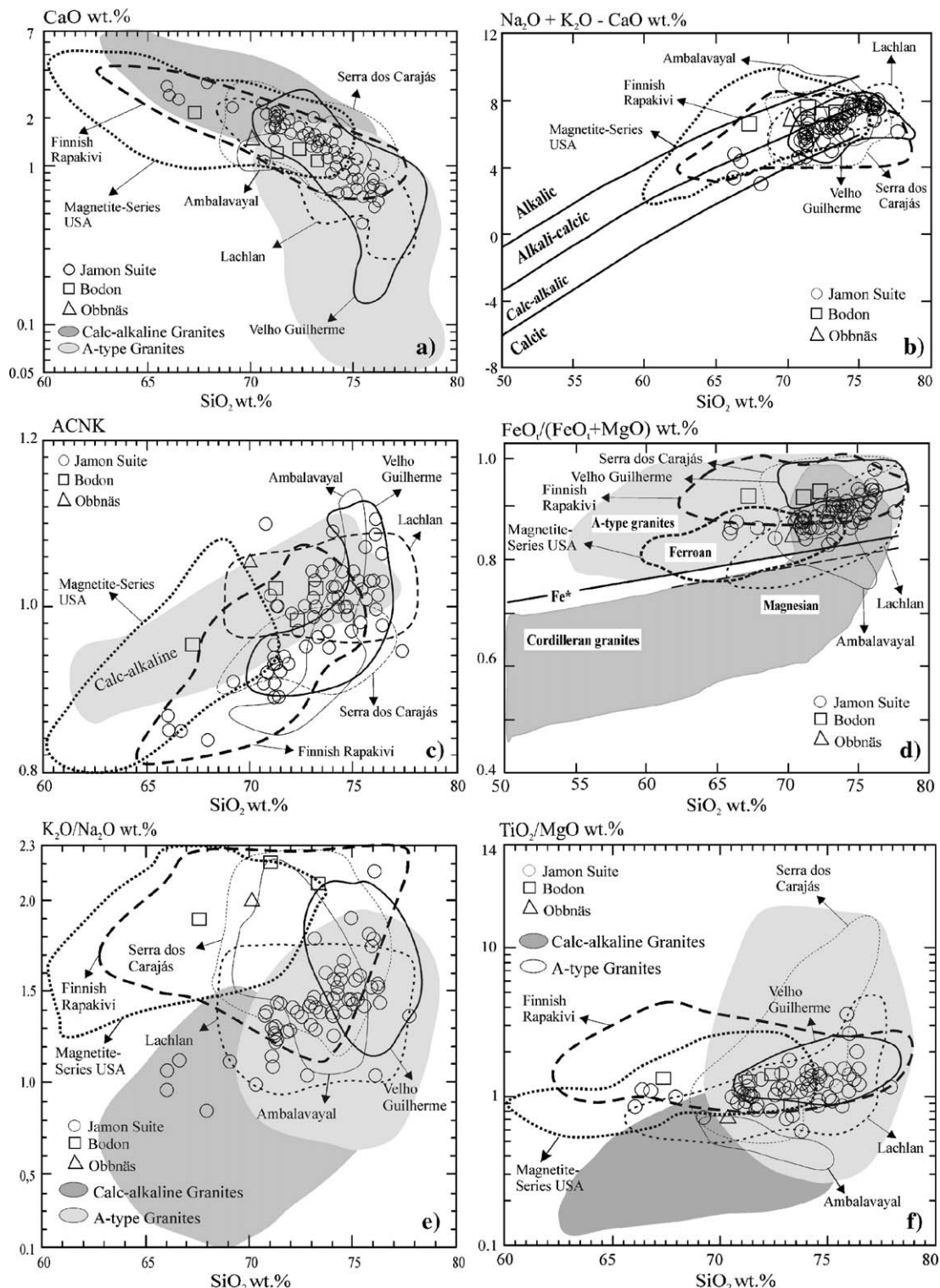
differences in whole-rock  $\text{FeO}_t/(\text{FeO}_t + \text{MgO})$  ratios; (3) the Mesoproterozoic magnetite-series granites of Laurentia (Anderson and Bender, 1989); (4) the A-type granites of the Lachlan Fold Belt (King et al., 1997, 2001); (5) the Ambalavayal A-type granite (Rajesh, 2000); (6) calc-alkaline Cordilleran granitoids (Sierra Nevada and Tuolumne batholiths; samples with more than 60 wt.% of  $\text{SiO}_2$  from the data set of Frost et al., 2001). Peralkaline granites have not been included, because they form an independent group of A-type granites. In the plots presented here, the Jamon suite samples, corresponding to the oxidized A-type granites of Carajás, are represented individually. The other suites are represented as fields, except for the average compositions of the main granite facies of the Bodom and Obbnäs plutons (Kosunen, 1999).

The data are shown in a selection of the diagrams proposed by Patiño Douce (1997) and Frost et al. (2001) in Fig. 2. In the  $\text{CaO}$  vs.  $\text{SiO}_2$  plot (Fig. 2a), the selected A-type granites have lower  $\text{CaO}$  contents than calc-alkaline granites but define fields that are almost parallel to the calc-alkaline field. In general, the Jamon suite granites plot in the area of overlap between the calc-alkaline and A-type fields, and extend into the A-type field (silica-rich samples) and the calc-alkaline field (silica-poor samples). They also plot almost in the same area as the Finnish rapakivi granites and the magnetite-series granites of the United States. The reduced Velho Guilherme suite granites of Carajás plot in the A-type field of Patiño Douce (1997). In the  $\text{Na}_2\text{O} + \text{K}_2\text{O} - \text{CaO}$  vs.  $\text{SiO}_2$  diagram (Fig. 2b), the A-type granite suites plot preferentially in the calc-alkalic and alkali-calcic fields (Frost et al., 2001). The Jamon suite samples are concentrated in the calc-alkalic field. The magnetite-series granites of the United States are enriched in alkalies compared to the Jamon granites and in part fall into the alkali field. In the  $\text{A/CNK}$  vs.  $\text{SiO}_2$  diagram (Fig. 2c), the fields of A-type granites and calc-alkaline granites are partially superposed. It is clear that these diagrams do not clearly discriminate A-type granites and calc-alkaline granites.

On the other hand, in the  $\text{FeO}_t/(\text{FeO}_t + \text{MgO})$  vs.  $\text{SiO}_2$  (Frost et al., 2001) and  $\text{K}_2\text{O}/\text{Na}_2\text{O}$  vs.  $\text{SiO}_2$ ,  $\text{TiO}_2/\text{MgO}$  vs.  $\text{SiO}_2$  (Patiño Douce, 1997) diagrams (Fig. 2d,e,f), the selected A-type granites are concentrated in the A-type and ferroan fields, and are better discriminated from calc-alkaline and Cordilleran granites. Compared to the latter, A-type granites show generally higher  $\text{FeO}_t/(\text{FeO}_t + \text{MgO})$ ,  $\text{K}_2\text{O}/\text{Na}_2\text{O}$ , and  $\text{TiO}_2/\text{MgO}$ . Some of the differences in the selected A-type granite fields and the fields of Patiño Douce (1997) relate to the fact that some peralkaline granites are included in the

indicated A-type field (Patiño Douce, 1997; see NK/A plot, his Fig. 1) and that dispersed samples with less than 70 wt.% SiO<sub>2</sub> are not represented in our schematic field.

The oxidized Jamon suite granites display geochemical trends that are similar to those of the magnetite-series granites of Laurentia (Fig. 2a to f), however the



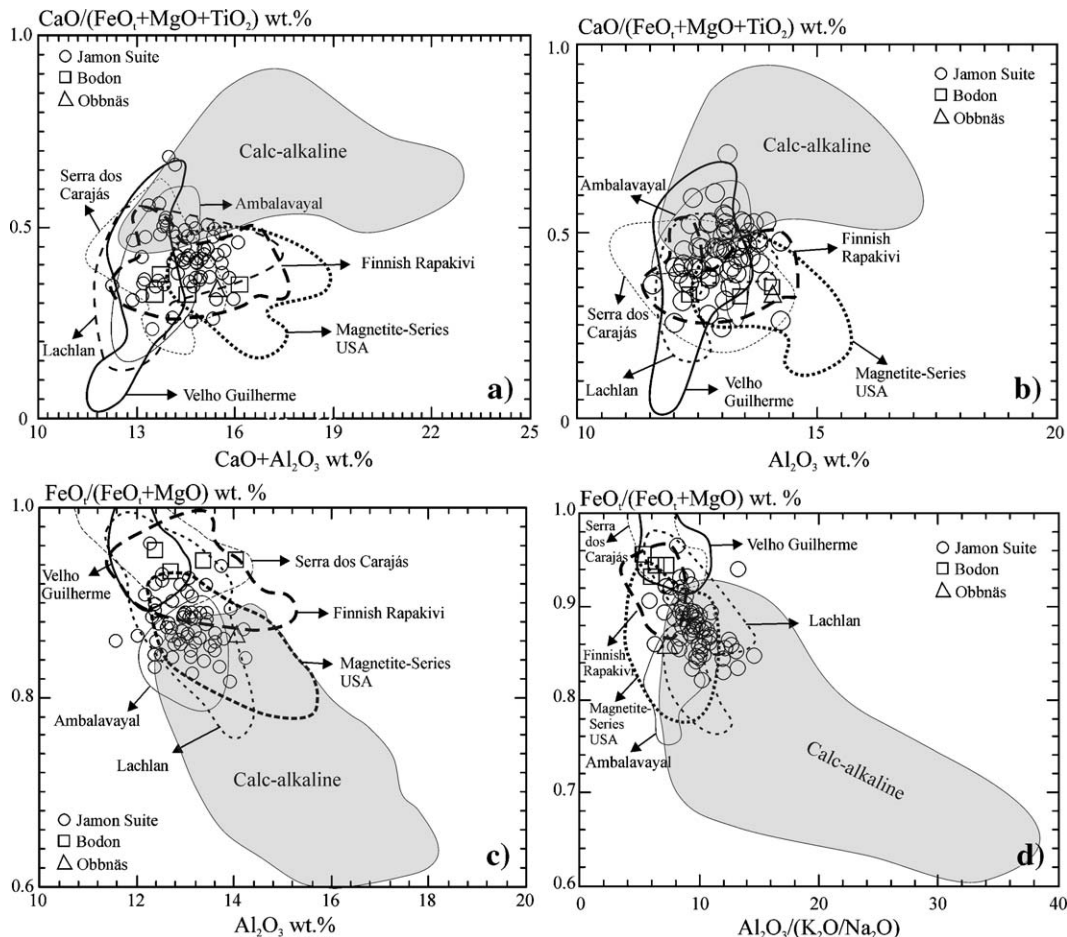


Fig. 3. Whole-rock  $\text{CaO}/(\text{FeO}_t + \text{MgO} + \text{TiO}_2)$  vs.  $\text{CaO} + \text{Al}_2\text{O}_3$  (a),  $\text{CaO}/(\text{FeO}_t + \text{MgO} + \text{TiO}_2)$  vs.  $\text{Al}_2\text{O}_3$  (b),  $\text{FeO}/(\text{FeO}_t + \text{MgO})$  vs.  $\text{Al}_2\text{O}_3$  (c), and  $\text{FeO}/(\text{FeO}_t + \text{MgO})$  vs.  $\text{Al}_2\text{O}_3/(\text{K}_2\text{O}/\text{Na}_2\text{O})$  (d) diagrams showing composition of representative oxidized and reduced A-type granites compared with calc-alkaline granites. Calc-alkaline fields are based on Sierra Nevada and Tuolumne granitoids with >60 wt.% of  $\text{SiO}_2$  (Frost et al., 2001). Data sources from A-type granites as in Fig. 2.

lower  $\text{K}_2\text{O}/\text{Na}_2\text{O}$  and higher  $\text{SiO}_2$  of Jamon distinguish this suite from the Laurentian granites in some of the plots. The fields of rapakivi granites and the reduced Velho Guilherme and Serra dos Carajás granites are similar to those of the oxidized granites, but their  $\text{FeO}_t/(\text{FeO}_t + \text{MgO})$  and  $\text{TiO}_2/\text{MgO}$  ratios are generally higher than in the A-type oxidized granites (Fig. 2d,f). The Ambalavayal granites and some samples of the Lachlan Belt A-type

granites show the lowest  $\text{FeO}_t/(\text{FeO}_t + \text{MgO})$  and fall in both the magnesian and ferroan fields (Fig. 2d). The Ambalavayal granites display also the lowest  $\text{TiO}_2/\text{MgO}$  ratios (Fig. 2f).

Patiño Douce (1999) compared Cordilleran granites, metaluminous A-type granites and basalt plateau rhyolites with the composition of experimental melts from varied sources. He showed that the  $\text{CaO}/(\text{FeO}_t +$

Fig. 2. Whole-rock (a)  $\text{CaO}$  vs.  $\text{SiO}_2$ , (b)  $\text{Na}_2\text{O} + \text{K}_2\text{O} - \text{CaO}$  vs.  $\text{SiO}_2$ , (c)  $[\text{Al}_2\text{O}_3/(\text{CaO} + \text{Na}_2\text{O} + \text{K}_2\text{O})]_{\text{Mol}}$  vs.  $\text{SiO}_2$ , (d)  $\text{FeO}/(\text{FeO}_t + \text{MgO})$  vs.  $\text{SiO}_2$ , (e)  $\text{K}_2\text{O}/\text{Na}_2\text{O}$  vs.  $\text{SiO}_2$ , and (f)  $\text{TiO}_2/\text{MgO}$  vs.  $\text{SiO}_2$  diagrams showing composition of representative A-type granites compared with calc-alkaline granites. A-type and calc-alkaline granite fields in (a), (e), and (f) from Patiño Douce (1997); alkalic, alkalic-calcic, calc-alkalic, and calcic fields in (b) and  $\text{Fe}^*$  divide line, magnesian Cordilleran granites and ferroan A-type granites fields in (d) are from Frost et al. (2001a). Data sources: Rämö and Haapala (1995) [Finnish rapakivi plutons from the Wiborg area]; Kosunen (1999) [Bodom and Obbnäs rapakivi plutons, southern Finland]; Anderson and Bender (1989) [Mesoproterozoic magnetite-series granites of the United States]; King et al. (1997, 2001) [Lachlan Fold Belt A-type granites]; Rajesh (2000) [Ambalavayal granites]; Dall'Agnol et al. (2005, and references therein) [Carajás A-type granite suites?Jamon (oxidized), Serra dos Carajás (moderately reduced), and Velho Guilherme (reduced); Frost et al. (2001) (calc-alkaline field in (c), Sierra Nevada and Tuolumne granitoids with >60 wt.% of  $\text{SiO}_2$ ].

$\text{MgO} + \text{TiO}_2$ ) ratio and  $\text{CaO} + \text{Al}_2\text{O}_3$  contents are useful in discriminating A-type and calc-alkaline granites. Accordingly, we have plotted the selected granites in the  $\text{CaO}/(\text{FeO}_t + \text{MgO} + \text{TiO}_2)$  vs.  $\text{CaO} + \text{Al}_2\text{O}_3$  diagram (Fig. 3a). Clearly distinct fields for the calc-alkaline granites and A-type granites emerge—this reflects the lower  $\text{CaO}$  and  $\text{Al}_2\text{O}_3$  contents of A-type granites and stresses the contrast in  $\text{Al}_2\text{O}_3$  content between these granite types. In fact,  $\text{Al}_2\text{O}_3$  content is a critical parameter in the characterization of calc-alkaline series (Irvine and Baragar, 1971; Ringwood, 1975; Wilson, 1989) and it should be considered in the geochemical distinction of these two granite series. It turns out that the  $\text{CaO}/(\text{FeO}_t + \text{MgO} + \text{TiO}_2)$  vs.  $\text{Al}_2\text{O}_3$  diagram (Fig. 3b) offers a good discrimination between A-type and calc-alkaline granites. However, in these diagrams (Fig. 3a,b), the fields of oxidized and reduced A-type granites are largely superposed, and these diagrams are not useful in distinguishing these two A-type granite groups.

As the next step,  $\text{Al}_2\text{O}_3$  was plotted against  $\text{FeO}_t/(\text{FeO}_t + \text{MgO})$  (Fig. 3c), a parameter for evaluation of the oxidizing character of magmatic rocks (Frost, 1991; Emslie, 1991; Frost et al., 2001; Anderson and Morrison, 2005; see Fig. 2d). This plot discriminates A-type and calc-alkaline granites, and allows a clear distinction between oxidized and reduced A-type granites. Due to their relatively low  $\text{FeO}_t/(\text{FeO}_t + \text{MgO})$  ratios, the Jamon suite samples and the magnetite-series granites of the United States are partially superposed with the calc-alkaline granite field. The  $\text{FeO}_t/(\text{FeO}_t + \text{MgO})$  vs.  $\text{Al}_2\text{O}_3/(\text{K}_2\text{O}/\text{Na}_2\text{O})$  diagram (Fig. 3d) employs some prominent geochemical parameters for the distinction of A-type granites (high in  $\text{FeO}_t/(\text{FeO}_t + \text{MgO})$  and  $\text{K}_2\text{O}/\text{Na}_2\text{O}$ ) and calc-alkaline granites (high in  $\text{Al}_2\text{O}_3$ ). This diagram discriminates calc-alkaline and A-type granites and also allows a good distinction between oxidized and reduced A-type granites.

It is concluded that: (1) the  $\text{FeO}_t/(\text{FeO}_t + \text{MgO})$  vs.  $\text{SiO}_2$ ,  $\text{K}_2\text{O}/\text{Na}_2\text{O}$  vs.  $\text{SiO}_2$ , and  $\text{TiO}_2/\text{MgO}$  vs.  $\text{SiO}_2$  diagrams (Fig. 2d,e,f), as well as the new proposed  $\text{CaO}/(\text{FeO}_t + \text{MgO} + \text{TiO}_2)$  vs.  $\text{CaO} + \text{Al}_2\text{O}_3$  and  $\text{CaO}/(\text{FeO}_t + \text{MgO} + \text{TiO}_2)$  vs.  $\text{Al}_2\text{O}_3$  diagrams (Fig. 3a,b), are well suited to distinguish between A-type and calc-alkaline granites; (2) the oxidized A-type granites are geochemically distinct from I-type, calc-alkaline or Cordilleran granitoids and similar in most geochemical aspects to typical A-type, including rapakivi, granites; and (3) the  $\text{FeO}_t/(\text{FeO}_t + \text{MgO})$  vs.  $\text{Al}_2\text{O}_3$  and  $\text{FeO}_t/(\text{FeO}_t + \text{MgO})$  vs.  $\text{Al}_2\text{O}_3/(\text{K}_2\text{O}/\text{Na}_2\text{O})$  diagrams (Fig. 3c, d) can be used to distinguish oxidized and reduced A-type granites, as well as for general discrimination of A-type from calc-alkaline granites.

## 6. $\text{FeO}_t/(\text{FeO}_t + \text{MgO})$ ratio vs. magnetite-series and ilmenite-series

Anderson and Morrison (2005) stated that whole-rock  $\text{FeO}_t/(\text{FeO}_t + \text{MgO})$  ratios of magnetite-series granites of Laurentia typically range between 0.80 and 0.88, while those of ilmenite-series granites are generally higher ( $>0.88$ ). Similar values (Figs. 2d, 3c,d) are shown by, respectively, the oxidized Jamon granites (0.83 to 0.94; Dall'Agnol et al., 1999c; Oliveira, 2001; Dall'Agnol et al., 2005) and the reduced Velho Guilherme and moderately reduced Serra dos Carajás granites (0.89 to 0.99; Teixeira, 1999; Dall'Agnol et al., 2005). However, some ilmenite-series granites of Laurentia (Anderson and Morrison, 2005; their Fig. 2) and some Finnish rapakivi granites (Fig. 3c,d) display whole-rock  $\text{FeO}_t/(\text{FeO}_t + \text{MgO})$  ratios lower than 0.88 and can not be distinguished from magnetite-series by this parameter. The Bodom and Obbnäs plutons are good examples of the contrasts in whole-rock  $\text{FeO}_t/(\text{FeO}_t + \text{MgO})$  ratios observed in rapakivi granites (Fig. 2d). The Bodom granites have higher whole-rock, biotite, and amphibole  $\text{FeO}_t/(\text{FeO}_t + \text{MgO})$  compared to Obbnäs (Kosunen, 1999, 2004; see Dall'Agnol et al., 2005). The dominant granitic facies of Obbnäs contains primary titanite and undefined iron oxide minerals as accessory minerals (Kosunen, 1999) and has whole-rock  $\text{FeO}_t/(\text{FeO}_t + \text{MgO})$  similar to those of Jamon and magnetite-series granites of Laurentia (Fig. 3c,d). However,  $\text{FeO}_t/(\text{FeO}_t + \text{MgO})$  in biotite and amphibole from Obbnäs is high ( $\sim 0.85$ –0.80; Kosunen, 2004) and similar to what is observed for moderately reduced A-type granites. This suggests that whole-rock and mafic mineral  $\text{FeO}_t/(\text{FeO}_t + \text{MgO})$  ratios must be employed with caution to define the reduced or oxidized character of A-type granites. There is a partial overlap between the fields of rapakivi granites, representative of the ilmenite-series, and oxidized, magnetite-series granites (Fig. 3c,d). This indicates that, for granites with whole-rock  $\text{FeO}_t/(\text{FeO}_t + \text{MgO})$  ratios near the limit for both series (0.88, as proposed by Anderson and Morrison, 2005), other aspects besides this ratio need to be considered in search of magmatic  $f\text{O}_2$  values. The identities and modal contents of Fe–Ti oxide minerals will be extremely relevant in this respect (see Ishihara, 1981; Frost, 1991; Dall'Agnol et al., 1997a).

Another aspect of the same problem is illustrated by some A-type granites of Carajás, e.g., the Cigano granite (Dall'Agnol et al., 2005), which contain magnetite and are classified as magnetite-series, but also display very high whole-rock, biotite, and amphibole  $\text{FeO}_t/(\text{FeO}_t + \text{MgO})$  ratios, indicating crystallization in relatively reducing conditions. This suggests that the magnetite-

series and ilmenite-series granites, as originally defined by Ishihara (1977, 1981), and, respectively, oxidized and reduced A-type granites, cannot always be considered strictly equivalent.

The A-type granites of the Lachlan Fold Belt have been generally interpreted as reduced (see King et al., 1997, 2001). However, whole-rock  $\text{FeO}_t/(\text{FeO}_t + \text{MgO})$  ratios in these granites tend to be lower than in other A-type granites (see Frost et al., 2001) and their fields (Fig. 3c,d) are superposed with both ilmenite-series and magnetite-series granites. This suggests that the Lachlan A-type granites were crystallized from both reduced and oxidized magmas. This hypothesis is reinforced by the content (0.2% modal) of early magmatic magnetite in the Watergums granite (Clemens et al., 1986; see their Fig. 1).

The Ambalavayal granites contain primary titanite and magnetite and whole-rock  $\text{FeO}_t/(\text{FeO}_t + \text{MgO})$  ratios similar or even lower than those of oxidized A-type granites (0.76 to 0.90; Rajesh, 2000; Fig. 3c,d). They evolved in oxidizing conditions, around or above NNO (Rajesh, 2000), and should also be classified as magnetite-series (Ishihara, 1981). However, the  $\text{FeO}_t/(\text{FeO}_t + \text{MgO})$  ratios in amphibole and biotite are extremely high (>0.95; Rajesh, 2000) and coincident with those shown by ilmenite-series granites (Anderson and Bender, 1989; Anderson and Smith, 1995; Rämö and Haapala, 1995; Frost and Frost, 1997; Frost et al., 1999; Anderson and Morrison, 2005). The reason for this ambiguous behavior is not clearly understood.

It is concluded that: (1) all magnetite-bearing granites are not necessarily oxidized and there is not a strict equivalence between the magnetite-series and ilmenite-series classification of Ishihara (1981) and, respectively, reduced and oxidized granites in general; (2) whole-rock and mafic mineral  $\text{FeO}_t/(\text{FeO}_t + \text{MgO})$  ratios must be employed with caution to define the reduced or oxidizing character of A-type granites near the boundary of ilmenite and magnetite-series granites; (3) definition of nature and modal contents of Fe–Ti oxide minerals of A-type granites, coupled with mineralogical and geochemical data, are relevant for estimation of  $f\text{O}_2$  conditions during magma crystallization.

## 7. Experimental constraints on the origin of oxidized A-type granites

Clemens et al. (1986) carried out crystallization experiments on the Watergums A-type granite at a pressure of 1 kbar,  $f\text{O}_2$  at FMQ+0.3 and variable water contents in melt. The studied rock is a low-CaO (1.24 wt.%) syenogranite containing modal biotite, amphibole, and

magnetite (1.5, 0.7, and 0.2 vol.%, respectively). The low pressure favored water saturation at relatively low water content in melt (~4 wt.%  $\text{H}_2\text{O}$ ) and, associated with low CaO content (see experimental results at 2 kbar in the AB422 granite of Wangrah Suite with similar CaO content; Klimm et al., 2003), inhibited amphibole crystallization in experiments. The liquidus phases were magnetite or quartz, depending on the water content, both followed by plagioclase and at lower temperature clinopyroxene. Clemens et al. (1986) estimated high temperatures (>830 °C) and appreciable water contents (2.4 to 4.3 wt.%) for the Watergums granite magma.

Patiño Douce and Beard (1995) performed vapor-absent dehydration melting and some coupled crystallization experiments of a biotite gneiss and a quartz amphibolite from 3 to 15 kbar. The low pressure experiments (3 to 5 kbar) were performed at  $f\text{O}_2$  above NNO and those at higher pressures (7 to 15 kbar) at  $f\text{O}_2$  below FMQ. In the dehydration melting experiments with the biotite gneiss (2.1 wt.% of CaO), the major mafic residual phase for pressures between 3 and 10 kbar is orthopyroxene, accompanied by garnet at 12.5 kbar, and by garnet and clinopyroxene at 15 kbar (Patiño Douce and Beard, 1995). In similar experiments, the quartz amphibolite (7.6 wt.% of CaO) contained orthopyroxene and clinopyroxene as the major residual phases for all pressures, accompanied by garnet at 12.5 and 15 kbar. These results indicated that, independent of pressure, orthopyroxene and clinopyroxene are important residual phases for CaO-enriched sources, while for low-CaO compositions, clinopyroxene is found as a major residual phase only at high pressure (~15 kbar). It is also worth noting that at low pressure (3 to 5 kbar) and  $f\text{O}_2$  above NNO, the molar  $\text{Al}_2\text{O}_3/(\text{MgO} + \text{FeO})$  ratio decreased with increasing pressure (Patiño Douce and Beard, 1995, their Fig. 13). This suggests that, in oxidizing conditions, melts generated by dehydration melting at low pressures ( $\leq 4$  kbar) should contain higher  $\text{Al}_2\text{O}_3$  than those formed at more elevated pressures. If an origin by dehydration melting of crustal igneous sources is true for oxidized, metaluminous A-type granites, this indicates that the low  $\text{Al}_2\text{O}_3$  contents (Fig. 3b, c) shown by these A-type granites will probably not be favored by low pressure melting.

Patiño Douce (1997) performed dehydration melting experiments at 950 °C,  $f\text{O}_2$  1 log unit below FMQ, and pressures of 4 and 8 kbar on calc-alkaline hornblende–biotite granitoids from Sierra Nevada. Generated melt volume decreased from tonalite (~40 to 30%) to granodiorite (~20 to 15%) and with increasing pressure. At 4 kbar, melting reactions produced neoblastic Ca-rich plagioclase, abundant orthopyroxene, and scarce

clinopyroxene. At 8 kbar, clinopyroxene was abundant, orthopyroxene rare, and plagioclase growth negligible. Melt compositions are similar to A-type granites, but those obtained at 4 kbar have more definite A-type characteristics than those formed at 8 kbar (Patiño Douce, 1997). This difference was attributed to the presence of plagioclase+orthopyroxene as dominant residual phases at shallow pressure ( $\leq 4$  kbar) dehydration melting, in contrast to the dominance of clinopyroxene at higher pressure (~8 kbar). Patiño Douce concluded that low pressure dehydration melting of calc-alkaline granitoids is a likely origin for ‘high-silica metaluminous A-type granites’, including rapakivi granites, and that the A-type chemical characteristics are lost in melts generated in the deep crust.

Patiño Douce (1999) presented a similar reasoning to explain the origin of his group of metaluminous, alkali-rich granites (MAGS). These A-type granites and rapakivi granites were discussed together with the rhyolites associated with continental flood-basalt provinces (FBRS). Patiño Douce (1999) emphasized that these ‘silicic igneous rocks of shallow origin’ have several geochemical characteristics in common. He presented geochemical diagrams where MAGS and FBRS are compared, among others, to calc-alkaline granitoids and compositional ranges of experimental metasediment-derived melts, and low pressure melts of calc-alkaline granitoids. Patiño Douce (1999) concluded that metaluminous A-type and rapakivi granites and

rhyolites associated with continental flood-basalts may be the products of low pressure melting of calc-alkaline rocks and that varying degrees of hybridization with basalts played an important role in their origin.

The MAGS, FBRS, and CAGS (calc-alkaline granites) of Patiño Douce (1999) are plotted together with A-type granites on the  $\text{CaO}/\text{Al}_2\text{O}_3$  vs.  $\text{CaO}+\text{Al}_2\text{O}_3$  and  $\text{CaO}/(\text{FeO}_t+\text{MgO}+\text{TiO}_2)$  vs.  $\text{CaO}+\text{FeO}_t+\text{MgO}+\text{TiO}_2$  diagrams (Fig. 4a,b). The A-type granite fields are disposed parallel to the FBRS field, partially superposed with the MAGS field, and clearly separated from the CAGS field. Oxidized and reduced A-type granites (e.g., the Jamon, Serra dos Carajás, and Velho Guilherme suites) do not define distinct fields in these diagrams and the fields of rapakivi granites, magnetite-series from the United States and Jamon are largely coincident. A-type granites follow the reaction curves for low pressure hybridization of calc-alkaline granites with high-Al olivine tholeiites and also the low pressure ( $\leq 5$  kbar) reaction curves for melt compositions produced by hybridization of high-Al olivine tholeiite with metagraywacke (Patiño Douce, 1999) (Fig. 4a,b). This suggests that plagioclase and orthopyroxene should be dominant residual phases of A-type magma sources. At the same time, it does not favor the formation of reduced and oxidized A-type granites at different pressures.

Dall'Agnol et al. (1999c) performed crystallization experiments on a hornblende–biotite monzogranite (2.2 wt.% CaO) of the Jamon suite at 3 kbar, varying

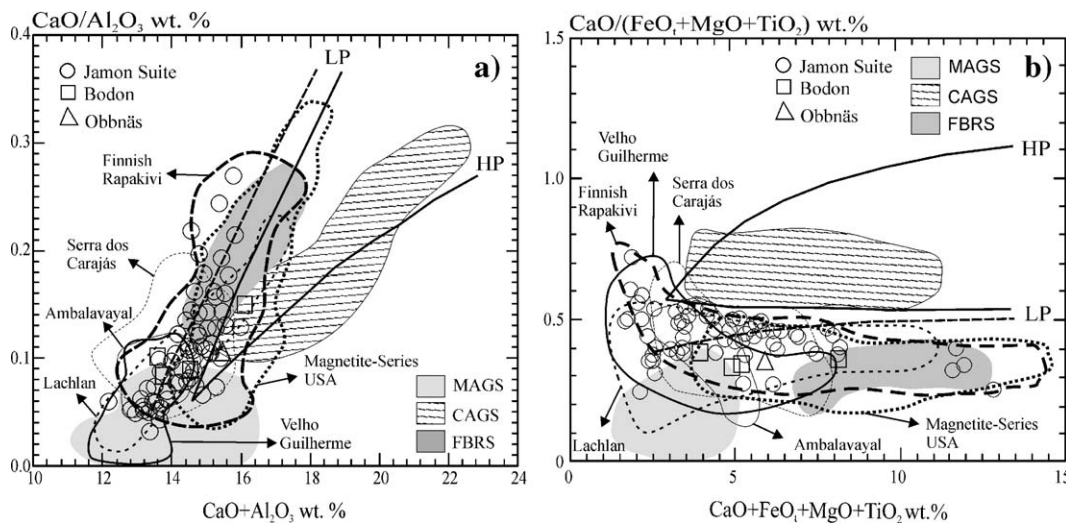


Fig. 4. Whole-rock  $\text{CaO}/\text{Al}_2\text{O}_3$  vs.  $\text{CaO}+\text{Al}_2\text{O}_3$  (a) and  $\text{CaO}/(\text{FeO}_t+\text{MgO}+\text{TiO}_2)$  vs.  $\text{CaO}+\text{FeO}_t+\text{MgO}+\text{TiO}_2$  (b) diagrams showing composition of representative oxidized and reduced A-type granites compared with calc-alkaline granites (CAGS), metaluminous alkali-rich granites (MAGS), and rhyolites associated with continental flood-basalt provinces (FBRS) (fields from Patiño Douce, 1999). Data sources for A-type granites as in Fig. 2. The dashed lines are reaction curves for low pressure hybridization of calc-alkaline granites with high-Al olivine tholeiites, with production of plagioclase+orthopyroxene. The solid lines labeled LP and HP imply melt compositions that would be produced by hybridization of high-Al olivine tholeiite with metagraywacke, at low pressure (LP,  $\leq 5$  kbar) or at high pressure (HP, 12 to 15 kbar) (Patiño Douce, 1999).

$f\text{O}_2$  (at NNO+2.5 and NNO−1.5) and water content in melt. In reducing conditions, clinopyroxene and orthopyroxene were the liquidus phases independent of water content. In oxidizing conditions, orthopyroxene was stable only at low  $\text{H}_2\text{O}$  content (<4 wt.%) and high temperatures. At higher water contents, clinopyroxene and plagioclase were the liquidus phases. Amphibole was stable only for liquids containing >4 wt.% of water, and its crystallization was thus strongly dependent on melt water contents (see Naney, 1983; Dall'Agnol et al., 1999c; Klimm et al., 2003). The amphibole probably derived from peritectic reactions between clinopyroxene±orthopyroxene and melt. The results obtained by Dall'Agnol et al. (1999c) indicate that, besides pressure,  $f\text{O}_2$  and water content in the melt also exert a strong influence on the nature of liquidus phases and, therefore, on the residual phases of A-type magmas produced by dehydration melting. Moderately high water contents

(>4 wt.%) and oxidizing conditions should inhibit the presence of orthopyroxene in the residue and favor that of clinopyroxene. In consequence, the A-type magmas generated under these conditions should be oxidized and have similar geochemical characteristics to the high pressure (~8 kbar) magmas derived from calc-alkaline sources of Patiño Douce (1997, 1999). Dall'Agnol et al. (1999c) also verified that  $\text{Fe}/(\text{Fe}+\text{Mg})$  in experimental mafic phases decreases with increasing temperature and  $f\text{O}_2$ . They estimated a 4 to 6 wt.% of water content for the Jamon hornblende–biotite monzogranite and dacite porphyry magmas and a crystallization at NNO+0.5 and temperatures between 900 and ~700 °C. Dall'Agnol et al. (1999b,c) also suggested that the Jamon magma could have been derived by relatively high pressure (>6 kbar) dehydration melting of an Archean source geochemically similar to a sanukitoid biotite–hornblende quartz diorite.

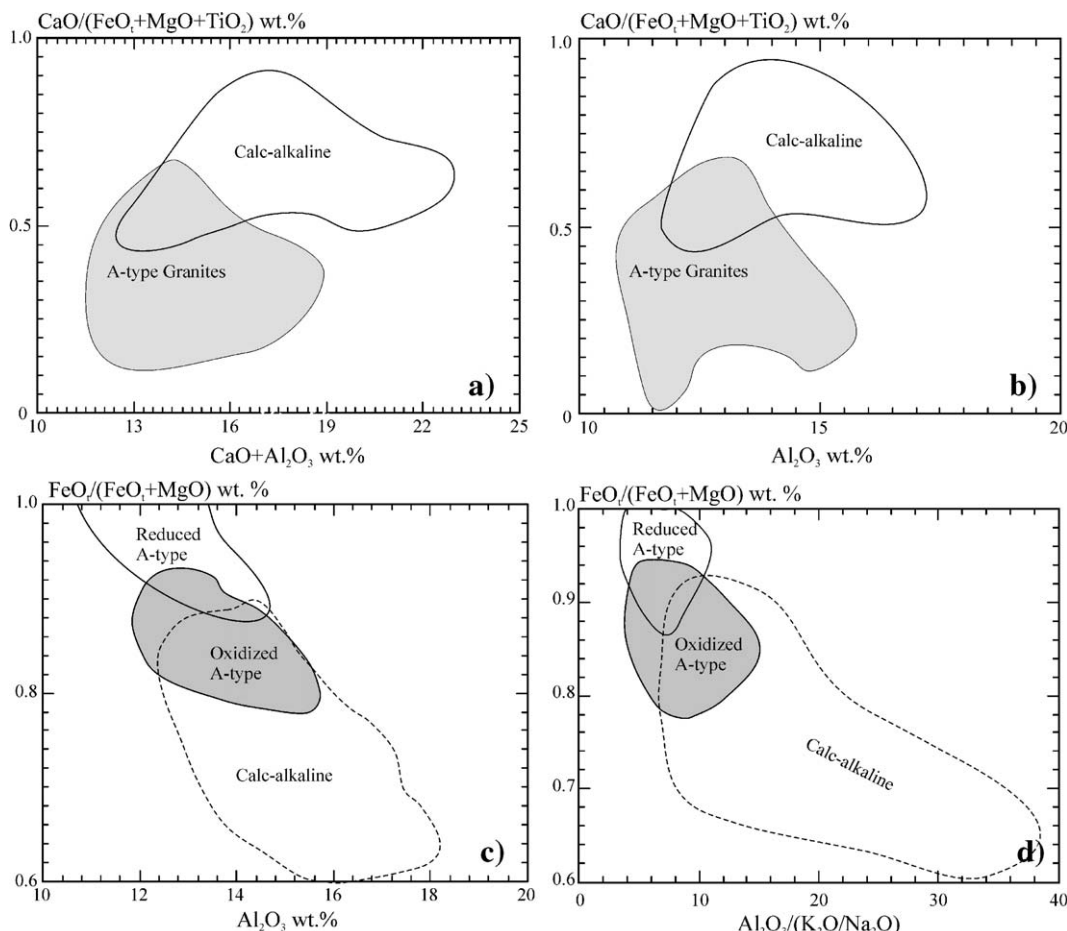


Fig. 5. Whole-rock  $\text{CaO}/(\text{FeO}_t+\text{MgO}+\text{TiO}_2)$  vs.  $\text{CaO}+\text{Al}_2\text{O}_3$  (a),  $\text{CaO}/(\text{FeO}_t+\text{MgO}+\text{TiO}_2)$  vs.  $\text{Al}_2\text{O}_3$  (b),  $\text{FeO}_t/(\text{FeO}_t+\text{MgO})$  vs.  $\text{Al}_2\text{O}_3$  (c), and  $\text{FeO}_t/(\text{FeO}_t+\text{MgO})$  vs.  $\text{Al}_2\text{O}_3/(\text{K}_2\text{O}/\text{Na}_2\text{O})$  (d) diagrams showing the compositional fields of calc-alkaline and A-type granites (a, b) and reduced and oxidized A-type granites and calc-alkaline granites (c, d). All fields were defined on the basis of data presented in Fig. 3.

Two hornblende–biotite granites (AB412 and AB422) of the Wangrah suite of the Lachlan Fold Belt were studied experimentally by Klimm et al. (2003) at 2 kbar,  $f\text{O}_2$  between NNO and NNO – 1.05, temperature between 900 and 700 °C, and for various melt  $\text{H}_2\text{O}$  contents. The AB412 granite is enriched in CaO (1.93 wt.%) and modal amphibole compared to the AB422 granite (CaO = 1.31 wt.%). Obtained liquidus temperatures were high (900 to 850 °C) and orthopyroxene and plagioclase were the liquidus phases for both compositions. Initial water content in the original magma of AB412 was estimated to be 2 to 3 wt.%  $\text{H}_2\text{O}$ . Klimm et al. (2003) suggested that the geologically relevant conditions for the Wangrah granites' crystallization were  $f\text{O}_2 < \text{NNO} - 2.2$ . They observed also that Fe/(Fe + Mg) in experimental orthopyroxene, amphibole, and biotite decreased with increasing  $f\text{O}_2$  and temperature and, in the case of orthopyroxene, also with increasing wt.%  $\text{H}_2\text{O}$  in melt.

The absence of clinopyroxene in the experimental phases of the Wangrah granites is noteworthy. In this aspect, they contrast with the results obtained on the Jamon granite. This difference could possibly be due to the higher CaO content and more oxidizing conditions of the Jamon granite. This indicates the relevance of source composition and  $f\text{O}_2$ , in determining the nature of residual phases during dehydration melting.

In summary, experimental evidence suggests that the geochemical signature of A-type granites is not dependent only on the pressure of melting. Source composition and  $f\text{O}_2$  conditions also exert a strong influence on the composition of generated magmas. These parameters are extremely relevant for the definition of the nature of residual phases during dehydration melting of crustal sources. Another important factor is water content, which is also related to the nature of the magma source, and is determinant for the crystallization of water-bearing silicates (e.g., amphibole).

Contrasts in crustal sources (including water content) and  $f\text{O}_2$ , associated with varying pressure may explain the geochemical characteristics of oxidized and reduced A-type granites.

## 8. Conclusions

Geochemical data demonstrate that, whatever the nature of magmatic processes involved in the origin of oxidized A-type granites is, these processes are certainly able to produce the dominant characteristics of A-type granites. This is shown by the fact that oxidized A-type granites are clearly distinguished from calc-alkaline Cordilleran granites in several major elements diagrams (Figs. 2d,e,f, 3a,b) and define fields largely coincident

with those of reduced A-type granites. Besides the  $\text{FeO}/(\text{FeO}_t + \text{MgO})$  vs.  $\text{SiO}_2$  (Frost et al., 2001),  $\text{K}_2\text{O}/\text{Na}_2\text{O}$  vs.  $\text{SiO}_2$ ,  $\text{TiO}_2/\text{MgO}$  vs.  $\text{SiO}_2$  (Patiño Douce, 1997) diagrams (Fig. 2d,e,f), the  $\text{CaO}/(\text{FeO}_t + \text{MgO} + \text{TiO}_2)$  vs.  $\text{CaO} + \text{Al}_2\text{O}_3$  and  $\text{CaO}/(\text{FeO}_t + \text{MgO} + \text{TiO}_2)$  vs.  $\text{Al}_2\text{O}_3$  diagrams can be used to distinguish A-type and calc-alkaline granites (Fig. 5a,b). Oxidized and reduced A-type granites are better discriminated in the  $\text{FeO}_t/(\text{FeO}_t + \text{MgO})$  vs.  $\text{Al}_2\text{O}_3$  and  $\text{FeO}_t/(\text{FeO}_t + \text{MgO})$  vs.  $\text{Al}_2\text{O}_3/(\text{K}_2\text{O}/\text{Na}_2\text{O})$  diagrams (Fig. 5c,d). We propose the two latter diagrams to distinguish between oxidized and reduced A-type granites. Preferentially, geochemical characterization should be accompanied by petrographic, Fe–Ti oxide, and magnetic susceptibility studies.

It is also concluded that all magnetite-bearing granites are not necessarily oxidized and a strict correspondence between oxidized and reduced A-type granites and, respectively, magnetite-series and ilmenite-series granites is not observed.

We have argued that oxidized granites like those of the Jamon suite and the Mesoproterozoic magnetite-series of the United States are better classified as A-type. It is also suggested that the classic rapakivi granites are more commonly ilmenite-series, reduced A-type granites. However, the relationship between oxidized A-type and rapakivi granites remains unresolved. In a classification scheme proposed for Laurentia–Baltica, the magnetite-series and ilmenite-series granites are spatially separated, implying broad regional changes in the composition of the lower crust sources of these granites (Anderson and Morrison, 2005). However, the A-type granites of Carajás region display near identical ages, occur in the same crustal province, and the processes involved in their origin are considered to be similar. These granites are stratigraphically correlated and are considered to differ as a function of contrasts in their sources. Furthermore, the porphyritic facies of Jamon granites commonly contains plagioclase-mantled K-feldspar megacrysts. For these reasons, we prefer to consider the Jamon granites as a distinct member of the rapakivi assemblage, but this point needs further discussion.

Experimental data indicate that the characteristics of A-type granites are strongly dependent on  $f\text{O}_2$  conditions and water content in magma sources. Besides pressure, these parameters, which are related to the nature of magma sources, should also be considered to explain the contrasts between different A-type granites. Oxidized A-type granites are considered to crystallize from magmas with appreciable water contents ( $\geq 4$  wt.%). Such conditions favor the presence of clinopyroxene as an important residual phase during dehydration melting (Dall'Agnol et al., 1999c) and can explain the less typical A-type

geochemical signature of oxidized A-type granites (see Anderson and Morrison, 2005).

An Archean, sanukitoid biotite–hornblende quartz diorite source was proposed for the oxidized Jamon magmas (Dall'Agnol et al., 1999b,c) and lower crustal calc-alkaline plutons for Laurentia magnetite-series granites (Anderson and Bender, 1989; Anderson and Morrison, 2005). In general, oxidized A-type granites probably derived from oxidized lower crustal quartz-feldspathic igneous sources. Reduced A-type granites could be derived from quartz-feldspathic igneous sources, with a reduced character (Anderson and Morrison, 2005) or, possibly, with a metasedimentary rock contribution (Dall'Agnol et al., 2005), or, alternatively, from differentiated tholeiitic sources (Frost and Frost, 1997; Frost et al., 1999). The imprint of these different magma sources is largely responsible for the geochemical and petrological contrasts between distinct A-type granite groups.

## Acknowledgments

J.A.C. Almeida contributed to the research on the Jamon Suite oxidized granites. O.T. Rämö, M. Pichavant, B. Scaillet, and colleagues of the Group of Research on Granite Petrology for stimulating discussions about rapakivi and A-type granites geochemistry and petrogenesis. O. T. Rämö, T. Andersen and L. Ashwal for invitation to participate in the Goldschmidt Conference at Copenhagen. P. Kosunen for unpublished data on the Bodom and Obbnäs plutons. Ilmari Haapala, Tod Waight and the volume editor's for criticisms and detailed reviews that substantially improved the paper. This research received support from CNPq (RD — 550739/2001-7, 476075/2003-3, 307469/2003-4; DCO — scholarship April04 up to present), CAPES (DCO — scholarship Nov01 to March04), and Federal University of Pará (UFPA). This paper is a contribution to PRONEX/CNPq (Proj. 103/98 — Proc. 66.2103/1998-0) and IGCP-510 project (IUGS-UNESCO).

## References

- Almeida, J.A.C., Dall'Agnol, R., Oliveira, D.C., submitted for publication. Geologia, petrografia e geoquímica do granito anorogênico Bannach, Terreno Granito-Greenstone de Rio Maria, Pará. Revista Brasileira de Geociências (in Portuguese).
- Althoff, F.J., Barbey, P., Boullier, A.-M., 2000. 2.8–3.0 Ga plutonism and deformation in the SE Amazonian craton: the Archean granitoids of Marajoara (Carajás Mineral Province, Brazil). *Precambrian Research* 104, 187–206.
- Amelin, Y.V., Larin, A.M., Tucker, R.D., 1997. Chronology of multiphase emplacement of the Salmi rapakivi granite-anorthosite complex, Baltic Shield: implications for magmatic evolution. *Contributions to Mineralogy and Petrology* 127, 353–368.
- Anderson, J.L., Bender, E.E., 1989. Nature and origin of Proterozoic A-type granitic magmatism in the southwestern United States of America. *Lithos* 23, 19–52.
- Anderson, J.L., Cullers, R.L., 1999. Paleo- and Mesoproterozoic granite plutonism of Colorado and Wyoming. *Rocky Mountain Geology* 34, 149–164.
- Anderson, J.L., Morrison, J., 1992. The role of anorogenic granites in the Proterozoic crustal development of North America. In: Condie, K.C. (Ed.), *Proterozoic Crustal Evolution*. Elsevier, pp. 263–299.
- Anderson, J.L., Morrison, J., 2005. Ilmenite, magnetite, and peraluminous Mesoproterozoic anorogenic granites of Laurentia and Baltica. *Lithos* 80, 45–60.
- Anderson, J.L., Smith, D.R., 1995. The effects of temperature and  $fO_2$  on the Al-in-hornblende barometer. *American Mineralogist* 80, 549–559.
- Barbarin, B., 1999. A review of the relationships between granitoid types, their origins and their geodynamic environments. *Lithos* 46, 605–626.
- Barnes, M.A., Anthony, E.Y., Williams, I., Asquith, G.B., 2002. Architecture of a 1.38–1.34 Ga granite–rhyolite complex as revealed by geochronology and isotopic and elemental geochemistry of subsurface samples from West Texas, USA. *Precambrian Research* 119, 9–43.
- Barros, C.E.M., Dall'Agnol, R., Vieira, E.A.P., Magalhães, M.S., 1995. Granito Central da Serra dos Carajás: avaliação do potencial metalogenético para estanho com base em estudos da borda oeste do corpo. *Boletim do Museu Paraense Emílio Goeldi. Série Ciências da Terra* 7, 93–123 (in Portuguese).
- Bettencourt, J.S., Tosdal, R.M., Leite Jr., W.B., Payolla, B.L., 1999. Mesoproterozoic rapakivi granites of the Rondônia Tin Province, southwestern border of the Amazonian craton, Brazil — I. Reconnaissance U–Pb geochronology and regional implications. *Precambrian Research* 95, 41–67.
- Bogaerts, M., Scaillet, B., Liégeois, J.-P., Vander Auwera, J., 2003. Petrology and geochemistry of the Lyngdal granodiorite (Southern Norway) and the role of fractional crystallization in the genesis of Proterozoic ferro-potassic A-type granites. *Precambrian Research* 124, 149–184.
- Chappell, B.W., White, J.R., 1974. Two contrasting granite types. *Pacific Geology* 8, 173–174.
- Chappell, B.W., White, J.R., 2001. Two contrasting granite types: 25 years later. *Australian Journal of Earth Sciences* 48, 489–499.
- Clemens, J.D., Holloway, J.R., White, A.J.R., 1986. Origin of the A-type granite: experimental constraints. *American Mineralogist* 71, 317–324.
- Collins, W.J., Beams, S.D., White, A.J., Chappell, B.W., 1982. Nature and origin of A-type granites with particular reference to Southeastern Australia. *Contributions to Mineralogy and Petrology* 80, 189–200.
- Costi, H.T., 2000. Petrologia de granitos alcalinos com alto flúor mineralizados em metais raros: o exemplo do albíta-granito da Mina Pitinga, Amazonas, Brasil. Doctor Thesis, Federal University of Pará, Belém, Brazil (in Portuguese).
- Creaser, R.A., Price, R.C., Wormald, R.J., 1991. A-type granites revisited: assessment of a residual-source model. *Geology* 19, 163–166.
- Christiansen, E.H., 2003. Are topaz rhyolites the erupted equivalents of rapakivi granites? In: Rämö, O.T., Kosunen, P.J., Lauri, L.S., Karhu, J.A. (Eds.), *Granitic Systems — State of the Art and Future Avenues. An International Symposium in Honor of Professor Ilmari Haapala, January 12–14, 2003*. Helsinki University Press. Abstract Volume, 120 pp.
- Christiansen, E.H., Sheridan, M.F., Burt, D.M., 1986. The geology and geochemistry of Cenozoic topaz rhyolites from the Western United States. *Geological Society of America, Special Paper* 205, 1–82.

- Dall'Agnol, R., Teixeira, N.P., Magalhães, M.S., 1993. Diagnostic features of the tin-specialized anorogenic granites of the Eastern Amazonian region. *Anais da Academia Brasileira de Ciências* 65 (Supl. 1), 33–50.
- Dall'Agnol, R., Lafon, J.M., Macambira, M.J.B., 1994. Proterozoic anorogenic magmatism in the Central Amazonian province: geochronological, petrological and geochemical aspects. *Mineralogy and Petrology* 50, 113–138.
- Dall'Agnol, R., Pichavant, M., Champenois, M., 1997a. Iron–titanium oxide mineral of the Jamon granite, Eastern Amazonian region, Brazil: implications for the oxygen fugacity in Proterozoic A-type granites. *Anais da Academia Brasileira de Ciências* 69, 325–347.
- Dall'Agnol, R., Souza, Z.S., Althoff, F.J., Barros, C.E.M., Leite, A.A.S., Jorge João, X.S., 1997b. General Aspects of the granitogenesis of the Carajás metallogenetic province. Second International Symposium on Granites and Associated Mineralizations, Excursions Guide, Salvador. Companhia Baiana de Pesquisa Mineral. Superintendência de Geologia e Recursos Minerais, pp. 135–161.
- Dall'Agnol, R., Costi, H.T., Leite, A.A., Magalhães, M.S., Teixeira, N.P., 1999a. Rapakivi granites from Brazil and adjacent areas. *Precambrian Research* 95, 9–39.
- Dall'Agnol, R., Rämö, O.T., Magalhães, M.S., Macambira, M.J.B., 1999b. Petrology of the anorogenic, oxidised Jamon and Musa granites, Amazonian craton: implications for the genesis of Proterozoic A-type granites. *Lithos* 46, 431–462.
- Dall'Agnol, R., Scaillet, B., Pichavant, M., 1999c. An experimental study of a Lower Proterozoic A-type granite from the Eastern Amazonian craton, Brazil. *Journal of Petrology* 40, 1673–1698.
- Dall'Agnol, R., Silva, C.M.G., Scheller, T., 1999d. Fayalite–hedembergite rhyolites of the Iriri formation, Tapajós Gold Province, Amazonian craton: implications for the Uatumã volcanism. Simpósio sobre Vulcanismo e Ambientes Associados, 1. Gramado. 1999. Boletim de resumos. Gramado. Instituto de Geociências/UFRGS, p. 31.
- Dall'Agnol, R., Teixeira, N.P., Rämö, O.T., Moura, C.A.V., Macambira, M.J.B., Oliveira, D.C., 2005. Petrogenesis of the Paleoproterozoic rapakivi, A-type granites of the Archean Carajás Metallogenic Province, Brazil. *Lithos* 80, 101–129.
- Eby, G.N., 1990. The A-type granitoids: a review of their occurrence and chemical characteristics and speculations on their petrogenesis. *Lithos* 26, 115–134.
- Eby, G.N., 1992. Chemical subdivision of the A-type granitoids: petrogenesis and tectonic implications. *Geology* 20, 641–644.
- Emslie, R.F., 1991. Granitoids of rapakivi granite–anorthosite and related associations. *Precambrian Research* 51, 173–192.
- Frost, B.R., 1991. Introduction to oxygen fugacity and its petrologic importance. In: Lindsley, D.H. (Ed.), Oxide minerals: petrologic and magnetic significance. *Reviews in Mineralogy*, vol. 25. Mineralogical Society of America, pp. 489–509.
- Frost, C.D., Frost, B.R., 1997. Reduced rapakivi type granites: the tholeiitic connection. *Geology* 25, 647–650.
- Frost, C.D., Frost, B.R., Chamberlain, K.R., Edwards, B., 1999. Petrogenesis of the 1.43 Ga Sherman batholith, SE Wyoming, USA: a reduced, rapakivi-type anorogenic granite. *Journal of Petrology* 40, 1771–1802.
- Frost, B.R., Barnes, C.G., Collins, W.J., Arculus, R.J., Ellis, D.J., Frost, C.D., 2001. A geochemical classification for granitic rocks. *Journal of Petrology* 42, 2033–2048.
- Galindo, A.C., Dall'Agnol, R., McReath, I., Lafon, J.M., Teixeira, N.P., 1995. Evolution of Brasiliano-age granitoids types in a shear-zone environment, Umarizal–Carauábas region, Rio Grande do Norte, Northeast Brazil. *Journal of South American Earth Sciences* 8, 79–96.
- Haapala, I., 1977. Petrography and geochemistry of the Eurajoki stock, a rapakivi–granite complex with greisen-type mineralization in southwestern Finland. *Geological Survey of Finland, Bulletin* 286, 1–128.
- Haapala, I., 1995. Metallogeny of the rapakivi granites. *Mineralogy and Petrology* 54, 149–160.
- Haapala, I., Rämö, O.T., 1992. Tectonic setting and origin of the Proterozoic rapakivi granites of the southeastern Fennoscandia. *Transactions of the Royal Society of Edinburgh. Earth Sciences* 83, 165–171.
- Hogan, J.P., Gilbert, M.C., Weaver, B.L., 1992. A-type granites and rhyolites: is A for ambiguous? *EOS, Transactions, American Geophysical Union* 73, 508 (newsletter).
- Irvine, T.N., Baragar, W.R.A., 1971. A guide to the chemical classification of the common volcanic rocks. *Canadian Journal of Earth Sciences* 8, 523–548.
- Ishihara, S., 1977. The magnetite-series and ilmenite-series granitic rocks. *Mining Geology* 27, 293–305.
- Ishihara, S., 1981. The granitoid series and mineralization. *Economic Geology* 75th Anniversary volume, 458–484.
- King, P.L., White, A.J.R., Chappell, B.W., Allen, C.M., 1997. Characterization and origin of aluminous A-type granites from the Lachlan Fold Belt, southeastern Australia. *Journal of Petrology* 38, 371–391.
- King, P.L., Chappell, B.W., Allen, C.M., White, A.J.R., 2001. Are A-type granites the high-temperature felsic granites? Evidence from fractionated granites of the Wangrah Suite. *Australian Journal of Earth Sciences* 48, 501–514.
- Klimm, K., Holtz, F., Johannes, W., King, P.L., 2003. Fractionation of metaluminous A-type granites: an experimental study of the Wangrah Suite, Lachlan Fold Belt, Australia. *Precambrian Research* 124, 327–341.
- Kosunen, P., 1999. The rapakivi granite plutons of the Bodom and Obbnäs, Southern Finland: petrography and geochemistry. *Bulletin of the Geological Society of Finland* 71, 275–304.
- Kosunen, P.J., 2004. Petrogenesis of A-type mid-Proterozoic A-type granites: Case studies from Fennoscandia (Finland) and Laurentia (New Mexico). Ph.D. Thesis, Department of Geology, University of Helsinki, Finland.
- Lamarão, C.N., Dall'Agnol, R., Lafon, J.-M., Lima, E.F., 2002. Geology, geochemistry, and Pb–Pb zircon geochronology of the Paleoproterozoic magmatism of Vila Riozinho, Tapajós Gold Province, Amazonian craton, Brasil. *Precambrian Research* 119, 189–223.
- Lamarão, C.N., Dall'Agnol, R., Pimentel, M.M., 2005. Nd isotopic composition of Paleoproterozoic volcanic and granitoid rocks of Vila Riozinho: implications for the crustal evolution of the Tapajós Gold Province, Amazonian craton. *Journal of South American Earth Sciences* 18, 277–292.
- Lenharo, S.L., Moura, M.A., Botelho, N.F., 2002. Petrogenetic and mineralization processes in Paleo- to Mesoproterozoic rapakivi granites: examples from Pitinga and Goiás, Brazil. *Precambrian Research* 119, 277–299.
- Loiselle, M.C., Wones, D.R., 1979. Characteristics and origin of anorogenic granites. *Geological Society of America Abstracts with Programs* 11, 468.
- Macambira, M.J.B., Lafon, J.-M., 1995. Geocronologia da Província mineral de Carajás: síntese dos dados e novos desafios. *Boletim do Museu Paraense Emílio Goeldi, Ciências da Terra* 7, 263–288 (in Portuguese).
- Machado, N., Lindenmayer, Z., Krogh, T.E., Lindenmayer, D., 1991. U–Pb geochronology of Archean magmatism and basement reactivation in the Carajás area, Amazon Shield, Brazil. *Precambrian Research* 49, 329–354.

- McReath, I., Galindo, A.C., Dall'Agnol, R., 2002. The Umarizal igneous association, Borborema Province, NE Brazil: implications for the genesis of A-type granites. *Gondwana Research* 5, 339–353.
- Naney, M.T., 1983. Phase equilibria of rock-forming ferromagnesian silicates in granitic systems. *American Journal of Science* 283, 993–1033.
- Oliveira, D.C., 2001. Geologia, geoquímica e petrologia magnética do granito paleoproterozóico Redenção, SE do Cráton Amazônico. M. Sc. Thesis, Federal University of Pará, Belém, Brazil (in Portuguese).
- Patiño Douce, A.E., 1997. Generation of metaluminous A-type granites by low-pressure melting of calc-alkaline granitoids. *Geology* 25, 743–746.
- Patiño Douce, A.E., 1999. What do experiments tell us about the relative contributions of crust and mantle to the origin of granitic magmas? In: Castro, A., Fernandez, C., Vigneresse, J.L. L. (Eds.), *Understanding Granites: New and Classical Techniques*, vol. 168. Geological Society, London, Special Publication, pp. 55–75.
- Patiño Douce, A.E., Beard, J.S., 1995. Dehydration-melting of biotite gneiss and quartz amphibolite from 3 to 15 kbar. *Journal of Petrology* 36, 707–738.
- Pearce, J.A., Harris, N.B.W., Tindle, A.C., 1984. Trace element discrimination diagrams for the tectonic interpretation of granitic rocks. *Journal of Petrology* 25, 956–983.
- Pitcher, W.S., 1993. *The Origin and Nature of Granite*. Chapman & Hall, London.
- Poitrasson, F., Pin, C., Douthou, J.-L., Platevoet, B., 1994. Aluminous subsolvus anorogenic granite genesis in the light of Nd isotopic heterogeneity. *Chemical Geology* 112, 199–219.
- Rajesh, H.M., 2000. Characterization and origin of a compositionally zoned aluminous A-type granite from South India. *Geological Magazine* 137, 291–318.
- Rämö, O.T., 1991. Petrogenesis of the Proterozoic rapakivi granites and related basic rocks of the southeastern Fennoscandian: Nd and Pb isotopic and general geochemical constraints. *Geological Survey of Finland Bulletin* 355.
- Rämö, O.T., Haapala, I., 1995. One hundred years of rapakivi granite. *Mineralogy and Petrology* 52, 129–185.
- Rämö, O.T., Dall'Agnol, R., Macambira, M.J.B., Leite, A.A.S., de Oliveira, D.C., 2002. 1.88 Ga oxidized A-type granites of the Rio Maria region, eastern Amazonian craton, Brazil: positively anorogenic! *Journal of Geology* 110, 603–610.
- Ringwood, A.E., 1975. *Composition and Petrology of the Earth's Mantle*. McGraw-Hill Book Company, New York.
- Scaillet, B., Macdonald, R., 2001. Phase relations of peralkaline silicic magmas and petrogenetic implications. *Journal of Petrology* 42, 825–845.
- Scaillet, B., Macdonald, R., 2003. Experimental constraints on the relationships between peralkaline rhyolites of the Kenya Rift Valley. *Journal of Petrology* 44, 1867–1894.
- Skjerlie, K.P., Johnston, A.D., 1993. Fluid-absent melting behavior of F-rich tonalitic gneiss at mid-crustal pressures: implications for the generation of anorogenic granites. *Journal of Petrology* 34, 785–815.
- Souza, Z.S., Potrel, A., Lafon, J.-M., Althoff, F.J., Pimentel, M.M., Dall'Agnol, R., Oliveira, C.G., 2001. Nd, Pb and Sr isotopes of the Identidade Belt, an Archean greenstone belt of the Rio Maria region (Carajás Province, Brazil): implications for the Archaean geodynamic evolution of the Amazonian Craton. *Precambrian Research* 109, 293–315.
- Sylvester, P.J., 1989. Post-collisional alkaline granites. *Journal of Geology* 97, 261–280.
- Takahashi, M., Aramaki, S., Ishihara, S., 1980. Magnetite-series/ilmenite-series vs. I-type/S-type granitoids. *Mining Geology Special Issue* 8, 13–28.
- Teixeira, N.P., 1999. Contribuição ao estudo das rochas granítoides e mineralizações associadas da Suite Intrusiva Velho Guilherme, Província Estanifera do Sul do Pará. Ph.D. Thesis, University of São Paulo, Brazil (in Portuguese).
- Teixeira, N.P., Bettencourt, J.S., Moura, C.A.V., Dall'Agnol, R., Macambira, E.M.B., 2002. Archean crustal sources for Paleoproterozoic tin-mineralized granites in the Carajás Province, SSE Pará, Brazil: Pb–Pb geochronology and Nd isotope geochemistry. *Precambrian Research* 119, 257–275.
- Whalen, J.B., Currie, K.L., Chappell, B.W., 1987. A-type granite: geochemical characteristics, discrimination and petrogenesis. *Contributions to Mineralogy and Petrology* 95, 407–419.
- Whalen, J.B., Jennifer, G.A., Longstaffe, F., Robert, F., Gariépy, C., 1996. Geochemical and isotopic (O, Nd, Pd and Sr) constraints on A-type granite petrogenesis based on the Topsails Igneous Suite, Newfoundland Appalachians. *Journal of Petrology* 37, 1463–1489.
- Wilson, M., 1989. *Igneous Petrogenesis*. Unwin Hyman, London.
- Wones, D.R., 1989. Significance of the assemblage titanite+magnetite+quartz in granitic rocks. *American Mineralogist* 74, 744–749.

## CAPÍTULO - 4

### ***GRAVIMETRIC, RADIOMETRIC, AND MAGNETIC SUSCEPTIBILITY STUDY OF THE PALEOPROTEROZOIC REDENÇÃO AND BANNACH PLUTONS: IMPLICATIONS FOR ARCHITECTURE AND ZONING OF A-TYPE GRANITES***

**Davis Carvalho de Oliveira**

**Roberto Dall'Agnol**

**João Batista C. da Silva**

**José de Arimatéia C. de Almeida**

*Submetido: JOURNAL OF SOUTH AMERICAN EARTH SCIENCES*

**GRAVIMETRIC, RADIOMETRIC, AND MAGNETIC SUSCEPTIBILITY STUDY OF THE PALEOPROTEROZOIC REDENÇÃO AND BANNACH PLUTONS: IMPLICATIONS FOR ARCHITECTURE AND ZONING OF A-TYPE GRANITES**

Davis Carvalho de Oliveira<sup>1</sup>, Roberto Dall'Agnol<sup>1\*</sup>, João Batista Corrêa da Silva<sup>2</sup>, and José Arimatéia Costa de Almeida<sup>1</sup>

<sup>1</sup>Group of Research on Granite Petrology, Centro de Geociências, Universidade Federal do Pará, Caixa Postal 8608, 66075-100 Belém, PA, Brazil

<sup>2</sup>Department of Geophysics, Centro de Geociências, Universidade Federal do Pará, Caixa Postal 8608, 66075-100 Belém, PA, Brazil

\*Corresponding author. Tel.: +55 91 3183 1477; fax +55 91 3183 1609. E-mail address:  
robdal@ufpa.br

**Abstract**

The 1.88 Ga, anorogenic, A-type Redenção and Bannach granites, representative of the Jamon suite, and associated dikes, are intrusive in Archean granitoids of the Rio Maria Granite-Greenstone Terrane in the eastern Amazonian craton in northern Brazil. Petrographic and geochemical aspects associated with magnetic susceptibility and gamma-ray spectrometry data showed that the Redenção and the northern part of Bannach plutons are normally zoned. They were formed by two magmatic pulses: (1) a first magma pulse was fractionated in situ after emplacement at shallow crustal level generating a series of coarse, even-grained monzogranites with variable modal proportions of biotite and hornblende; (2) a second, slightly younger magma pulse, located to the center of the plutons, was composed of a more evolved liquid from which even-grained leucogranites derived. Gravity modelling indicates that the Redenção and Bannach plutons are sheeted-like composite laccolithic intrusions, ~6 km and ~2 km thick, respectively. These plutons follow the general power law for laccolith dimension and are similar in this respect to classical rapakivi granite plutons. Gravity data suggest that the growth of the northern part of

the Bannach pluton results of the amalgamation of smaller sheeted-like plutons that intruded in sequence from northwest to southeast. The Jamon suite plutons were emplaced in an extensional tectonic setting and the stress was oriented approximately along NNE-SSW to ENE-WSW, as indicated by the occurrence of diabase and granite porphyry dyke swarms, orientated WNW-ESE to NNW-SSE and coeval with the Jamon suite. The 1.88 Ga A-type granite plutons and stocks of Carajás are disposed along a belt that follows the general trend defined by the dikes. The inferred tabular geometry of the studied plutons and the high contrast of viscosity between the granites and their Archean country rocks can be explained by magma transport via dikes.

**Keywords:** Gravity; Magmatic zoning; Laccolith; Anorogenic; Amazonian craton

## 1. Introduction

During the last two decades, Proterozoic, A-type granites, dominantly rapakivi, have been described from many Precambrian shield areas, e.g., North America (Anderson and Bender, 1989; Emslie, 1991; Barnes et al., 1999; Anderson and Morrison, 2005), Fennoscandia (Haapala and Rämö, 1990; Rämö and Haapala, 1995; Kosunen, 2004), and the Amazonian craton (Dall'Agnol et al., 1994, 2005; Bettencourt et al., 1995). In the Amazonian craton, felsic volcanic rocks, as well as mafic and charnockitic plutonic rocks, are also associated with rapakivi granites (Bettencourt et al., 1995; Dall'Agnol et al., 1999a; Fraga, 2002; Fraga et al., 2003).

A-type, rapakivi granites show a pronounced peak in the Proterozoic (~1.88 to 1.0 Ga), and show a bimodal mafic-felsic magmatic association (Rämö, 1991; Rämö and Haapala, 1995). The Proterozoic A-type granites also show quite a large variation in their redox behavior, ranging from reduced to oxidized (Haapala and Rämö, 1990; Anderson and Morrison, 1992; Anderson and Smith, 1995; Frost and Frost, 1997; Frost et al, 1999; Elliot, 2001; Dall'Agnol and Oliveira, submitted), and thus show evidence for substancial variation in crystallization conditions and protolith composition.

The tectonic setting of the Proterozoic A-type, rapakivi granites has remained an issue of controversy. The classic Proterozoic rapakivi granites are associated with mafic dike swarms, listric shear zones, and thinned crust (Rämö and Haapala, 1995). They were intruded into a crust that predates them by some hundred million years (e.g., Rämö and Haapala, 1995; Rämö et al., 2002; Dall'Agnol et al., 2005), and are found as discordant multiple plutons. This indicates an

extensional tectonic setting and anorogenic origin (lack of direct association to convergent processes and resulting mountain building; Haapala and Rämö, 1999, and references therein). However, others authors suggested that rapakivi granites could be related to distal orogenesis (Åhäll et al., 2000). Rapakivi granites and related “anorogenic” granites have become an important tool for modelling Precambrian intraplate crustal processes and global-scale lithospheric evolution. An origin associated with crustal anatexis promoted by magmatic underplating is generally admitted (Huppert and Sparks, 1988; Rämö and Haapala, 1995; Dall'Agnol et al., 1999a).

Another common feature of the A-type granite plutons is their internal compositional zoning (Paradella et al., 1998; Costi et al., 2000; Rajesh, 2000; Teruiya, 2002; Richardson, 2004); generally they are more mafic at the margins and grade inward, with or without discontinuities, to more felsic zones (near normal zoning). Reverse zoning (more mafic core than outer zones) may also be observed (Ceci and Frederick, 2002), but is most common in calc-alkaline granitoid plutons (Zorpi et al., 1989; Paterson and Vernon, 1995). Generally, the zoned plutons are interpreted as having been intruded in a continuous series of magmatic pulses leading to an in situ growing of the pluton (Bateman and Chappel, 1979; Pitcher, 1979; Zorpi et al., 1989; Petford, 1996). Their cores are formed by later emplaced, more mobile, differentiated rocks. In the case of ‘anorogenic granites’, nor the mechanisms neither the timing for zoning development are entirely understood.

Deep seismic sounding studies in the classical Wiborg rapakivi batholith indicated that it is a shallow laccolith-type intrusion having associated mafic intrusions in deeper crustal levels (Rämö et al., 1994, and references therein). The common occurrence of granite intrusions as laccoliths is now recognized (Rocchi et al., 2002; Aranguren et al., 2003; Ponz et al., 2006) and models for laccolith formation have been discussed (Roman-Berdiel et al., 1995). The classic diapiric models for granite intrusion (Ramberg, 1970; Weinberg et al., 1996) have been criticized and the role of dikes in the ascent of felsic magmas was emphasized (Clemens and Mawer, 1992; Petford et al., 1994; Petford, 1996).

Proterozoic A-type granites have been described from the Archean Rio Maria region in the eastern Amazonian Craton in Brazil (Dall'Agnol et al., 1994, 1999a, 2004). The Jamon Paleoproterozoic A-type granite suite has been dated at 1.88 Ga and was intruded into a ~3-Ga-old crust characterized by greenstone belts and granitoid rocks. The Archean crust remained

stable to the point when the 1.88 Ga granite magmatism commenced. The Jamon suite is formed by the Redenção, Bannach, Jamon, Musa, Marajoara, Manda Saia, Seringa, São João, and Gradaús plutons (Fig. 1b). These granites are usually non-deformed, shallow-level plutons that are associated with bimodal dyke swarms, locally forming composite mafic-felsic dikes. They are high-K granites with subalkaline A-type chemistry, show a pronounced oxidized character (Dall'Agnol et al., 1997b, 1999a; Dall'Agnol and Oliveira, submitted) and display many characteristics of the oxidized, mid-Proterozoic A-type granites of the western United States (Anderson and Bender, 1989; Barnes et al., 2002; Anderson and Morrison, 2005).

The mineralogy, geochemistry, and petrology of the Jamon suite granites are relatively well studied (Dall'Agnol et al., 1999, 2005; Dall'Agnol and Oliveira, submitted). However the internal zoning, tridimensional shape and emplacement history of its plutons needed additional investigation. Airborne magnetic and radarsat image analysis provided an integrated view of the regional geological features of the area of occurrence of the Redenção and Bannach plutons, selected for study. Aeroradiometric (gamma ray) surveys and magnetic susceptibility data were associated with field, petrographic, and geochemical data to put in evidence their internal zoning. In parallel, it was carried out a gravity survey on the mentioned plutons. Tridimensional modeling provided an estimate of the mass distribution at depth and allowed estimation of the shape and thickening of the plutons. The new geophysical data acquired in the Redenção and Bannach plutons enable a re-interpretation of their magmatic evolution and is employed as a basis for an initial discussion about the mechanisms of their emplacement.

## 2. Geologic Setting

The Jamon Suite is situated in the Carajás province of the eastern Amazonian craton (Dall'Agnol et al., 2005, and references therein). The Carajás province has been included into the Central Amazonian province (Tassinari and Macambira, 1999; Fig. 1a) and it is dominated by Archean terrains intruded by Paleoproterozoic anorogenic granites. To the west, it is limited by a terrane dominated by Proterozoic granitoids and Uatumã volcanic-pyroclastic assemblages; to the east, by the Neoproterozoic Araguaia Belt, whose evolution is associated with the Brasiliano (Pan-African) cycle that did not significantly affect the Amazonian Craton; to the north, by the Maroni-Itacaiúnas province, formed in the 2.2-2.1-Ga Trans-Amazonian event (Fig. 1a).

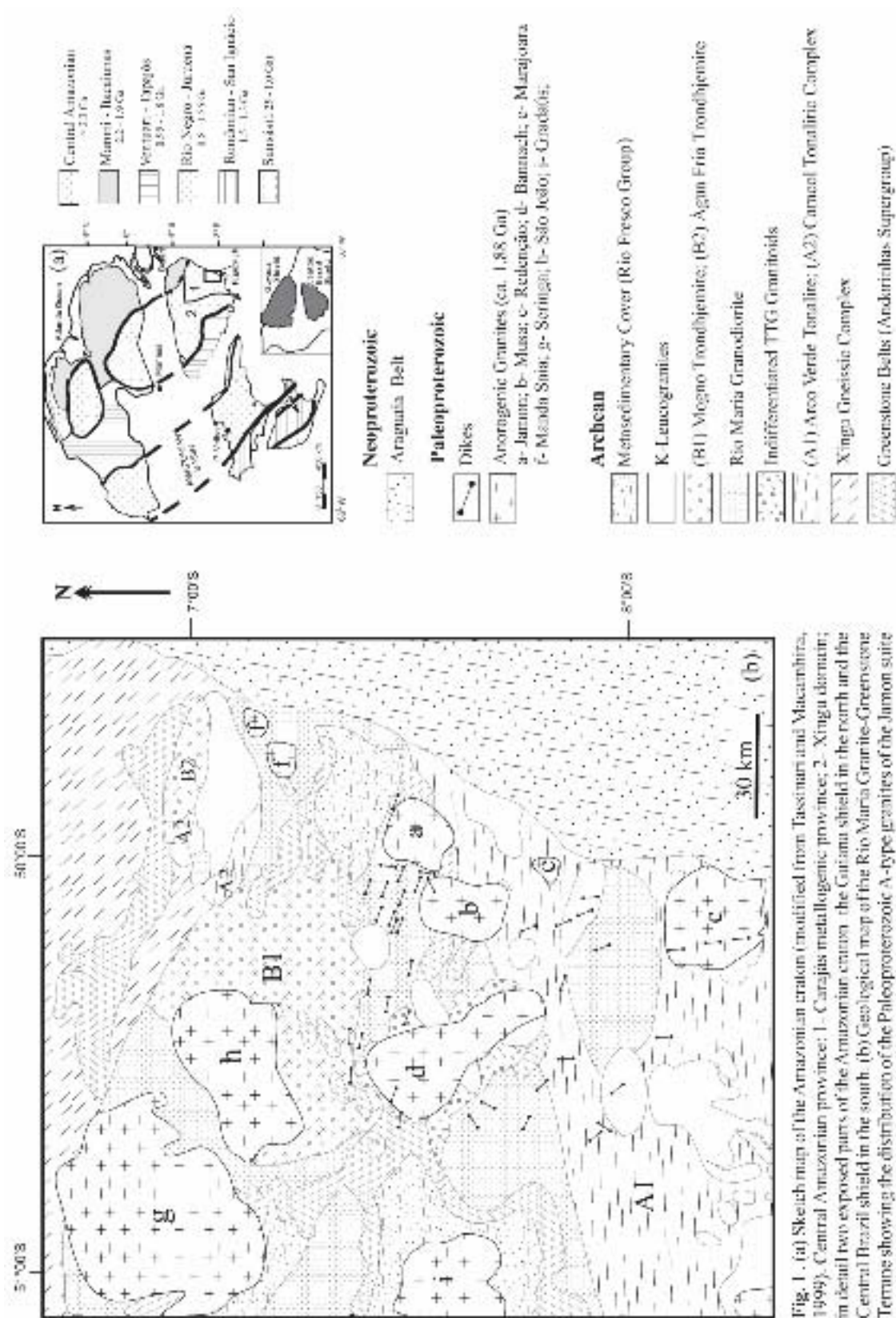


Fig. 1. (a) Sketch map of the Amazonian craton (modified from Tessmann and Macambira, 1999). Central Amazonian province: 1- Carajás metallocogenic province; 2- Xingu domain; 3- two exposed parts of the Amazonian craton: the Gurani shield in the north and the Central Brazil shield in the south. (b) Geological map of the Rio Maria Granite-Greenschist Terrane showing the distribution of the Paleoproterozoic A-type granites of the Jamon suite (modified from Almeida, 2005, and references therein).

The Carajás province was cratonised at the end of the Archean and remained stable until the emplacement of A-type granites at ~1.88 Ga (Machado et al., 1991; Macambira and Lafon, 1995; Dall'Agnol et al., 1999a, b, 2005; Teixeira et al., 2002), as a direct response of the extensional tectonic regime involving underplating of mafic magmas in a continental lithosphere. In the Rio Maria terrane, this is indicated by dike swarms that are coeval with the granites and include mafic-felsic composite dikes (Dall'Agnol et al., 2005). In the adjacent provinces, orogenic events are significantly older (the Trans-Amazonian event in the north) or younger (the Brasiliano event in the east) than these granites. Lamarão et al. (2002, 2005) and Dall'Agnol et al. (2005) suggest that the A-type granite magmatism of the Carajás province was related to a continental event that marks the beginning of the breakup of the Paleoproterozoic continent formed at the end of the Trans-Amazonian orogenic cycle.

The Carajás province is divided into two Archean tectonic domains, the 3.0-2.86-Ga Rio Maria Granite-Greenstone Terrane (Macambira and Lafon, 1995; Dall'Agnol et al., 1997b) and the rift-related Carajás Basin dominantly composed of 2.76-2.55-Ga metavolcanic rocks, banded iron formations, and granitoids (Machado et al., 1991; Macambira and Lafon, 1995; Barros et al., 2001). The granite plutons of the Jamon suite are intrusive in Archean granitoids and greenstone belts of the Rio Maria Granite-Greenstone Terrane, which corresponds to the southern part of the Carajas Metallogenic Province (Fig. 1b). The greenstone belts (Andorinhas Supergroup) are composed dominantly of komatiites and tholeiitic basalts (Souza and Dall'Agnol, 1995). Four principal groups of Archean granitoids have been distinguished (Macambira and Lafon, 1995; Dall'Agnol et al., 1997b; Leite et al., 2004): (1) Older tonalitic-trondhjemitic series (TTG) represented by the Arco Verde and Caracol tonalites (~2.97-2.93-Ga) (2) 2.87 Ga sanukitoid Rio Maria Granodiorite and associated rocks, which are intrusive into the greenstone sequence; (3) Younger TTGs series, represented by the Mogno and Água Fria trondhjemites (2.87 Ga); and (4) Potassic leucogranites of calc-alkaline affinity, represented by the Xinguara, Mata Surrão, Guarantã and similar granites (~2.86-Ga).

### 3. General aspects of the studied plutons

The Redençao and Bannach plutons are unfoliated and deformational structures are practically restricted to fracturing and faulting. Magmatic foliation is only locally developed on the border. Both granite intrusions are subcircular and remarkably discordant cross-cutting the E-

W or NW-SE earlier structural trends of the Archean country rocks (Fig. 2a and b). The Bannach pluton was interpreted as composed of at least three independent near-circular intrusions, migrating from north to south (Almeida, 2005). External contacts are sharp and angular xenoliths of Archean rocks are commonly observed near the margin of the plutons, indicating a high viscosity contrast between the magmas and the Archean bedrock. The country rocks are strongly affected by contact metamorphism. Hornblende hornfels contact aureoles around the 1.88 Ga plutons are well developed in both granitoids and greenstones (Dall'Agnol et al 1994, 1999c). Al-in-hornblende barometer and mineral assemblages developed in the contact aureole suggested that the plutons of the Jamon suite were emplaced at shallow crustal levels (~1 to 3 kbar; Dall'Agnol et al., 1999b). Swarms of mafic, intermediate, and felsic dikes are associated with the Jamon Suite (Silva Jr. et al., 1999). Composite mafic-felsic dikes cutting Archean sanukitoid granodiorites have been locally described (Dall'Agnol et al., 2005). The felsic dikes yielded Pb-Pb zircon ages of  $1885 \pm 4$  and  $1885 \pm 2$  Ma (Oliveira D.C., unpublished data). One of these dikes, rhyolite porphyry, shows evidence of mingling with an associated mafic dike, demonstrating that the mafic and felsic magmas were contemporaneous. Therefore, as indicated by dike swarms that are coeval with the granitic magma, the granite plutons were emplaced in an extensional tectonic regime. The Redenção and other Jamon suite plutons are disposed nearly parallel to northwest-southeast faults in the basement, consistent with magma ascent along pre-existing deep fault lineaments. This is consistent with the dominant WNW-ESE to NNW-SSE trends of Paleoproterozoic dikes. It indicates also that a distensional stress disposed along NNE-SSW to ENE-WSW strongly controlled the Jamon suite emplacement.

#### 4. Zoning of the plutons

##### 4.1. Petrographic and Geochemical Data

The petrography and the magmatic evolution of the Redenção and Bannach granites were discussed by Oliveira et al. (in press) and Almeida (2005), respectively. Both granites are very similar in textures and mineralogy. These plutons consist of several intrusive phases disposed in near-concentric zones and cut by syenogranitedikes. They are formed essentially of coarse-grained, equigranular to porphyritic or coarse- to medium-grained seriated monzogranites with subordinate medium, even-grained types. All facies are leucocratic with contents of mafic minerals normally between 15% and 6%; in the less evolved facies, they reach >25% and are

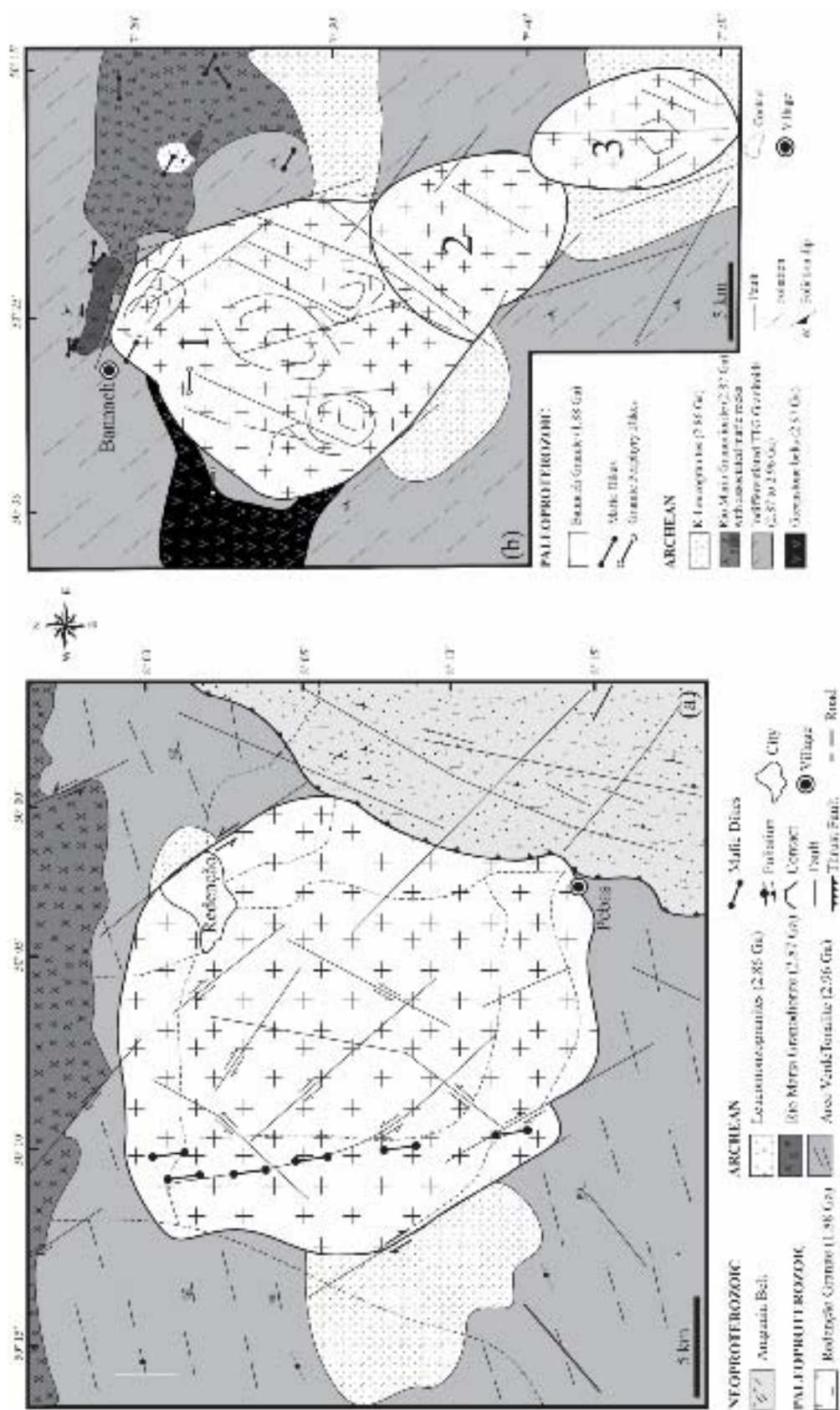


**Fig. 2.** Detailed geological map of the (a) Redenção (Oliveira, 2001) and (b) Bannach (Almeida, 2005) plutons. 1, 2, and 3 indicate the successive intrusions of the Bannach pluton.

<5% in the differentiated leucogranites. Biotite is the dominant mafic mineral and is found in all granite varieties; amphibole, sometimes with relics of clinopyroxene, is abundant only in the less evolved facies. The assemblage of accessory minerals includes zircon, apatite, iron-titanium oxides (magnetite/ilmenite), sulphide phases (pyrite/chalcopyrite), allanite, titanite and, in the more evolved facies, fluorite. Subsolidus processes were limited to alteration of plagioclase and mafic phases; epidote, sericite, and chlorite are alteration products.

In the granitic plutons, the distribution of the different facies is relatively well ordered (Figs. 3 and 4). In the Redençao granite, the less evolved rocks are even-grained, coarse biotite+hornblende monzogranites, locally enriched in cumulitic amphibole=clinopyroxene, which occurs in the southern part of the pluton. They grade to the interior of the pluton to dominantly coarse-grained, equigranular, seriated or porphyritic biotite monzogranites. The seriated and porphyritic biotite monzogranite facies configure annular structures in the central and southern areas of the pluton. In the central part of the pluton, evolved leucogranites define small circular structures (Fig. 3). Field relationships showed that the seriated and porphyritic biotite monzogranite facies are intrusive in the coarse- even-grained (hornblende)-biotite monzogranite. Aplitic dikes are common and coincide in orientation with the main NE-SW and NW-SE faulting system.

In the Jamon Suite, except locally in composite dikes evidences of magma mingling between mafic and felsic magmas have not been reported (Dall'Agnol et al., 2005). However, in the Redençao and Bannach plutons, evidences of ‘mingling’ of the coarse porphyritic facies with other felsic magmas are frequently observed. In these ‘mingled’ rocks, plagioclase mantled K-feldspar megacrysts are common but typical wiborgitic and pyterlitic rapakivi textures are absent (cf. Rämö and Haapala, 1995).

The internal zoning of the northern intrusion of Bannach (Fig. 4) is similar to that of the Redençao pluton. However, in the Bannach pluton, some significant differences are worthwhile: the (clinopyroxene)-amphibole-bearing, less evolved monzogranites are more abundant and show a regular distribution occurring along all pluton margins; the coarse-equigranular and the medium- to coarse-grained seriated biotite monzogranites are not found; four pulses of leucogranites, situated generally towards the central parts of the pluton, have been identified; the porphyritic biotite monzogranites are disposed as NE-SW elongated discordant bodies, cutting

the other facies; felsic granitic dikes are systematically associated with the porphyritic monzogranites (Fig. 4).

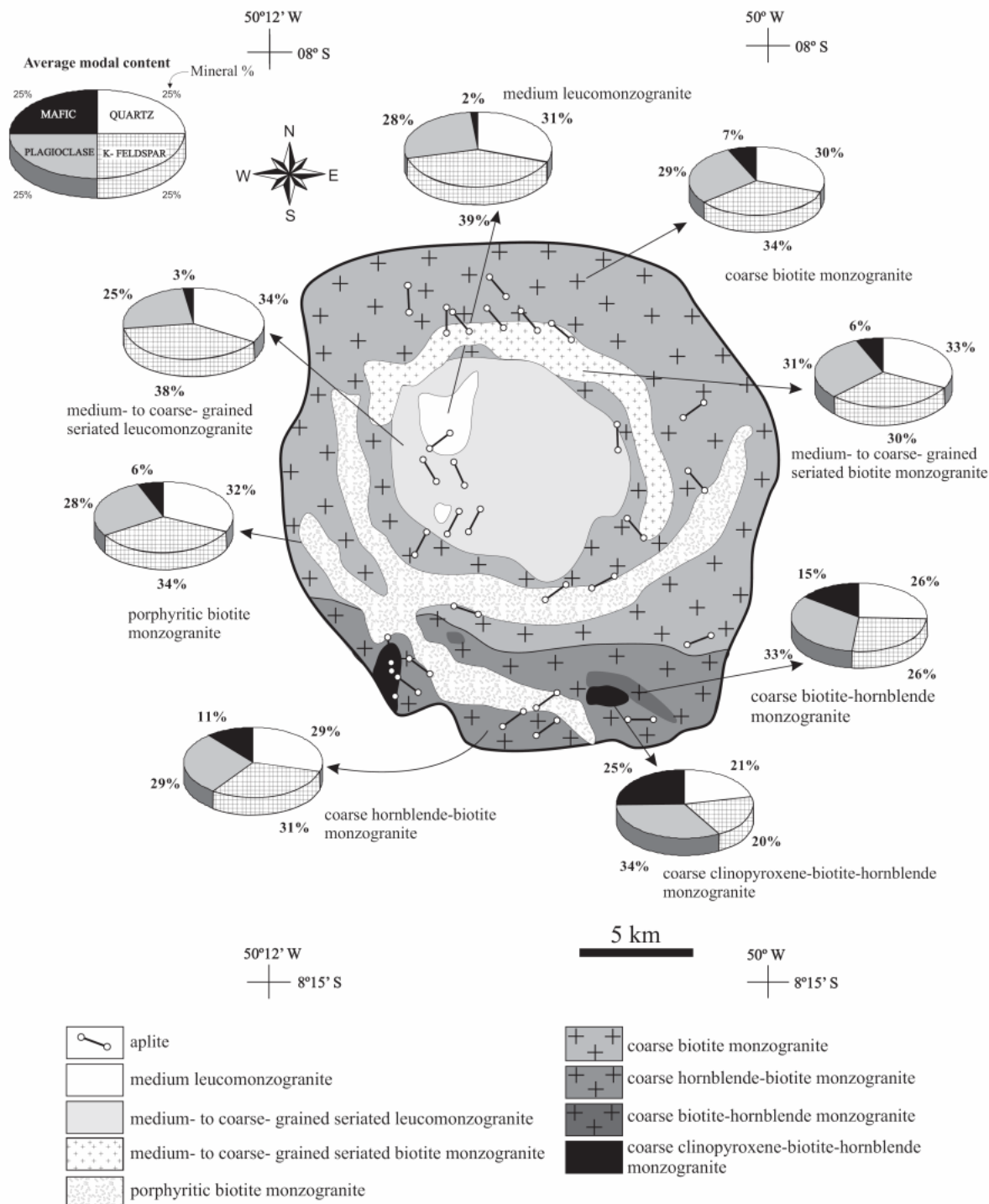


**Fig. 3.** Sketch geological map of the Redenção pluton showing the areal distribution of granitic facies. The average modal contents of the essential felsic minerals and mafic mineral totals of each facies are also shown in pie diagrams (Oliveira, 2001).

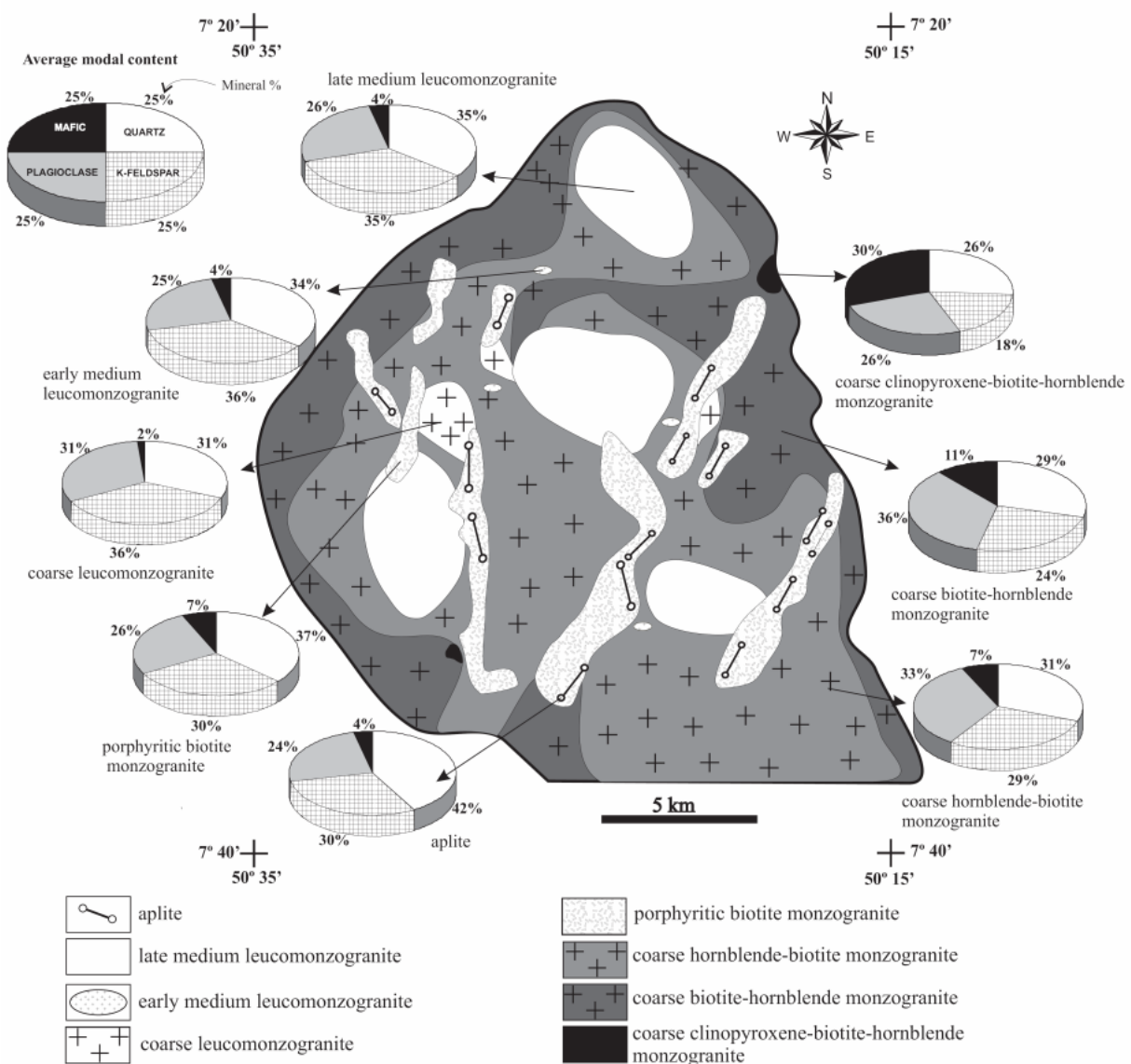


**Fig. 4.** Sketch geological map of the Bannach pluton showing the areal distribution of granitic facies. Average modal contents of the essential felsic minerals and mafic mineral totals of each facies are also shown in pie diagrams (Almeida, 2005).

The magmatic zoning is marked in both plutons by the systematic decrease of modal mafic mineral content, plagioclase/potassium feldspar and amphibole/biotite ratios and anorthite content of plagioclase ( $An_{32-15}$ ) from the (clinopyroxene)+ amphibole+biotite monzogranite toward the leucogranites. On the other hand, the abundance of alkali feldspar and quartz increases towards the inner zone.  $TiO_2$ ,  $MgO$ ,  $FeO_t$ ,  $CaO$ ,  $P_2O_5$ ,  $Ba$ ,  $Sr$ , and  $Zr$  decrease, and  $SiO_2$ ,  $K_2O$ , and  $Rb$  increase in the same way. Magmatic differentiation was controlled by fractionation of early crystallized phases, including amphibole  $\pm$  clinopyroxene, andesine to calcic oligoclase,

ilmenite, magnetite, apatite, and zircon. Negative Eu anomalies increased with differentiation. Oliveira (2001) proposed that the fractional crystallization was the dominant process of magmatic evolution of the Redenção pluton. Nevertheless, magma mingling processes had also influenced the evolution of this granitic pluton as suggested by the relationships between porphyritic biotite granites and leucogranites. Similar magmatic processes were proposed to explain the zoning of the Bannach pluton (Almeida, 2005). The leucogranite facies of both plutons were interpreted as probable late, independent injections of evolved, felsic magmas (Oliveira, 2001; Almeida, 2005).

#### 4.2. Magnetic Susceptibility Data

In the Redenção and Bannach plutons, the bulk magnetic susceptibility (K) shows similar values, varying between  $1.05 \times 10^{-3}$  and  $54.72 \times 10^{-3}$  SIv with an average of  $11.55 \times 10^{-3}$  SI in the Redenção pluton (Oliveira et al., 2002), and between  $1.07 \times 10^{-3}$  and  $72.74 \times 10^{-3}$  with an average of  $9.26 \times 10^{-3}$  in the Bannach pluton (Almeida, 2005). K has a unimodal and bimodal distribution, respectively, in the Redenção and Bannach plutons (Fig. 5a and b). Magnetite is always dominant over ilmenite and modal contents of Fe-Ti oxide minerals vary between 3.5 and 0.4 % in the Redenção, and between 3.8 and ~0.1% in the Bannach pluton. Both granites are typical magnetite series ferromagnetic granites (Ishihara, 1981; Ferré et al., 2002). Magnetic susceptibility (MS) reflects essentially variations in the magnetite content of different granitic facies.

Average MS values decrease from the (clinopyroxene)-amphibole-biotite monzogranites to the biotite monzogranites, attaining the lowest value in the leucomonzogranites. In other words, magnetic susceptibility decreases from the facies with higher modal contents of mafic minerals to the leucogranites. In Bannach, this implies decrease of MS from the border to the center of the pluton with a normal and concentric zoning (Fig. 5b; Almeida, 2005); in the Redenção pluton, the highest MS values are concentrated in the southern part of the pluton, decreasing to the NE and mid-central domains, the lowest MS values being found in the center of the intrusion (Fig. 5a; Oliveira et al., 2002). The MS behavior is consistent with the pattern indicated by petrographic and geochemical data. Gleizes et al. (1993) also signalized that the bulk rock magnetic susceptibility variation in ferromagnetic granites, that are more common in Archean and Proterozoic terranes, is a good guide to unravel their compositional variations and can be correlated with petrographic varieties. The highest MS values correspond to the more mafic rocks. It increases with Fe content and can be used as a magmatic differentiation index.

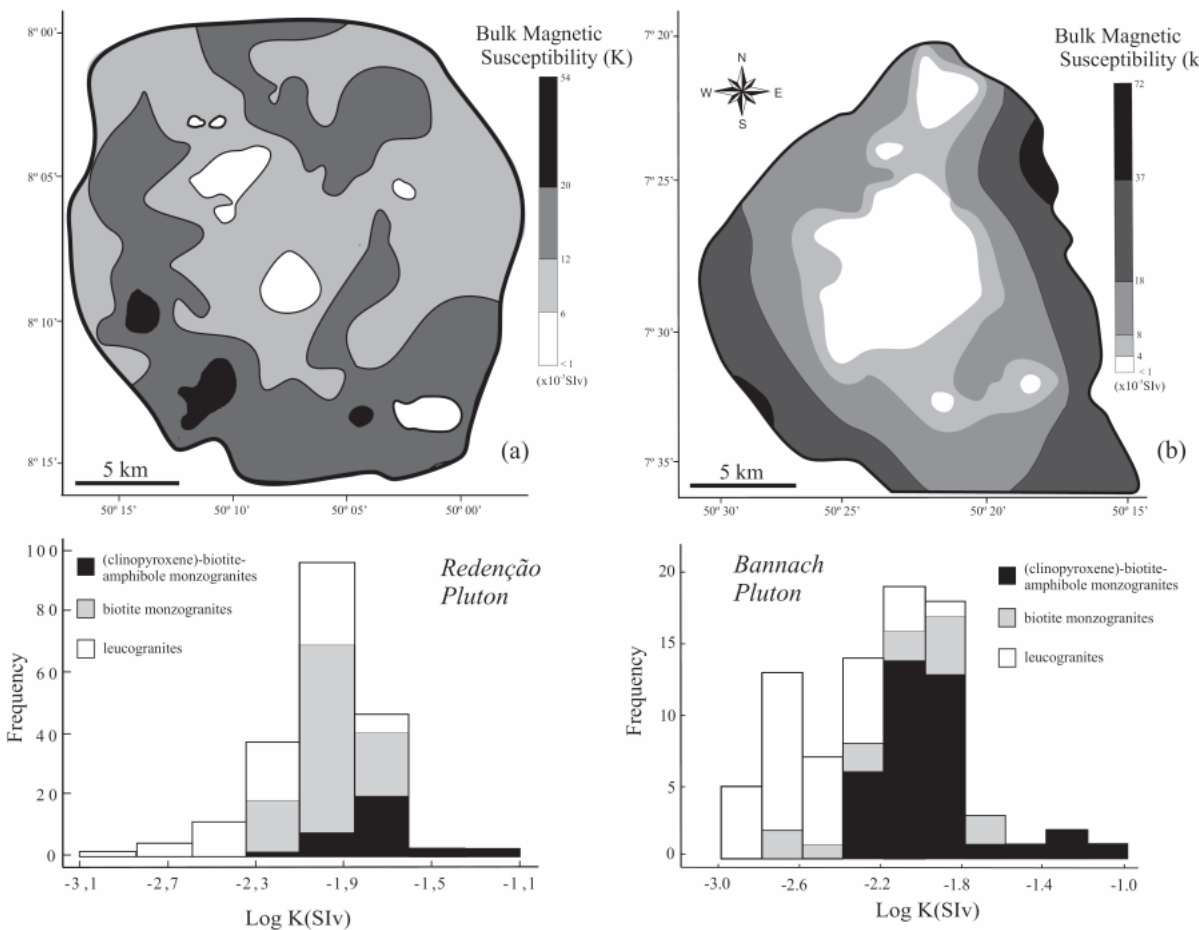


**Fig. 5.** Variation of bulk magnetic susceptibility values and frequency histogram (K in SIv) of the (a) Redenção and (b) Bannach plutons rock varieties. In the Redenção pluton the bulk susceptibility was measured with the SI-1 and Kappabridge KLY-3 magnetic susceptibilimeters; in the Bannach pluton all measurements were acquired with the SI-1.

#### 4.3. Remote Sensing and Aerogamma Spectrometry

The sources of natural gamma radiation are associated with common rock-forming minerals (feldspars, micas and clays) in the case of K, and to accessory minerals (e.g zircon and monazite) in the case of the U and Th. The Total Count channel (CT), with a broad spectrum that includes the contribution of K, U, and Th radiations, presents higher intensity and is statistically more reliable for the discrimination of rock units (Paradella et al., 1998). On the other hand, U and Th channels are more indicated for rock type identification and detection of hidrotermal/metassomatic processes (Vasconcelos et al., 1994; Richardson, 2004). It is worthwhile also to remember that U behaves geochemically as a mobile element, while Th is generally immobile or less mobile as compared to U during secondary processes.

As mentioned by Paradella et al. (1998), in interpreting the results of this integration, certain factors which could have affected the measured values must be considered (e.g. variation in the vegetation cover). Interpretations based on K-channel should be treated with caution due to the possibility of false responses induced by the vegetation. This is not the case for U and Th channels (Pereira and Nordemann, 1983). The more important effect is the spatial correlation of higher gamma responses with the geomorphology of the area.

In the Redençao granite, the SRTM/Gamma products revealed a strong correlation between gamma ray anomalies and higher topographic levels (Fig. 6a). Results from Bannach pluton obtained with orbital remote sensing and gamma integration also showed that the strongest gamma responses are mainly related to high and moderate relief areas within the pluton (Fig. 6b).

In the interior of the studied plutons, the SRTM/U product showed clearly higher gamma U activities in the central areas of the intrusions compared to their borders. Similar positive gamma anomalies are also indicated by Th in the central parts of the massifs (Fig. 6a and b). The analysis of the airborne and SRTM/Gamma TC products reinforced the results obtained through the RADAR/U-Th products. The gamma anomalies in the plutons are coincident with the area distribution of their more evolved, generally leucogranitic facies. These rocks are enriched in K, Th, and U, explaining their radiometric contrast with the more mafic biotite-amphibole monzogranites, dominant in the border of the plutons (Figs. 3 and 4). Thus, the aerogamma spectrometry gives useful information for the understanding of the internal magmatic zoning in the plutons.

The whole rock geochemical data on the Redençao and Bannach plutons (Oliveira et al., in preparation; Almeida et al., submitted) demonstrate that K contents are higher toward the central sector of the plutons when compared to the borders, but the K contribution alone would not be able to determine the main gamma patterns registered in the whole intrusions. U and Th also increase during magmatic differentiation, explaining the observed gamma U and Th behaviors (Fig. 6a and b). The same evolution trends and general radiometric features were observed in the Musa, Jamon, and Marajoara plutons of the Jamon suite. A similar magmatic evolution was also assumed for the Paleoproterozoic, tin-mineralized Antonio Vicente pluton (W of the Carajás Province), which more evolved facies are enriched in U and Th (Dall'Agnol et al., 1993).

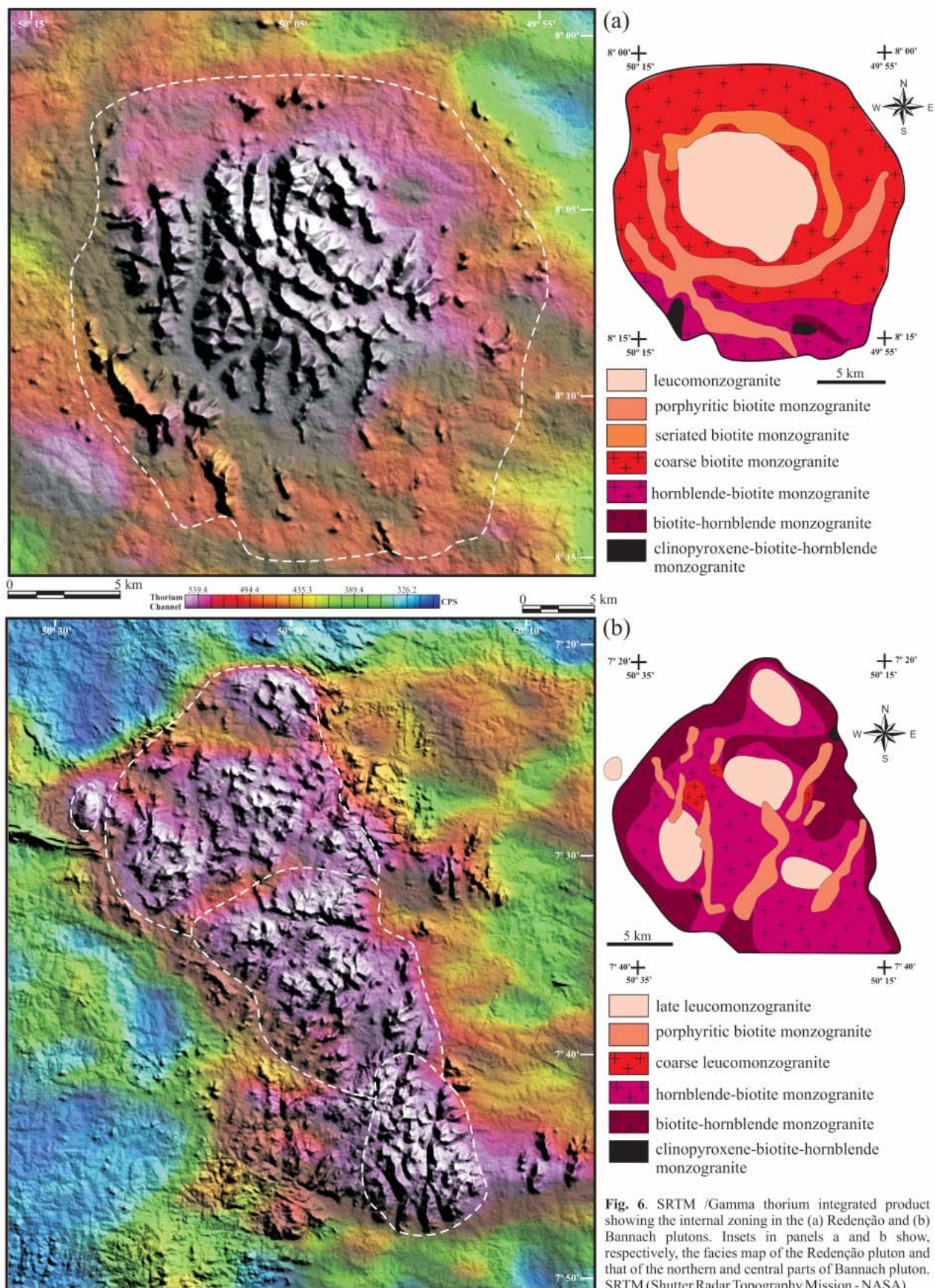


**Fig. 6.** SRTM /Gamma thorium integrated product showing the internal zoning in the (a) Redenção and (b) Bannach plutons. Insets in panels a and b show, respectively, the facies map of the Redenção pluton and that of the northern and central parts of Bannach pluton. SRTM (Shuttle Radar Topography Mission - NASA).

## 5. Gravity method

### 5.1. Gravity survey and corrections

#### 5.1.1 Bannach Area

Given the importance of altimetric information and the absence of reference base-stations in the Bannach region for the gravity survey on the Bannach pluton, it was necessary to define a new altimetric base in that area. To this end, a new reference base-station has been transferred from the Brazilian Fundamental Gravity Net (Escobar, 1980), taking as altimetric reference an IBGE base located at Rio Maria city (985 L; 7°16'18" S / 50°05'48" W), with a g value in the system GRS-67 of 978044,87 (Carvalho, 1988). The new gravimetric base-station, with a g value of 978010.49, was located in the Bannach town, and denominated Hotel Catarinense (7°20'52" S / 50°24'39" W). Gravity was measured at 147 stations following approximately north-south and east-west trending traverses on the Bannach pluton and its neighboring country rocks. The distance between gravity stations are about 500 m and 1000 m, in the border and in the center of the pluton, respectively. The gravity measurements were referred to the international gravity net (IGSN 1971) at the new Bannach gravimetric base.

A Lacoste-Romberg Model G gravity meter, with a precision of  $\pm 0.01$  mGal, was employed for measurements. Geographic coordinates and elevations were obtained using a Magellan Pro Mark X differential GPS, with average precision of  $\sim 10$  m and  $\sim 0.4$  m in the horizontal and vertical directions, respectively. The altitudes relative to the sea level were obtained with a Paulin altimeter accurate to the meter. The instrument drift, latitude, free-air, and Bouguer corrections were applied to the observed data. A reduction density of  $2.67 \text{ g/cm}^3$ , was used to perform the Bouguer corrections. The gravity response a regional field, approximated by a first-order polynomial has been removed from the data along each traverse, where necessary, in order to produce an anomaly falling off to zero at both ends of the profile

#### 5.1.2 Redenção Area

The results of gravity surveying of the Redenção pluton presented here constitute part of a larger scale gravity exploration campaign accomplished by Mineração Jenipapo (Western Mining Company – WMC) on an area covering the border between the eastern Amazonian craton and the Brasiliano Araguaia Belt. In that area Archean units of the Rio Maria Granite-Greenstone Terrane

are exposed and intruded by Paleoproterozoic A-type granites, and low grade metasedimentary rocks of the Araguaia Belt.

Between 1999 and 2000, 135 observations were collected along roads crossing the Redenção pluton and adjacent country rocks, with a constant spacing of 1 km between the stations. The reference base-station used is located in the city of Redenção. The gravity meter was a Scintrex CG3 Autograv Meter with a precision of 0.01 mGal. The positioning was carried out with a Trimble Geodetic Base Station System 4700 with accuracy between 5 cm and 10 cm. The latitude, free-air, Bouguer, topographic, tide and instrument drift corrections were applied to the data. For the Bouguer and topographic corrections, a reference density of  $2.67 \text{ g/cm}^3$  has been assumed. The gravity response of a regional field, approximated by a first-order polynomial, has been removed from the data along the traverses, where necessary, to produce an anomaly falling off to zero at both ends of the profile

### 5.2. Density Measurements

Density measurements were carried out on selected samples considered to be representative of both the different granite varieties and its surrounding country rocks. In the Redenção and Bannach plutons, the average density values of each facies generally decrease from the border to the center. The biotite monzogranites and leucogranites have density smaller than  $2.66 \text{ g/cm}^3$ , while the clinopyroxene-bearing cumulitic monzogranites and the biotite-amphibole monzogranites density is greater than  $2.70 \text{ g/cm}^3$  (Table 1). These plutons are composed of approximately 80% of biotite  $\pm$  amphibole monzogranite ( $\rho = 2.64\text{--}2.65 \text{ g/cm}^3$ ). The denser facies occur locally as enclaves or along the borders of the plutons. The leucogranites are less dense ( $\rho = 2.61 \text{ g/cm}^3$ ) as compared to other varieties and occur either as stocks in the center of the intrusions or as dikes. In spite of the above mentioned internal density variations, in both plutons, the density distribution within the plutons is uniform enough to justify the adoption of a unique average density of  $2.64 \text{ g/cm}^3$ .

The density of the country rocks of the studied plutons are quite variable decreasing from the mafic greenstone belts ( $\rho = 2.97 \text{ g/cm}^3$ ), to the Rio Maria granodiorite and associated monzonites ( $\rho = 2.74$  to  $2.85 \text{ g/cm}^3$ ), and attaining the lowest values in the tonalites and leucomonzogranites ( $\rho = 2.65$  to  $2.63 \text{ g/cm}^3$ ). For a simplified, integrated modeling taking into account the overall dominance of granitoids, an average density of  $2.73 \text{ g/cm}^3$  was assumed for

the country rocks. An average density contrast of  $0.09 \pm 0.01 \text{ g/cm}^3$  between the country rocks and the Paleoproterozoic granites was, therefore, assumed for the gravity inversion of the anomalies produced by both plutons.

**Table 1** - Mean density values estimated for the Redenção and Bannach granite varieties and country rocks.

<b>Redenção and Bannach Plutons</b>	density, $\text{g/cm}^3$
Clinopyroxene-hornblende-biotite monzogranite	$2.77 \pm 0.03$
Biotite-hornblende monzogranite	$2.70 \pm 0.01$
Hornblende-biotite monzogranite	$2.65 \pm 0.01$
Biotite monzogranite	$2.63 \pm 0.02$
Leucomonzogranite	$2.61 \pm 0.01$

<b>Country Rocks (Redenção Pluton)</b>	density, $\text{g/cm}^3$
Rio Maria Granodiorite	$2.74 \pm 0.01$
K-leucomonzogranite	$2.72 \pm 0.02$
Arco Verde Tonalite	$2.65 \pm 0.02$

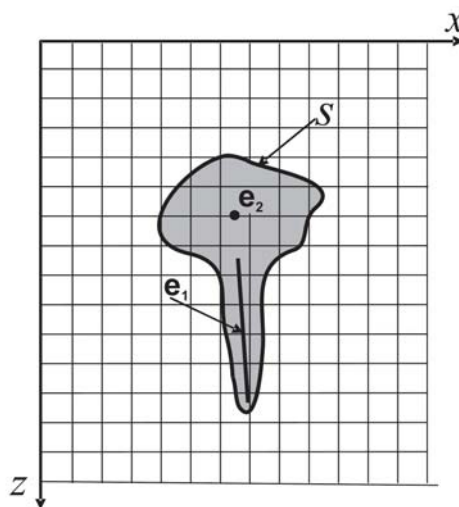
  

<b>Country Rocks (Bannach Pluton)</b>	density, $\text{g/cm}^3$
Greenstone Belts	$2.97 \pm 0.03$
Mafic Rocks/Monzonites	$2.85 \pm 0.02$
Rio Maria Granodiorite	$2.74 \pm 0.01$
K-leucogranite	$2.63 \pm 0.02$
Arco Verde Tonalite	$2.65 \pm 0.02$

### 5.3. Inversion Methodology

The mathematical details of the gravity inversion method are presented in Silva and Barbosa (2006). Here we present an overview of the method's rationale. Let  $S$  be a 2D gravity source having arbitrary shape and arbitrary density contrast distribution and assume that an outline of this source may be defined by a combination of geometric elements consisting of axes and points ( $e_1$  and  $e_2$  in Fig. 7). We discretize the subsurface region, containing the sources, into a grid of 2D rectangular cells (Fig. 7) and allow different density contrasts be assigned to each cell, approximating, in this way the continuous distribution of density contrast by a discrete one. The purpose of the method is to estimate density contrasts for all cells, which fit the observations and present non-null estimates close to the geometric elements. To this end, the interpreter specifies a set of line segments and points, which presumably outlines the true sources and assigns to each

geometric element a target density contrast. The method then estimates the shapes of the sources by estimating the density contrast of each cell of the grid, generating, in this way, a discrete distribution of density contrast producing the best fit to the observed anomaly and concentrating the non-null estimated density contrasts about the specified geometric elements. The estimated density contrasts of the cells about a given geometric element will tend to be close to the target density contrast assigned to the geometric element. The user may then accept the solution or modify the target, densities, and /or the number and position of the geometric elements and start a new inversion, repeating this interactive procedure until a satisfactory solution is obtained. Because the interpretation model consists of a grid of prisms with different density contrasts, this technique allows for lateral facies changes. This interpretation method has been implemented in a user-friendly environment by means of suitable graphical interfaces, allowing a fast and efficient interactivity.



**Fig. 7.** Outline of a 2D gravity source ( $S$ ) defined by a combination of geometric elements consisting of axes and points ( $e_1$  and  $e_2$ ; Silva and Barbosa, 2006).

#### 5.4. Results

The Bouguer anomaly of the Redenção and Bannach plutons along six traverses are presented in Figures 8 and 9, respectively. Both plutons produce gravity lows, a typical behavior of most granite plutons, due to their lower density relative to the surrounding rocks (Aranguren, 1997; Singh et al., 2004).

Each gravity profile has been inverted using the interactive inversion procedure described in the previous section by assuming that each pluton may be outlined by a single axis at surface (Figs. 8b and 9b) and by assigning to each axis a density contrast of  $0.09 \text{ g/cm}^3$ . Because the

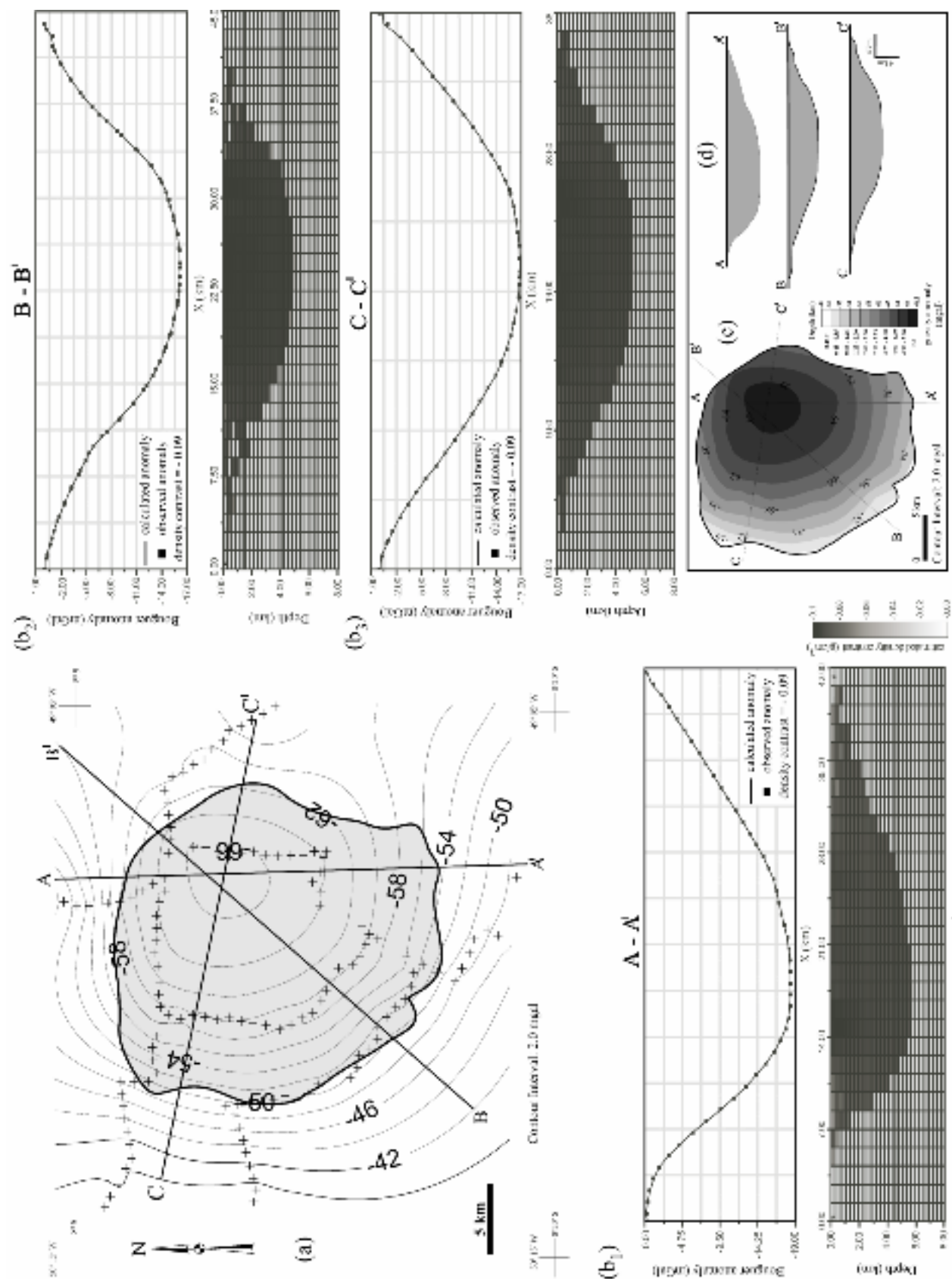


**Fig. 8.** Redenção pluton. (a) Bouguer anomaly map showing the gravity stations (crosses) and contours in 1.0 mgal. (b) Observed gravity (squares) and calculated Bouguer anomaly (continuous lines) obtained from the modeling of the residual anomalies associated with the modeled geometry of the pluton. Gravity inversion profiles with the regional field removed as computed by 2D modeling. (b1) A-A', approximate N-S profile; (b2) B-B', approximate SW-NE profile; (b3) C-C', approximate W-E profile. (c) Contour map of the Redenção pluton depth drawn from gravity anomalies modeling using the method of Silva and Barbosa (2006). (d) Cross-sections through the Redenção pluton showing its morphology with depth; all sections obtained from 2D gravity inversion. All sections are shown at the same horizontal and vertical scales with no vertical exaggeration. The profiles are indicated in Fig. 8a, c. Depths are in kilometers. A density of  $2.64 \text{ g/cm}^3$  was employed for the granite varieties of the Redenção pluton and  $2.73 \text{ g/cm}^3$  for the country rocks.

Redenção and Bannach plutons outcrop, the feature of interest, which will be extracted from the gravity data, is the spatial variation of the plutons' thickness. The results of the inversion of the gravity anomaly along the traverses are shown in Figures 8b and 9b for Redenção and Bannach, respectively.

A remarkable feature of both plutons, disclosed by the gravity inversion, is that they exhibit a lateral extension substantially larger than vertical one, outlining a sheeted geometry. An approximate N-S cross-section (A-A' in Figure 8a and b1) through the strongest negative residual anomaly over the Redenção intrusion, for example, indicates, according to the assumed density contrast between the granite and its country rocks, that a maximum deepening of the granite's floor to 5.6 km is necessary to explain the gravity anomaly. Similar results were obtained along the B-B' and C-C' cross-sections (Fig. 8a, b2, and b3). The estimates of the plutons' depth to the bottom indicates a progressive thinning from the center to the borders and maximum thickness values of 5.6 km and 2.2 km, respectively, for the Redenção and Bannach plutons (Figs. 8b, c, d, 9b, c, and d). In the former, the main concentration of granitic mass is situated in the central to northeastern part of the intrusion. In the latter, it is located in the central-northern and southern areas of the intrusion. Because 2D gravity inversion has been performed on data produced by 3D sources, the maximum depths of the plutons may in fact be slightly greater than the estimated figures of 5 km and 2 km.

A contour map of the Redenção massif's depth to the bottom was draw from the gravity inversion of the isolated gravity profiles shown in Figure 8c and d. From this map, it can be seen that the overall trend is a progressive deepening of the floor of the pluton from its border to its center. The subcrop map of the pluton almost coincides with the outcrop area map (Fig. 2a), except at the eastern margin, where the intrusion is covered by the Araguaia belt metasediments. Gravity data provides, therefore, strong evidence that the Redenção intrusion has a laccolithic shape.

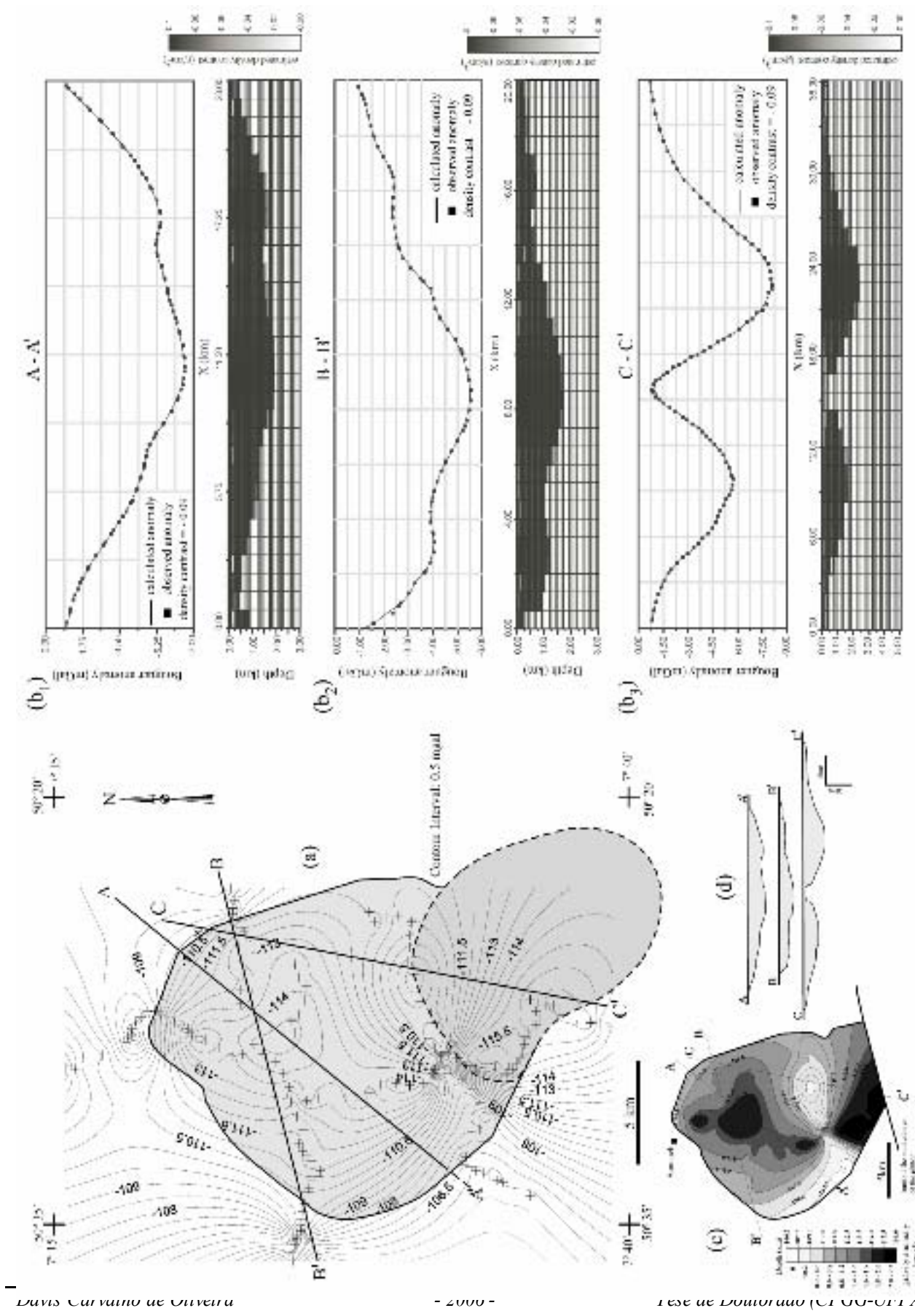


**Fig. 9.** Bannach pluton. (a) Bouguer anomaly map showing the distribution of the gravity stations (crosses) and 0.5 mgal contours in the studied area of the pluton. (b) Observed gravity (squares) and calculated Bouguer anomaly (continuous lines) obtained from the modeling of the residual anomalies associated with the modeled geometry of the pluton. Gravity inversion profiles with the regional field removed as computed by 2D modeling. (b1) A-A', approximate NE-SW profile; (b2) B-B', approximate E-W profile; (b3) C-C', approximate N-S profile. (c) Contour map of the Bannach pluton depth drawn from gravity anomalies modeling using the method of Silva and Barbosa (2006). (d) Cross-sections through the Bannach pluton showing its morphology with depth; all sections obtained from 2D gravity inversion. All sections are shown at the same horizontal and vertical scales with no vertical exaggeration. The profiles are indicated in Fig. 9a, c. Depths are in kilometers. It was assumed a density contrast of -0.09 g/cm<sup>3</sup> between the granite varieties and the country rocks.

In the Bannach pluton, the gravity survey was restricted to its northern and central parts that correspond to the first intrusion and to part of the second intrusion that compose the pluton (Almeida, 2005). The different gravimetric cross sections suggest that the pluton is also a laccolith. However, it differs from the Redenção because of its smaller thickness, being only locally thicker than 2 km. Besides, the gravity data revealed the existence of a gravity high, approximately coinciding with the limit between the first and second intrusions. A gravity high is also identified along the western border of the first intrusion. It reinforces the hypothesis of an origin of the pluton by multiple sequential intrusions, evolving from the north to the south. The steep increase of the gravity response in the limit between the first and second intrusions, also observed in the western border of the first intrusion, is a strong evidence of a shallow contact between the granite and the country rocks in the mentioned areas (Fig. 9d; C-C' profile). It is concluded that the general shape of the Bannach pluton is similar to that of the Redenção pluton, but they differ in thickness. The origin by sequential multiple center intrusion is also a distinct aspect of the Bannach pluton not observed at Redenção, but probably also present in the Musa pluton of the Jamon suite.

## 6. Discussion

### 6.1. Tridimensional shape of the plutons

A remarkable feature of the Redenção pluton and the northern intrusion of the Bannach pluton is that they exhibit a lateral extent larger than the vertical one, outlining a sheeted geometry. They are near circular bodies with approximate diameters of 25 km and 20 km, respectively, extending to a maximum depth of 5.6 km in the case of Redenção and of 2.2 km for Bannach (Figs. 10a and b). Several granite plutons display sheeted-like geometries with fractal thickness/length ratios

(Mcffrey and Petford, 1997). The average thickness/length ratios of the studied plutons are similar to those indicated by the general power law for laccolith dimension (Mcffrey and Petford, 1997; Rocchi et al., 2002), and to those observed in classical rapakivi granite batholiths (Vigneresse, 2005, and references therein): Wiborg (350 km x 200 km x 5 km) from Finland; Åland (110 km x 90 km x 8 km), and Nordingrå (50 km x 20 km x 5 km), from Sweden; Korosten ( 125 km x 100 km x 0.5 – 3 km) from Ukraine.

In general, the global shape of rapakivi granites strongly differs from that of other massifs (Vigneresse 2005). The diagram L/W vs. W/T discriminates the three-dimensional characteristics of intrusive plutons (Améglio et al., 1997; Mcffrey and Petford, 1997). The relation between the length/width (L/W) and width/thickness (W/T) ratios clearly separates wedge-shaped plutons from flat-floored ones, and reflects the control of the emplacement mechanism and shape of the plutons by regional tectonics (Fig. 11). In this respect, the rapakivi granites are characterized by a very large width/thickness (W/T) ratio, whereas the length/width (L/W) ratio remains close to 1, reflecting a quasi-square shape at the surface. This indicates the anisotropic character of the crust at the time of emplacement (Hogan et al., 1998; Vigneresse et al., 1999).

The Bannach pluton reaches in all its extension a length of 45 km in the NW-SE direction (Fig. 2b). However, it should be take into account that this pluton is a composite intrusion formed by at least three coalescent plutons (Almeida et al., submitted; Figs. 2b, 6b, and 9b3, c, and d; cross-section C-C'). Gravity data reinforce the hypothesis that the growth of the northern part of the Bannach pluton results of the amalgamation of smaller sheeted-like plutons that intruded in sequence from northwest to southeast.

In an extensional tectonic setting it would be expected the occurrence of thin-sheeted intrusions, rarely more than 5 km thick, better than thick plutons. The results of gravity inversion in the Redenção and Bannach plutons indicate that their three-dimensional shape is in agreement with this model. This conclusion can be extrapolated to the entire Jamon suite.

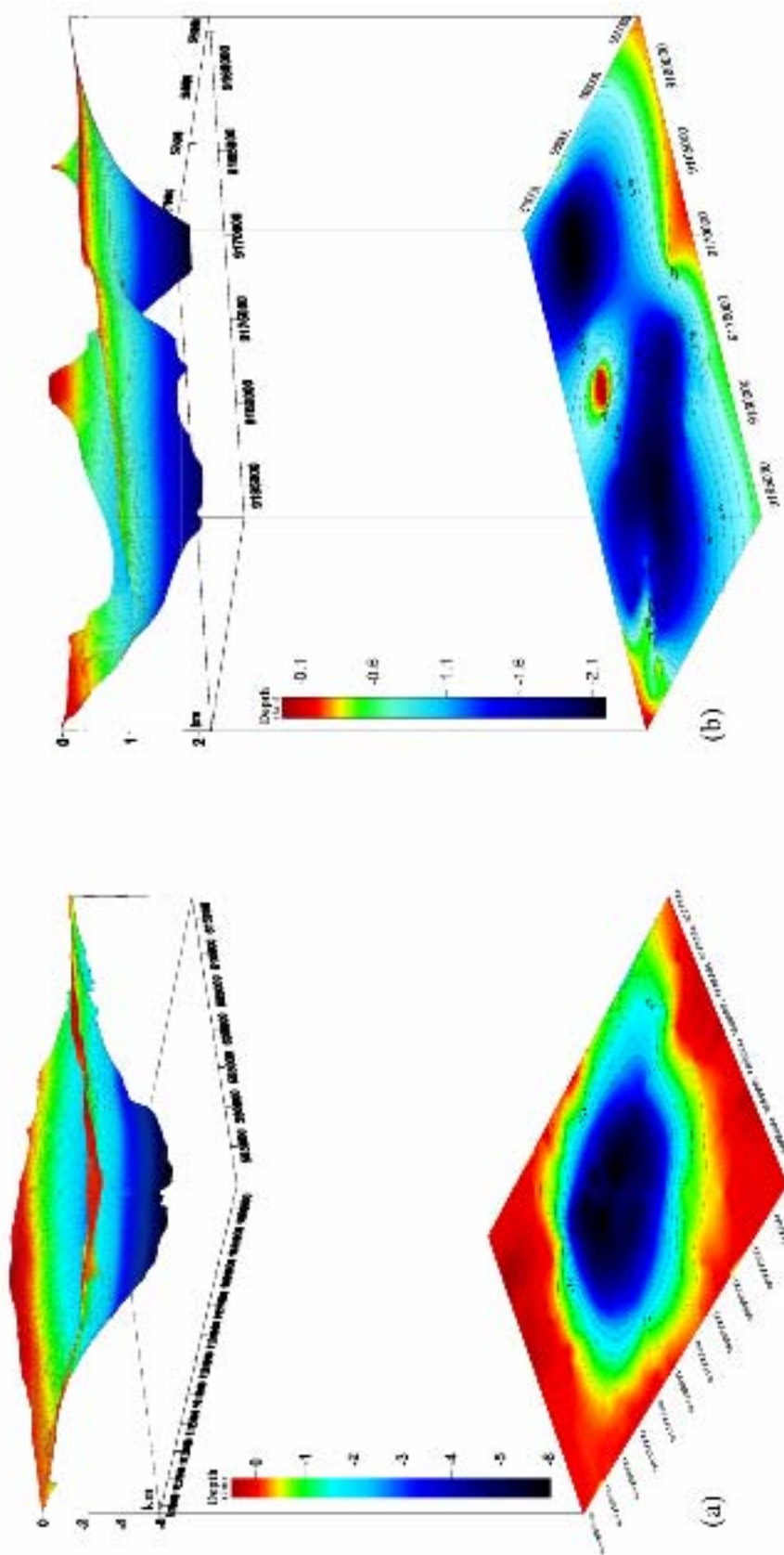


**Fig. 10.** Perspective views of the three-dimensional geometry of the Redenção and Bannach plutons through gravity data analysis associated with depth maps (in km) (a) Redenção pluton. View from SW to NE. (b) Bannach pluton. View from WNW to ESE.

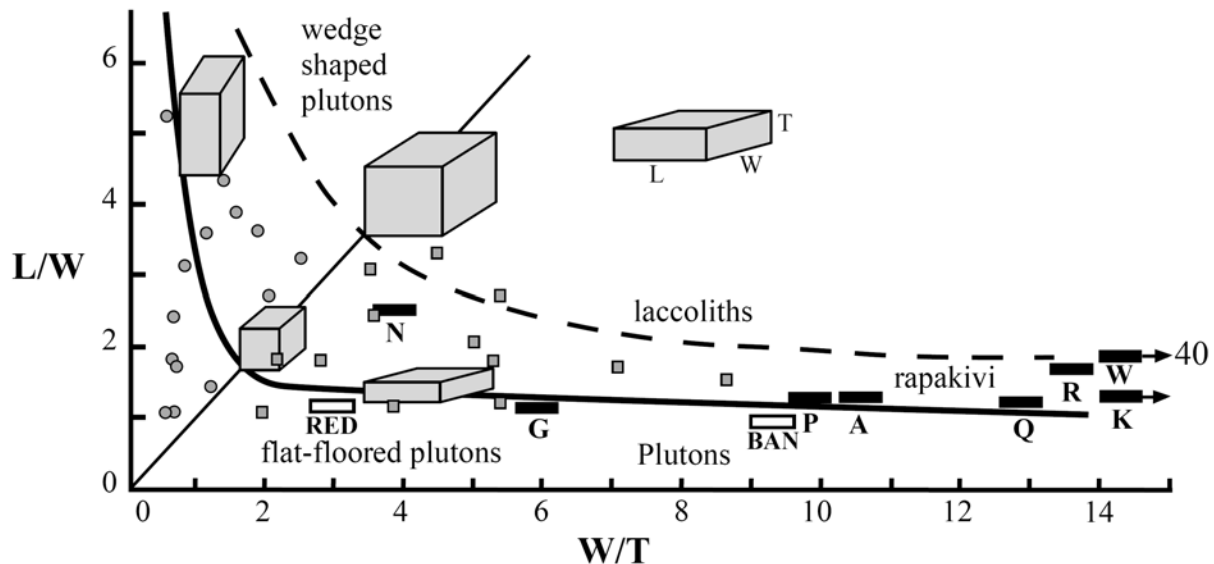


**Fig. 11.** Diagram length/width ( $L/W$ ) as a function of the ratio width/thickness ( $W/T$ ) of various plutons, as deduced from gravity data inversion (Améglio et al., 1997), based on Vigneresse (2005, and references therein). Circles reflect wedge-shaped plutons, and squares flat floored massifs. Also plotted are curves for laccoliths and plutons deduced from 2D models (Petford et al., 2000). Rapakivi granites (Wiborg, Ahvenisto, both in Finland; Nordingrå, Sweden; Riga in Latvia; Korosten, Ukraine; Grahf Fjelde, Paatusoq and Qernertoq, southern Greenland) are shown by black boxes. The Redençao and Bannach plutons are indicated by unfilled boxes labeled, respectively, RED and BAN.

## 6.2. Tectonic setting and emplacement of the studied plutons

The extensive A-type, rapakivi magmatism developed during the Mesoproterozoic appears to be a very specific, world scale event. This magmatism has been recognized in most old cratonic blocks, especially in North America, Baltica and Amazonia (Rämö and Haapala, 1995). It has been, generally, associated with the breakup of a supercontinent formed at the late Paleoproterozoic or early Mesoproterozoic (Hofmann, 1989; Windley, 1993, 1995; Brito Neves, 1999; Frost et al., 1999; Condie, 2002; Lamarão et al., 2002, 2005; Zhao et al., 2004; Dall'Agnol et al. 2005; Vigneresse, 2005). The origin of rapakivi granites and associated rocks is generally considered as typical of ‘anorogenic’, extensional settings. They are not associated with major episodes of large-scale deformation that would mark any model of local plate convergence. However, they could represent the reflex in stabilized areas of distal orogenic events (cf. Åhäll et al., 2000; Zhao et al., 2004).

In the Amazonian Craton, the emplacement of the Jamon suite granites takes place ~200 Ma after the latest peak of convergence of the Transamazonian event during the Paleoproterozoic. Moreover, the A-type plutons of Carajás province are ~1.0 Ga older than their Archean country rocks (Macambira and Lafon, 1995; Rämö et al., 2002; Dall'Agnol et al., 2005). The development of this extensive granite magmatism is considered to be associated with the fragmentation of a ~2.0 Ga, Paleoproterozoic supercontinent and postdates the Archean crust of the Carajás province by ca. one billion year.

The generation of the A-type rapakivi granites of the Carajás province is admitted to be linked to asthenosphere upwelling and magma production in the mantle, followed by partial melting of the lower continental crust provoked by the heat provided by the underplating of mantle magmas (Dall'Agnol et al., 2005). The resulting anatetic liquids ascend in the crust and are emplaced as high-level granite complexes. In this model, extension is associated to the mantle upwelling and it is indicated by the occurrence of diabase and granite porphyry dyke swarms coeval with the Jamon suite. The dikes follow WNW-ESE to NNW-SSE trends demonstrating that the tectonic extensional stress was oriented approximately along NNE-SSW to ENE-WSW. The 1.88 Ga A-type granite plutons and stocks of Carajás are also disposed along a belt extending from the border between the Amazonian craton and the Araguaia belt, in the east, to the Xingu region domain, in the west. This belt also follows the general trend defined by the dikes (Fig. 1b).

A wealth of geological evidence argues in favor of an emplacement of the Jamon suite in an extensional setting. In this context, dikes are the most efficient way to feed upper crustal plutons (Petford, 1996; Petford et al., 2000). Moreover, important information on the emplacement mechanism of granitic magmas is preserved in the three-dimensional (3D) shape of the plutons. The inferred tabular geometry of the studied plutons, similar to that assumed for rapakivi complexes, is not predicted by diapiric models (Cruden, 1990). It is, however, consistent with what would be expected in the case of granitic magma transport via a series of dyke feeder channels (Petford, 1996).

Assuming a dike-like ascent model, two stages during the construction of the Bannach and Redenção plutons can be recognized. The relationships of the Jamon suite plutons with coeval, NW-SE trending dyke swarms indicate that, in a first stage, the ascent of magma took place through similarly orientated fracture zones, perpendicular to the principal extensional stress. Mingling structures, locally found in composite dike, indicate the ascent of mafic and

felsic magmas through the same fissures and the contemporaneous character of these magmas. The second stage corresponds to the switch from upward flow to lateral spread of magma at upper-crustal levels and is responsible for the sheet-like shape of the plutons. The high viscosity contrast and absence of deformation aureole within the country rocks suggest that the lateral spreading of the plutons was not the main mechanism for space creation during emplacement; space was mostly created by the vertical displacement of country rock. On a regional scale, the Redençao and Bannach plutons are aligned nearly parallel to NNW-SSE faults in the Archean basement, consistent with magma ascent along pre-existing deep fault lineaments. Deep faults have served as channels for the magma upwelling and tectonic discontinuities represented weaker zones that favored magma emplacement at shallow crustal level.

### 6.3. Internal zoning of the plutons

All studied plutons of the Jamon suite display normal zoning (this paper; Dall'Agnol et al., 2005, and references therein). A common explanation for this feature is a magmatic evolution by fractional crystallization, with gradual differentiation from the margins to the center of the plutons (Bateman and Chappell, 1979). Zorpi et al. (1989) and Richardson (2004) discussed the hypotheses presented to explain this type of zoning and mentioned that granite plutons are more commonly formed of a series of continuous pulses of magmas differentiated elsewhere. They emphasized the role of magma mingling processes in the origin of normal zoned calc-alkaline plutons and concluded that *in situ* fractional crystallization should be ruled out as the dominant mechanism for zoning development. They admitted that zoning was inherited from an earlier stage of pluton's evolution. In spite of the geochemical contrasts between the calc-alkaline granites and those of the Jamon suite (Dall'Agnol and Oliveira, in press), the general conclusions of Zorpi et al. (1989) are probably also applicable for the Redençao and Bannach plutons, with the important difference that mingling processes in the later are restricted to felsic, porphyritic granites, without evidence of involvement of mafic magmas except in local composite dikes.

The geochemical characteristics of the Redençao and Bannach granite varieties indicate that the leucogranites of both plutons are not derived directly by fractional crystallization of the less evolved amphibole-biotite-bearing facies (Oliveira, 2001; Almeida et al., submitted). They were interpreted as late-emplaced varieties of more evolved magmas derived from similar sources and processes but not necessarily from the same magma. This interpretation is consistent

with the general features observed in these plutons and could partially explain their normal zoning. The coarse biotite monzogranites should be derived from the amphibole-biotite monzogranites by fractional crystallization. The gradual compositional transition in between these facies, associated with the late emplacement of leucogranite magmas, could explain the general zoning of these plutons. Local occurrences of clinopyroxene-bearing mafic-enriched monzogranites are related to cumulitic processes involving the less evolved rocks.

## 7. Conclusions

At the end of Paleoproterozoic times (~1.88 Ga), the Amazonian Craton recorded a tectonothermal event that resulted in major lithospheric reorganization associated with mantle upwelling, mafic underplating, crustal extension, and emplacement of “anorogenic”, A-type granites. Petrographic and geochemical aspects associated with magnetic susceptibility and gamma-ray spectrometry data showed that the Redenção and the northern part of Bannach plutons are normally zoned. They were formed by two magmatic pulses: a first pulse, resulting in a fractionation series of coarse, even-grained monzogranites with variable modal proportions of biotite and hornblende; a slightly younger pulse, located to the center of the plutons, composed of even-grained leucogranites.

Composite 2-D gravity inversions along profiles allowed us to determine the approximate 3-D geometry of these massifs that correspond to sheet-shaped laccolithic intrusions (Rocchi et al., 2002; Araguren et al., 2003). The studied plutons follow the general power law for laccolith dimension (Mcffrey and Petford, 1997; Rocchi et al., 2002; Cruden, 2005), and their dimensional ratios are similar to those observed in classical rapakivi granite batholiths (Vigneresse, 2005). Gravity data suggest that the growth of the northern part of the Bannach pluton results of the amalgamation of smaller sheeted-like plutons that intruded in sequence from northwest to southeast. This is consistent with evidence that the Bannach pluton is a composite intrusion formed by at least three coalescent plutons (Almeida, 2005).

The occurrence of diabase and granite porphyry dyke swarms, orientated WNW-ESE to NNW-SSE and coeval with the Jamon suite, demonstrates that, at that time, the tectonic extensional stress was oriented approximately along NNE-SSW to ENE-WSW. The 1.88 Ga A-type granite plutons and stocks of Carajás are disposed along a belt that follows the general trend defined by the dikes. The inferred tabular geometry of the studied plutons and the high contrast of

viscosity between the granites and their Archean country rocks are not consistent with diapiric or ballooning models (Castro et al., 1987; Cruden 1990, 2005; Barros et al., 2001), but can be explained by magma transport via dikes (Petford, 1996).

### Acknowledgments

We acknowledge: Grant Osborne and Keith Martin, of the former Western Mining Company, for the gravity data obtained in the Redenção area; J. L. Gouvêa and A. L. Quaresma for support in the acquisition and the treatment of gravimetric data; the Geological Survey of Brazil (CPRM) for supply and L. T. Rosa-Costa and A. G. Vale for the treatment of aerogeophysical data; C. E. M. Barros for participation in the geological mapping of Redenção pluton and F. V. Guimarães for magnetic susceptibility data on the Bannach pluton. This research received financial support from CNPq (RD – 550739/2001-7, 476075/2003-3, 307469/2003-4; DCO – scholarship April04 to Nov05), CAPES (DCO – scholarship Nov01 to March04), and Federal University of Pará (UFPA). This paper is a contribution to PRONEX/CNPq (Proc. 66.2103/1998-0) and IGCP-510 project (IUGS-UNESCO).

### References

- Åhäll, K.I., Connelly, J.N., Brewer, T.S., 2000. Episodic rapakivi magmatism due to distal orogenesis: correlation of 1.69–1.50 Ga orogenic and inboard, “anorogenic” events in the Baltic Shield. *Geology* 28, 823– 826.
- Almeida, J.A.C., 2005. Geologia, petrografia e geoquímica do granito anorogênico Bannach, Terreno Granito-Greenstone de Rio Maria, PA. M.Sc. Thesis, Federal University of Pará, Belém, Brazil (in Portuguese), 171p.
- Almeida, J.A.C., Dall'Agnol, R., Oliveira, D.C., Submitted. Geologia, petrografia e geoquímica do granito anorogênico bannach, terreno granito-greenstone de rio maria, Pará. *Revista Brasileira de Geociências*.
- Améglio, L., Vigneresse, J. L. & Bouchez, J. L., 1997. An assessment of combined fabrics and gravity data in granites. In: Bouchez, J. L., Hutton, D. & Stephens, W. E. (eds) *Granite: from Segregation of Melt to Emplacement Fabrics*. Dordrecht: Kluwer Academic, pp. 199– 214.
- Anderson, J.L., Bender, E.E., 1989. Nature and origin of Proterozoic A-type granitic magmatism in the southwestern United States of America. *Lithos* 23, 19-52.

- Anderson, J.L., Morrison, J., 1992. The role of anorogenic granites in the Proterozoic crustal development of North America. In: Condie, K.C. (Ed.), Proterozoic Crustal evolution. Elsevier, p. 263-299.
- Anderson, J.L., Smith, D.R., 1995. The effects of temperature and  $fO_2$  on the Al-in-hornblende barometer. American Mineralogist 80, 549-559.
- Anderson, J.L., Morrison, J., 2005. Ilmenite, magnetite, and peraluminous Mesoproterozoic anorogenic granites of Laurentia and Baltica. Lithos 80, 45-60.
- Aranguren, A., 1997. Magnetic fabric and 3D geometry of the hambreiro-Sta. Eulalia pluton: implications for the Variscan structures of eastern Galicia, NW Spain. Tectonophysics, 273, 329-344.
- Aranguren, A., Cuevas, J., Tubía, J.M., Román-Berdiel, T., Casas-Sainz, A., Casas-Ponsati, A., 2003. Granite laccolith emplacement in the Iberian arc: AMS and gravity study of the La Tojiza pluton (NW Spain). Journal of the Geological Society, London, vol. 160, p. 435-445.
- Barnes, M. A., Rohs, C. R., Anthony, E. Y., Van Schmus, W. R., Denison, R. E., 1999. Isotopic and elemental chemistry of subsurface Precambrian igneous rocks, west Texas and eastern New Mexico. Rocky Mt. Geol. 34:245-262.
- Barnes, M.A., Anthony, E.Y., Williams, I., Asquith, G.B., 2002. Architecture of a 1.38-1.34 granite-rhyolite complex as revealed by geochronology and isotopic and elemental geochemistry of subsurface samples from west Texas, USA. Pre-cambriam Research. 119, 9-43.
- Barros, C.E.M., Sardinha, A.S., Barbosa, J.P.O., Krimski, R., Macambira, M.J.B., 2001. Pb-Pb and U-Pb zircon ages of Archean syntectonic granites of the Caraja's metallogenic province, Northern Brazil. 3th Simposio Sudamericano de Geologia Isotopica, 3, Pucon, Chile, Resumos Expandidos. Servicio Nacional de Geología Y Minería. CD-ROM.
- Bateman, P.C., Chappel, B.W. 1979. Crystallization, fractionation, and solidification of the Tuolumne Intrusive Series, Yosemite National Park, California: GSA Bull, 90: 456-482.
- Bettencourt, J.S., Tosdal, R., Leite, W.B., JR., Payolla, B.L., 1995. Overview of the rapakivi granites of the Rondônia Tin Province (RTP). In: Symposium on Rapakivi Granites and Related Rocks. Excursion Guide and Programs... Belém, pp. 5-14.
- Brito Neves, B.B., 1999. América do Sul: quarto fusões, quatro fissões e o processo acrescionário

- andino: Revista Brasileira de Geociências 29, 379-392 (in Portuguese).
- Carvalho, J.S., 1988. Aplicação dos Métodos Gravimétrico e Magnetométrico para a Definição do Comportamento Estrutural da Faixa de Dobramentos Araguaia. Belém. 108 p. (M.Sc. Thesis, CPGG/UFPA).
- Castro, A., 1987. On granitoid emplacement and related structures. A review. Geologische Rundschau, 76: 101-124.
- Ceci, V.M., Frederick, M.D. 2002. The Stripedrock pluton, a reversely zoned, A-type, Neoproterozoic granite in the Blue Ridge of Southwestern Virginia: Annual meeting of Southeastern (51st) / North-Central (36th) Section of the Geological Society of America, GSA, Lexington, Kentucky. Abstracts with Programs. Vol. 34, No. 12, April 2002.
- Clemens, J.D., Mawer, C.K., 1992. Granitic magma transport by fracture propagation. Tectonophysics, 204: 339-360.
- Condie, K.C., 2002. Breakup of a Paleoproterozoic supercontinent. Gondwana Research 5, 41-43.
- Costi, H.T., Dall'Agnol, R., Moura, C.A.V., 2000. Geology and Pb-Pb geochronology of Paleoproterozoic volcanic and granitic rocks of Pitinga province, Amazonian craton, Northern Brazil. International Geology Review 42, 832– 849.
- Cruden, A.R., 1990. Flow and fabric development during the diapiric rise of magma. Journal of Geology, 98, 681-698.
- Cruden, A.R. 2005. Emplacement and growth of plutons: implications for rates of melting and mass transfer in continental crust. In: Brown, M. & Rushmer, T. (Eds.): *Evolution and Differentiation of the Continental Crust*, Cambridge University Press. In Press.
- Dall'Agnol, R., Teixeira, N.P., Magalhães, M.S., 1993. Diagnostic features of the Tin-specialized anorogenic granites of the Eastern Amazonian Region. Anais da Academia Brasileira de Ciências, 65 (Suplemento 1): 33-50.
- Dall'Agnol, R., Lafon, J.M., Macambira, M.J.B., 1994. Proterozoic anorogenic magmatism in the Central Amazonian province: geochronological, petrological and geochemical aspects. Mineralogy and Petrology 50, 113-138.
- Dall'Agnol, R., Souza, Z.S., Althoff, F.J., Barros, C.E.M., Leite, A.A.S., Jorge João, X.S., 1997b. General Aspects of the granitogenesis of the Carajás metallogenetic province. In: Second International Symposium on Granites and Associated Mineralizations, Excursions Guide,

- Salvador, Companhia Baiana de Pesquisa Mineral, Superintendência de Geologia e Recursos Minerais, pp.135-161.
- Dall'Agnol, R., Costi, H.T., Leite, A.A., Magalhães, M.S., Teixeira, N.P., 1999a. Rapakivi granites from Brazil and adjacent areas. *Precambrian Research* 95, 9-39.
- Dall'Agnol, R., Rämö, O.T., Magalhães, M.S., Macambira, M.J.B., 1999b. Petrology of the anorogenic, oxidised Jamon and Musa granites, Amazonian craton: implications for the genesis of Proterozoic A-type granites. *Lithos* 46, 431-462.
- Dall'Agnol, R., Scaillet, B., Pichavant, M., 1999c. An Experimental Study of a Lower Proterozoic A-Type Granite from the Eastern Amazonian Craton, Brazil. *Journal of Petrology* 40, 1673-1698.
- Dall'Agnol, R., Teixeira, N.P., Rämö, O.T., Moura, C.A.V., Macambira, M.J.B., Oliveira, D.C. 2005. Petrogenesis of the Paleoproterozoic, rapakivi, A-type granties of the Archean Carajás Metallogenic Province, Brazil. *Lithos* 80, 101-129.
- Dall'Agnol, R., Oliveira, D.C. Submitted. Oxidized, magnetite-series, rapakivi-type granites of Carajás, Brazil: implications for classification and petrogenesis of A-type granites. *Lithos*.
- Elliott, B.A., 2001. Crystallization conditions of the Wiborg rapakivi batholith, SE Finland: an evaluation of amphibole and biotite mineral chemistry. *Mineralogy and Petrology*. 72, 305–324.
- Emslie, R.F., 1991. Granitoids of rapakivi granite-anorthosite and related associations. *Precambrian Research* 51, 173-192.
- Escobar I.P. 1980. Metodos de levantamentos e ajustamento de observações gravimétricas visando a implantação da Rede Gravimetrica Fundamental Brasileira. Rio de Janeiro, Observatorio Nacional, Publ. No. 1, 32p.
- Ferré, E.C., Gleizes, G. & Caby, R., 2002. Tectonics and post-collisional granite emplacement in an obliquely convergent orogen: the Trans-Saharan belt, Eastern Nigeria. *Precambrian Research*, 114, 199-219
- Fraga, L.M.B. 2002 - A Associação anortositio - mangerito - granito rapakivi (AMG) do Cinturão Guiana Central, Roraima, e suas encaixantes paleoproterozóicas: evolução estrutural geocronologia e petrologia. Ph.D. Thesis, Federal University of Pará, Belém, Brazil (in Portuguese).
- Fraga, L.M., Dall'Agnol, R., Macambira, M.J.B., 2003. The Mucajai anorthosite-mangerite

- rapakivi granite (AMG) complex, north Amazonian craton, Brazil. EGS–AGU–EUG Joint Assembly, Nice, France. VGP6 Granite Systems and Proterozoic Lithospheric Processes, EAE03-A-14489.
- Frost, C.D., Frost, B.R., 1997. Reduced rapakivi type granites: the tholeiitic connection. *Geology* 25, 647–650.
- Frost, C.D., Frost, B.R., Chamberlain, K.R., Edwards, B., 1999. Petrogenesis of the 1.43 Ga Sherman batholith, SE Wyoming, USA: a reduced, rapakivi-type anorogenic granite. *Journal of Petrology* 40, 1771–1802.
- Gleizes, G., Nedelec, A., and Bouchez, J., 1993. Magnetic Susceptibility of the Mont-Louis Andorra Ilmentite-Type Granite (Pyrenees): A New Tool for the Petrographic Characterization and regional mapping of Zoned Granite Plutons: *Journal of Geophysical Research*, v. 98, p. 4317–4331.
- Haapala, I., Rämö, A., 1990. Petrogenesis of the Proterozoic rapakivi granites of Finland. In: Stein, H.J., Hannah, J.L. (Eds.), *Ore-bearing Granite Systems: Petrogenesis and Mineralizing Processes*. Special Paper-Geological Society of America, vol. 246. pp. 275–286.
- Haapala, I., Rämö, O.T., 1999. Rapakivi granites and related rocks: an introduction. *Precambrian Research* 95, 1–7.
- Hoffmann, P., 1989. Speculations on Laurentia's first gigayear (2.0 to 1.0 Ga). *Geology* 17, 135–138.
- Hogan, J.P., Price, J.D., Gilbert, M.C., 1998. Magma traps and driving pressure: consequences for plúton shape and emplacement in an extensional regime. *Journal of Structural Geology* 20, 1155–1168.
- Huppert, H.E., Sparks, R.S., 1988. The generation of granitic magmas by intrusion of basalt into continental crust. *Journal of Petrology* 29, 599–624.
- Ishihara, S., 1981. The granitoid series and mineralization. *Economic Geology*, 75 th Anniversary volume, pp. 458–484.
- Kosunen, P.J., 2004. Petrogenesis of A-type mid-Proterozoic A-type granites: Case studies from Fennoscandia (Finland) and Laurentia (New Mexico). Ph.D. Thesis, Department of Geology, University of Helsinki, Finland.
- Lamarão, C.N., Dall'Agnol, R., Lafon, J.-M., Lima, E.F., 2002. Geology, geochemistry, and Pb-

- Pb zircon geochronology of the Paleoproterozoic magmatism of Vila Riozinho, Tapajós Gold Province, Amazonian craton, Brasil. *Precambrian Research* 119, 189-223.
- Lamarão, C.N., Dall'Agnol, R., Pimentel, M.M., 2005. Nd isotopic composition of Paleoproterozoic volcanic and granitoid rocks of Vila Riozinho: implications for the crustal evolution of the Tapajos Gold Province, Amazonian Craton. *Journal of South American Earth Sciences* 18, 277-292.
- Leite, A. A. S., Dall'Agnol, R., Macambira, M. J. B., Althoff, F. J., 2004. Geologia e geocronologia dos granítóides arqueanos da região de Xinguara (PA) e suas implicações na evolução do Terreno Granito-Greenstone de Rio Maria. *Revista Brasileira de Geociências*. 34, 447-458.
- Macambira, M.J.B., Lafon, J.-M., 1995. Geocronologia da Província mineral de Carajás: síntese dos dados e novos desafios. *Boletim do Museu Paraense Emílio Goeldi, Ciências da Terra* 7, 263-288 (in Portuguese).
- McCaffrey K.J.W., Petford N., 1997. Are granitic intrusions scale invariant? *Journal of the Geological Society of London* 154:1-4.
- Machado, N., Lindenmayer, Z., Krogh, T.E., Lindenmayer, D., 1991. U-Pb geochronology of Archean magmatism and basement reactivation in the Carajás area, Amazon Shield, Brazil. *Precambrian Research* 49, 329-354.
- Oliveira, D.C., 2001. Geologia, geoquímica e petrologia magnética do granito paleoproterozóico Redenção, SE do Cráton Amazônico. M.Sc. Thesis, Federal University of Pará, Belém, Brazil (in Portuguese), 202p.
- Oliveira, D.C., Dall'Agnol, R., Barros, C.E.M., Figueiredo, M.A.B.M., 2002. Petrologia magnética do Granito Paleoproterozóico Redenção, SE do Cráton Amazônico. *Contribuições Geologia da Amazônia*, 3:115-132.
- Oliveira, D.C., Dall'Agnol, R., Barros, C.E.M., Vale, A.G., In press. Geologia e Petrografia do Granito Paleoproterozóico Redenção, SE do Cráton Amazônico. *Boletim do Museu Paraense Emílio Goeldi, série Ciências Naturais*, Belém, v. 2, n. 1, p. 155-172.
- Oliveira, D.C., Dall'Agnol, R., Barros, C.E.M., In preparation. Magmatic evolution of the Paleoproterozoic, anorogenic zoned A-type Redenção Granite of the Jamon suite from Amazonian Craton.
- Paradella, W.R.; Santos, A.R.; Dall'Agnol, R.; Pietsch, R.W.; Sant'Anna, M.V. A., 1998.

- Geological investigation based on airborne (SAREX) and spaceborne (RADARSAT- 1) SAR integrated products in the Central Serra dos Carajás granite area, Brazil. Canadian Journal of Remote Sensing, v.24, n.4, p.376-392.
- Paterson, S.R., Vernon, R.H., 1995. Bursting the bubble of ballooning plutons: a return to nested diapirs emplaced by multiple processes. Geology Society of America Bulletin 107, 1356-1380.
- Pereira, E.B., Nordemann, D.J.R., 1983. The effects of a tropical rain forest cover on airborne gamma-ray spectrometry. Brazilian Journal of Geophysics, 1(2): 99-108.
- Petford, N., Lister, J.R., Kerr, R.C., 1994. The ascent of felsic magmas indikes. Lithos 32:161-68.
- Petford, N., 1996. dikes or diapirs? Transactions of the Royal Society of Edinburgh: Earth Sciences 87, 105-114.
- Petford, N., Cruden, A.R., McCaffrey, K.J.W. and Vigneresse, J.-L., 2000. Granite magma formation, transport and emplacement in the Earth's crust. Nature, 408: 669-673.
- Pitcher, W.S., 1979. The nature, ascent and emplacement of granitic magmas. Journal of the Geological Society of London, 136: 627-662.
- Pons J., Barbey P., Nachit H., Burg J.-P., 2006. Development of igneous layering during growth of pluton: The Tarçouate Laccolith (Morocco). Tectonophysics, 413, 3-4, 271-286.
- Rajesh, H.M., 2000. Characterization and origin of a compositionally zoned aluminous A-type granite from South India. Geological Magazine 137, 291-318.
- Ramberg, H., 1970. Model studies in relation to intrusion of plutonic bodies. In: Mechanics of Igneous Intrusions. Liverpool: Seel House Press, p.261-286.
- Rämö, O.T., 1991. Petrogenesis of the Proterozoic rapakivi granites and related basic rocks of the southeastern Fennoscandian: Nd and Pb isotopic and general geochemical constraints. Geological Survey of Finland Bulletin 355.
- Rämö, O.T., Haapala, I., Salonsaari, P., 1994. Rapakivi granite magmatism: implications for lithospheric evolution. Geological Survey of Finland, Guide 37, 61-68
- Rämö, O.T., Haapala, I., 1995. One hundred years of rapakivi granite. Mineralogy and Petrology 52, 129-185.
- Rämö, O.T., Dall'Agnol, R., Macambira, M.J.B., Leite, A.A.S., de Oliveira, D.C., 2002. 1.88 Ga oxidized A-type granites of the Rio Maria region, eastern Amazonian craton, Brazil:

- Positively anorogenic! *Journal of Geology* 110, 603-610.
- Richardson, P. D. 2004. Pluton Zonation Unveiled by Gamma-ray Spectrometry and Magnetic Susceptibility; A Case Study of the Sheeprock Granite, Western, Utah: M.Sc. Thesis Thesis, Department of Geology, Brigham Young University, 44p.
- Rocchi, S., Westerman, D.S., Dini, A., Innocenti, F., Tonarini, S., 2002. Two-stage growth of laccoliths at Elba Island, Italy. *Geology*, v. 30, no. 11, p. 983-986.
- Román-Berdiel, T., Gapais, D., Brun, J.P., 1995. Analogue models of laccolith formation. *Journal of Structural Geology*. 17, p. 1337–1346.
- Silva, J.B.C., Barbosa, V.C.F., 2006, Interactive gravity inversion: *Geophysics*, vol 71, p. J1-J9.
- Silva, Jr., R.O., Dall'Agnol, R., Oliveira, E. P., 1999. Geologia, petrografia e geoquímica dos diques proterozóicos da região de Rio Maria, sudeste do Pará. *Geochimica Brasiliensis*, 13.
- Singh, A.P., Kumar, N., Singh B., 2004. Magmatic underplating beneath the Rajmahal Traps: Gravity signature and derived 3-D configuration. *Proceedings of the Indian Academy of Sciences. Earth and Planetary Sciences*, 113, No. 4, pp. 759–769.
- Souza, Z.S., Dall'Agnol, R., 1995. Geochemistry of metavolcanic rocks in the Archean Greenstone Belt of Identidade, SE, Pará, Brazil. *Anais Academia Brasileira de Ciências*. 67, 217-233.
- Tassinari, C. C. G.; Macambira, M. J. B. 1999. Geochronological Provinces of the Amazonian Craton. *Episodes*, 22: 174-182.
- Teixeira, N.P., Bettencourt, J.S., Moura, C.A.V., Dall'Agnol, R., Macambira, E.M.B., 2002. Archean crustal sources for Paleoproterozoic tin-mineralized granites in the Carajás Province, SSE Pará, Brazil: Pb-Pb geochronology and Nd isotope geochemistry. *Precambrian Research* 119, 257-275.
- Teruiya, R. K. 2002. Integração digital de dados multifontes no estudo geológico do Granito Cigano, Província Mineral de Carajás – PA. M.Sc. Thesis, INPE-SP, 137p.
- Vasconcellos, R.M., Metelo, M.J., Motta, A.C., Gomes, R.D., 1994. Geofísica em levantamentos geológicos no Brazil. CPRM, Rio de Janeiro, Brazil, pp. 165.
- Vigneresse, J.L., Tikoff, B., Améglio, L. 1999. Modification of the regional stress field by magma intrusion and formation of tabular granitic plutons. *Tectonophysics* 302, 203-224.
- Vigneresse, J.L., 2005. The specific case of the Mid-Proterozoic rapakivi granites and associated suite within the context of Columbia supercontinent. *Precambrian Research*, 137, 1-34.

- Weinberg, R.F., 1996. The ascent mechanism of felsic magmas: news and views. *Trans. R. Soc. Edinburgh: Earth Sciences*, 87: 95-103.
- Windley, B.F., 1993. Proterozoic anorogenic magmatism and its orogenic connections. *Journal of the Geological Society of London*, 150, 39-50.
- Windley, B. F. 1995. *The Evolving Continents*. 3 ed. London, Wiley, 526 p.
- Zhao, G., Sun, M., Wilde, S.A., Li, S., 2004. A Paleo-Mesoproterozoic supercontinent: assembly, growth and breakup. *Earth Science Review* 67, 91–123.
- Zorpi, M.J., Coulon, C., Orsini, J.B., Cocirata, C., 1989. Magma mingling, zoning and emplacement in calc-alkaline granitoid plutons. *Tectonophysics*, 157:315-329.

## CAPÍTULO - 5

### ***ANISOTROPY OF MAGNETIC SUSCEPTIBILITY OF THE REDENÇÃO GRANITE, EASTERN AMAZONIAN CRATON: IMPLICATIONS FOR THE EMPLACEMENT OF A PALEOPROTEROZOIC ANOROGENIC A-TYPE PLUTON***

**Davis Carvalho de Oliveira**

**Sérgio Pacheco Neves**

**Roberto Dall'Agnol**

**Gorki Mariano**

**Paulo B. Correia**

*Submetido: PRECAMBRIAN RESEARCH*

Dear Dr Oliveira,

Your submission entitled "*Anisotropy of Magnetic Susceptibility of the Reden Granite, Eastern Amazonian Craton: Implications for the Emplacement of a Paleoproterozoic Anorogenic A-type Pluton*" has been received by Precambrian Research

Please note that submission of an article is understood to imply that the article is original and is not being considered for publication elsewhere. Submission also implies that all authors have approved the paper for release and are in agreement with its content.

Your submission *entitled "Anisotropy of Magnetic Susceptibility of the Redenção Granite, Eastern Amazonian Craton: Implications for the Emplacement of a Paleoproterozoic Anorogenic A-type Pluton"* has been assigned the following manuscript number:  
PRECAM2235.

You will be able to check on the progress of your paper by logging on  
<http://ees.elsevier.com/precam/> as Author.

Thank you for submitting your work to this journal.

Kind regards,

Brenda Kaldenbach  
Journal Manager  
Precambrian Research

**ANISOTROPY OF MAGNETIC SUSCEPTIBILITY OF THE REDENÇÃO GRANITE,  
EASTERN AMAZONIAN CRATON: IMPLICATIONS FOR THE EMPLACEMENT OF  
A PALEOPROTEROZOIC ANOROGENIC A-TYPE PLUTON**

Davis Carvalho de Oliveira<sup>1</sup>, Sérgio Pacheco Neves<sup>2</sup>, Roberto Dall'Agnol<sup>1</sup>, Gorki Mariano<sup>2</sup>, and  
Paulo Barros Correia<sup>2</sup>

<sup>1</sup>Group of Research on Granite Petrology, Centro de Geociências, Universidade Federal do Pará,  
Caixa Postal 8608, 66075-100 Belém, PA, Brazil

<sup>2</sup>Departament of Geology, Universidade Federal de Pernambuco, 50740-530 Recife, PE, Brazil

\*Corresponding author. Tel.: +55 91 3183 1477; fax +55 91 3183 1609. E-mail address:  
[robdal@ufpa.br](mailto:robdal@ufpa.br)

**Abstract**

Mechanisms responsible for emplacement of granitic plutons, and in particular of anorogenic A-type plutons, are still debated. Here, a magnetic fabric study through anisotropy of magnetic susceptibility (AMS) measurements has been applied to the Redenção pluton in an attempt to understand its emplacement history. The Redenção pluton is part of the 1.88 Ga, anorogenic, A-type Jamon suite. It was intruded into 2.97 – 2.86 Ga-old Archean granitoids of the Rio Maria Granite-Greenstone Terrane in the eastern Amazonian craton (northern Brazil). Gravity survey shows that the Redenção pluton is a 6 km-thick, sheeted-like intrusion emplaced

at shallow crustal level. The pluton is characterized by normal zoning, with mingling relationships that indicates multiple magma injections in its construction. High magnetic susceptibilities ( $K$  from  $1 \times 10^{-3}$  SI to  $54 \times 10^{-3}$  SI) and thin-section examination indicate that the magnetic fabric is primarily carried by ferromagnetic minerals (magnetite). Low  $P'$  values and microstructural observations (absence of intracrystalline deformation features) indicate that the magnetic fabric is of magmatic origin. The magnetic fabric is well organized and characterized by concentric steep foliations associated with gently to moderately plunging lineations. The lack of a well-defined unidirectional linear fabric at pluton scale suggests reduced or null influence of regional stresses during granite emplacement. Three stages are proposed for construction of the Redenção pluton, which reconcile the tabular shape of the intrusion with the occurrence of steep magnetic foliations: (1) ascent of magmas in vertical, northwest-striking feeder dikes and accommodation by translation along east-west-striking regional foliation planes; (2) switch from upward flow to lateral spread of magma. Space for injection of successive magma pulses is created by floor subsidence; (3) in situ inflation of the magma chamber in response to intrusion of the central, late-emplaced facies, accompanied by evacuation of resident magmas through ring fractures.

**Keywords:** AMS, Ferromagnetic, Magnetite, A-type granites, Anorogenic, Amazonian craton

## 1. Introduction

The end of the Paleoproterozoic Era and the entire Mesoproterozoic Era were characterized by intense magmatic activity in different cratonic areas of the world. The rapakivi granite suites and associated rocks of the Fennoscandian Shield (Haapala and Rämö, 1992; Rämö and Hapala, 1995; Amelin et al., 1997; Eklund and Shebanov, 1999) and North American continent (Emslie, 1991; Frost et al., 1999; Anderson and Morrison, 2005) are typical examples of the rocks formed during these Proterozoic magmatic events. Similar magmatic events have also been identified in the Amazonian craton (Dall'Agnol et al., 1999a, 2005; Bettencourt et al., 1999).

The tectonic setting of the Proterozoic A-type, rapakivi granites has remained an issue of controversy. The classic Proterozoic rapakivi granites are associated with mafic dike swarms, listric shear zones, and thinned crust (Rämö and Haapala, 1995). They were intruded into a crust

that predates them by some hundred million years (e.g., Rämö and Haapala, 1995; Rämö et al., 2002; Dall'Agnol et al., 2005), and are found as discordant multiple plutons. This suggests an extensional tectonic setting and “anorogenic” origin, i.e., lack of direct association with convergent processes and absence of plate-scale deformation (Hutton et al., 1990, Haapala and Rämö, 1999 and references therein). However, other authors have suggested that rapakivi granites could be related to distal orogenesis (Nyman et al., 1994; Nyman and Karlstrom, 1997; Åhäll et al., 2000). Rapakivi granites and related “anorogenic” granites have become an important tool for modelling Precambrian intraplate crustal processes and global-scale lithospheric evolution. An origin associated with crustal anatexis promoted by magmatic underplating is generally admitted (Huppert and Sparks, 1988; Rämö and Haapala, 1995; Dall'Agnol et al., 1999a).

The emplacement mechanism of granitic plutons in the continental crust remains a fundamental tectonic problem and the emplacement model of A-type granites, in particular, is still poorly understood. Rock fabrics provide a wealth of information on the emplacement mechanisms of plutons and their tectonic settings. However, very few fabric studies have been carried out on A-type granites, possibly because they are often even-grained and isotropic, without visible crystal orientations (Bonin, 1986; Ferré et al., 1999). Recent studies have shown that the low-field anisotropy of magnetic susceptibility (AMS) technique can provide fabric information for weakly deformed or apparently undeformed plutons from various tectonic settings, and with different composition and mineralogy (Bouchez, 1997). Thus far, few AMS studies have been performed on A-type plutons (Geoffroy et al., 1997; Ferré et al., 1999; Bolle et al., 2002). Here we report the results of an AMS study carried out in the Redenção pluton (eastern Amazonian craton). The Redenção pluton, representative of the Paleoproterozoic oxidized A-type Jamon suite (~1.88 Ga old), is an intrusion hosted by ~3.0 to 2.86-Ga-old granitic rocks of the Archean Rio Maria Granite-Greenstone Terrane (Oliveira et al. 2002, 2005). This contribution aims to investigate the emplacement mechanisms involved in the construction of the Redenção pluton and, by comparison with similar A-type and rapakivi plutons emplaced elsewhere, to evaluate the utility of magnetic fabric studies in this kind of intrusion. This work may lead the way for further research on the factors controlling emplacement of anorogenic, A-type granites in general.

## 2. Geological setting

The Redenção granite is situated in the eastern border of the Central Amazonian province of the Amazonian craton (Tassinari and Macambira, 2004; Fig 1a). It occurs in the Archean Rio Maria Granite-Greenstone Terrane, the southern part of the Carajás metallogenic province (DOCEGEO, 1988). This province is limited in the north by the Maroni-Itacaiúnas province (Fig. 1a) that was formed in the 2.2-2.1 Ga Trans-Amazonian event. In the east, it is bordered by the Neoproterozoic Araguaia Belt, which is related to the Brasiliiano (Pan-African) cycle that did not significantly affect the Amazonian craton; to the west, it is limited by the Xingu domain dominated by Proterozoic granitoids and volcanic-pyroclastic assemblages, with ages concentrated around 1.88 Ga (Teixeira et al., 2002; Fig. 1a).

The Carajás province is divided into two tectonic domains, the 3.0-2.86 Ga Rio Maria Granite-Greenstone Terrane (Macambira and Lafon, 1995, Dall'Agnol et al., 2006) and the rift-related Carajás Basin dominantly composed of 2.76-2.55 Ga metavolcanic rocks, banded iron formations, and granitoids (Machado et al., 1991, Macambira and Lafon, 1995, Barros et al., 2001). The Rio Maria Granite-Greenstone Terrane corresponds to an Archean terrane intruded by Paleoproterozoic anorogenic granites (Fig. 1b; Dall'Agnol et al., 1999b, 2005; Rämö et al., 2002). The area is dominated by granitoids and supracrustal greenstone belts with zircon ages of 2.97 to 2.86 Ga (Macambira and Lafon, 1995; Macambira and Lancelot, 1996; Leite et al., 2004) and younger, yet Archean, sedimentary rocks of the Rio Fresco sequence. The greenstone belts (Andorinhas Supergroup) are composed dominantly of komatiites and tholeiitic basalts (Souza and Dall'Agnol, 1995) and four principal groups of Archean granitoids have been distinguished (Althoff et al., 2000; Leite et al., 2004; Dall'Agnol et al., 2006; Oliveira et al., submitted): (1) Granitoids of the older tonalitic-trondhjemite series (TTG) represented by the Arco Verde and Caracol tonalites (2.97 to 2.93 Ga); (2) 2.87 Ga sanukitoid Rio Maria granodiorite and associated intermediate rocks, which had intruded the greenstone sequence; (3) Younger TTG series represented by the Mogno and Água Fria trondhjemites (~2.87 Ga); (4) Potassic leucogranites of calc-alkaline affinity, represented by the Xinguara, Mata Surrão, and Guarantã granites.

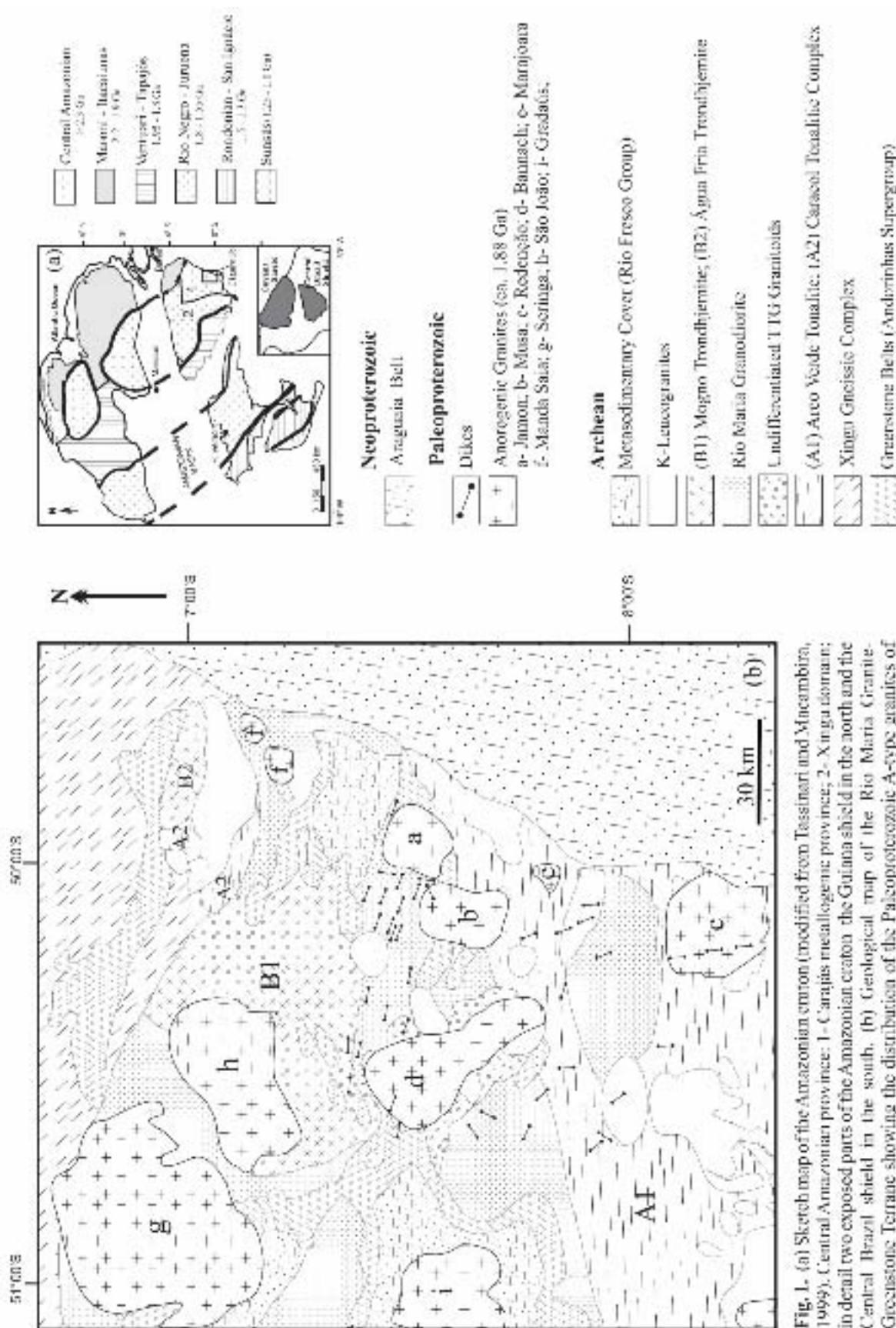


Fig. 1. (a) Sketch map of the Amazonian craton (modified from Tessmann and Micanmbira, 1999); Central Amazonian province: 1- Carajás metallocgenic province; 2- Xingu domain; in detail two exposed parts of the Amazonian craton: the Guiana shield in the north and the Central Brazil shield in the south. (b) Geological map of the Central Brazil Terrane showing the distribution of the Paleoproterozoic A-type granites of the Jamon suite (modified from Almeida, 2005, and references therein).

The eastern part of the Amazonian Craton was stabilized at the end of the Archean and remained stable until 1.88 Ga when generation and emplacement of oxidized A-type granites of the Jamon suite and associated mafic and felsic dikes occurred (Dall'Agnol et al., 1994, 1999b, 2005). In the adjacent provinces, orogenic events are significantly older (the Trans-Amazonian event in the north) or younger (the Brasiliano event in the east) than these granites. Lamarão et al. (2002, 2005) and Dall'Agnol et al. (2005) suggest that the A-type granite magmatism of the Carajás province was related to a continental event marking the beginning of breakup of a Paleoproterozoic continent formed at the end of the Trans-Amazonian orogenic cycle.

The Redençao pluton is an intrusion hosted by the Arco Verde tonalite and potassic leucoxenites (Vale and Neves, 1996; Oliveira, 2001; Oliveira et al., 2005). In addition to the Redençao pluton, the Jamon Suite is formed by the Jamon, Musa, Bannach, Marajoara, Manda Saia, Seringa, São João, and Gradaús plutons (Fig. 1b; Dall'Agnol et al., 2005; Almeida et al., submitted). Nd isotope data for the Jamon Suite show that their  $\epsilon_{\text{Nd}}$  (at 1880 Ma) values are strongly negative ranging generally from -10.5 to -8.1 (mean value -9.4). On the other hand,  $T_{\text{DM}}$  ages are all Archean but show considerable variation (~2.60 to 3.02 Ga; Dall'Agnol et al., 1999b, 2005; Rämö et al., 2002). The Nd evolution lines of Rio Maria Archean granitoids suggest that the Paleoproterozoic A-type granites of the Jamon Suite were derived from relatively deeper parts of the Archean crust.

### 3. The Redençao pluton: general outline

#### 3.1. Field relationships and magmatic evolution

The Redençao and other plutons of the Jamon Suite are generally unfoliated, except for the local development of magmatic foliation at their borders. Deformational structures are restricted to fractures and faults. The intrusion is subcircular and remarkably discordant, cross-cutting the E-W to NW-SE structural trend of the host Archean granitoids (Fig. 2). External contacts are sharp with angular xenoliths of the Arco Verde Tonalite commonly observed near the border of the pluton.

The Redençao pluton comprises several petrographic facies disposed in near-concentric zones (Fig. 2). The less evolved rocks are even-grained, coarse-grained biotite+hornblende monzogranites, locally enriched in cumulitic amphibole±clinopyroxene, which occur in the

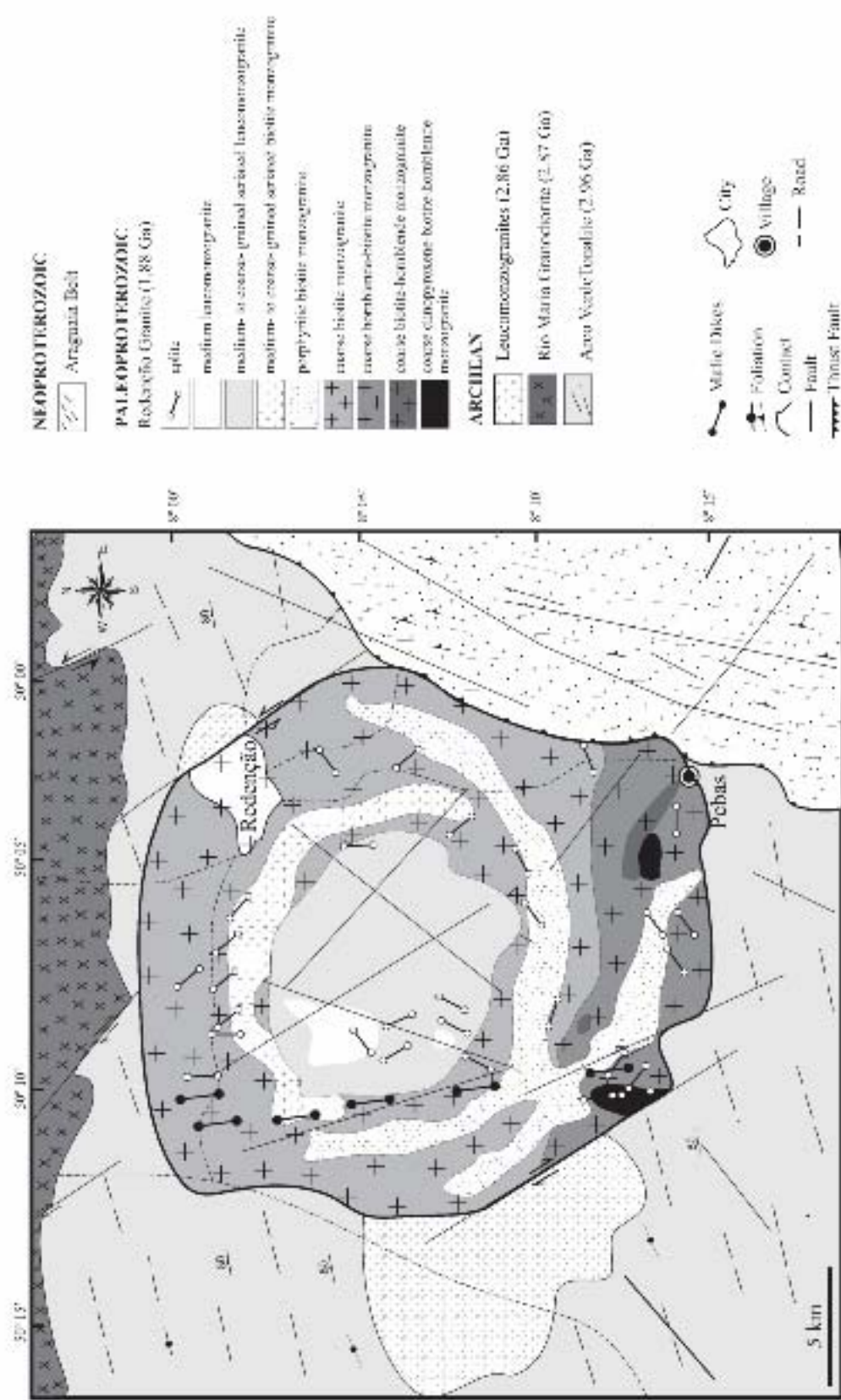


**Fig. 2.** Detailed geological map of the Redenção region showing the areal distribution of granitic facies of the pluton (Oliveira, 2001; Oliveira et al., submitted).

southern part of the pluton. Coarse-grained, (hornblende)-biotite monzogranites are dominant in the northern, eastern, and western borders of the pluton. Coarse- to medium-grained seriated and porphyritic biotite monzogranites configure annular structures in the central and southern areas of the pluton and are intrusive in the coarse-grained biotite monzogranite (Fig. 2). In the central part of the pluton, evolved leucogranites define small circular structures. Aplitic dikes are common and coincide in orientation with the main NE-SW and NW-SE fracturing systems that cross-cut the pluton and its country rocks.

Oliveira (2001) proposed that fractional crystallization, controlled by fractionation of early crystallized phases, including amphibole  $\pm$  clinopyroxene, andesine to calcic oligoclase, ilmenite, magnetite, apatite, and zircon, was the dominant process of magmatic evolution of the Redenção pluton. Nevertheless, magma mingling processes have also influenced its evolution. This is more clearly demonstrated by the relationships between porphyritic biotite granites and leucogranites (Oliveira et al., submitted). However, there is also evidence of interaction between the less evolved, mafic-rich varieties and the comparatively more evolved granites. This indicates the coexistence in a partially molten state of different magmas batches. The leucogranite facies was interpreted as probable late, independent injections of evolved, felsic magmas from a different source (Oliveira, 2001; Oliveira et al., 2005).

A remarkable aspect in all granitic facies is the absence of significant solid state recrystallization. Igneous textures are perfectly preserved, except for local effects of subsolidus alteration processes. The sequence of mineral crystallization has been deduced from clear textural relationships (Oliveira et al., 2002) and, is considered similar to the Jamon monzogranite, for which experimental data show that magnetite is a near liquidus phase (Dall'Agnol et al., 1999c). It registered initially the high temperature evolution of the liquid, but it was also affected by the gradual decrease of temperature and displays textural evidence of re-equilibration, due mostly to oxi-exsolution or to late local oxidation (martitization) processes (Dall'Agnol et al. 1997).

### 3.2. 3-D Geometry

The 3-D shape of the Redenção pluton was estimated by forward modeling of Bouguer gravity anomalies after removal of a regional field (Oliveira et al., submitted). A remarkable feature of the pluton is that it exhibits a lateral extension substantially larger than the vertical one (Fig. 3). According to the density contrast between the granites and their country rocks ( $-0.09 \pm$

0.01 g/cm<sup>3</sup>), a maximum thickness value of ~ 6 km, with a progressive thinning from the center to the borders, is necessary to explain the gravity anomaly.

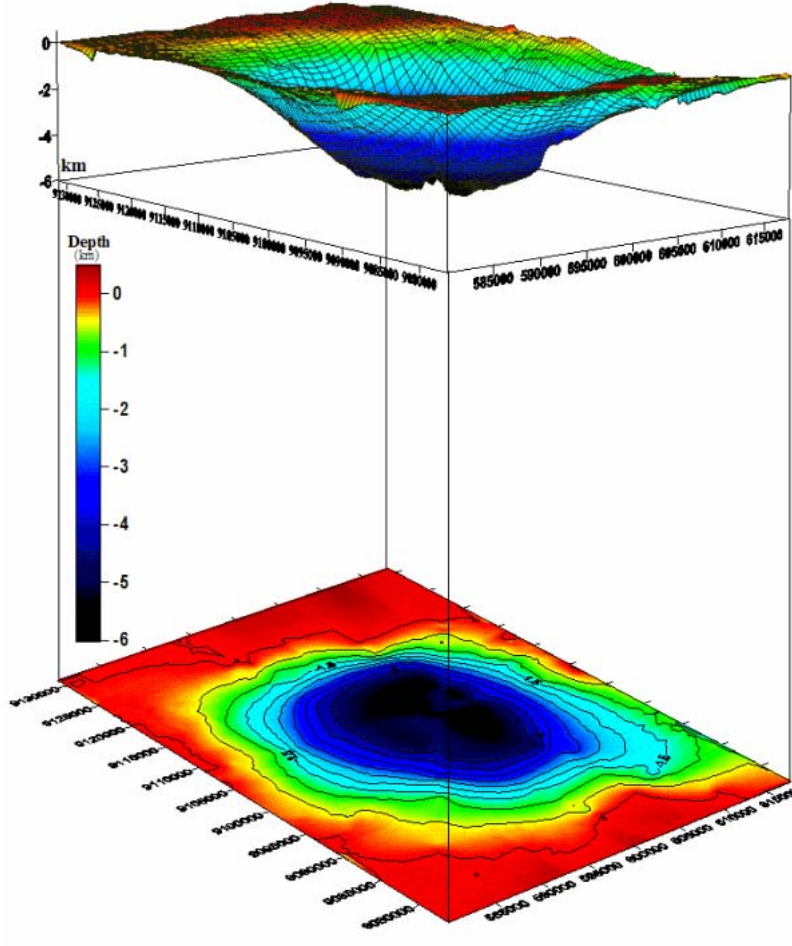


**Fig. 3.** Perspective views of the three-dimensional geometry of the Redenção pluton through gravity data analysis associated with depth maps (in km). View from SW to NE (Oliveira et al., submitted).

#### 4. Anisotropy of magnetic susceptibility study

##### 4.1. Sampling and measurements

Anisotropy of magnetic susceptibility (AMS) is particularly well adapted for the study of granitic rocks, like the Redenção Granite, that show weak mineral shape-preferred orientations implying that the mineral fabric can not be measured by conventional methods. In this work, specimens obtained from 127 distinct stations were studied for their AMS according to the procedure described in Bouchez (1997). At least three oriented cylindrical samples, 7 to 9 cm long and 2.54 cm in diameter, were drilled from each station using a gasoline-powered portable drill with an average spacing between stations of 1-2 km (Fig. 6a). In the laboratory, the samples were cut into specimens of 2.2 cm in height using a diamond-coated wheel saw. Each core

provided two or three specimens yielding a total of 729 specimens, from which the site mean AMS parameters were calculated (Table 1).

The specimens were analyzed using a Kappabridge KLY-3 (AGICO, Brno, Czech Republic) susceptibility meter, whose resolution is better than  $10^{-8}$  SI, at the Laboratório Helmo Rand (Federal University of Pernambuco, Brazil). The ANISOFT package program (Jelínek, 1978; Hrouda et al., 1990) was used to obtain a statistical evaluation of the AMS in individual sites. The magnitudes and orientations of the principal axes of the AMS ellipsoid were determined for each specimen using a sequence of fifteen susceptibility measurements in different orientations. Each station is characterized by the average AMS parameters of a minimum of three specimens, whose representation is an ellipsoid with  $k_1 \geq k_2 \geq k_3$  as principal susceptibilities axes. Table 1 gives averages of the AMS data at each of the 127 stations: vectorial averages of the  $k_1$ ,  $k_2$  and  $k_3$  orientations, and arithmetic average of the magnitude of  $k_1$ ,  $k_2$  and  $k_3$  from which the anisotropy parameters have been derived.

## 4.2. Results

### 4.2.1. Magnetic susceptibility

Available data of magnetic susceptibility ( $K$ ) for the Redenção pluton were acquired using a SI-1 susceptometer (Saphire Instruments; Oliveira et al., 2002). The  $K$  values obtained have a unimodal distribution (Fig. 4), varying between  $1.05 \times 10^{-3}$  SI and  $54.72 \times 10^{-3}$  SI with an average of  $11.55 \times 10^{-3}$  SI. These high values ( $> 10^{-3}$  SI) are typical of magnetite series ferromagnetic granites (Ishihara, 1981; Ferré et al., 2002), in accord with the high abundance of magnetite in these rocks (0.4 to 3.5 % modal content of opaque minerals, dominantly magnetite with subordinate ilmenite and rare sulfides; Oliveira, 2001; Oliveira et al., 2002).

Average  $K$  values decrease from the (clinopyroxene)-biotite-amphibole monzogranites to the biotite monzogranites, attaining the lowest value in the leucogranites. In other words, magnetic susceptibility decreases from the facies with higher modal contents of mafic minerals to the leucogranites.  $K$  increases with increasing opaque, mafic minerals, and amphibole contents and decreasing quartz and K-feldspar contents (Fig. 5). The highest values are concentrated in the southern part of the pluton, decreasing to the NE and mid-central domains, the lowest  $K$  values being found in the center of the intrusion (Fig. 6b; Oliveira et al., 2002). This behavior is

consistent with the pattern of internal zonation of the pluton indicated by petrographic and geochemical data (Oliveira et al., submitted).

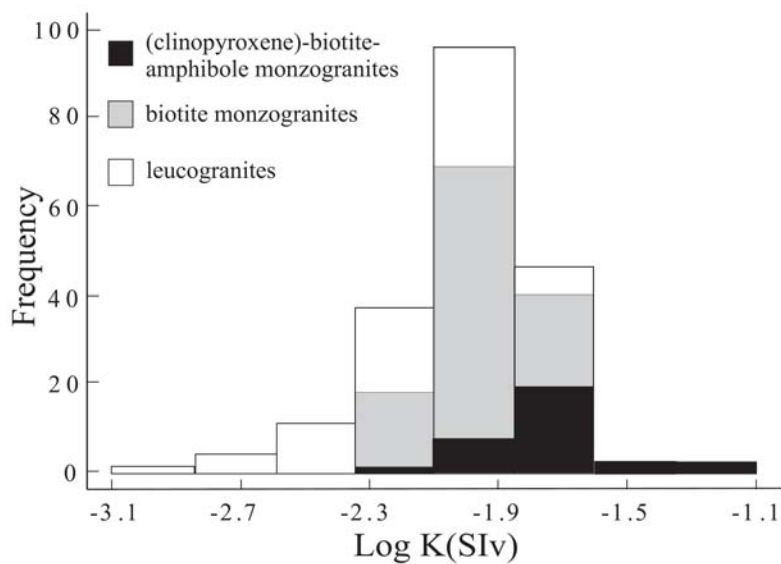


**Fig. 4.** Frequency histogram showing the variation of bulk magnetic susceptibility values ( $K$  in SIv) of the Redenção pluton rock varieties. The bulk susceptibility was measured with the SI-1 and Kappabridge KLY-3 magnetic susceptibilimeters.

The behavior of  $K$  values obtained in the AMS study is quite similar to that in the previous study discussed above. The mean bulk susceptibility,  $K$  [ $(k_1 + k_2 + k_3)/3$ ], from the investigated specimens ranges from  $0.259 \times 10^{-3}$  SI to  $31.995 \times 10^{-3}$  SI with an average value of  $11.274 \times 10^{-3}$  SI (Table 1). The maximum value of  $K$  obtained in the AMS study is slightly lower compared with the previous study. This can be explained by the absence of AMS measurements in rocks with cumulitic features.

$K$  is higher in the hornblende-biotite monzogranite with mean of  $18.477 \times 10^{-3}$  SI and decreases from the coarse-grained biotite monzogranite ( $12.749 \times 10^{-3}$  SI), to the seriated biotite monzogranite ( $12.597 \times 10^{-3}$  SI), to the porphyritic biotite monzogranite ( $9.148 \times 10^{-3}$  SI), and to the leucogranites ( $6.806 \times 10^{-3}$  SI). As the  $K$  value of magnetite is two orders of magnitude higher than that of any ferromagnesian mineral and the contribution of paramagnetic silicates should not exceed  $5 \times 10^{-3}$  SI (Rochette et al., 1992), the  $K$  values reflect essentially variations in the magnetite content of the different granitic facies and indicate that they are ferromagnetic in origin.

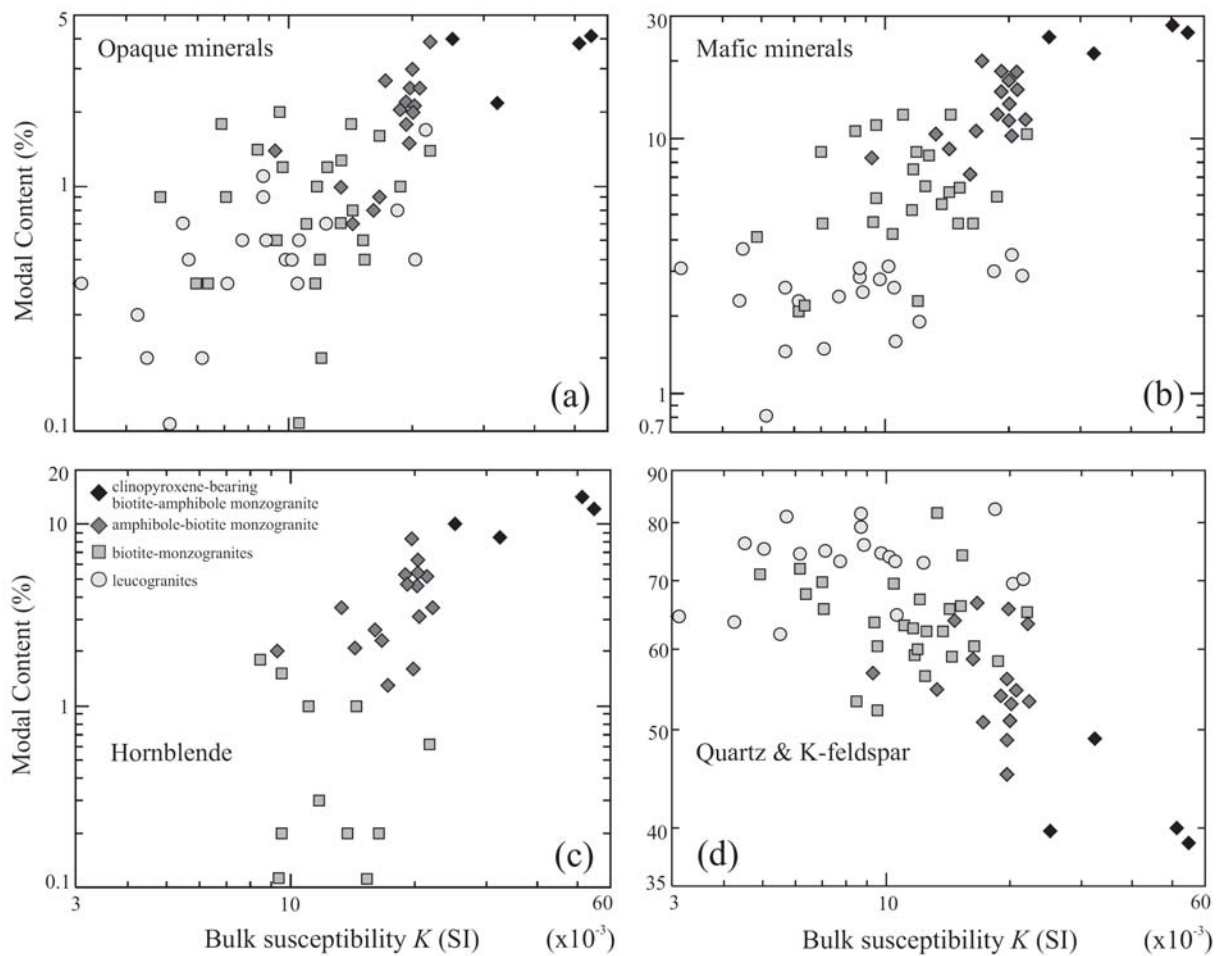


**Fig. 5.** Relationships between magnetic susceptibility ( $K = 10^3$  SI) and modal compositions of the Redenção pluton. (a) opaque minerals, (b) mafic minerals, (c) hornblende, (d) quartz + K-feldspar contents vs.  $K$  (Oliveira et al., 2002).

#### 4.2.2. Shape and anisotropy of AMS ellipsoids

AMS ellipsoids are characterized using the degree of anisotropy,  $P' = k_1/k_3$ , that indicates the intensity of the preferred orientation of magnetic minerals, and a shape factor,  $T = 2\ln(k_2/k_3)/\ln(k_1/k_3) - 1$ , that characterize the shape of the AMS ellipsoid, both introduced by Jelínek (1981). The  $T$  parameter varies from -1 for prolate (perfectly linear magnetic fabric, i.e.  $k_2 = k_3$ ) through 0 (neutral) to +1 for oblate (perfectly planar magnetic fabric, i.e.  $k_1=k_2$ ).  $P'$  varies from 1, corresponding to an isotropic sample (0% anisotropy, sphere) upwards, with values in igneous rocks rarely exceeding 1.3 (~ 30% anisotropy). The variation of both parameters within plutons has been used in previous studies to deduce styles of deformation of the magma during emplacement (e.g. Bouchez et al., 1990; Bouillin et al., 1993; Archanjo et al., 1995; Cruden et al., 1999; Neves et al., 2003; Talbot et al., 2004; Chadima et al., 2006).

**Table1** - Parameters of AMS for individual sampling sites

Site ( <i>n</i> )	Localization		Scalar data		Direction of principal axes						Facies	
	UTM coordinate		$K_m$ ( $10^{-3}$ SI)	<i>P</i> *	<i>T</i>	$K_1$	$\alpha_{95} (k_1)$	$K_2$	$\alpha_{95} (k_2)$	$K_3$	$\alpha_{95} (k_3)$	
Hornblende-biotite monzogranite												
RED09 (7)	595759	9096278	20.1714	1.015	-0.012	212/38	46.3	93/32	41.9	337/36	28.6	HBMzG
RED10 (6)	595316	9094950	25.6712	1.052	0.288	306/1	22.5	59/87	22.2	216/3	23.6	HBMzG
RED12 (6)	598171	9090301	13.0138	1.040	0.365	96/38	38.6	321/42	37.7	207/25	27.3	HBMzG
RED17 (5)	607270	9094443	24.6160	1.023	0.122	91/17	41.9	345/42	62.3	198/43	49.8	HBMzG
RED18 (13)	604802	9092932	21.0952	1.031	-0.389	281/71	24.0	11/0	31.3	101/19	27.1	HBMzG
RED57 (5)	588343	9098352	24.6921	1.075	-0.102	217/21	31.2	317/24	23.9	91/57	31.4	HBMzG
RED59 (5)	589291	9097736	18.6834	1.067	0.136	130/40	34.1	234/17	26.8	342/46	38.0	HBMzG
RED61 (7)	591151	9094722	16.9929	1.060	0.237	140/10	21.7	241/45	31.4	40/43	20.9	HBMzG
RED62 (8)	591945	9093615	13.9163	1.158	0.936	162/17	29.9	253/3	43.7	354/73	6.5	HBMzG
RED63 (6)	592316	9095703	12.2757	1.062	0.007	153/60	23.1	60/1	28.6	330/30	25.0	HBMzG
RED64 (6)	592208	9102490	20.9683	1.020	0.242	336/60	54.5	128/27	44.0	224/12	45.6	HBMzG
RED65 (6)	590824	9099114	31.9950	1.084	0.516	302/15	34.0	210/6	32.5	101/74	16.9	HBMzG
RED74 (7)	593168	9093397	21.3714	1.048	0.003	329/20	29.8	68/23	37.0	201/59	19.2	HBMzG
RED75 (8)	593748	9092659	25.6063	1.047	-0.388	92/36	19.8	275/54	35.2	183/1	37.1	HBMzG
RED78 (7)	597905	9090715	12.2117	1.058	0.509	131/29	43.3	132/29	33.6	344/57	9.6	HBMzG
RED79 (7)	599343	9090712	11.7814	1.025	0.073	239/26	30.6	120/46	31.6	348/33	48.1	HBMzG
RED82 (7)	603294	9092454	18.4900	1.031	-0.327	282/25	12.7	185/15	18.4	67/61	16.9	HBMzG
RED83 (4)	605929	9093768	10.9525	1.024	-0.361	45/12	10.5	203/77	54.1	314/5	10.7	HBMzG
RED87 (6)	599584	9116264	17.1118	1.048	0.252	76/57	29.9	261/33	35.6	170/2	34.8	HBMzG
RED101 (7)	604119	9091684	9.9770	1.017	0.852	107/5	45.9	198/4	34.1	325/84	37.1	HBMzG
RED104 (6)	607484	9091338	18.0250	1.040	0.244	68/22	24.3	240/67	33.6	337/3	19.4	HBMzG
RED106 (4)	607832	9095882	19.5400	1.051	0.251	48/51	16.1	262/34	12.1	160/17	12.2	HBMzG
RED108 (5)	609090	9097384	20.5314	1.045	-0.128	228/22	31.0	355/56	35.4	127/24	43.1	HBMzG
RED121 (8)	604126	9094847	14.8729	1.031	-0.632	64/35	22.6	322/16	38.4	212/51	39.3	HBMzG
RED125 (4)	599470	9092770	17.3550	1.038	-0.329	269/18	21.4	167/34	6.1	22/51	29.8	HBMzG
Coarse biotite-monzogranite												
RED02 (2)	593510	9109399	7.4405	1.04	0.500	130/10	49.6	45/80	47.4	220/35	46.1	cBmzG
RED20 (4)	590221	9111872	7.5370	1.046	0.142	52/35	68.5	241/54	62.6	145/4	66.8	cBmzG
RED21 (4)	592987	9112235	7.5595	1.029	0.408	251/71	62.3	71/19	38.6	161/0	51.1	cBmzG
RED23 (9)	603880	9107562	16.0512	1.027	-0.672	91/43	24.7	268/47	35.3	360/1	31.9	cBmzG
RED37 (7)	590998	9109463	13.8270	1.041	-0.755	55/37	44.8	161/21	-	274/46	43.4	cBmzG
RED38 (4)	591084	9106454	13.5213	1.045	0.147	34/71	46.7	242/17	24.2	149/8	23.8	cBmzG
RED39 (4)	591632	9105163	6.8985	1.041	0.248	9/49	79.0	136/28	59.9	242/28	47.0	cBmzG
RED40 (3)	593662	9109949	4.3067	1.026	0.019	52/32	45.9	175/41	91.6	299/32	77.0	cBmzG
RED41 (5)	593653	9105619	9.5450	1.034	0.814	54/16	55.5	299/56	27.7	153/29	23.4	cBmzG
RED42 (3)	593068	9103870	22.6993	1.061	0.230	112/30	77.1	231/40	31.3	358/35	28.9	cBmzG
RED43 (6)	592788	9101936	7.3750	1.035	-0.854	134/3	19.0	43/24	35.0	231/65	29.1	cBmzG
RED44 (5)	595080	9100150	10.7178	1.033	0.593	280/41	57.2	51/37	36.7	163/27	16.7	cBmzG
RED45 (5)	600221	9113528	8.5396	1.040	-0.559	88/4	18.8	357/18	22.7	192/71	49.3	cBmzG
RED46 (5)	599912	9112393	12.6026	1.040	-0.478	106/10	31.8	198/13	54.4	340/73	53.7	cBmzG
RED47 (6)	593606	9112314	10.5933	1.027	-0.020	77/18	39.8	334/34	42.1	191/50	37.1	cBmzG
RED48 (7)	592720	9113268	8.9249	1.018	0.726	342/43	38.2	227/24	33.0	117/37	38.5	cBmzG
RED49 (5)	592663	9114344	6.5532	1.035	-0.722	215/85	35.5	28/5	34.9	118/1	40.6	cBmzG
RED50 (5)	604752	9113795	5.9632	1.050	-0.067	266/12	23.8	163/47	39.1	6/40	35.3	cBmzG
RED51 (5)	603897	9114964	10.2834	1.074	0.638	311/7	60.1	188/77	45.1	42/11	46.6	cBmzG

(continued on next page)

**Table 1 (continued)**

Site ( <i>n</i> )	Localization		Scalar data			Direction of principal axes						Facies
	UTM coordinate		<i>K<sub>m</sub></i> (10 <sup>-3</sup> SI)	<i>P</i> *	<i>T</i>	<i>K<sub>1</sub></i>	$\alpha_{95}(k_1)$	<i>K<sub>2</sub></i>	$\alpha_{95}(k_2)$	<i>K<sub>3</sub></i>	$\alpha_{95}(k_3)$	
<i>Coarse biotite-monzogranite (continued)</i>												
RED52 (5)	604750	9112904	14.1998	1.041	0.427	197/33	35.7	290/6	55.6	29/56	36.4	cBMzG
RED53 (6)	587407	9104711	10.1330	1.096	0.592	95/18	30.6	355/27	36.8	215/56	12.8	cBMzG
RED54 (5)	588753	9104309	17.6500	1.042	0.675	204/43	41.7	79/31	68.8	328/31	23.6	cBMzG
RED56 (6)	587584	9101025	8.8926	1.051	-0.240	81/45	19.0	324/25	25.6	215/35	27.0	cBMzG
RED66 (5)	591042	9100926	10.3936	1.075	-0.463	336/8	16.1	74/44	34.5	238/45	27.9	cBMzG
RED70 (6)	593180	9099017	6.5185	1.087	0.605	1/20	33.3	270/1	27.8	178/70	13.4	cBMzG
RED84 (7)	604045	9112476	13.4193	1.054	-0.450	128/32	23.5	316/58	40.0	220/3	46.9	cBMzG
RED85 (5)	603224	9114873	11.2368	1.038	-0.801	138/58	34.5	316/32	34.0	46/1	-	cBMzG
RED86 (4)	600958	9114939	13.8488	1.072	0.360	144/51	47.3	235/0	77.2	325/39	57.2	cBMzG
RED88 (6)	597429	9110740	12.1555	1.039	0.561	292/12	32.0	28/25	32.1	179/62	28.2	cBMzG
RED93 (4)	609672	9110036	7.1808	1.006	-0.013	157/64	65.3	252/3	46.7	30/20	84.8	cBMzG
RED94 (6)	609455	9109054	11.2325	1.049	0.001	169/23	48.3	281/42	48.7	59/39	30.0	cBMzG
RED95 (6)	609906	9105644	8.3802	1.042	0.188	350/21	21.1	91/26	36.5	226/56	23.9	cBMzG
RED96 (6)	610729	9104321	7.4378	1.034	0.278	151/76	40.4	327/14	-	58/1	38.0	cBMzG
RED97 (6)	612626	9102788	6.7368	1.042	0.265	334/62	33.1	176/27	39.7	81/9	20.5	cBMzG
RED99 (6)	601533	9111867	11.2863	1.034	-0.679	107/20	20.0	209/30	46.0	348/53	55.9	cBMzG
RED107 (5)	608019	9097633	13.3800	1.016	-0.898	358/20	11.6	243/49	37.4	102/34	61.8	cBMzG
RED109 (5)	606244	9110198	17.8220	1.041	-0.184	108/70	31.8	342/12	46.6	248/16	44.0	cBMzG
RED110 (3)	604167	9099024	8.4527	1.052	0.472	63/14	79.0	321/39	81.4	168/48	48.3	cBMzG
RED113 (4)	591003	9112289	6.7958	1.056	0.522	20/3	56.9	120/76	67.2	289/14	27.9	cBMzG
RED114 (5)	593726	9111270	12.5862	1.045	-0.036	332/60	36.0	153/30	42.7	63/0	60.4	cBMzG
RED115 (4)	597461	9111661	16.7475	1.044	0.244	269/59	43.4	33/18	58.5	131/24	43.2	cBMzG
RED116 (3)	596030	9115073	18.6367	1.099	0.464	84/20	57.3	229/67	84.6	349/12	35.5	cBMzG
RED117 (4)	597221	9113596	12.7338	1.042	0.243	86/22	76.1	182/15	76.7	304/63	46.3	cBMzG
RED119 (4)	603308	9098227	13.9255	1.027	-0.320	25/35	42.6	120/6	19.8	219/55	61.7	cBMzG
RED122 (6)	601953	9094607	8.1902	1.057	0.316	240/12	15.3	332/11	17.0	103/74	12.4	cBMzG
<i>Seriated biotite-monzogranite</i>												
RED01 (4)	600338	9111648	16.265	1.060	0.450	234/71	22.6	112/11	25.4	18/16	14.6	sBMzG
RED03 (9)	593776	9108210	15.5266	1.05	0.561	87/13	27.9	283/76	30.7	178/4	10.0	sBMzG
RED16 (6)	606824	9100843	10.7938	1.062	-0.082	294/67	42.0	132/22	37.0	40/7	54.0	sBMzG
RED22 (7)	602538	9109347	12.1819	1.033	-0.236	141/71	23.2	2/15	27.2	269/12	32.1	sBMzG
RED92 (6)	597483	9105138	13.2740	1.066	0.621	325/24	28.4	201/52	37.8	68/28	16.0	sBMzG
RED100 (6)	599238	9111995	12.0808	1.055	0.431	308/13	16.1	57/54	27.4	210/33	17.9	sBMzG
RED118 (5)	598442	9111997	13.8220	1.039	0.117	321/18	18.0	57/17	19.5	187/64	17.1	sBMzG
RED127 (5)	605929	9108562	6.8290	1.050	0.299	170/58	26.4	4/31	27.1	270/6	8.4	sBMzG
<i>Porphyritic biotite-monzogranite</i>												
RED11 (5)	598428	9091151	5.7602	1.015	0.586	279/79	64.9	88/11	32.6	179/2	44.0	pBMzG
RED13 (5)	595629	9097778	12.6730	1.043	-0.433	345/52	46.4	141/36	44.6	239/12	42.2	pBMzG
RED15 (7)	608122	9102546	7.0980	1.053	0.969	172/41	42.2	333/48	22.4	74/10	11.1	pBMzG
RED55 (4)	588873	9103080	6.4023	1.218	-0.305	223/35	58.1	121/16	40.2	12/50	33.3	pBMzG
RED58 (8)	588957	9098934	9.8378	1.056	-0.172	165/15	38.3	261/24	38.2	46/61	28.0	pBMzG
RED58I (3)	588475	9098694	8.0870	1.080	0.223	313/7	50.3	50/44	84.2	216/45	36.0	pBMzG
RED60 (7)	590144	9096076	8.6120	1.070	0.484	339/15	39.0	85/46	36.4	235/40	13.5	pBMzG
RED71 (6)	592747	9096899	14.0567	1.080	0.492	182/40	40.3	79/15	47.1	332/46	18.2	pBMzG
RED72 (9)	594709	9098431	10.0334	1.046	0.651	202/7	26.3	293/9	28.9	78/79	15.4	pBMzG
RED76 (9)	594511	9091890	7.3061	1.042	-0.965	133/9	11.1	41/15	35.5	253/73	34.3	pBMzG

(continued on next page)

**Table 1 (continued)**

Site ( <i>n</i> )	Localization UTM Coordinate	Scalar data			Direction of principal axes						Facies	
		$K_m$ (SI)	$P'$	$T$	$K_1$	$\alpha_{95} (k_1)$	$K_2$	$\alpha_{95} (k_2)$	$K_3$	$\alpha_{95} (k_3)$		
<i>Porphyritic biotite-monzogranite (continued)</i>												
RED77 (6)	596161 9090873	3.4882	1.060	-0.130	233/70	18.1	84/17	23.7	351/9	21.7	pBMzG	
RED80 (5)	600813 9091016	9.7062	1.044	0.492	48/21	42.0	313/14	41.2	191/64	30.6	pBMzG	
RED81 (6)	602222 9091719	11.1320	1.036	0.159	185/56	26.3	287/8	26.3	22/32	18.0	pBMzG	
RED98 (4)	611743 9105762	8.7770	1.030	0.453	303/20	-	41/19	75.0	170/61	67.0	pBMzG	
RED102 (5)	607460 9094010	7.7636	1.028	-0.031	155/63	34.1	53/6	55.4	320/26	42.2	pBMzG	
RED103 (6)	608406 9093025	7.4595	1.055	-0.086	60/8	8.3	169/66	14.6	327/23	12.3	pBMzG	
RED105 (5)	605863 9091741	11.9600	1.046	-0.576	99/28	23.2	262/60	50.8	5/7	64.1	pBMzG	
RED120 (6)	604834 9096412	8.9795	1.030	-0.519	182/43	30.3	1/47	-	91/1	55.4	pBMzG	
RED123 (4)	598496 9095075	8.7325	1.069	0.770	212/47	42.4	83/31	50.3	335/28	12.0	pBMzG	
RED124 (3)	597672 9096152	11.9597	1.072	0.321	164/48	47.1	331/42	44.2	67/6	37.6	pBMzG	
RED126 (4)	596715 9092100	12.2828	1.060	0.470	257/27	38.3	164/5	39.9	64/62	8.3	pBMzG	
<i>Leucogranites</i>												
RED04 (6)	593797 9106352	2.4145	1.014	0.770	50/33	53.8	150/16	44.2	262/52	29.6	sLMzG	
RED05 (6)	594289 9106216	0.9573	1.023	0.679	172/0	43.4	263/73	55.5	81/17	30.0	sLMzG	
RED06 (5)	594459 9106478	5.5662	1.043	-0.626	354/10	25.4	237/70	51.8	87/18	44.6	sLMzG	
RED07 (4)	595682 9105178	12.5757	1.034	-0.120	354/24	44.7	233/50	60.1	99/30	44.3	sLMzG	
RED08 (3)	595410 9104675	0.2599	1.024	-0.324	223/11	30.3	115/60	16.4	319/28	27.3	sLMzG	
RED14 (8)	606351 9106276	0.8670	1.077	0.012	302/5	14.0	36/40	20.2	206/50	18.8	sLMzG	
RED19 (5)	601389 9098025	11.2738	1.020	0.009	124/32	44.0	352/47	49.2	231/26	47.3	sLMzG	
RED24 (13)	603542 9106580	10.7110	1.027	-0.029	326/68	29.2	158/8	27.9	250/18	26.1	sLMzG	
RED25 (4)	603475 9104369	4.7337	1.057	0.160	325/26	62.2	110/60	44.2	227/15	29.0	sLMzG	
RED26 (5)	603167 9103479	8.5454	1.030	0.471	10/4	48.2	275/48	57.0	104/41	41.1	sLMzG	
RED27 (6)	602860 9102927	5.3848	1.026	-0.113	333/17	29.0	102/64	52.7	237/19	47.3	sLMzG	
RED28 (8)	601910 9102684	11.4721	1.039	-0.047	17/30	28.8	249/47	25.0	125/28	20.2	sLMzG	
RED29 (8)	601602 9101579	9.2970	1.030	-0.440	96/48	21.4	240/37	40.9	344/18	44.5	sLMzG	
RED30 (8)	601570 9100903	7.2033	1.044	0.407	290/71	32.7	183/6	44.0	91/18	31.6	sLMzG	
RED31 (9)	601230 9099798	4.6624	1.032	-0.311	53/62	27.8	144/0	-	234/28	37.8	sLMzG	
RED32 (4)	600498 9100537	2.6353	1.027	-0.422	322/47	30.3	88/28	69.6	195/29	67.8	sLMzG	
RED33 (8)	599215 9101830	0.7879	1.027	0.641	274/9	38.9	176/39	33.3	15/49	15.4	sLMzG	
RED34 (5)	598600 9102154	10.3438	1.029	-0.221	18/46	43.3	122/12	44.1	223/41	52.2	sLMzG	
RED35 (5)	601390 9102654	10.7504	1.040	-0.201	248/39	29.5	51/49	32.8	151/8	16.3	sLMzG	
RED36 (6)	600565 9103147	4.461	1.059	0.449	324/26	22.6	106/59	32.0	226/17	13.9	sLMzG	
RED67 (6)	597198 9103308	6.7367	1.030	0.314	156/6	17.5	252/51	25.6	61/39	8.0	sLMzG	
RED68 (4)	596920 9101866	0.5188	1.050	0.542	141/19	21.1	26/50	47.1	244/33	6.5	sLMzG	
RED69 (5)	596367 9100792	15.2424	1.036	-0.928	123/43	31.6	328/44	57.2	225/13	57.1	sLMzG	
RED73 (6)	592618 9093736	4.8093	1.070	0.205	299/34	13.9	201/12	15.5	95/53	9.8	sLMzG	
RED89 (6)	597334 9109327	6.4000	1.049	0.056	274/39	29.9	167/19	30.2	57/44	20.1	sLMzG	
RED90 (4)	597483 9107638	0.4577	1.033	0.699	152/22	30.7	16/61	34.5	250/18	11.8	sLMzG	
RED91 (6)	597483 9106138	8.3542	1.043	0.232	172/61	31.9	271/5	34.0	41/28	29.4	sLMzG	
RED111 (5)	602439 9106429	17.0256	1.072	0.189	286/72	28.9	116/18	27.6	25/3	26.2	sLMzG	
RED112 (7)	600819 9107262	12.9181	1.047	-0.325	255/36	23.9	119/45	39.5	3/23	24.2	sLMzG	

The site name; numbers of specimens measured (*n*); longitude, latitude - UTM;  $K_m$  = mean magnetic susceptibility ( $10^{-3}$ ) of the stations in SI unit;  $K_1$  = trend and plunge of the magnetic lineation (in degrees);  $K_3$  = trend and plunge of the pole of the magnetic foliation;  $P'$  = total anisotropy of the magnetic susceptibility;  $T$  = Jelinek's (1981) AMS ellipsoid shape parameter; the parameter values represent arithmetical means of  $K_m = (k_1+k_2+k_3)/3$ ,  $P = k_1/k_3$ ,  $T = 2 \ln(k_3/k_1)/\ln(k_1/k_3)-1$ ;  $e_1$ ,  $e_2$  and  $e_3$  are the semi-angle (measured in degrees) of the 95 per cent confidence ellipse of AMS axes; facies abbreviations: B - biotite; H - hornblende; MzG - monzogranite; L - leuco; C - coarse, even-grained; s - medium- to coarse- grained seriated; p - porphyritic; e - medium-, even-grained.

The anisotropy degree in the Redenção pluton varies from 1.016 to 1.46, but it is low (less than 1.2) in most samples (Table 1; Fig. 6c and Fig. 7a, b). It is less than 1.10 in 75% of specimens and in 98% of stations, suggesting that deformation in the solid state is not important, since high  $P'$  values are generally acquired during later solid-state deformation (Hrouda, 1982). This is consistent with petrographic observations showing a lack of intracrystalline deformation features in the constituent minerals of the different petrographic facies.  $P'$  does not show clear correlation with petrographic domains. Sites with  $P' > 1.10$  are found locally in the southwestern border. Moderate values,  $1.05 < P' < 1.10$ , are located along the western border and locally in the northern, mid-central and southeastern domains (Fig. 6c). The spatial variation is poorly coincident with that shown by  $K$ , and lack of correlation of  $P'$  and  $K$  is also evident on a  $P'$  versus  $K$  plot (Fig. 7a), contrary to what is commonly observed in ferromagnetic granites (Archanjo et al., 1994; Bouchez, 1997). However, a slightly positive correlation is observed up to a sudden increase of  $P'$  occurs at ‘ferromagnetic’ values of  $K$  ( $\sim 10^{-2}$  SI). The nonlinear dependence between these parameters is typical of magnetite bearing igneous rocks (Rochette et al., 1992; Borradaile and Henry, 1997), indicating that AMS fabric strength is independent of composition in these rocks. Except for those specimens with lowest  $K$  ( $< 5 \times 10^{-4}$  SI), our data fall outside the domain of paramagnetic granitoids (Fig. 7a).

The shape of the AMS ellipsoids varies widely within the pluton, with oblate ellipsoid ( $T > 0$ ) being slightly more abundant than prolate ones (Figs. 6d and 7b, c). The site mean shape parameter ranges from -0.965 to 0.969 and displays a fairly neutral magnetic ellipsoid on average with a mean  $T$  of 0.09 (Table 1; Fig. 8b, c). The  $T - P'$  plot (Fig. 7b) illustrates the symmetrical disposition of the specimens on both sides of the  $T = 0$  line. Therefore, there is no obvious correlation among  $T$ ,  $P'$  and  $K$  in the pluton (Fig. 6b, c, d and 7a, b, c).

#### 4.2.3. Magnetic fabric

The magnetic lineation (parallel to  $k_1$ ) and foliation (normal to  $k_3$ ) for each station were acquired from the average of  $k_1$  and  $k_3$  orientations of individual specimens, respectively. The precision of the magnetic fabric data is given by the opening angle of the confidence cone at 95% about  $k_1$  and  $k_3$  ( $\alpha_{95}$ ; Table 1). Directional data are considered well defined if  $\alpha_{95} < 25^\circ$  and poorly defined if  $\alpha_{95} > 30^\circ$ . Within-station variability,  $\alpha k_1$  and  $\alpha k_3$ , is usually fairly large (Fig. 8) with  $\alpha k_1$  and  $\alpha k_3$  varying jointly:  $< 30^\circ$  in 45% of the stations, between  $30^\circ$  and  $50^\circ$  in 40% of the

stations, and above 50° in the remainder 15%. The average within-station variability is 35° for  $k_1$  and 32° for  $k_3$ . For  $\alpha_{95} > 30^\circ$  the data were utilized if the directional AMS parameters of the nearest sites are coherent; otherwise the data was discarded. A positive correlation exists between measurement error (instrumental error, holder and operator errors, and the errors due to the irregular shape of the specimen) and  $\alpha k_1$  (within-site variability). Repeated measurements on specimens with large measurement errors displayed the same orientation of the principal AMS axes. This indicates that the  $\alpha k_1$  error is primarily due to measurement errors and not to the heterogeneous distribution of the magnetic grains.

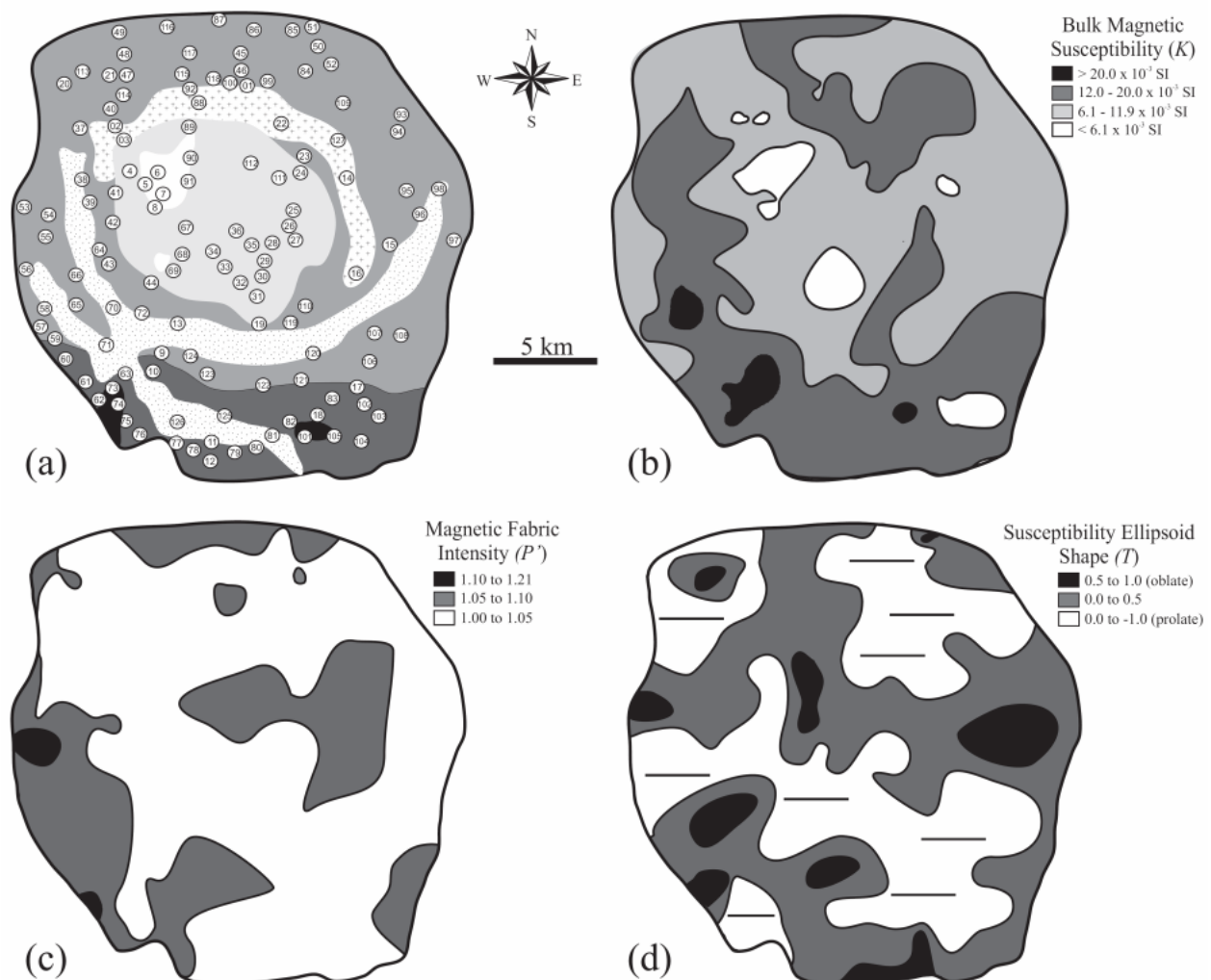


**Fig. 6.** (a) Sample sites in the Redenção Pluton. (b) Variation of bulk magnetic susceptibility values ( $K$  SI) in the pluton. (c) Variation in the magnetic fabric intensity ( $P'$ ) in the pluton. (d) Variation of magnetic susceptibility shape factor ( $T$  values).  $T = 1$ ,  $T = 0$ , and  $T = -1$  represent a perfectly oblate, neutral, and prolate ellipsoids, respectively (Jelinek, 1981). All scalar parameters contoured by hand, based on analyses at all 127 AMS sites in the pluton.

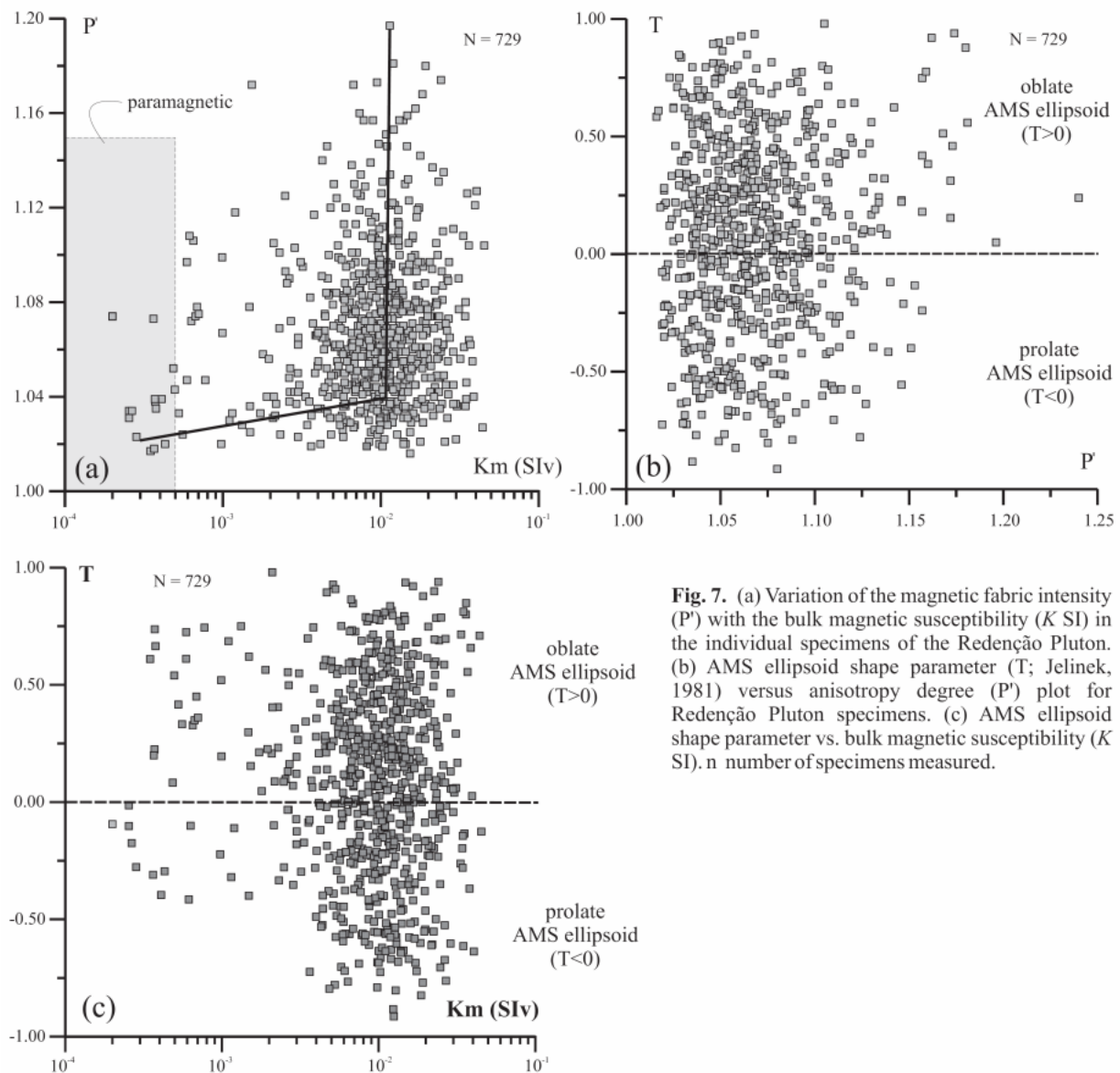


**Fig. 7.** (a) Variation of the magnetic fabric intensity ( $P'$ ) with the bulk magnetic susceptibility ( $K_m$  SI) in the individual specimens of the Redenção Pluton. (b) AMS ellipsoid shape parameter ( $T$ ; Jelinek, 1981) versus anisotropy degree ( $P'$ ) plot for Redenção Pluton specimens. (c) AMS ellipsoid shape parameter vs. bulk magnetic susceptibility ( $K_m$  SI). n = number of specimens measured.

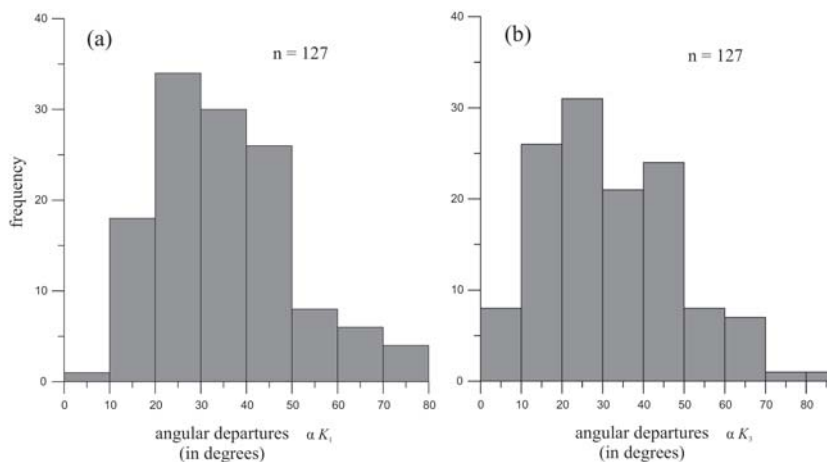


**Fig. 8.** Principal AMS axes angular departure from the mean (in degrees). (a)  $\alpha K_1$  and (b)  $\alpha K_3$  for each station are respectively the average angular departure between  $K_1$  and  $K_3$  of the specimens and the vectorial mean of the station specimens. Stations display large variability of  $K_1$  and  $K_3$ . n = number of stations.

Most sites fall into one of three categories that are a function of the shape of the mean AMS ellipsoid (Fig. 9). Sites with oblate ellipsoids have well-clustered magnetic foliations ( $k_3$ ) and a smearing of  $k_1$  and  $k_2$  directions within the foliation plane. Those with prolate ellipsoids show well-defined magnetic lineations ( $v k_1$ ) and a wide scatter of  $k_2$  and  $k_3$  directions within the plane normal to  $k_1$ . Mean principal susceptibility directions tend to be well defined in sites with neutral AMS ellipsoids, provided  $P'$  is sufficiently high (Fig. 9).

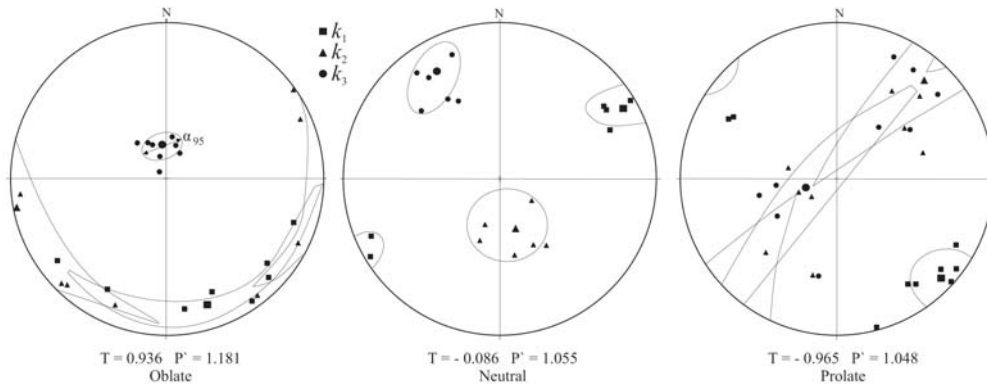


**Fig. 9.** AMS directional data types showing examples of an oblate fabric (RED 62,  $T = 0.936$ ), neutral fabric (RED 103,  $T = 0.086$ ), and prolate fabric (RED 76,  $T = 0.965$ ). The 95% confidence ellipses around each site mean principal direction (large symbol) are described by maximum  $\alpha_{95}$  angle.

The orientation of magnetic foliations and lineations in the Redenção pluton are shown in Figures 10 and 11. Magnetic foliations have generally moderate to steep dips ( $> 60^\circ$  to subvertical) and magnetic lineations plunge gently to moderately (usually  $< 60^\circ$ ). The foliation and lineation trajectories are curvilinear (Fig. 12 a, b), and show a general concentric arrangement, with inward dips of the magnetic foliation. Near the margins, they follow the shape of the pluton. In the coarse biotite monzogranite facies, strikes of magnetic foliation and lineation are systematically parallel to the contact of the pluton with the country rocks and the other facies. Along the contact between the (later emplaced) porphyritic biotite monzogranite and the coarse amphibole-biotite monzogranite at the southwestern part of the pluton the foliation and lineation trends perfectly follow the trace of the contact. The same is observed in the contact between coarse biotite monzogranite and the seriated biotite monzogranite at the northern of the pluton. The foliation dip is predominantly steep in the central part of the pluton and decreases to moderate in the south-western border, where magnetic lineations dip gently (commonly  $< 30^\circ$ ), almost sub-horizontal. In the central leucogranites, the magnetic fabric is apparently near concentrically disposed. This pattern is generally parallel to the lithological zoning.

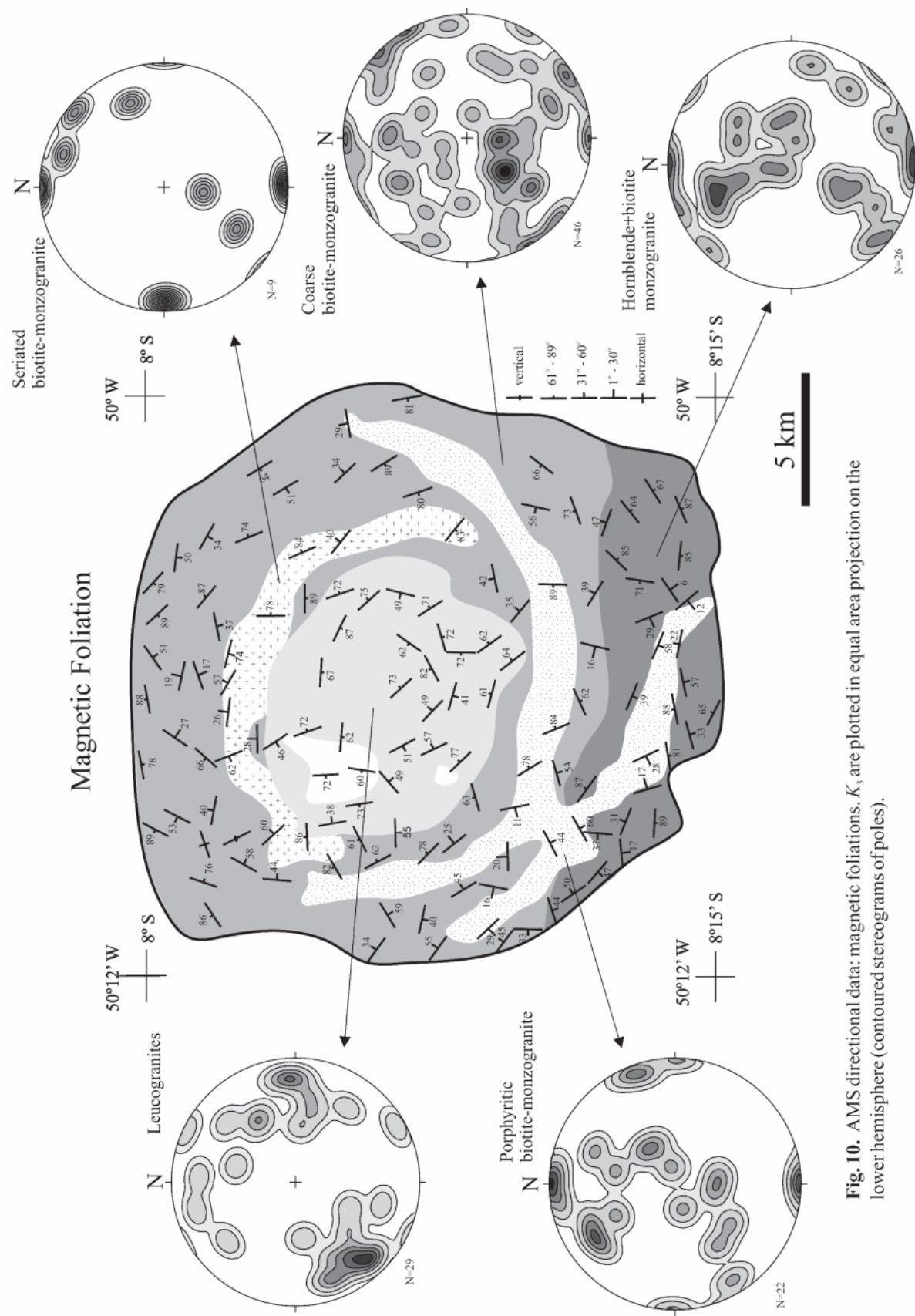
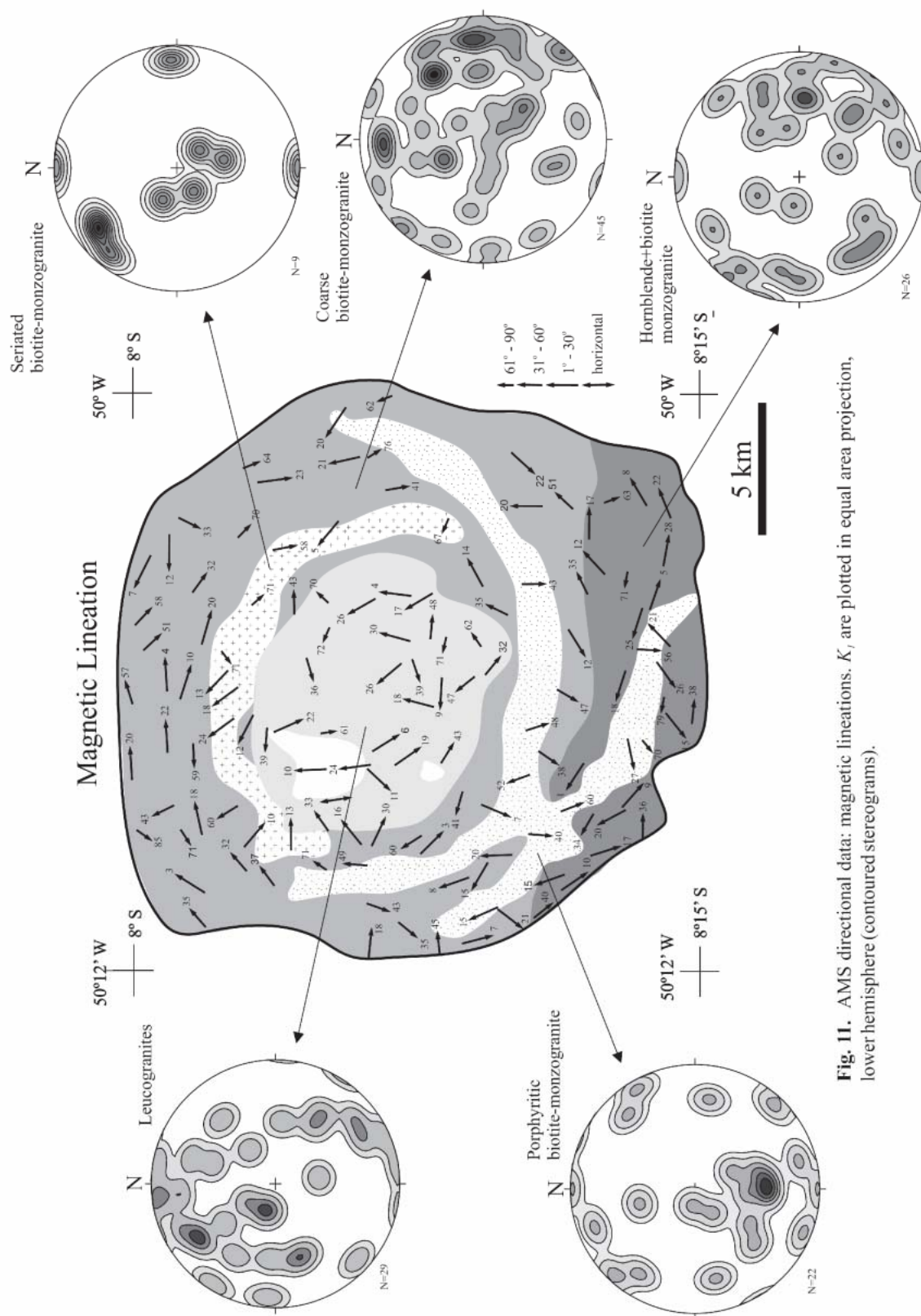
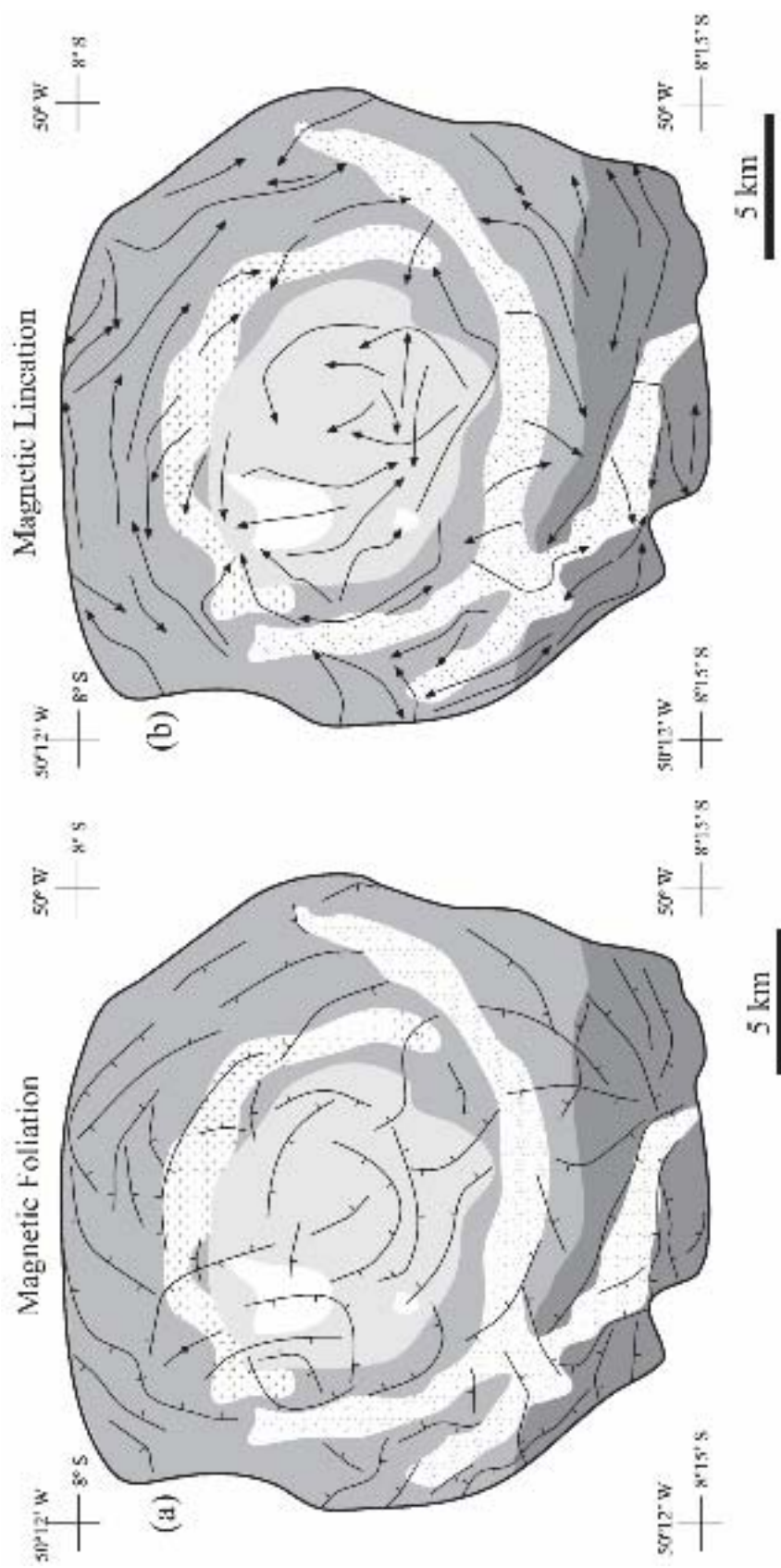


Fig. 10. AMS directional data: magnetic foliations,  $K_3$ , are plotted in equal area projection on the lower hemisphere (contoured stereograms of poles).



**Fig. 11.** AMS directional data: magnetic lineations.  $K_i$  are plotted in equal area projection, lower hemisphere (contoured stereograms).



**Fig. 12.** Magnetic fabric trajectories constructed manually from the data in Figures 10 and 11. (a) magnetic foliations and (b) magnetic lineations trajectories.

## 5. Discussion

### 5.1. Regional context of pluton emplacement

A-type, rapakivi granites have been described from many old cratonic blocks, especially in North America, Baltica and Amazonia (Rämö and Haapala, 1995). With their worldwide distribution, distinct silicic-mafic magmatic association, and emplacement history, this magmatism appears to be a very specific, world-scale event. The A-type magmatism shows a pronounced occurrence in the Paleo- and Mesoproterozoic (commonly from 1.88 to 1.3 Ga), several hundred Ma after the orogenic peak that gave place to the amalgamation of a proposed supercontinent formed at the late Paleoproterozoic or early Mesoproterozoic (Hofmann, 1989; Windley, 1993, 1995; Brito Neves, 1999; Frost et al., 1999; Condie, 2002; Lamarão et al., 2002, 2005; Rogers and Santosh, 2002; Zhao et al., 2002, 2004; Dall'Agnol et al., 2005; Vigneresse, 2005). For this reason, the origin of rapakivi granites and associated rocks is generally considered typical of ‘anorogenic’ settings. They are not associated with major episodes of large-scale deformation related to local plate convergence. However, they could represent the response in stabilized areas to distal orogenic events (cf. Nyman et al., 1994; Nyman and Karlstrom, 1997; Åhäll et al., 2000; Zhao et al., 2004).

In the Carajás province, A-type plutons postdate their Archean country rocks by ca. one billion years (Macambira and Lafon, 1995; Rämö et al., 2002; Dall'Agnol et al., 2005). Moreover, the emplacement of the Jamon suite granites took place ~ 150 Ma after the last major Paleoproterozoic Trans-Amazonian compressional event recorded in the Maroni-Itacaiúnas province (Fig. 1; Delor et al., 2003; Rosa-Costa, 2006). It is clear that the Carajás province was an extremely stable domain of the craton at 1.88 Ga. The emplacement of the Jamon suite granites of the Carajás province is admitted to be linked to asthenospheric upwelling and magma production in the mantle, followed by partial melting of the lower continental crust provoked by heat provided by underplating of mantle magmas (Dall'Agnol et al., 2005). The resulting anatetic liquids ascended in the crust and were emplaced as high-level granite complexes. In this model, extension is proposed to be associated with mantle upwelling. The occurrence of diabase dike swarms coeval with the Jamon suite (Fig. 13) have WNW-ESE to NNW-SSE trends, suggesting extension oriented approximately along the NNE-SSW to ENE-WSW direction. The 1.88 Ga A-type granite plutons and stocks of Carajás province are also disposed along a belt that follows the

general trend defined by the dikes (Fig. 1b), suggesting that their emplacement may have been controlled by NE-SW extension.

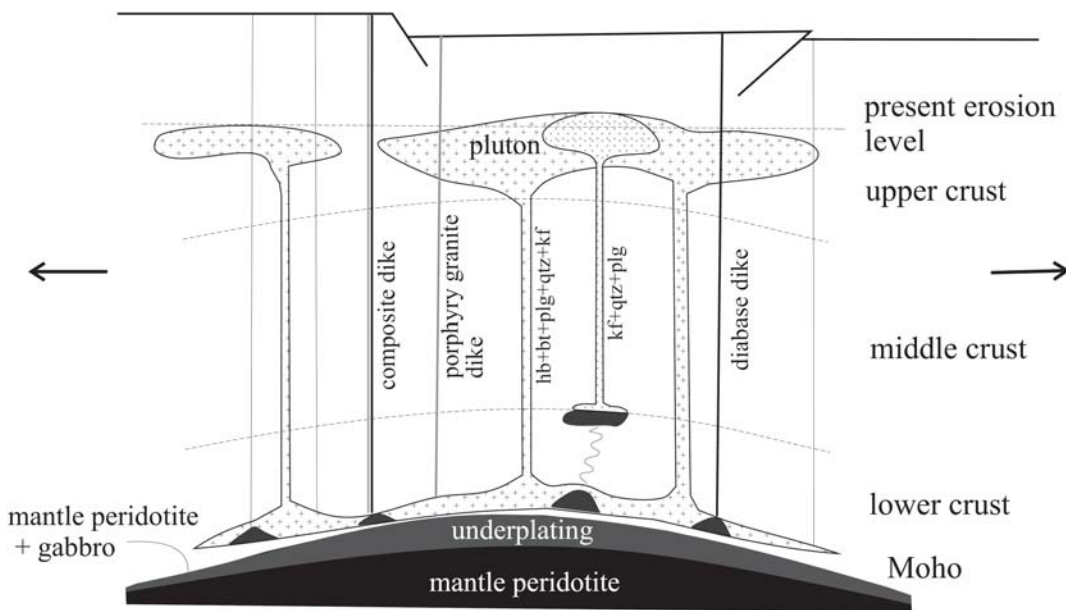


**Fig. 13.** Model for the generation of the Palaeoproterozoic bimodal magmatism in the Rio Maria Granite-Greenstone Terrane (Carajás province), showing the relationship between diabase dikes, A-type granites, and quartz feldspar porphyries. The scheme is based on Huppert and Sparks (1988) and modified from Rämö and Haapala (1996). Mantle-derived mafic magmas are intruded at the crust–mantle boundary, where they form a magmatic underplate, a hybrid of mantle peridotite, gabbro, and crustal material. The thermal effect of the mafic magmas cause extensive partial melting of the lower crust, forming A-type granitic magmas and quartz porphyry dikes. Ascending mantle-derived mafic magmas are partly trapped to higher crustal levels or reach the surface through diabase dikes. The first causes partial melting in the lower/middle crust, producing more evolved A-type granitic magmas (K-feldspar + quartz + plagioclase). Successive intrusion of silicic magmas in the middle/upper crust form A-type granite plutons and silicic dikes. The mafic and silicic magmas may locally use the same channelways, forming composite dikes with or without hybridization. hb – hornblende, bt – biotite, plg – plagioclase, kf – K-feldspar, qtz – quartz.

In the Redenção pluton, the AMS fabric is controlled mostly by magnetite, which is an early-crystallized accessory mineral. In rocks in which  $K$  is carried dominantly by ferromagnetic minerals the AMS probably results from the shape anisotropy of magnetite grains (e.g., Archanjo et al., 1995; Grégoire et al., 1998; Ferré et al., 1999). Considering the textural relationships of magnetite with other mineral grains and the absence of subsolidus deformation and recrystallization, the AMS can be interpreted as of magmatic origin. As a consequence, the magnetic lineation corresponds to the dominant magma stretching direction, which reflects emplacement-related processes, dynamic processes which occur within the magma chamber, regional deformation, or a combination of these (e.g., Paterson et al., 1998; McNulty et al., 2000;

Benn et al., 2001; Neves et al., 1996, 2003; Zák et al., 2005). The lack of a well-defined unidirectional linear fabric at pluton scale suggests a reduced or null influence of regional tectonic stresses during granite emplacement. This is in agreement with low  $P'$  values, the predominance of neutral ellipsoids, and absence of any clear correlation between  $P'$  and  $K$ . Therefore, granite emplacement was not related to a major orogeny and its fabric was not controlled by syn-emplacement regional deformation. This is in agreement with the “anorogenic” tectonic setting admitted for the Jamon suite (Dall’Agnol et al., 2005).

### 5.2. Zoning and magnetic susceptibility

A near-concentric normal zoning is a remarkable feature observed in the Redenção pluton and in others plutons of the Jamon suite (Oliveira et al., submitted; Almeida et al., submitted; Dall’Agnol et al., 2005). Gradual differentiation from the margins to the center of the plutons could be an explanation for this zoning. The coarse-grained biotite monzogranites could be derived from the amphibole-biotite monzogranites by fractional crystallization. However, geochemical data indicate that the leucogranites cannot be derived directly by fractional crystallization of the less evolved amphibole-biotite-bearing facies (Oliveira, 2001).

The high values of  $K$  ( $> 10^{-3}$  SI) found in the Redenção pluton indicate that it is ferromagnetic in origin, in accord with the high abundance of magnetite ( $> 1\%$  vol.). The unimodal distribution of  $K$  and petrographic aspects suggest that post-magmatic processes have not been intense nor penetrative.  $K$  values decrease from the southern border to the center of the pluton. The apparent zoning pattern in  $K$  values is similar to that observed for geochemical and petrographic zoning. The positive and negative correlation between  $K$  values and, respectively, mafic mineral and quartz + K-feldspar content reinforce the link between magnetic and compositional zoning. There is good agreement that in magnetite-bearing granites, the magnitude of  $K$  increases in the more mafic units (Archanjo et al., 1995; Ferré et al., 1995). Effectively, in the Redenção pluton, the highest  $K$  values correspond to the more mafic rocks. As a consequence,  $K$  displays negative correlation with  $[FeOt/(FeOt+MgO)]$  and could be used as a magmatic differentiation index.

### 5.3. Magnetic fabric and emplacement model

Although apparently isotropic in the field, the Redençao pluton displays well-defined magnetic foliation and lineation trajectories. Trajectories of the magnetic fabrics and zoning of the Redençao pluton are nearly concentric and parallel to the contact pluton/country rocks. These characteristics are similar to those expected for diapiric or concentrically expanded plutons (Cruden, 1990; Paterson and Vernon, 1995; Dietl and Koyi, 2002). However, in the present case, these two possibilities can be ruled out due to the absence of ductile deformation of country rocks and the tabular shape of the intrusion. This latter constraint suggests an emplacement similar to those of lacolith intrusions, but, in lacolith plutons, subhorizontal, not steep, magmatic foliations are expected (e.g., Román-Bediel et al., 1995; Scaillet et al., 1995; Rocchi et al., 2002). Any emplacement model for the Redençao pluton has therefore to explain how subvertical fabrics were developed in a tabular intrusion. In the following, we propose that this feature can be resolved by combining emplacement by floor depression and magmatic deformation related to the intrusion of the late leucogranite facies.

Swarms of mafic, intermediate, and felsic dikes are associated with the Jamon Suite (Silva Jr. et al., 1999). Composite mafic-felsic dikes cutting Archean granodiorites have also been locally described (Dall'Agnol et al., 2005). The felsic dikes yielded Pb-Pb zircon ages of  $1885 \pm 4$  and  $1885 \pm 2$  Ma (Oliveira D.C., unpublished data). One of these dikes, rhyolite porphyry, shows evidence of mingling with an associated mafic dike, demonstrating that the mafic and felsic magmas were contemporaneous. The occurrence of dike swarms coeval with the granites of the Jamon suite suggests that the granite plutons were emplaced in an extensional tectonic regime. This is consistent with the tabular shape of the Redençao and Bannach plutons inferred from gravity data (Oliveira et al., submitted), since subhorizontal intrusions are favored in extensional settings (e.g., Vigneresse, 1995; Vigneresse et al., 1999).

Dikes are the most efficient way to feed upper crustal plutons (Petford, 1996; Petford et al., 2000). Assuming a dike-like ascent model, three stages during the construction of the Redençao pluton are proposed. The orientation of the biotite-hornblende monzogranite facies and its magnetic foliation and lineation are close to the direction of the regional WNW-striking subvertical foliation. Field relations show that this facies was the first to be emplaced. So, initial pluton construction could have involved ascent of magmas along fractures developed parallel to

foliation planes, with space for emplacement being provided by subsidence and/or uplift of blocks at the intersection with the NNW-striking fractures or by NNE-SSW-directed translation (Fig. 14a). Steeply-plunging magnetic lineations locally found in the biotite-amphibole monzogranite facies may record vertical flow during magma emplacement.

The second stage corresponds to the switch from upward flow to lateral spread of magma at upper-crustal levels and is responsible for the tabular shape of the pluton. The high viscosity contrast and absence of deformation aureole within the country rocks indicate that forceful lateral spreading of the pluton was not the main mechanism for making space during emplacement. Instead, room was mostly created by vertical displacement of country rock as the pluton grew from an initial thin sill to attain its maximum observed thickness of 6 km (Fig. 3). Space for emplacement of successive magma pulses was likely generated by floor subsidence (Cruden, 1998) rather than by uplift of country rocks, the usual situation in laccoliths (Román-Berdiel et al., 1995; Petford et al., 2000; Saint Blanquat et al., 2001). Downwarping of the underlying country rocks can account for the observation of inward dipping magnetic foliation in the coarse-grained biotite monzogranite (Fig. 14b), instead of the expected domal structure resulting from laccolith-like emplacement.

In the third stage, emplacement of the late leucogranite facies resulted in *in situ* inflation of the magma chamber and a coaxial magmatic strain. The magma-pressure driven deformation led to further steepening of the magnetic fabric and development of concentrically arranged magnetic lineations in the early emplaced and partially crystallized coarse-grained biotite monzogranite (Fig. 14c). Since space creation by lateral displacement was probably inefficient to accommodate the new incoming magma, overpressure of the magma chamber may have resulted. This induced fracturing of the roof, with development of ring fractures. Migration of interstitial liquid to these fractures and its subsequent eruption is required in order to maintain a near constant volume. The geochemistry of the porphyritic facies suggests it probably represents an evolved liquid derived from a parental magma similar in composition to the coarse-grained monzogranite (Oliveira et al., submitted). Therefore, the arcuate shape of this facies may represent sites of magma expulsion of part of the resident magma. A similar explanation could also be proposed for the seriated monzogranite. However, this is less likely, since this facies does not appear to be genetically related with the coarse-grained biotite monzogranite. It is suggested that it may have resulted from intrusion of new magma batches from below, with its bow-shaped

structure again reflecting the radial stress field induced by the leucogranite facies, with which it shows textural affinity (Oliveira et al., submitted).

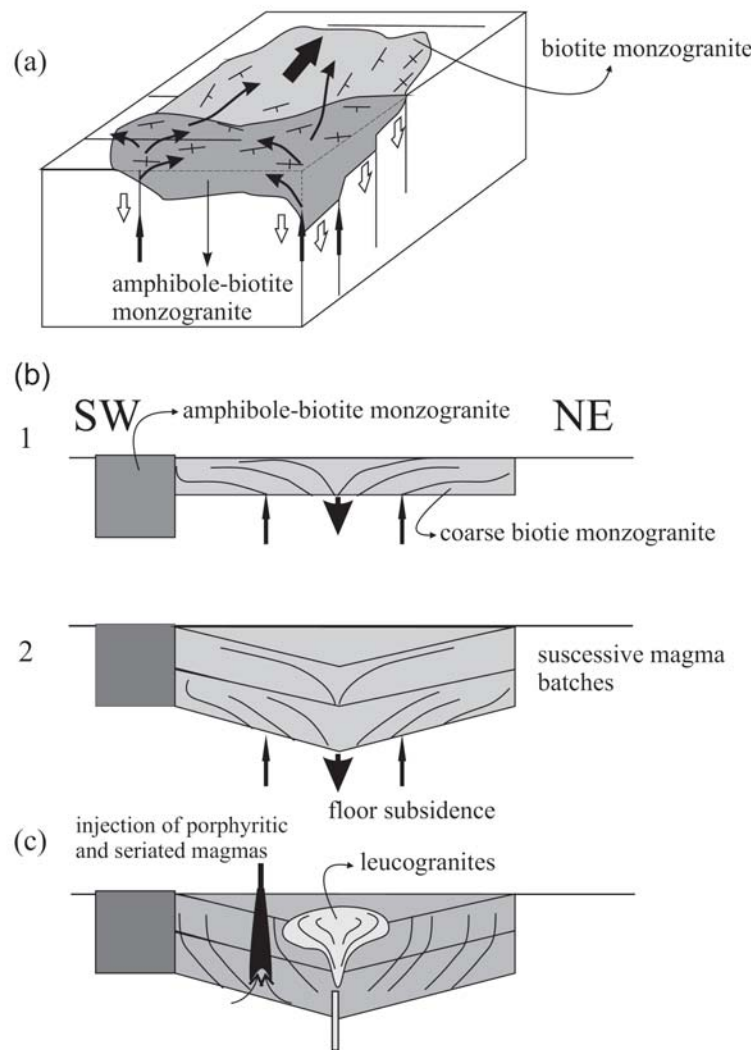


**Fig. 14.** Proposed emplacement model for the Redenção granite. (a) Block-diagram showing magma ascent exploiting the subvertical foliation of country rocks. Due to the pressure of magma intrusion, the horizontal stresses eventually overcome the lithostatic load (Vigneresse et al., 1999) and the opening plane becomes horizontal. Subvertical foliations and steep to shallow lineations related to magma ascent and emplacement are preserved in the early-emplaced amphibole-biotite monzogranite. (b1, b2) SW-NE cross-sections showing growth of the pluton by floor subsidence (Cruden, 1998), possibly accommodated by ductile extension at deeper crustal levels. A shallow to moderately-inward dipping foliation develops in the differentiating successive magma batches. (c) Intrusion of the late leucogranite facies induces a radial stress field and causes foliation in the partially crystallized biotite monzogranite to become steeper. Overpressure of the magma chamber induces arcuate fractures in the pluton roof, which drain part of the residual melt present in the magma chamber.

#### 5.4. Perspectives on the application of the AMS technique in the structural study of A-type granites

Few AMS studies have been conducted in A-type plutons. Ferré et al. (1999) and Bolle et al. (2000, 2002) studied granitoids associated with the Bushveld Complex (South Africa) and the Rogaland Igneous Complex (Norway), respectively. In both cases the granites are part of larger layered intrusions. Ferré et al. (1999) found that magnetite-rich granites in the Bushveld Complex display well-defined subhorizontal magnetic foliations but lack a well-defined linear fabric, which they interpreted as evidence for laccolith emplacement of crystal-poor magma batches followed by in-situ static crystallization. In contrast, the AMS study of the Rogaland Igneous Complex (Bolle et al., 2000, 2002) revealed that magnetic lineations show a clear convergent pattern towards the center of the intrusion, where they become subvertical. This pattern was attributed to continuous downward drag of the crystallizing granite magma caused by sinking of the underlying mafic rocks. Alkaline granites from ring-complexes are usually also included within the anorogenic granites category. In a study of one such ring-dike complex from Skye (Scotland), Geoffroy et al. (1997) found a consistent magnetic fabric pattern, with magnetic foliations dipping steeply towards the convex wall of each intrusion and with shallow-plunging magnetic lineations generally parallel to the strikes of the foliation. This was inferred to be consequence of a radial and compressive stress field acting after each injection of magma.

Compared with granites emplaced in orogenic settings, anorogenic granites are expected to display lower anisotropies and, consequently, weaker fabrics. However, the studies summarized above, in conjunction with the new study reported here, point out that the AMS is a promising technique in the analysis of the internal fabric of these rocks. They also highlight that there is no universal rule, with each particular case requiring a different interpretation. In fact, clues on emplacement mechanisms of granitic magmas and on internal magma chamber processes may be better uncover by studies of these types of plutons because orogenic granites may acquire an internal fabric by a multitude of mechanisms. This may result in composite fabrics and sometimes render the results so complicated as to hamper an unambiguous interpretation. However, it must be kept in mind that these initial results were obtained in magnetite-rich granites. In the reduced A-type granites, including the more typical rapakivi granites (Rämö and Haapala, 1995), the results may be less conclusive or not easily interpretable. It would be interesting to undertake AMS technique studies in moderately reduced A-type

plutons, as the Serra dos Carajás and Cigano plutons of the Serra dos Carajás suite (Dall'Agnol et al., 2005) and similar plutons. These granites have significant modal content of magnetite, but display also mineralogical evidence, e.g. the composition of mafic minerals, of crystallization in relatively reducing conditions (Dall'Agnol and Oliveira, 2006). Finally, as pointed out by Ferré et al. (1999), replacement of magnetite by haematite during hydrothermal alteration may also constitute a complication in the study of anorogenic plutons.

## 6. Conclusions

At the end of the Paleoproterozoic (~1.88 Ga), the Carajás province recorded a tectonothermal event that resulted in the emplacement of several “anorogenic”, A-type granites. The Jamon suite plutons were emplaced in an extensional tectonic setting oriented approximately NNE-SSW to ENE-WSW, as indicated by the coeval intrusion of WNW-ESE- to NNW-SSE-striking diabase and granite porphyry dike swarms. We have carried out the first magnetic fabric study of one of the members of the Jamon suite, the Redenção pluton. Together with existing petrographic, geochemical and gravity data, the results show that the Redenção pluton is a normally zoned, tabular intrusion. High magnetic susceptibilities, early-crystallization of magnetite, and low  $P'$  values indicate that the magnetic fabric is of magmatic origin and carried by magnetite. Absence of a well-defined unidirectional linear fabric at pluton scale suggests reduced or null influence of regional stresses during granite emplacement. The concentric orientation of steeply dipping magnetic foliations and shallow to moderately plunging magnetic lineations in the different facies of the pluton are interpreted as resulting mainly from (a) floor subsidence, which created space for injection of successive magma pulses, (b) *in situ* inflation of the magma chamber in response to the intrusion of the central, late-emplaced facies, and (c) ejection of part of the residual resident magma through cylindrical fractures. The successful application of the AMS technique to the study of the internal fabric of the Redenção granite opens up the possibility that a similar approach can provide important insights into the emplacement mechanism of A-type anorogenic granites, including rapakivi granites.

## Acknowledgments

The authors would like to express the special thanks to M. A. Oliveira, J. A. C. Almeida, and A. L. Quaresma for the support in the acquisition of data during field works. Grant Osborne

and Keith Martin, of the former Western Mining Company, for the gravity data obtained in the Redenção area and C. E. M. Barros for participation in the geological mapping of Redenção pluton. This research received financial support from CNPq (RD – 550739/2001-7, 476075/2003-3, 307469/2003-4; DCO – scholarship April04 to Nov05), CAPES (DCO – scholarship Nov01 to March04), and Federal University of Pará (UFPA). This paper is a contribution to PRONEX/CNPq (Proc. 66.2103/1998-0) and IGCP-510 project (IUGS-UNESCO).

## References

- Åhäll, K.I., Connelly, J.N., Brewer, T.S., 2000. Episodic rapakivi magmatism due to distal orogenesis: correlation of 1.69–1.50 Ga orogenic and inboard, “anorogenic” events in the Baltic Shield. *Geology* 28, 823– 826.
- Almeida, J.A.C., 2005. Geologia, petrografia e geoquímica do granito anorogênico Bannach, Terreno Granito-Greenstone de Rio Maria, PA. M.Sc. Thesis, Federal University of Pará, Belém, Brazil (in Portuguese), 171p.
- Almeida, J.A.C., Dall'Agnol, R., Oliveira, D.C., Submitted. Geologia, petrografia e geoquímica do granito anorogênico Bannach, Terreno Granito-Greenstone de Rio Maria, Pará. *Revista Brasileira de Geociências*.
- Althoff, F.J., Barbey, P., Boullier, A.-M., 2000., 2.8–3.0 Ga plutonism and deformation in the SE Amazonian craton: the Archean granitoids of Marajoara (Carajás mineral province). *Precambrian Research* 104, 187– 206.
- Amelin, Y.V., Larin, A.M, Tucker, R.D., 1997. Chronology of multiphase emplacement of the Salmi rapakivi granite–anorthosite complex, Baltic shield: implications for magmatic evolution. *Contributions to Mineralogy and Petrology* 127, 353–368.
- Anderson, J.L., Morrison, J., 2005. Ilmenite, magnetite, and peraluminous Mesoproterozoic anorogenic granites of Laurentia and Baltica. *Lithos* 80, 45-60.
- Archango, C.J., Bouchez, J.-L., Corsini, M., Vauchez, A., 1994. The Pombal granite pluton: magnetic fabric, emplacement and relationships with the Brasiliano strike-slip setting of NE Brazil (Paraiba State). *Journal of Structural Geology* 16, 323-335.
- Archango, C.J., Launeau, P., Bouchez, J.L., 1995. Magnetic fabric vs. magnetite and biotite shape fabrics of the magnetite-bearing granite pluton of Gameleiras (northeast Brazil). *Phys. Earth Planet. Interiors.* 89, 63–75.

- Barros, C.E.M., Sardinha, A.S., Barbosa, J.P.O., Krimski, R., Macambira, M.J.B., 2001. Pb-Pb and U-Pb zircon ages of Archean syntectonic granites of the Carajás metallogenetic province, Northern Brazil. 3<sup>th</sup> Simposio Sudamericano de Geología Isotópica, 3, Pucon, Chile, Resumos Expandidos. Servicio Nacional de Geología Y Minería. CD-ROM.
- Benn, K., Paterson, S.R., Lund, S.P., Pignotta, G.S., Kruse, S., 2001. Magmatic fabrics in batholiths as markers of regional strains and plate kinematics: example of the Cretaceous Mt. Stuart batholith. *Phys. Chem. Earth (A)* 26, 343-354.
- Bettencourt, J. S., Tosdal, R. M., Leite Jr., W. B, Payolla, B. L., 1999. Mesoproterozoic rapakivi granites of the Rondônia Tin Province, southwestern border of the Amazonian craton, Brazil - I. Reconnaissance U-Pb geochronology and regional implications. *Precambrian Research*. 95, 41-67.
- Bolle, O., Diot, H., Duchesne, J.C., 2000. Magnetic fabric and deformation in charnockitic igneous rocks of the Bjerkreim-Sokndal layered intrusion (Rogaland, Southwest Norway). *Journal of Structural Geology* 22, 647-667.
- Bolle, O., Trindade, R.I.F., Bouchez, J.L., Duchesne, J.C., 2002. Imaging downward granitic magma transport in the Rogaland Igneous Complex, SW Norway. *Terra Nova* 14, 87-92.
- Bonin, B., 1986. Ring complex granites and anorogenic magmatism. *Studies in Geolgy*, North Oxford Academic, Oxford, 188 p.
- Borradaile, G.L., Henry, B., 1997. Tectonic applications of magnetic susceptibility and its anisotropy. *Earth Science Review* 42, 49-93.
- Bouchez, J.L., Gleizes, G., Djouadi, T., Rochette, P., 1990. Microstructure and magnetic susceptibility applied to emplacement kinematics of granites: the example of the Foix pluton (French Pyrenees). *Tectonophysics*, 184, 157±171.
- Bouchez, J.L., 1997. Granite is never isotropic: an introduction to AMS studies of granitic rocks. In: Bouchez, J.L., Hutton, D.H.W., Stephens, W.E. (Eds.), *Granite: from Segregation of Melt to Emplacement Fabrics*, vol. 8. Kluwer Publishing Co., Dordrecht, pp. 95–112.
- Bouillin, J.P., Bouchez, J.L., Lespinasse, P., Pêcher, A., 1993. Granite emplacement in an extensional setting: an AMS study of the magmatic structures of Monte Capanne (Elba, Italy). *Earth and Planetary Science Letters* 118, 263-279.
- Brito Neves, B.B., 1999. América do Sul: quatro fusões, quatro fissões e o processo acrecional andino: *Revista Brasileira de Geociências* 29, 379-392 (in Portuguese).

- Chadima, M., Hrouda, F., Melichar, Rostislav., 2006. Magnetic fabric study of the SE Rhenohercynian Zone (Bohemian Massif): Implications for dynamics of the Paleozoic accretionary wedge. *Tectonophysics* 418, 93-109.
- Condie, K.C., 2002. Breakup of a Paleoproterozoic supercontinent. *Gondwana Research* 5, 41-43.
- Cruden, A.R., 1990. Flow and fabric development during the diapiric rise of magma. *Journal of Geology* 98, 681-698.
- Cruden, A. R. (1998) On the emplacement of tabular granites. *Journal of the Geological Society, London* 154, 853 - 862.
- Cruden, A.R., Tobish, O.T., Launeau, P., 1999. Magnetic fabric evidence for conduit-fed emplacement of a tabular intrusion: Dinkey Creek pluton, central Sierra Nevada batholith, California. *Journal of Geophysical Research* 104, 10511-30.
- Dall'Agnol, R., Lafon, J.M., Macambira, M.J.B., 1994. Proterozoic anorogenic magmatism in the Central Amazonian province: geochronological, petrological and geochemical aspects. *Mineralogy and Petrology* 50, 113-138.
- Dall'Agnol, R., Pichavant, M., Champenois, M., 1997. Iron–titanium oxide mineral of the Jamon granite, Eastern Amazonian region, Brazil: implications for the oxygen fugacity in Proterozoic A-type granites. *Anais da Academia Brasileira de Ciências* 69, 325–347.
- Dall'Agnol, R., Costi, H.T., Leite, A.A., Magalhães, M.S., Teixeira, N.P., 1999a. Rapakivi granites from Brazil and adjacent areas. *Precambrian Research* 95, 9-39.
- Dall'Agnol, R., Rämö, O.T., Magalhães, M.S., Macambira, M.J.B., 1999b. Petrology of the anorogenic, oxidised Jamon and Musa granites, Amazonian craton: implications for the genesis of Proterozoic A-type granites. *Lithos* 46, 431-462.
- Dall'Agnol, R., Scaillet, B., Pichavant, M., 1999c. An Experimental Study of a Lower Proterozoic A-Type Granite from the Eastern Amazonian Craton, Brazil. *Journal of Petrology* 40, 1673-1698.
- Dall'Agnol, R., Teixeira, N.P., Rämö, O.T., Moura, C.A.V., Macambira, M.J.B., Oliveira, D.C., 2005. Petrogenesis of the Paleoproterozoic, rapakivi, A-type granites of the Archean Carajás Metallogenic Province, Brazil. *Lithos* 80, 101-129.
- Dall'Agnol, R., Oliveira, D.C., 2006. Oxidized, magnetite-series, rapakivi-type granites of Carajás, Brazil: implications for classification and petrogenesis of A-type granites. *Lithos* (In press).

- Dall'Agnol, R., Oliveira, M.A., Almeida, J.A.C., Althoff, F.J., Leite, A.A.S., Oliveira, D.C., Barros, C.E.M., 2006. Archean and Paleoproterozoic granitoids of the Carajás metallogenetic province, eastern Amazonian craton. In: Dall'Agnol, R., Rosa-Costa, L.T., Klein, E.L. (eds.). Symposium on Magmatism, Crustal Evolution, and Metallogenesis of the Amazonian Craton. Abstracts Volume and Field Trips Guide. Belém, PRONEX-UFPA/SBG-NO, 150p.
- Delor, C., Lahondère, D., Egal, E., Lafon, J.M., Cocherie, A., Guerrot, C., Rossi, P., Trufert, C., Theveniaut, H., Phillips, D., Avelar, V.G., 2003. Transamazonian crustal growth and reworking as revealed by the 1:500.000-scale geological map of French Guiana (2<sup>nd</sup> edition). Géologie de la France, 2-3-4: 5-57.
- Dietl, C., Koyi, H.A., 2002. Emplacement of nested diapirs: results of centrifuge modelling. Journal of the Virtual Explorer 6, 81-88.
- DOCEGEO (Rio Doce Geologia e Mineração), 1988. Revisão litoestratigráfica da Província Mineral de Carajás. 35th Congresso Brasileiro de Geologia, Belém, pp. 11-54.
- Eklund, O., Shebanov, A.D., 1999. The origin of rapakivi texture by sub-isothermal decompression. Precambrian Research. 95, 129–146.
- Emslie, R.F., 1991. Granitoids of rapakivi granite-anorthosite and related associations. Precambrian Research 51, 173-192.
- Ferré , E., Gleizes, G., Bouchez, J.L., Nnabo, P.N., 1995. Internal fabric and strike-slip emplacement of the Pan-African granite of Solli Hills, northern Nigeria. Tectonics 14, 1205-1219.
- Ferré, E.C., Wilson, J. and Gleizes, G., 1999. Magnetic susceptibility and AMS of the Bushveld alkaline granites, South Africa. Tectonophysics, 307: 113-133.
- Ferré, E.C., Gleizes, G. and Caby, R., 2002. Tectonics and post-collisional granite emplacement in an obliquely convergent orogen: the Trans-Saharan belt, Eastern Nigeria. Precambrian Research 114, 199-219.
- Frost, C.D., Frost, B.R., Chamberlain, K.R., Edwards, B., 1999. Petrogenesis of the 1.43 Ga Sherman batholith, SE Wyoming, USA: a reduced, rapakivi-type anorogenic granite. Journal of Petrology 40, 1771-1802.

- Geoffroy, L., Olivier, P., Rochette, P., 1997. Structure of a hypovolcanic acid complex inferred from magnetic susceptibility anisotropy measurements: the Western red Hills granite (Skye, Scotland, Thulean Igneous Province). *Bulletin of Volcanology*, 59: 147- 159.
- Grégoire, V., Darrozes, J., Gaillot, P., Nédélec, A., Launeau, P., 1998. Magnetite grain shape fabric and distribution anisotropy vs rock magnetic fabric: a three-dimensional case study. *Journal of Structural Geology* 20, 937–944.
- Haapala, I., Rämö, O.T., 1992. Tectonic setting and origin of the Proterozoic rapakivi granites of the southeastern Fennoscandia. *Transactions of the Royal Society of Edinburgh. Earth Sciences* 83, 165–171.
- Haapala, I., Rämö, O.T., 1999. Rapakivi granites and related rocks: an introduction. *Precambrian Research* 95, 1–7.
- Hoffmann, P., 1989. Speculations on Laurentia's first gigayear (2.0 to 1.0 Ga). *Geology* 17, 135–138.
- Hrouda, F., 1982. Magnetic anisotropy of rocks and its application in geology and geophysics. *Geophysical Survey* 5, 37-82.
- Hrouda, F., Jelínek, V., Hrusková, L., 1990. A package of programs for statistical evaluation of magnetic data using IBM-PC computers. *EOS Trans. AGU, Fall Meeting*, San Francisco, 1289.
- Huppert, H.E., Sparks, R.S., 1988. The generation of granitic magmas by intrusion of basalt into continental crust. *Journal of Petrology* 29, 599–624.
- Hutton, D.H.W., Dempster, T.J., Brown, P.E., Becker, S.M., 1990. A new mechanism of granite emplacement: rapakivi intrusions in active extensional shear zones. *Nature* 343, 452 – 454.
- Ishihara, S., 1981. The granitoid series and mineralization. *Economic Geology*, 75<sup>th</sup> Anniversary volume, pp. 458-484.
- Jelínek, V., 1978. Statistical processing of anisotropy of magnetic susceptibility measured on groups of specimen. *Studia Geophysica et Geodaetica* 22, 50–62.
- Jelínek, V., 1981. Characterization of the magnetic fabrics of rocks. *Tectonophysics* 79, 63– 67.
- Lamarão, C.N., Dall'Agnol, R., Lafon, J.-M., Lima, E.F., 2002. Geology, geochemistry, and Pb-Pb zircon geochronology of the Paleoproterozoic magmatism of Vila Riozinho, Tapajós Gold Province, Amazonian craton, Brasil. *Precambrian Research* 119, 189-223.

- Lamarão, C.N., Dall'Agnol, R., Pimentel, M.M., 2005. Nd isotopic composition of Paleoproterozoic volcanic and granitoid rocks of Vila Riozinho: implications for the crustal evolution of the Tapajos Gold Province, Amazonian craton. *Journal of South American Earth Sciences* 18, 277-292.
- Leite, A.A.S., 2001. Geoquímica, petrogênese e evolução estrutural dos granitóides arqueanos da região de Xinguara, SE do Cráton Amazônico. Belém, Universidade Federal do Pará, Centro de Geociências. Doctor thesis, Federal University of Pará, Belém, Brazil (in Portuguese). 490p.
- Leite, A.A.S., Dall'Agnol, R., Macambira, M.J.B., Althoff, F.J., 2004 Geologia e geocronologia dos granitóides arqueanos da região de Xinguara-PA e suas implicações na evolução do Terreno Granito-'Greenstone' de Rio Maria, Cráton Amazônico. *Revista Brasileira de Geociências* 34 (4), 447-458.
- Macambira, M.J.B., Lancelot, J.R., 1996. Time constraints for the formation of the Archean Rio Maria crust, southeastern Amazonian craton, Brazil. *International Geology Review* 38, 1134-1142.
- Macambira, M.J.B., Lafon, J.-M., 1995. Geocronologia da Província mineral de Carajás: síntese dos dados e novos desafios. *Boletim do Museu Paraense Emílio Goeldi, Ciências da Terra* 7, 263-288 (in Portuguese).
- Machado, N., Lindenmayer, Z., Krogh, T.E., Lindenmayer, D., 1991. U-Pb geochronology of Archean magmatism and basement reactivation in the Carajás área, Amazon Shield, Brazil. *Precambrian Research* 49, 329-354.
- McNulty, B.A., Tobish, O.T., Cruden, A.R.Gilder, S., 2000. Multistage emplacement of the Mount Givens pluton, Central Sierra Nevada batholith. *Geological Society of America Bulletin* 112, 119-135.
- Neves, S.P., Vauchez, A., Archanjo, C.J., 1996. Shear-zone controlled magma emplacement or magma-assisted nucleation of shear zones? Insights from Northeast Brazil. *Tectonophysics* 262, 349-365.
- Neves, S.P., Araujo, A.M.B., Correia, P.B., Mariano, G., 2003. Magnetic fabrics in the Cabanas granite (NE Brazil): interplay between emplacement and regional fabrics in a dextral transpressive regime. *Journal of Structural Geology* 25, 441-453.

- Nyman, M.W., Karlstrom, K.E., Kirby, E., Graubard, C.M., 1994. Mesoproterozoic contractional orogeny in western North America: Evidence from ca. 1.4 Ga plutons. *Geology* 22, 901-904.
- Nyman, M.W., Karlstrom, K.E., 1997. Pluton Emplacement processes and tectonic setting of the 1.42 Ga signal batholith, SW USA: important role of crustal anisotropy during regional shortening. *Precambrian Research* 82, 237-263.
- Oliveira, D.C., 2001. Geologia, geoquímica e petrologia magnética do granito paleoproterozóico Redenção, SE do Cráton Amazônico. M.Sc. Thesis, Federal University of Pará, Belém, Brazil (in Portuguese), 202p.
- Oliveira, D.C., Dall'Agnol, R., Barros, C.E.M., Figueiredo, M.A.B.M., 2002. Petrologia magnética do Granito Paleoproterozóico Redenção, SE do Cráton Amazônico. In: Klein, E.L., Vasquez, M.L., Rosa-Costa, L.T. (Eds.) Contribuições à Geologia da Amazônia. Sociedade Brasileira de Geologia Núcleo Norte, Belém, vol. 3, p. 115-132.
- Oliveira, D.C., Dall'Agnol, R., Barros, C.E.M., Vale, A.G., 2005. Geologia e Petrografia do Granito Paleoproterozóico Redenção, SE do Cráton Amazônico. Boletim do Museu Paraense Emílio Goeldi, Série Ciências Naturais, Belém, v. 2, n. 1, p. 155-172.
- Oliveira, D.C., Dall'Agnol, R., Silva, J.B.C., Almeida, J.A.C., Submitted. Gravimetric, radiometric, and magnetic susceptibility study of the Paleoproterozoic Redenção and Bannach plutons: implications for architecture and zoning of A-type granites. *Journal of South American Earth Sciences*.
- Paterson, S.R., Vernon, R.H., 1995. Bursting the bubble of ballooning plutons: a return to nested diapirs emplaced by multiple processes. *Geology Society of America Bulletin* 107, 1356-1380.
- Paterson, S.R., Fowler Jr., T.K., Schmidt, K.L., Yoshinobu, A.S., Yuan, E.S., Miller, R.B., 1998. Interpreting magmatic fabric patterns in plutons. *Lithos* 44, 53-82.
- Petford, N., 1996. Dikes or diapirs? *Transactions of the Royal Society of Edinburgh: Earth Sciences* 87, 105–114.
- Petford, N., Cruden, A.R., McCaffrey, K.J.W. and Vigneresse, J.-L., 2000. Granite magma formation, transport and emplacement in the Earth's crust. *Nature* 408, 669-673.
- Rämö, O.T., Haapala, I., 1995. One hundred years of rapakivi granite. *Mineralogy and Petrology* 52, 129–185.

- Rämö, O.T., Haapala, I., 1996. Rapakivi granite magmatism: a global review with emphasis on petrogenesis. In: Demaiffe, D. (Ed.), Petrology and Geochemistry of Magmatic Suites of Rocks in the Continental and Oceanic Crust. A volume dedicated to Jean Michot. Université Libre de Bruxelles, Royal Museum for Central Africa, pp. 177– 200.
- Rämö, O.T., Dall'Agnol, R., Macambira, M.J.B., Leite, A.A.S., de Oliveira, D.C., 2002. 1.88 Ga oxidized A-type granites of the Rio Maria region, eastern Amazonian craton, Brazil: Positively anorogenic! *Journal of Geology* 110, 603-610.
- Rochette, P., Jackson, M., Aubourg, C., 1992. Rock magnetism and the interpretation of anisotropy of magnetic susceptibility. *Reviews of Geophysics* 30 (3), 209–226.
- Rocchi, S., Westerman, D.S., Dini, A., Innocenti, F., Tonarini, S., 2002. Two-stage growth of laccoliths at Elba Island, Italy. *Geology* 30, 983-986.
- Rogers, J.J.W., Santosh, M., 2002, Configuration of Columbia, a Mesoproterozoic supercontinent: *Gondwana Research* 5, 123–132.
- Roman-Berdiel, T., Gapais, D., Brun, J.P., 1995. Analogue models of laccolith formation. *Journal of Structural Geology* 17, 1337-1346.
- Rosa-Costa, L.T., 2006. Geocronologia  $^{207}\text{Pb}/^{206}\text{Pb}$ , Sm-Nd, U-Th-Pb E $^{40}$  Ar- $^{39}$  Ar do Segmento sudeste do Escudo das Guianas: Evolução crustal e termocronologia do evento Transamazônico. Doctor Thesis, Federal University of Pará, Belém, Brazil (in Portuguese), 226p.
- Saint-Blanquat, M., Law, R.D., Bouchez, J.L., Morgan, S.S., 2001. Internal structure and emplacement of the Papoose Flat pluton: An integrated structural, petrographic, and magnetic susceptibility study. *Geological Society of America Bulletin* 113, 976-995.
- Santos, J.O.S., Hartmann, L.A., Gaudette, H.E., Groves, D.I., McNaughton, N.J., Fletcher, I.R., 2000. A new understanding of the provinces of the Amazon craton based on integration of field mapping and U-Pb and Sm-Nd geochronology. *Gondwana Research* 3(4), 453-488.
- Santos, J.O.S., Van Breemen, O.B., Groves, D.I., Hartmann, L.A., Almeida, M.E., McNaughton, N.J., Fletcher, I.R., 2004. Timing and evolution of multiple Paleoproterozoic magmatic arcs in the Tapajós Domain, Amazon craton: constraints from SHRIMP and TIMS zircon, baddeleyite and titanite U-Pb geochronology. *Precambrian Research* 131, 73-109.

- Scaillet, B., Pêcher, A., Rochette, P., Champenois, M., 1995. The Gangotri granite (Garhwal Himalaya): Laccolic emplacement in an extending collisional belt. *Journal of Geophysical Research* 100, 585-607.
- Silva, Jr., R.O., Dall'Agnol, R., Oliveira, E.P., 1999. Geologia, petrografia e geoquímica dos diques proterozoicos da região de Rio Maria, sudeste do Pará. *Geochimica Brasiliensis*, 13.
- Souza, Z.S., Dall'Agnol, R., 1995. Geochemistry of metavolcanic rocks in the Archean Greenstone Belt of Identidade, SE, Pará, Brazil. *Anais da Academia Brasileira de Ciências*. 67, 217-233.
- Talbot, J.-Y., Martelet, G., Courrioux, G., Chen, Y., Faure, M., 2004. Emplacement in an extensional setting of the Mont Lozére-Borne granitic complex (SE France) inferred from comprehensive AMS, structural and gravity studies. *Jounal of Structural Geology* 26, 11-28.
- Tassinari, C. C. G.; Macambira, M. J. B. 1999. Geochronological Provinces of the Amazonian Craton. *Episodes*, 22: 174-182.
- Tassinari, C.C.G., Macambira, M.J.B., 2004. Evolução tectônica do Cráton Amazônico. In: Mantesso-Neto, V., Bartorelli, A., Carneiro, C.D.R., Brito Neves, B.B. de. (Org.). *Geologia do Continente Sul Americano: Evolução da obra de F.F.M. de Almeida*. São Paulo: BECA, 2004, v. , p. 471-486.
- Teixeira, N.P., Bettencourt, J.S., Moura, C.A.V., Dall'Agnol, R., Macambira, E.M.B., 2002. Archean crustal sources for Paleoproterozoic tin-mineralized granites in the Carajás Province, SSE Pará, Brazil: Pb-Pb geochronology and Nd isotope geochemistry. *Precambrian Research* 119, 257-275.
- Vale, A.G., Neves, P.N., 1994. O Granito Redenção: Estado do Pará. In: Congresso Brasileiro de Geologia, 38, Balneário Camboriú-SC. SBG, vol. 1, p. 149 - 150.
- Vigneresse, J.L., 1995. Control of granite emplacement by regional deformation. *Tectonophysics* 249, 173-186.
- Vigneresse, J.L., 2005. The specific case of the Mid-Proterozoic rapakivi granites and associated suite within the context of Columbia supercontinent. *Precambrian Research*, 137, 1-34.
- Vigneresse, J.L., Tikoff, B., Améglio, L., 1999. Modification of the regional stress field by magma intrusion and formation of tabular granitic plutons. *Tectonophysics* 302, 203-224.
- Windley, B.F., 1993. Proterozoic anorogenic magmatism and its orogenic connections. *Journal of the Geological Society of London* 150, 39-50.

- Windley, B.F. 1995. *The Evolving Continents*. 3 ed. London, Wiley, 526 p.
- Zák, J., Schulmann, K., Hrouda, F., 2005. Multiple magmatic fabrics in the Sázava pluton (Bohemian Massif, Czech Republic): a result of superposition of wrench-dominated regional transpression on final emplacement. *Journal of Structural Geology* 27, 805-822.
- Zhao, T.-P., Zhou, M.-F., Zhai, M.-G., Xia, B. 2002, Paleoproterozoic rift-related Volcanism of the Xiongier Group, North China Craton: implications for the breakup of Columbia. *International Geology Review*, 44, 336-351.
- Zhao, G., Sun, M., Wilde, S.A., Li, S., 2004. A Paleo-Mesoproterozoic supercontinent: assembly, growth and breakup. *Earth Science Reviews* 67, 91–123.

## **CAPÍTULO - 6**

### ***DISCUSSÕES E CONCLUSÕES FINAIS***

## DISCUSSÕES E CONCLUSÕES FINAIS

As rochas que constituem os maciços da Suíte Jamon possuem composições monzograníticas, excetuando-se diques de leucomicro-sienogranito. As suas características texturais e mineralógicas permitem subdividi-las em fácies petrográficas que incluem monzogranitos equigranulares com diferentes proporções modais de anfibólio e biotita, leuogranitos e, subordinadamente, variedades porfiríticas.

Observações de campo aliadas a dados aerogamaespectrométricos, petrográficos, geoquímicos e de suscetibilidade magnética, demonstraram que os corpos graníticos que constituem a Suíte Jamon possuem um zoneamento normal concêntrico com as fácies mais ricas em minerais máficos situando-se na periferia dos corpos e as fácies mais leucocráticas as porções mais centrais. As fácies porfiríticas afloram em elevações alinhadas ou formam estruturas anelares, como no caso do Granito Redenção. De modo geral, os líquidos formadores do granito evoluíram das bordas para o centro, onde se concentraram os líquidos mais diferenciados. As composições modais, que tal evolução se traduziu por aumentos moderados nos conteúdos de quartzo e da razão feldspato potássico/plagioclásio e, de modo mais acentuado, pela diminuição gradual das percentagens de minerais máficos e da razão anfibólio/biotita. Esta tendência é acompanhada pelo aumento de  $\text{SiO}_2$ ,  $\text{K}_2\text{O}$  e Rb e uma nítida diminuição dos teores de  $\text{TiO}_2$ ,  $\text{MgO}$ ,  $\text{Fe}_2\text{O}_3\text{t}$ ,  $\text{CaO}$ ,  $\text{P}_2\text{O}_5$ , Ba, Sr e Zr.

Os dados geoquímicos obtidos para o Granito Redenção sugerem que a evolução das suas variedades de rocha não se deu por simples cristalização fracionada, com outros processos tendo papel importante. Com base nas relações entre os óxidos de elementos maiores e menores, dos elementos traço litófilos (Rb, Sr e Ba) e ETR, foi possível distinguir pelo menos três estágios de evolução magnética nestes granitos: o primeiro corresponde à geração da fácie hornblenda  $\pm$  clinopiroxênio-monzogranito a partir do líquido hornblenda+biotita monzogranito localmente enriquecido em anfibólio e clinopiroxênio cumuláticos. Esta hipótese é coerente com o gap composicional entre a fácie hornblenda  $\pm$  clinopiroxênio-monzogranito e as demais variedades. Ela explica também as acentuadas anomalias de Eu observadas na fácie hornblenda  $\pm$  clinopiroxênio-monzogranito, inconsistentes com a hipótese de o líquido formador da fácie hornblenda-biotita-monzogranito ter sido derivado do primeiro por cristalização fracionada. O segundo estágio evolutivo é marcado pela geração das diferentes variedades de biotita-monzogranitos por processo de cristalização fracionada a partir da fácie biotita+hornblenda-

monzogranito. Os padrões dos ETR apresentados pelos biotita-monzogranitos, com pronunciadas anomalias de Eu, favorecem a hipótese de um fracionamento dominado por plagioclásio e feldspato potássico. O terceiro estágio corresponde à geração dos leucogranitos a partir de um magma félscico mais evoluído e independente. Outros processos, como *magma mingling*, foram importantes para geração das variedades porfiríticas do corpo, havendo evidências de interação entre as fácies biotita-monzogranito e os leucogranitos. De modo geral, as características geoquímicas e petrográficas e a evolução magmática do Granito Redenção são semelhantes às dos demais granitos da Suíte Jamon (Jamon, Musa e Bannach).

A Suíte Jamon é subalcalina, metaluminosa a peraluminosa e possui afinidade geoquímica com granitos intra-placa, tipo-A. A ocorrência de magnetita e titanita, bem como os altos valores de suscetibilidade magnética demonstram que os granitos da Suíte Jamon foram formados em condições oxidantes. Granitos tipo-A oxidados possuem altas razões de  $\text{FeOt}/(\text{FeOt}+\text{MgO})$ ,  $\text{TiO}_2/\text{MgO}$  e  $\text{K}_2\text{O}/\text{Na}_2\text{O}$  e baixos valores de  $\text{CaO}$  e  $\text{Al}_2\text{O}_3$  comparado aos granitos cálcio-alcalinos. Valores ligeiramente mais baixos da razão  $\text{FeO}_t/(\text{FeO}_t+\text{MgO})$ , os distinguem dos granitos tipo-A reduzidos. Os granitos da Suíte Jamon são similares aos granitos mesoproterozóicos do tipo-A da série magnetita do SW da América do Norte e diferem dos granitos rapakivi reduzidos do Escudo da Fennoscandia e das suítes Serra dos Carajás e Velho Guilherme da Província Mineral de Carajás em vários aspectos, provavelmente pela diferença de fontes magmáticas. A Suíte Jamon cristalizou próximo ou levemente acima do tampão óxido de níquel-níquel (NNO) e um biotita-honblenda-quartzo-diorítico sanukitóide arqueano foi a fonte proposta para os seus magmas.

As formas tridimensionais dos granitos Redenção e Bannach, modeladas através de estudo gravimétrico, indicam que os mesmos são intrusões tabulares com ~6.0 km e ~2.2 km de espessura máxima, respectivamente. Estes plútuns apresentam formas lacolíticas e são similares neste aspecto aos clássicos plútuns graníticos rapakivi. Os dados gravimétricos sugerem que a parte norte do plúton Bannach resultou da amalgamação de dois plútuns tabulares menores, colocados em seqüência de noroeste para sudeste. Isto é consistente com as interinterpretações anteriores de que o Granito Bannach corresponde a uma intrusão composta formada por pelo menos três plútuns coalescentes.

Os plútuns da Suíte Jamon foram colocados em um ambiente tectônico extensional com o esforço seguindo o trend NNE-SSW to ENE-WSW, como indicado pela ocorrência de enxames

de diques de diabásio e granito pórfiro, de orientação WNW-ESE a NNW-SSE, coexistentes com a suíte. Os plútuns graníticos paleoproterozóicos da Província de Carajás estão dispostos ao longo de um cinturão que segue o *trend* geral definido pelos diques. A geometria tabular dos plútuns estudados e o alto contraste de viscosidade entre os granitos e suas rochas encaixantes arqueanas podem ser explicados pela colocação dos magmas em baixa profundidade, em uma crosta rígida, sendo assumido que o transporte do magma se deu por diques.

Os altos valores de suscetibilidade magnética ( $1 \times 10^{-3}$  SI to  $54 \times 10^{-3}$  SI) obtidos em amostras do Granito Redenção, indicam que a sua trama magnética é controlada principalmente pelos minerais ferromagnéticos (magnetita). Os baixos valores do grau de anisotropia ( $P'$ ), a formação da magnetita nos estágios iniciais da cristalização magmática e certos aspectos texturais, como a ausência de feições deformacionais, indicam que a trama magnética é de origem magmática. A trama magnética é bem definida e caracterizada por uma foliação concêntrica de alto ângulo associada com linhas de mergulho moderado a fraco. A falta de uma trama linear unidirecional bem definida na escala do plúton sugere uma influência reduzida ou nula de esforços regionais durante a colocação do corpo granítico. Três estágios são propostos para a construção do Granito Redenção, conciliando a forma tabular da intrusão com o comportamento da trama magnética nas diferentes fácies do plúton: (1) ascensão vertical de magma através de diques alimentadores noroeste-sudeste e acomodação pela translação ao longo dos planos da foliação regional E-W; (2) mudança do fluxo, passando de vertical para um espalhamento lateral do magma, com subsidência do assoalho criando espaço para injeção de pulsos magmáticos sucessivos; (3) expansão *in situ* da câmara magmática em resposta às intrusões mais tardias na porção central, acompanhada pela injeção de magma residual através de fraturas anelares.

A aplicação bem sucedida das técnicas de AMS no estudo da trama magnética do Granito Redenção forneceu importantes informações sobre o mecanismo de colocação dos granitos anorogênicos tipo-A. Os resultados obtidos neste trabalho estimulam futuras pesquisas, no sentido da busca de um melhor entendimento dos fatores que controlam a colocação de corpos graníticos intraplacas e seu papel na evolução crustal, em especial do Cráton Amazônico.